

---

# Optimisation of transplantation methodology in mouse models of Huntington's Disease

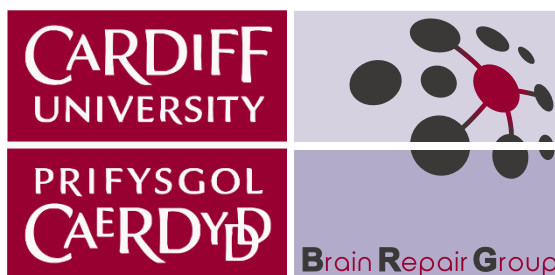
— David John Harrison —

---

This dissertation is submitted for the degree of Doctor of Philosophy  
at Cardiff University

December 2018

Supervisor:  
Prof. Stephen B. Dunnett



# Summary

The objective of the experiments described in this thesis was to optimise transplantation protocols to improve the outcome of striatal mouse-to-mouse grafts in lesion models of Huntington's Disease. There is a need to develop the model since the results observed, both in published studies and from within the lab, show typically small and pencil-like grafts, with little integration into the host compared to the widely-used rat model.

The starting point was current practice – procedures based on the efficacious rat model - with studies designed to probe the effect of altering key components of the protocol. These are grouped into three experimental chapters;

- Exploring the effect of host

These experiments examine potential reasons a poorer outcome is seen in mice. By comparing the mouse and rat quinolinic acid lesion models it was shown that mice maintain a greater inflammatory response. This result prompted studies into the effect of delaying grafting until beyond peak post-lesion inflammation, and if the inflammatory response was strain-specific. Whilst no differences were detected, it was concluded that group sizes were not adequate to make a definitive conclusion.

- Exploring the effect of donor

The first experiment focussing on donor parameters compared different methods of cell preparation and identified that E14 single-cell suspension yielded the best results. However, all groups demonstrated large variance in the graft outcome. This led to the exploration of the cell suspension and cell viability, finding that the trypan blue method may not be ideal for measuring the health of cell suspensions.

- Functional outcome measures

These experiments demonstrated a variety of graft outcomes; however, none could describe which were 'best' in terms of functional efficacy, a fundamental outcome for cell transplantation therapies. A field-wide lack of systematic behavioural testing of the mouse quinolinic acid models was identified, and the final experiments describe a comprehensive motor and cognitive characterisation of the model, culminating in recommendations for appropriate test batteries to identify functional recovery.

# Contents

Summary	i
<b>Chapter 1 - Introduction</b>	
1.1 Huntington's disease	1
1.2 Animal models of Huntington's disease	6
1.3 Potential therapeutic options in HD	9
1.4 Factors affecting the quality of transplants	17
1.5 Outcome measures in preclinical graft assessment	20
1.6 Aims	23
<b>Chapter 2 - Methods</b>	
2.1 Animal models	24
2.2 Surgical procedures	25
2.3 Histological techniques	29
2.4 Cell culture procedures	35
2.5 Behavioural testing	37
<b>Chapter 3 - Exploring the effect of host in QA lesion models</b>	
<b>Experiment 1 – A species comparison of excitotoxic lesions</b>	
3.1 Summary	54
3.2 Introduction	56
3.3 Methods	59
3.4 Results	62
3.5 Discussion	71
3.6 Conclusions and future work	75
<b>Experiment 2 – Extending the post-lesion period and the effect of host age</b>	
3.7 Summary	77
3.8 Introduction	78
3.9 Methods	79
3.10 Results	82
3.11 Discussion	88
3.12 Conclusions and future work	91
<b>Experiment 3 – The effect of host and donor strains</b>	
3.13 Summary	92
3.14 Introduction	93
3.15 Methods	96
3.16 Results	100
3.17 Discussion	109
3.18 Conclusions and future work	111

## **Chapter 4 – Exploring the effects of donor tissue and cell preparations**

### **Experiment 4 – The effect of tissue preparation and donor age**

4.1	Summary	113
4.2	Introduction	115
4.3	Methods	119
4.4	Results	126
4.5	Discussion	137
4.6	Conclusions and future work	143

### **Experiment 5 – The viability of cell suspension during the surgery period**

4.7	Summary	144
4.8	Introduction	145
4.9	Methods	148
4.10	Results	151
4.11	Discussion	156
4.12	Conclusions and future work	159

## **Chapter 5 – The functional assessment of the QA lesioned mouse model**

5.1	Summary	161
5.2	Introduction	162

### **Experiment 6 – Characterisation of deficits in a unilateral dorsolateral QA lesion mouse model**

5.3	Methods	164
5.4	Results	169
5.5	Experimental Discussion	186

### **Experiment 7 – Characterisation of deficits in a bilateral dorsomedial QA lesion mouse model**

5.6	Methods	189
5.7	Results	194
5.8	Experimental Discussion	211
5.9	Chapter Discussion	214
5.10	Conclusions and future work	221

## **Chapter 6 – General Discussion**

6.1	Key findings	224
6.2	The effect of host	225
6.3	The effect of donor	227
6.4	Functional assessment	227
6.5	Conclusions	228
	Bibliography	230
	Appendix 1 – Solution recipes	259
	Appendix 2 – Antibodies	261
	Appendix 3 – Operant test parameters	262
	Appendix 4 – Published article	267

# Chapter 1

## Introduction

### 1.1 Huntington's disease

Huntington's disease (HD) is a debilitating disorder characterised by motor, cognitive and psychological disturbances, for which the prognosis is extremely poor. Diagnosis is typically made when motor symptoms begin to manifest (Huntington Study Group, 1996), usually from around 35-40 years of age, although they can present at any age (Foroud et al., 1999). Chorea, loss of balance or perceived clumsiness are commonly the first reported signs, which can progress to dystonia, bradykinesia, rigidity, dysarthria and dysphagia (Novak and Tabrizi, 2010). Preceding diagnosis, however, the patient will often have had a period of subtle but worsening cognitive and psychological changes (Paulsen et al., 2008, 2001). These signs tend to be detected by close family members many years before the apparent disease onset, and often are not recognised by the patient themselves. Cognitive signs can include decline in executive function and difficulty in organising thoughts, problems initiating movement, perseveration of movement, increased impulsivity and distractibility, and difficulty in learning new information. Psychiatric features associated with the disease can include depression, anxiety, apathy, irritability and suicidal tendencies (Paulsen et al., 2005). Sleep disturbance and personality changes are also commonly seen. Any one of these symptoms in themselves can have a severely damaging effect on a patient's life, which makes HD a devastating disease not only for the patient but for their family, not least because of its hereditary nature.

Most patients will survive for just 10 to 20 years post-disease onset (Foroud et al., 1999), with symptoms becoming progressively more severe, resulting in a rapid deterioration in quality of life. The most common causes of death come from inter-related complications, such as pneumonia or cardiovascular problems, rather than as a direct result of the disease. There is currently no known treatment that can inhibit the progression of the disease and symptomatic relief is minimal.

The prevalence of HD in Europe and western countries is often reported to be between 5-7 in 100,000 people (Walker, 2007), however more recent estimates increased this to 12.3 in 100,000 (Evans et al., 2013). HD is genetically inherited and caused by an expansion of the trinucleotide repeat cytosine-adenine-guanine (CAG) in exon 1 of the Huntingtin gene (*HTT*) on chromosome 4, first identified in 1993 by the Huntington's Disease Collaborative Research Group (HDCRG, 1993). As an autosomal dominant disease with full penetrance, any person carrying the mutated gene (*mHTT*) will develop the disease and have a fifty percent chance of passing it on to any offspring. While the inheritance of *mHTT* accounts for the vast majority of HD cases, it is thought that 1-3% of new cases are due to sporadic mutations (Myers et al., 1993). Since symptoms will often present after childbearing age, and previous generations often have been misdiagnosed, it is common for patients to have had children before knowing about the condition – meaning diagnosis impacts greatly on the whole family. Genetic testing is available to confirm the presence of *mHTT*, however most people at risk decide not to take the test (Creighton et al., 2003), possibly due to the risk of negative social discrimination or the thought that it is unnecessary due to the lack of a cure, or simply because they would rather not know.

The age at which the onset of symptoms occurs is closely correlated to the *mHTT* CAG repeat length (Langbehn et al., 2004). Individuals in the normal population have <10 - 29 CAG repeats in the gene sequence (Kumar et al., 2010), whereas HD patients have an extended CAG repeat length of 36 or more. While the mean age of onset occurs around mid-life, those with repeats towards the lower end of the scale tend to have symptoms which manifest later in life, while juvenile onset of symptoms, and greater symptom severity, occurs in those with more than ~60 CAG repeats (Lee et al., 2012; Zdzienicka et al., 2002). It is thought that environmental factors and as yet unidentified genetic factors can also play a modifying role in the age of disease onset (The U.S.-Venezuela Collaborative et al., 2004).

The huntingtin protein (HTT), for which *HTT* codes, is known to be active in neural development, and also is thought to have many other functional roles in the body including intracellular vesicular trafficking, synaptic transmission, neuronal transcription and autophagy (Caviston and Holzbaur, 2009; Gauthier et al., 2004; Marcora and Kennedy, 2010; Martin et al., 2014; Steffan, 2010). The exaggerated length of the *mHTT* gene in people with HD translates an expanded polyglutamine repeat in the HTT protein which causes misfolding and interferes with its normal function and interactions (Borrell-Pagès et al., 2006).

The appearance of aggregated mutant huntingtin (mHTT), and its formation into insoluble inclusion bodies in neuronal cells throughout the brain, is a characteristic feature in HD. It remains unclear if these inclusions are protective or pathogenic in nature (Walker, 2007) as the exact pathological mechanisms of HD are yet to be determined. Some of the earliest pathological deterioration occurs in the olfactory tubercles and the caudate putamen, and is focussed specifically on the medium spiny neurons (MSNs) (Graveland et al., 1985) which constitute 90 – 95% of the total adult striatal neuron count. The progressive dysfunction and degeneration of these cells from the basal ganglia network trigger the cognitive, psychiatric and behavioural disruption seen in patients, possibly initiated through early synaptic dysfunction (Duff et al., 2007; Harrington et al., 2012; Paulsen et al., 2008; Twelvetrees et al., 2010). However, neurochemical alterations, mitochondrial dysfunction, oxidative stress, neuroinflammation and excitotoxicity have all been linked to the deterioration of MSNs and their associated neural networks (Alexi, 2000; Beal, 1994; Crotti et al., 2014; Tang et al., 2005).

### 1.1.1 The cortico-striatal circuitry in the normal brain

Striatal MSNs project and carry signals to the thalamus and output targets beyond, and the remaining 5-10% of striatal neurons (excitatory cholinergic interneurons) work to modulate their action (DiFiglia and Rafols, 1988; Lanciego et al., 2012; Wang et al., 2006). MSNs are GABAergic, secreting the inhibitory  $\gamma$ -aminobutyric acid (GABA) neurotransmitter which acts to dampen activity of post-synaptic target neurons. Movement, cognition and behaviour are thought to be controlled by the neuronal circuits of the cerebrum and basal ganglia (Albin et al., 1989; Brown and Robbins, 1989; Phillips and Carr, 1987; Steiner and Gerfen, 1998; Suri et al., 1997), with functionally distinct cortico-striatal loops mediating different aspects of behaviour (Alexander et al., 1986; Lopez-Paniagua and Seger, 2011). Together with the globus pallidus (GP), substantia nigra (SN) and subthalamic nucleus (STN), the striatum is one of the major nuclei of the basal ganglia of humans and other primates, and is the primary afferent structure. It receives input from the cerebral cortex, thalamus, SN and brain stem, and extends efferent neurons to the GP and SN (Lanciego et al., 2012), **Figure 1.1 A**.

Within the striatum MSNs are organised into two parallel processing circuits known as the direct and indirect pathways, each predominantly innervated by different dopaminergic receptor sub-populations. Dopamine D1 receptors are predominantly located on the MSNs of the direct pathway, while D2 receptors are associated more with the MSNs of the indirect

pathway (Doig et al., 2010), although there is thought to be some crossover between the two. The substantia nigra innervates phasic dopaminergic input into the basal ganglia, and differentially induces excitation and inhibition of the direct and indirect pathways respectively. The net balance of these two opposing circuits is critical for the stimulation of the thalamo-cortical feedback mechanisms which drive the system and determine optimal behaviour outputs (Albin et al., 1989; DeLong, 1990), as such, normal functioning control is coordinated through the action of the direct and indirect pathways. If the balance is disturbed, functional integrity is lost, resulting in a broad range of consequent effects on movement and cognitive ability. For example, through selective loss of MSNs as in HD, or through loss of dopamine through nigral cell loss as in Parkinson's disease, (Albin et al., 1989).

### 1.1.2 The cortico-striatal circuitry in Huntington's disease

The loss of MSNs from the indirect pathway is thought to be the principal cause of the neuropathological symptoms in HD (Albin et al., 1989; DeLong, 1990), disrupting the balance of the two signalling pathways of the basal ganglia, **Figure 1.1 B**, and inducing the progression of psychiatric, cognitive and motor deficits characteristic of HD.

As the disease progresses, the pathology extends to the neurons of the direct pathway and patients become progressively more hypokinetic. In the later stages, the pathology becomes more extensive and eventually develops into a whole brain disease (Aylward et al., 1998; Rosas et al., 2002).



## 1.2 Animal models of Huntington's disease

Aside from the pathogenic progression of HD, the mechanisms of the disease are still not completely understood. To fully explore the contribution of potential underlying aberrant processes and to test the capacity of novel treatments to ameliorate them, animal models must play a critical role. An appropriate model must reproduce some aspects of the disease, preferably relatable to signs exhibited in patients, from which the disease mechanisms can be explored.

Two of the major hallmarks of HD make it relatively amenable to modelling in animals. Firstly, it is caused by an identified single genetic mutation, enabling a plethora of transgenic and knock-in models to be constructed. Secondly, its primary pathogenic feature is loss of MSNs from the striatum, an aspect which can be replicated through striatal injection of excitotoxins which cause targeted cell death.

### 1.2.1 Genetic models of HD

Through replicating the genetic nature of HD, genetic models offer insight into its progressive features, as well as providing a method of understanding key molecular and cellular disturbances induced by the disease. This provides an opportunity to not only test the impact of pharmaceutical and other interventions on disease progression, but also to identify relevant pre-symptomatic changes which could be used to identify optimal timings for early therapeutic interventions, before the onset of cell loss.

There is now a wide array of HD mouse models commercially available, incorporating transgenics - in which all or part of the mouse or human mutant gene are inserted randomly into the genome, and knock-in models, where the mutation is inserted specifically into the huntingtin gene exon 1 locus. Whilst each of the models present a differing array of disease signs and severity, they commonly show progressive behavioural motor and cognitive deficits, and the presence of widespread intra-nuclear inclusions (Heng et al., 2008; Menalled and Chesselet, 2002). The first transgenic mouse models (R6/1 with ~115 CAG repeats and R6/2 with 150 CAG repeats) exhibit a rapid development of cognitive (learning and memory), motor (abnormal gait, claspability, hyperactivity) and physical decline (weight loss and muscle wastage), as well as early pathological signs (formation of intranuclear mHtt inclusions). The R6/2 model has a particularly aggressive disease progression and a life

expectancy of just 13-16 weeks. More recent models, such as the knock-in hdhQ175 line (~175-190 CAG repeats), are slower to develop inclusions and show signs of cognitive decline only after age 6 months. This makes them more amenable to longer-term studies and intervention probes than the R6s, which may not live long enough to benefit from treatment. In addition, a series of lines has been developed in which a range of CAG lengths have been incorporated, from 50 to 250 repeats, with the onset of HD signs occurring earlier, and disease severity increasing in proportion to the number of CAG repeats present. Cognitive decline in genetic HD mouse models has been demonstrated through attentional deficits (e.g. five-choice serial reaction time task), memory deficits (e.g. Morris water maze task) and decline in cognitive plasticity (e.g. set shifting tasks). Motor deficits have been shown through gait analysis, reduced motor coordination (e.g. rotarod, balance beam) and poorer manual dexterity (paw reaching) compared to wildtype controls.

Currently, a minimal number of transgenic rat models of HD have been developed, and the majority of transgenic work has been conducted in mice due to the ease of genetic manipulation in this species compared to rats (Brooks et al., 2009; Manfré et al., 2015).

Whilst clearly having the benefit of exhibiting high face validity and the genetic construct of the disease, critically, the genetic models demonstrate only minimal striatal cell loss (Brooks et al., 2012b, 2012c; Gil and Rego, 2008; Turmaine et al., 2000). Some degree of neuronal loss was evident in the YAC 128 model, although not until after 9 months of age (Slow et al., 2003). For studies examining this aspect of the disease, maintaining animals for so long before experiments is costly. In addition, if surgical interventions are to be performed, the impact on welfare is increased when conducted in older, more unwell animals, rather than younger and otherwise healthy animals. Importantly, reducing the period for which animals are kept, and improving welfare are priorities for animal research. Therefore, acute models of neurodegeneration present a viable alternative for studies focussed on this aspect of HD.

### 1.2.2 Excitotoxic lesion models of HD

Glutamatergic excitotoxicity is thought to be a major mechanism of neurodegeneration in HD. Binding of the neurotransmitter glutamate (GLU<sup>+</sup>) to the *N*-methyl-D-aspartate (NMDA) receptors, located on the dendrites of neurons, causes a massive and detrimental influx of Ca<sup>2+</sup> into the cell. MSNs have a relatively high number of NMDA receptors, and as such they are inherently more susceptible to the actions of the excitotoxin. As intracellular levels of Ca<sup>2+</sup> increase, a toxic series of metabolic disturbances and pathological damage is triggered,

including mitochondrial  $\text{Ca}^+$  overload (Beal, 1994; Tang et al., 2005) and the induction of apoptotic cell death (Beal et al., 1991, 1986; Schwarcz et al., 1979). Compromised cellular metabolism, such as that seen in the MSNs in HD, is thought to confer an increased predisposition to excitotoxic vulnerability, thus triggering cell death in response to normal levels of excitotoxins in the brain.

Quinolinic acid (QA) is an endogenous  $\text{GLU}^+$  analogue which acts upon the NMDA receptors and replicates some of the chemical pathways thought to play a role in the degeneration of MSNs (Beal et al., 1986; Bruyn and Stoof, 1990). Neurons with dendritic NMDA receptors stimulated by the excitotoxin exhibit specific depolarization and rapid degeneration (Foster, 1983). Therefore, the specific striatal neurodegeneration observed in early HD can be emulated in animal models through intracranial injection of QA directly into the striatum (Beal et al., 1991; Portera-Cailliau et al., 1995), whereby the NMDA-rich MSNs within the area of QA infusion will be subjected to its excitotoxic action, leading to their localised cell death. Much like in HD, the axons and non-neuronal tissue in this model are spared, as well as the cholinergic interneurons and non-spiny NADPH-diaphorase neurons (Beal et al., 1991; Davies and Roberts, 1988).

Other neurotoxins have been utilized in lesion models including  $\text{GLU}^+$ , kainic acid (KA), ibotenic acid (IBO), and NMDA. The  $\text{GLU}^+$  analogues, KA and IBO, were developed as they were found to have an increased potency over  $\text{GLU}^+$  (Coyle et al., 1983), however each had shortcomings including the development of extra-striatal lesions, in the case of KA (Guldin and Markowitsch, 1981), and degeneration of striatal target neurons and bi-lateral reduction of dopamine with IBO (Narang et al., 1993). The targeted action of QA lends the excitotoxin an advantage over other similar neurotoxins by inducing an acute working recapitulation of HD which produces the cellular dysfunction and many of the core symptoms associated with the disease (Beal et al., 1991). In addition, the ability to independently lesion just one hemisphere allows the use of the contralateral side as a within-subject control for lateralised deficits.

Whereas the genetic mouse models of HD have been extensively behaviourally characterised (Brooks et al., 2012a, 2012b, 2012c; Heng et al., 2008), the striatal QA lesion mouse model has not undergone such a systematic behavioural or pathological characterisation.

Protocols for testing cognitive function, and the effect of therapeutic strategies on these functions, are often based on traditional rat models of disease. The translation to mice is often expensive in time and resources, thus in certain fields of research, such as

transplantation therapy, there is rich history of trials in the rat that is largely absent in the mouse (Björklund et al., 1980a, 1980b; Dunnett and Björklund, 1997; Gage et al., 1997). In addition to benefitting from a comprehensive catalogue of established testing protocols, the larger size of the rat confers an advantage where the therapeutic application is surgical (Abbott, 2004; Bugos et al., 2009). A comparison of the pathology and response to QA lesioning in the rat and mouse models is discussed further in **Experiment 1**, and an in-depth characterisation of the behavioural deficits of the QA mouse model in **Chapter 5**.

### 1.3 Potential therapeutic options in HD

There is currently no treatment available which can reverse or slow the progression of HD. The burden of the disease is managed through physiotherapy and support from family and physicians, as well as through symptomatic pharmacological treatment, which can often cause problematic side-effects (Coppen and Roos, 2017).

A number of potential therapies are under consideration for clinical application, each tackling a different aspect of the disease, such as prevention of protein aggregation (Huntington Study Group, 2015), increasing beneficial neurotrophic factors in the brain (Reilmann et al., 2014), or most recently, promising trials aimed at lowering the amount of mHTT through suppression of the RNA (NIH, 2017).

These approaches show great promise for people in the pre-symptomatic and early stages of HD, however it remains unclear how appropriate they might be once significant neurodegeneration has occurred. Whilst preventing loss of affected cells is obviously extremely valuable, these approaches cannot repair those cells which have already been lost.

The relatively targeted nature of the neurodegeneration in HD presents an opportunity to replace those lost striatal cells with new MSNs, with the aim of restoring connections, and potentially to even reverse the progress of the disease.

#### 1.3.1 Cell transplantation as a viable therapeutic option in HD

Transplantation of whole ganglionic eminences (WGEs), which include the site of MSN precursors in foetal development, has been shown to be a viable therapeutic strategy. Clinical trials have so far focussed on safety and procedural aspects of the therapy, and

demonstrated long-term survival of grafts, with no graft-induced side effects or exacerbation of the disease (Freeman et al., 2000; Hauser et al., 2002; Rosser, 2002). With the focus primarily on safety, studies have shown limited functional improvement, however, improvements in neurological assessments have been reported in some cases. A review by Bachoud Lévi et al., (2017) reports the outcome of 30 patients transplanted with hPF tissue for all trials where clinical data and follow-up details are available. Of these, 4 have demonstrated long-term functional efficacy, including improvements in motor and cognitive function over 4 – 6 years. An additional 4 patients showed more transient improvements or slowing of symptom progression compared to non-transplanted patients in the cohort.

Post-mortem analysis of grafts have demonstrated successful integration of the transplanted tissue and differentiation into relevant striatal phenotypes (Capetian et al., 2009; Freeman et al., 2000), in some but not all cases, highlighting the need for continued refinement of transplantation procedure. The efficacy and consistency of this approach must be improved before it can be developed as a clinical treatment.

Cell replacement therapy has the potential to be a powerful therapeutic strategy for the treatment of HD, however, more work is required to test whether foetal transplantation can reliably improve function in people with HD.

Human transplantation trials have so far used primary foetal (hPF) tissue from termination of pregnancy as a source of neuronal precursors, and this is currently viewed as the gold standard for graft outcome measures. However, the recruitment of multiple embryos is necessary to obtain the cell numbers required for a transplantation in HD, making the process difficult to manage logistically due to the limited availability of tissue. In addition, the quality of the tissue can be inconsistent, leading to difficulties in replicating protocols from patient to patient.

Other obstacles facing the use of hPF tissue as a mainstream treatment, other than being a topic of controversy, include strict regulation and ethical constraints, and the need for patients to undergo an immunosuppressive regime to avoid immune rejection of the transplanted tissue. Advances in the use of embryonic stem cells (ESC) and mesenchymal stem cells (MSC) derived from adult bone marrow, have opened up the possibility of increasing not only the supply of donor cells, but also of improved quality control over the cell product (Dunnett and Rosser, 2007). Furthermore, the development of induced pluripotent stem cells (iPSC) and induced neurons (iN) allow conversion of adult somatic cells into the required cell types, which could lead the way in producing personalised treatment

products. Transplanting patient-derived cells could negate the requirement for immunosuppression and its associated side effects, and potentially improve the long-term graft outcome. However, cells taken from people with HD would retain a dysfunctional genotype and, as transplanted cells, could follow the same path of disease progression as those they are replacing. New techniques in the field have enabled the correction of CAG repeat length in manipulated iPSCs and have shown they can differentiate into new cells free of the expanded codon (An et al., 2012), thus furthering the potential of iPSCs for use in cell replacement therapies. This may be confounded however, by studies which show that even non-diseased transplanted cells will start to undergo degeneration in line with disease progression over time (Cicchetti et al., 2009).

These donor cell sources have great potential to benefit the field of cell replacement therapy, however, much preclinical work is still required before moving them forward to clinic. The time frame of transplantation studies in patients can range over decades and progress is often slow, which highlights the need for further work in animal models to address many issues in a much shorter term to progress the therapy.

### 1.3.2 Transplantation in rodents as model therapeutic systems

The techniques of transplantation have been studied since the 1970's (Seiger and Olson, 1977), with work mostly concentrated on rat lesion models and demonstrating the successful reversal of functional deficits and integration of donor tissue with the host striatum. A broad range of studies have shown healthy looking grafts which have connected extensively with the host tissue and alleviated some HD-like signs induced by lesioning (Brasted et al., 2000; Döbrössy and Dunnett, 2008, 2005; Dunnett and White, 2006; Mazzocchi-Jones et al., 2009), **Figure 1.2.** Rat grafts typically incorporate most of the lesioned striatum and, as a result of protocol refinement, are able to produce a high proportion of dopamine and cAMP regulated phosphoprotein (DARPP-32) positive MSN tissue. Typically, grafted tissue is organised into striosomal-like morphology, with areas of dense DARPP-32 staining striatal-like P-zones, and non-P-zones where this staining is much reduced or absent (Graybiel et al., 1989; Isacson et al., 1987). It has been suggested that these non-P-zones contain non-DARPP-32 neurons and glial cells (Nakao et al., 1996). Efferent projections from grafts are seen extending into the globus pallidus, as detected using retrograde tracers such as Fluorogold. Furthermore, afferent host cortical neurons and dopaminergic fibres are often observed innervating the grafted tissues, thus mirroring the natural patterns of the basal ganglia circuitry (Watts et al.,

2000b; Wictorin et al., 1989). Differentiation of transplanted tissue however, has been shown to be transplant site-specific, with donor cells apparently responding to local signals from within the host parenchyma (Campbell et al., 1995; Fricker et al., 1999).

The advancement of stem-cell derived precursors and the many advantages these hold over primary tissue, such as manipulations in labelling and genetics, along with the development of new genetic models of HD, meant that there was leap from transplanting primary tissue in the rat models to transplanting stem cells in mice. As a result, existing protocols were transferred directly to the mouse models, and systematic optimisation of methods translating from rat to mice were largely overlooked.

Few mouse transplantation studies have been published, and even fewer of these use mouse primary embryonic tissue (mPF). In contrast to those seen in rats, transplants of WGE in HD mouse models have generally produced relatively small grafts. Despite most studies reporting high graft survival rates, cell survival is low and the resultant grafts are often thin and pencil-like, with relatively little host interaction (Brasted et al., 2000; Cisbani et al., 2014; Dunnett and White, 2006; El Akabawy et al., 2012; Johann et al., 2007; Kelly et al., 2009, 2007), **Figure 1.3**. It is worth considering that often the best-looking grafts from an experiment may be the ones chosen for published images, even so, the mouse grafts do not compare to those depicted in rat studies. **Table 1.1** summarises the protocols and quantified graft outcomes reported in the literature for striatal mPF transplants in HD mouse models and demonstrates the small graft volumes and lack of consistency.

Graft outcome measures have mostly focussed on morphology rather than any functional assessments, however, a study of transplantation in the R6/2 transgenic mouse did test for graft-induced functional recovery (Dunnett et al., 1998). In this case no improvement was found, possibly due to a combination of small graft sizes, widespread pathology in the host and the reduced R6/2 lifespan restricting the time for adequate graft development.

Mouse studies of ESC and iPSC transplants are becoming increasingly common (Arber et al., 2015; Dihné et al., 2006; El Akabawy et al., 2012; Shin et al., 2012), but do not yet produce the quality of transplant observed in rat studies. There remains a need to re-evaluate the protocols of primary mouse-to-mouse transplantation in order to produce the optimum outcomes against which future cell products may be validated. This includes the need to optimise the transplantation procedure, from tissue preparation and delivery, to the development of precise methods for functional assessment.

The experiments described in this thesis compare the rat and mouse QA model and modifications to the standard transplantation protocols, with the aim of improving the quality of graft outcome. The starting point for these comparisons is based on those mouse studies which have produced the largest grafts (Döbrössy et al., 2011) **Figure 1.3 G**, and the protocols and models used in this study are those on which the experiments of this thesis are based, see **Chapter 2**.

Once robust protocols have been developed in the QA models to ensure healthy and integrating grafts can be reproduced consistently, the methods can then be tested in the progressive genetic models. Moreover, optimising the protocols for achieving successful embryonic WGE grafts will solve many issues that are also relevant to pluripotent stem cell-derived grafts, which are currently being developed as a more sustainable source of donor cells.

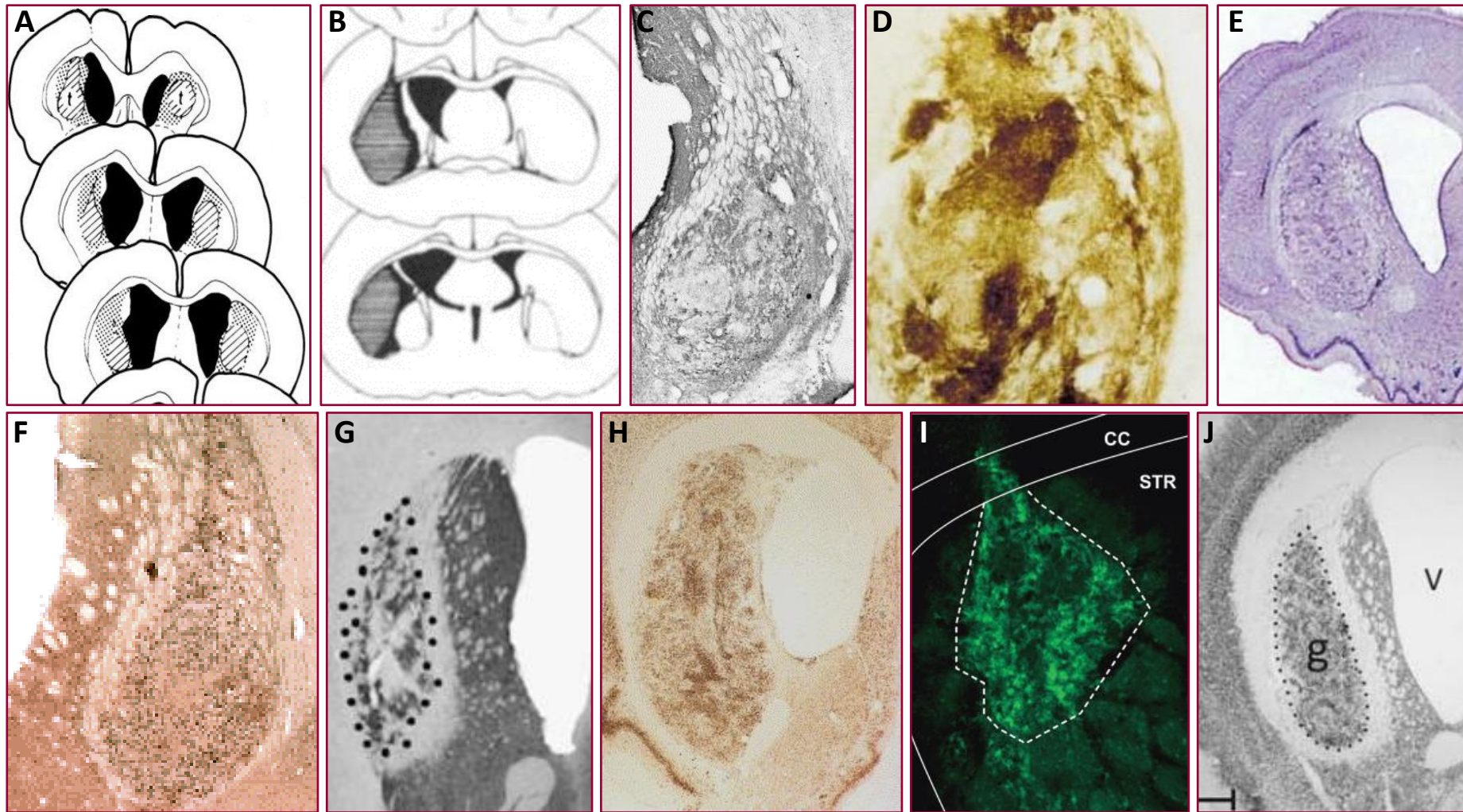


**Figure 1.2** Images of rat PF striatal transplants into rat hosts collated from existing literature **A** Isacson et al., (1986), **B** Mayer et al., (1992), **C** Fricker et al., (1997), **D** Watts et al., (2000), **E** Brasted et al., (2000), **F** Fricker-Gates et al., (2004), **G** Döbrössy and Dunnett, (2006), **H** Dunnett and White, (2006), **I** Mazzocchi-Jones et al., (2009) and **J** Klein et al., (2013).

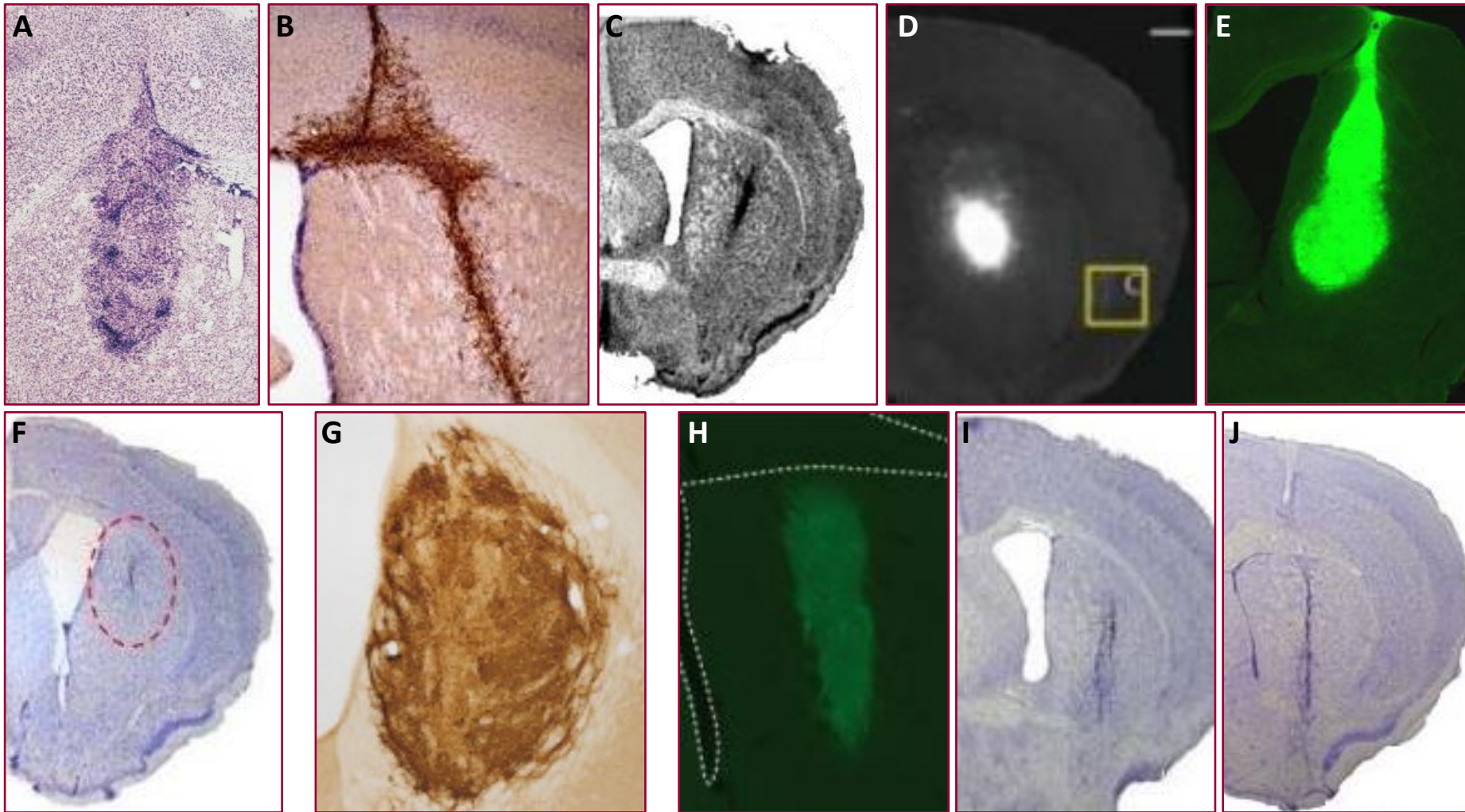


**Figure 1.3** Images of mouse PF striatal transplants into mouse hosts collated from existing literature **A** Dunnett et al., (1998), **B** Johann et al., (2007), **C** Kelly et al., (2007), **D** Magavi and Lois, (2008), **E** Stefanova et al., (2009), **F** Precious, (2010), **G** Döbrössy et al., (2011), **H** Cisbani et al., (2013), **I** Evans, (2013) and **J** Robertson, (2014).

Author	Lesion	Host strain	Host age	Time post-lesion	Donor strain	Donor age	Tissue type	Preparation	Ice	Cells/ $\mu$ l	Cells transplanted	Survival rate (%)	Graft cell number	Graft volume (mm <sup>3</sup> )
Dunnett et al., (1998)	X	R6/2 CBA X C57BL/6	10w	n/a	C57BL/6	E13-14	LGE	CS	N	½ WGE	1 WGE	100 100	- -	- -
Johann et al., (2007)	QA X	C57BL/6 R6/2	Adult	2, 7 & 14d	EGFP- C57BL/6 EGFP- R6/2	E14	Cultured WGE / NSC	CS / Neuro- spheres	-	200,000	200,000	- -	3 – 20,000 3 – 20,000	0.03 – 0.20 0.03 – 0.20
Kelly et al., (2007)	QA	C57BL/6	Adult	-	C57BL/6	E14	WGE	CS	Y	250,000	500,000	95	30,000	1.8
Magavi and Lois, (2008)	X	CD1	8w – 13m	n/a	CD1- GFP	E14	LGE	TP	Y	5,000	5,000	-	2 – 4,000	-
Stefanova et al., (2009)	3-NP	C57BL/6 PLP- $\alpha$ SYN	Adult	3d	C57BL/6	E13.5	WGE	CS	N	½ WGE	1 WGE	-	-	0.8 – 1.0
Precious, (2010)	QA	C57BL/6	Adult	14d	C57BL/6	E14	WGE LGE MGE	CS	Y	125,000	250,000	- - -	1,000 750 450	0.75 1.5 1.4
Mazzocchi-Jones et al., (2011)	QA	C57BL/6	Adult	7d	EGFP	E13	WGE	CS	Y	200,000	400,000	100	-	-
Döbrössy et al., (2011)	QA	CD1	8w	10d	C57BL/6 ( $\pm$ GFP)	E14	WGE	CS	N	150,000	300,000	100	-	-
Cisbani et al., (2013)	X	YAC128 C57BL/6	8m	n/a	C57BL/6 ( $\pm$ GFP)	E13.5	LGE	CS	Y	100,000	100,000	100 100	6,000 6,500	0.014 0.02
Evans, (2013)	QA	C57BL/6	Adult	6 – 10d	C57BL/6	E14 E12	WGE	CS	N	250,000 1 WGE	500,000 2 WGE	78 86	- -	1.25 4.4
Robertson, (2014)	QA	CD1	8w	-	CD1	E14	WGE	CS	N	125,000	300,000	37	-	-

**Table 1.1** Summary of mouse PF striatal transplants into mouse hosts. “-” denotes where information is unavailable. LGE = lateral ganglionic eminence, WGE = whole ganglionic eminence. CS = single-cell suspension, TP = tissue-piece preparation.

## 1.4 Factors affecting the quality of transplants

The process of transplanting cells, from the source of the tissue and the way it is processed, to the surgical protocols and the host into which it is being implanted, are subject to a huge range of potential variables, all of which could have a great impact on the outcome of cell transplantation. The current protocols for transplantation in rodents have been developed in the rat lesion model following studies aimed at optimising the conditions for large grafts containing a high proportion of striatal-like tissue and demonstrable functional efficacy (Barker, 1995; Schmidt et al., 1981). Such studies included probing the effects of embryonic dissection, donor age, the lesion-transplantation time window and the degree to which tissue is dissociated. However, very few of these experiments were conducted in mouse models.

### 1.4.1 Host effects

#### The immune response of the central nervous system (CNS)

The development and maturation of transplanted embryonic MSN precursors has been shown to be dependent on extrinsic factors relating to the host environment (Ivkovic and Ehrlich, 1999). This highlights that the environment into which the cells are deposited can have a direct effect on graft outcome. The host CNS immune response to transplanted tissue has become recognised as one of the most important features of graft survival (Barker and Widner, 2004), despite the CNS historically being considered an immunologically privileged site (Barker and Billingham, 1978). Whilst the blood brain barrier can limit the infiltration of some peripherally circulating large molecules and immune cells into healthy brain parenchyma, the tight junctions it forms, separating the CNS from the periphery, can become more permeable when under stress or damaged during the process of transplantation surgery (Finsen et al., 1991), as well as during the lesioning process in preclinical models. In these conditions, the neural tissue is not only exposed to circulating immune cells (Hickey et al., 1991), but the inflammatory and immune response within the CNS itself can also be activated.

The primary inflammatory and immune cells in the CNS are the microglia. In normal healthy individuals, microglia actively survey the brain in a ramified 'resting' state searching for foreign material, damaged tissue and debris. If these are encountered, the microglia can

transform into an 'activated' state and act as macrophages to engulf the offending material (Karperien et al., 2013; Olah et al., 2011; Streit et al., 2004), **Figure 1.4**.

In development, microglia are responsible for the pruning of unnecessary dendrites and synaptic connections, and in adulthood will remove those connections that are not used or dysfunctional (Perry and Teeling, 2013). An increase in activated microglia has been seen at an early disease stage in the brains of both people with HD (Tai et al., 2007a, 2007b) and the in genetic mouse models (Kwan et al., 2012), with the mHTT-expressing microglia showing an increased tendency to induce neuronal death (Crotti et al., 2014). Furthermore, otherwise healthy neurones can be phagocytised if they become stressed in the presence of activated microglia, a process which is exacerbated in HD and other neurodegenerative diseases in which patient exhibit dysfunctional microglial activity (Brown and Neher, 2014).

The microglia are highly reactive to insult and will increase in number to combat damage, recruiting non-local microglia to the region. This can lead to damage of healthy neural tissue if there is a sustained reaction to chronic insult. These reactive microglia could potentially be detrimental to transplanted cells being introduced during this reactive phase (Giulian, 1993). Conversely, some reports have hypothesised that the presence of microglia could be beneficial to the transplanted cells through supporting re-growth into damaged areas since they have been associated with the promotion of neural tissue repair by the secretion of neurotrophic factors such as brain-derived neurotrophic factor (BDNF) *in vitro*, (Miwa et al., 1997), however it is clear that *in vivo*, the reaction to transplanted tissue can be detrimental and severe (Cicchetti et al., 2011; Lawrence et al., 1990). Microglia and macrophages in fixed brain sections can be identified through immunohistochemical staining of antibodies, such as Ionized calcium binding adaptor molecule 1 (Iba1), and cell morphology used to predict the state of activation, as described in **Figure 1.4**. A more definitive description of the activated state of microglia could be achieved through double-labelling brain tissue with a combination of resting-state and activated-state specific antibodies, such as F4/80 and Cluster of differentiation 40 (CD40) respectively. An abundance of one marker over another could potentially inform on the type of effect that the microglia are exerting on the transplants, with increased numbers of CD40+ microglia indicating an activated state and inflammatory/hostile response to the transplant. Alternatively, more F4/80+ cells could indicate that the resting state microglia are contributing to a more anti-inflammatory, favourable environment. Using quantitative assays such as an enzyme-linked immunosorbent assay (ELISA), quantitative polymerase chain reaction (qPCR, for RNA transcription) and Western blots (for protein transcription) it is possible to further distinguish

between potentially beneficial or detrimental microglial presence in tissue using markers to identify what type of substances they are secreting, for example brain derived neurotrophic factor (BDNF) and Interleukin-10 (IL-10) would indicate beneficial/anti-inflammatory properties, while conversely QA and CD16 would show an inflammatory response.

Microglia clearly play an important role in both HD and in the survival of transplanted cells, and the microglial response in the QA lesion models and transplanted mice is discussed further in [Chapter 3](#).

It is often assumed that mice will function and behave as a smaller version of the rat, however, there are underlying differences between the way that rats and mice respond to cells transplanted into the lesioned striatum. Whether there are disparities between the two species in their physical or chemical response to lesioning, in how the striatum responds to transplantation, or how the donor tissue responds to being transplanted has not been fully explored or dissected. [Experiment 1](#) of this thesis directly compares the lesion response of the two species and discusses the differences between them.

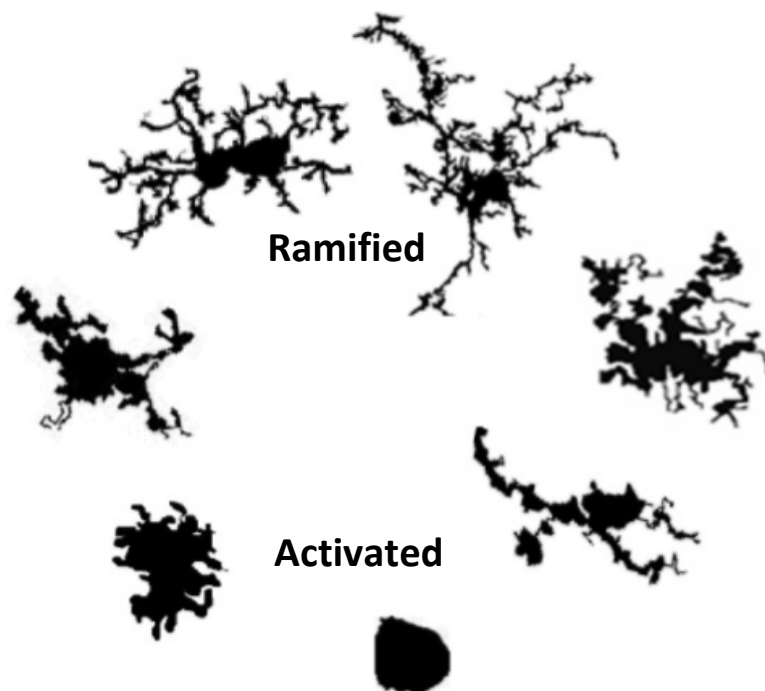


**Figure 1.4** Representation of microglial morphological changes from ramified to activated states. Adapted from Karperien et al (2013).

---

### 1.4.2 Donor effects and cell preparation

#### Donor age

The effect of donor age had been explored widely in rat-to-rat models and has been shown to impact greatly on the cellular content of the resultant grafts (Fricker et al., 1997; Schackel et al., 2013; Watts et al., 2000a, 1997). The embryonic age 14 days (E14) time-point was generally adopted and has been widely incorporated into the mouse protocols. However, differences between the developmental rates of mice and rats, and specifically the age at which the medial and lateral aspects of the WGE emerge, indicate that the optimum age for harvesting donor tissue in mice should be different to that of rats. The effects of donor age on graft outcome in mice are discussed further in [Chapter 4](#).

#### Tissue preparation

Early animal studies of neural transplantation engrafted chopped tissue pieces into cavity lesions generated by direct ablation of the brain parenchyma. This process was refined for rat tissue, firstly by introducing the process of cell dissociation (Schmidt et al., 1981), then through further systematic refinement of the tissue preparation protocol to improve efficacy of striatal grafts (Fricker et al., 1996). As a result, transplantation procedures were fine-tuned in the rat-to-rat model which has led to improvements in graft survival, graft volume and DARPP-32 content (Gage et al., 1997; Rosser et al., 2011; Watts et al., 2000b). The effects of tissue preparation on graft outcome is further discussed in [Chapter 4](#).

### 1.5 Outcome measures in preclinical graft assessment

The success (or failure) of transplantation in mouse models is typically evaluated by the morphological aspects of the grafts, such as cell survival, graft volume and cell type. Improvements in graft survival, size and striatal content can be good criteria to which protocols can be assessed and are relatively quick and simple to measure. However, they cannot by themselves tell us anything about the functional efficiency of the treatment. The fundamental aim of late-stage clinical trials is to produce a meaningful improvement in motor, cognitive and/or psychological disturbances to the person with HD, and so functional output should also be a critical part of pre-clinical studies. Whilst many rat-to-rat studies have described motor and cognitive improvements following successful grafting (Fricker et

al., 1997; Mayer et al., 1992; Reading and Dunnett, 1995), these outcome measures are mostly missing for the mouse.

### 1.5.1 Morphological outcome measures

Longitudinal monitoring or measuring of transplanted tissue can be difficult and expensive. As a result, preclinical grafts are most commonly assessed only at the end of the study, and certainly at the end of the subject's life. Morphological aspects of the grafts are taken as markers of 'success', such as increased proportion of graft survival, increased cell counts and graft volume. In addition, a greater degree of innervation of the transplanted tissue into the host parenchyma or a greater accuracy for efferent projections connecting to anatomically correct regions can be considered positive markers of success.

The majority of studies use immunohistochemical staining of tissue using specific antibodies to evaluate grafts post-mortem. The number of DARPP-32<sup>+</sup> neurons and the amount of striatal-like patches of DARPP-32<sup>+</sup> tissue (P-zones) within grafts have been shown to affect behavioural outcomes, with grafts exhibiting a greater proportion of P-zones demonstrating greater functional recovery in rats (Nakao et al., 1996). However, since these outcomes can only easily be measured post-mortem, it is hard to directly assess the progress of treatment.

### 1.5.2 Functional outcome measures

Transplantation studies in rat models have been able to utilise the large array of behavioural tests implemented and characterised for the QA model to gain proxy measures of longitudinal survival and graft-induced repair. Whilst some QA lesion-induced behavioural deficits have been reported in mice, such as amphetamine-induced rotation (Bernreuther et al., 2006), a full characterisation of the QA mouse model has not been published, consequently it is difficult to know which of the tests used in rats are the most appropriate to use in mice.

It is well established in rats that a lesion's location within the striatum impacts greatly on the degree and type of functional deficits seen (Hauber and Schmidt, 1994; Joel and Weiner, 2000; Voorn et al., 2004; Yin and Knowlton, 2006). The dorsal striatum is implicated in sensorimotor control, stimulus-response learning and habit learning (Featherstone and McDonald, 2004; Yin et al., 2004), whilst the ventral striatum, including the nucleus accumbens, is more associated with motivation and rewarded behaviours such as those

probed in the progressive ratio task (Eagle et al., 1999), with no impairment of motivation seen in rats lesioned in the dorsomedial (DMS) or dorsolateral striatum (DLS). However, the distinction between the function of the dorsal and ventral regions is blurred with some degree of cross-over between them, for example aspects of motivation have been associated with the DLS (Lelos et al., 2013). Further studies have dissected the relative contributions to different tasks of the DMS and DLS, analogous to the primate caudate and putamen respectively (Joel and Weiner, 2000). Featherstone and McDonald (2004), showed that the rats with a DLS QA lesion had a performance deficit in an operant conditional discrimination task in which they were required to make an appropriate response to a given stimulus, whereas DMS lesioned animals did not show impairment. In addition, the DLS rats completed fewer trials compared to DMS lesioned animals. Furthermore, cognitive flexibility was linked with the DMS by Ragozzino et al. (2002), who demonstrated its involvement in a reversal learning task in rats.

The disparate roles of different 'compartments' within the striatum are explained by the organisation of its efferent and afferent connections which project to and from distinct target regions. The afferent connections from the motor sensory cortex tend to form synapses within the dorsolateral striatum, whereas the pre-frontal cortex, associated with executive function, connects predominantly to the dorsomedial striatum. If lesions specific to these regions can illicit different behavioural outcomes, then it follows that grafts could demonstrate diverse types of functional recovery dependant on where they are placed.

Mid-striatal lesions in mice have shown disruption of acquisition learning and a decrease in accuracy in a serial procedural learning task (Brooks et al., 2007; Trueman et al., 2005). Although the extent of the penetration of the lesions into the DMS or DLS was not assessed, other studies have shown divergent behavioural effects of central dorsal and DMS lesioned mice (Baldan Ramsey et al., 2011).

For studies of mouse-to-mouse transplantation, lesions and grafts are typically targeted to the mid-striatum, either because this is a larger target, and/or no examination of behavioural outcome is to be performed. As a result, it is unclear as to which deficits are likely to be induced through mid-striatal lesioning, particularly as only a slight variance in the positioning of the mouse during surgery could alter the degree of medial or lateral spread of the toxin, far more so than in the larger rat model.

**There is a need to target specific regions of the striatum in order to test behavioural outcomes effectively**

Important considerations for testing functional efficacy of grafts include the need for a clear, relevant, lesion-induced behavioural deficit that can be measured and corrected. Additionally, for transplantation studies, a behavioural phenotype should maintain a consistent deficit throughout the period in which graft maturation and integration occurs, with minimal spontaneous recovery, against which graft-induced recovery can be compared. A behavioural characterisation of two QA lesion mouse models is performed and discussed in **Chapter 5**, to develop pertinent test batteries designed to probe specific deficits.

## 1.6 Aims

The experiments undertaken and presented in this thesis aim to identify the major factors influencing the poor outcomes observed when transplanting primary striatal mouse tissue into lesion mouse models of HD, and to determine how protocols could be adapted to improve results. In addition, they seek to determine if fine-tuning the lesioned models themselves can generate a behavioural test battery in which graft-induced functional recovery can be tested more precisely.

The contrast between the quality of rat-to-rat grafts and mouse-to-mouse grafts in QA lesioned models is considerable, given that the same protocols are applied to both paradigms. The first experiment seeks to identify any overt difference between the two models in their response to lesioning by comparing the effects of QA lesion protocols on the physical and inflammatory striatal environment.

The next series of experiments aims to test modifications to the host aspect of mouse transplantation protocols that could avoid the negative effects of the differences identified previously. The result of protocol manipulations designed to probe the effect of altering the length of time between lesioning and transplanting cells, and changing the strains used is examined.

Following this, the subsequent experiments aim to investigate the impact of altering aspects of the donor cell preparation protocol by manipulating the donor age and the processing treatment of the cells.

The objective of the final two experiments is to refine the targeting of the mouse QA lesions and produce an appropriate system of assessing functional recovery by defining the most apposite behavioural tests for assessing long-term graft-induced recovery.

# Chapter 2

## Methods

### 2.1 Animal models

All experiments were subject to project, personal and facilities licences and local ethical review in accordance with the United Kingdom Animals (Scientific Procedures) Act 1986.

Animals were housed under standard conditions in a 12:12 light/dark cycle with lights on between 6am and 6pm. Temperature and humidity were maintained at  $21\pm 2$  °C and  $60\pm 1\%$  respectively. Unless otherwise stated, food and water were available *ad libitum*. Animals were left to acclimatise for at least 1 week after arriving at the facility prior to the commencement of any study.

#### Mice

##### C57BL/6J

The C57BL/6J (Charles River, UK or Harlan, Bicester, UK) mouse strain was chosen as the standard host model for the experiments described in this thesis since this is the most commonly used mouse strain in scientific research (The Jackson Laboratory, 2017). Not only do the majority of published lesion, transplantation and behavioural studies in mice use C57BL/6J mice (see **Table 1.1**), it is also the background strain most widely used for the genetic models of HD. This is an important consideration for applying any potential protocol adaptations identified through the work presented here, since the translation from QA model studies to genetic models, which are more reflective of the progressive aspects of HD, would be the most appropriate step for preclinical studies of HD transplantation.

##### Chrm4-EGFP-CD1

Chrm4-EGFP-CD1 mice (MMRRC, USA) also known as M4-BAC-GFP, are a line expressing the enhanced green fluorescent protein (EGFP) within the protein coding Cholinergic Receptor Muscarinic 4 gene (*Chrm4*). In this model, GFP is expressed specifically in mature MSNs (Döbrössy et al., 2011). This strain was chosen primarily because it was the donor used in the mouse to mouse transplantation study identified by literature review as yielding the largest

grafts, see **Table 1.1**. A further benefit of using EGFP tissue is that it enables easy identification of grafted tissue post-mortem, which is often hard to distinguish from the host parenchyma - particularly in the case of small grafts. Throughout the experiments described in this thesis, the GFP-labelled tissue was detected by immunohistochemical staining rather than through direct observation of fluorescence, which presented two benefits; it avoided problems arising from auto-fluorescent background signals, which are known to increase within perfused and damaged (lesioned) tissues, and also it improved visualisation of the relative positioning of the transplanted tissue within the host.

### CD1

CD1 mice (Harlan, Bicester, UK) were selected as a comparison strain when exploring the effects of host or donor strain on graft outcome. This strain is widely used for transplantation experiments investigating immunosuppression and tolerisation methods but much less in studies with behavioural outcome measures. It was also the strain used by the Döbrösy et al., (2011) study which yielded the largest grafts.

### Rats

#### Lister hooded

Lister Hooded rats (Charles River, UK) were used in species comparison experiments. They are a strain commonly used for behavioural rat to rat transplantation studies which demonstrate consistent positive graft outcomes.

## 2.2 Surgical procedures

### 2.2.1 Lesion surgery

Striatal lesions were generated through direct administration of the neuroexcitotoxin quinolinic acid (QA, Sigma-Aldrich, UK, P6320-4) under general anaesthetic and targeted to the mid-striatum using stereotaxic coordinates. Fresh 0.09M QA solution was prepared on the morning of each surgery session in 0.1 M phosphate-buffer solution (PBS, Thermo Fisher, UK, 10010-056, **Appendix 1**) and stored at room temperature (RT).

Animals were anaesthetised in an induction chamber using 5% isoflurane gas (Abbott, UK) in oxygen, the head shaved and a subcutaneous (s.c.) injection of meloxicam 2.5mg/kg

(Metacam, Boehringer Ingelheim, Germany) given as pain relief prior to surgery. Once transferred to a stereotaxic frame (Kopf Instruments, Germany), anaesthesia was maintained through administration of 1.5 – 3% isoflurane in a mixture of oxygen and nitrous oxide (2:1) through a nose mask. The tooth bar was set to 0mm for mice and -2.3mm for rats for flat skull positioning. Following swabbing of the surgical site with dilute povidone-iodine solution (Ecolab, UK) and 70% ETOH solution, the skull was exposed, and a small hole drilled at the anterior-posterior (AP) and medio-lateral (ML) stereotaxic coordinates described in **Table 2.1**.

A 30-gauge stainless steel cannula attached to a 10 $\mu$ l microvolume syringe (SGE Analytical Sciences, Thermo Fisher, UK, 2035) driven by a mechanical pump was used to inject 0.75 $\mu$ l of QA per site. The QA was infused over 6 min and the cannula left in position for a further 3 min to prevent back flow of solution. The cannula was removed, and the incision closed using Vicryl dissolvable sutures (5-0 for mice, and 4-0 for rats, Ethicon, UK). 0.9% glucose saline (Baxter, UK, FKE1323) was administered subcutaneously during surgery to reduce dehydration (0.5ml for mice, 5ml for rats) and a 7.5mg/kg intramuscular injection of diazepam (Hameln Pharmaceuticals Ltd, UK) given at the end of anaesthetic to prevent seizures. Animals were placed into a warm recovery chamber for 2-3 hours until completely awake and returned to clean cages. Daily health checks were performed, and additional wet mash of standard food was placed in the cages for at least three days post-surgery.

Species		TB	AP	ML	DV
Mouse		-0.0	+0.8	-2.0	-3.0
Rat	Site 1	-2.3	-0.4	-3.4	-4.0 and -4.5
	Site 2	-2.3	+1.4	-2.8	-4.0 and -4.5

**Table 2.1** Stereotaxic coordinates (in mm) used for standard QA lesions in the mouse and rat. TB = tooth bar, AP = anterior-posterior, ML = mediolateral, DV = dorsoventral (as measured from dura).

### 2.2.2 Preparation of tissue for transplantation

Pregnant Chrm4-EGFP-CD1 mice of gestation age E14 were killed by cervical dislocation and the uterine horns collected into Hank's Balanced Salt Solution (HBSS, Gibco, UK). Embryos

were removed and the brains and both WGEs were dissected, as described in **Figure 2.1**, using a microscope under a laminar flow hood.

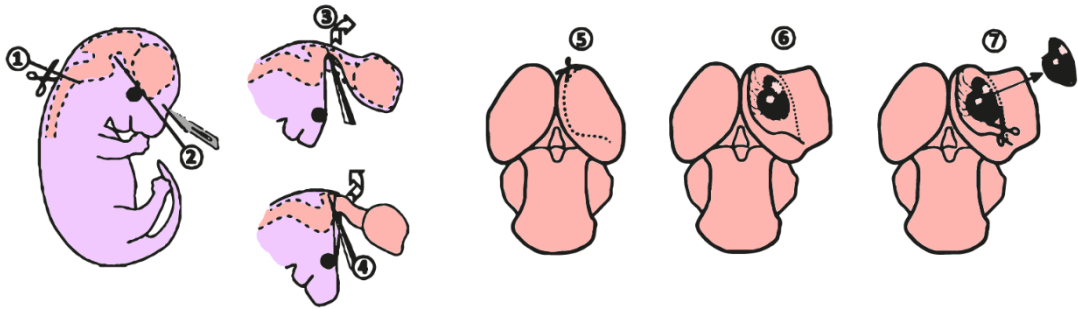


**Figure 2.1** Diagram depicting the dissection of WGE tissue. 1. Embryo is killed via decapitation. 2. A cut is made at the base of the brain, just above the eye towards the back of the head. 3. The skin and meninges are removed carefully from around the brain. 4. The brain is prised forward and pinched off at the base. 5. With the brain positioned dorsal surface upwards, a cut is made through the medial cortex. 6. The medial cortex flap is folded over to expose the WGE on the floor of the lateral ventricle. 7. WGE is removed with a lateral cut. Adapted from Dunnett & Björklund (2000).

WGE tissue was incubated at 37°C for 10mins in 0.1% bovine trypsin (Worthington, New Jersey, USA) + 0.05% DNase (Sigma-Aldrich, UK) in Dulbecco's Modified Eagle Medium (DMEM/F12, Invitrogen, UK). 0.01% bovine trypsin inhibitor (Sigma-Aldrich, UK) was added for an additional 5mins, before washing with direct addition of DMEM/F12 and centrifugation for 3mins at 1000rpm (\*). The resulting pellets were re-suspended in DMEM/F12 and triturated using a Gilson pipette with a 200µl tip to mechanically dissociate the cells into a single cell suspension. Cell number and viability were determined by trypan blue (0.4% trypan blue solution, Sigma) exclusion counting using a haemocytometer, as described below. Cell suspensions were transplanted only if viability was greater than 80%. Cells were concentrated at 150,000 cells/µl for transplantation in DMEM/F12. All suspensions were kept at room temperature and in the dark to minimise potential risks of light exposure decreasing the strength of the GFP signal.

For **Experiment 4** where tissue pieces were transplanted, the same procedure as described above was followed up until \*, whereby mechanical dissociation was forgone, and the tissue transferred directly to 4µl DMEM/F12 ready for transplantation.

### Trypan blue exclusion counting

10µl of cell suspension was diluted 1:125 with DMEM/F12 and then 1:1 with trypan blue (a total dilution factor of 500) before being transferred to a haemocytometer and viewed under a microscope. The total number of living and dead cells within five squares of the haemocytometer were counted (see **Figure 2.2**) and the number of cells per µl was estimated using the following formula: **Cells µl<sup>-1</sup> = (Cells counted / 5) x dilution factor x 10**.

Cell suspension viability was calculated using the following formula: **Viability (%) = Total live cells counted / (total live + dead cells counted) x 100**

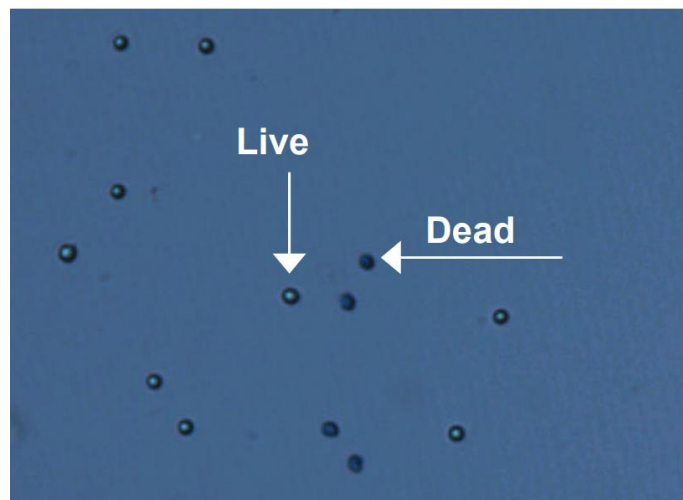


**Figure 2.2** Image depicting live and dead cells stained with trypan blue. Live cells have a bright centre and dark edges, whilst dead cells are dark throughout.

### 2.2.3 Transplantation surgery

After a post-lesion recovery time of 7 – 10 days, mice were anaesthetised (as described above) to receive unilateral transplantations into the lesioned striatum. 2 µl of suspension was injected over two depths (DV: -3.2 mm & -2.8 mm) using an SGE syringe, at the same AP and ML coordinates as the QA injection (AP: +0.8 mm, ML: -0.2 mm), depositing approximately 300,000 cells in total into the lesioned striatum over 2 min (1 µl/min). The syringe was manually depressed by gentle tapping of the plunger periodically. The syringe was left in situ for an additional 3 min to allow diffusion and reduce backflow of suspension, before being slowly removed, and the skin sutured as above. Animals were allowed to recover fully before returning to a clean home cage.

## 2.3 Histological techniques

### 2.3.1 Perfusion and sectioning

Animals received a terminal intraperitoneal injection of sodium pentobarbital (Euthatal) (0.3 ml for mice, 1 ml for rats), and were transcardially perfused with a prewash of 0.1M phosphate buffered solution (PBS, pH7.3) for 2 minutes using a peristaltic pump (set at 30.4mlmin<sup>-1</sup> for mice and 50mlmin<sup>-1</sup> for rats), immediately proceeded by 4% paraformaldehyde solution (PFA, pH7.3, Fisher Scientific, Loughborough UK, **Appendix 1**) for 5mins at the same rate. Brains were removed, post-fixed in 4% PFA for 4hrs and transferred to 25% sucrose solution in PBS (**Appendix 1**) for at least 48hrs.

A freezing-stage microtome was used to coronally section the brains at 40µm thickness. Sections were stored as 1:12 series in anti-freeze at -20°C.

### 2.3.2 Cresyl Violet staining

Tris buffered saline (TBS, pH7.4, **Appendix 1**) was used to wash brain sections (1:12 or 1:6 series) and mount onto microscope slides double-subbed with 1% gelatine. Slides were allowed to dry before being passed through the series of solutions (see **Table 2.2**), at room temperature (RT) and cover slipped using DPX mountant (Fisher Scientific, UK, 12658646).

Solution	Duration
70% ethanol	5 mins
95% ethanol	5 mins
100% ethanol	5 mins
1:1 chloroform ethanol	20 mins
100% ethanol	5 mins
95% ethanol	5 mins
70% ethanol	5 mins
Distilled water	5 mins
Cresyl Violet solution*	5 mins
Distilled water	5 mins
70% ethanol	5 mins
95% ethanol	5 mins
2.5% acetic acid in 95% ethanol	2-5 mins (until desired staining obtained)
95% ethanol	5 mins
100% ethanol	5 mins
Xylene	5 mins

**Table 2.2** Summarized protocol for Cresyl Violet staining. \*Recipe for Cresyl Violet solution is listed in **Appendix 1**.

### 2.3.3 Immunohistochemistry on free-floating sections

Tris buffered saline (TBS, pH7.4, **Appendix 1**) was used to wash brain sections (1:12 or 1:6 series) before undergoing the basic protocol for immunohistochemical staining of tissue listed in **Table 2.3**. The specific primary and secondary antibodies and associated blocking agents and concentrations are listed in **Appendix 2**.

Solution	Duration
TBS wash	10 mins x 2
Quench	5 mins
TBS wash	10 mins x 3
Block (3% ns* in TXTBS)	1 hour
Primary antibody* (in 1% ns in TXTBS)	Overnight at RT, or 3 nights at 4°C
TBS wash	10 mins x 3
Secondary antibody* (in 1% ns in TBS)	3 hours
TBS wash	10 mins x 3
TNS wash	5 mins x 2
DAB solution	Until light brown
TNS wash	5 mins x 3
TBS wash	10 mins x 2

**Table 2.3** Summarized protocol for immunohistochemical staining of free-floating brain sections. Recipes and protocols for solutions are listed in **Appendix 1**. \*Specific primary and secondary antibodies and associated blocking agents and concentrations are listed in **Appendix 2**. TBS = Tris buffered saline, ns = normal serum, TXTBS = Triton X-100 in TBS, TNS = Tris non-saline.

Following staining, the tissue sections were mounted on microscope slides double-subbed in 1% gelatine and allowed to dry. Slides were subsequently dehydrated by soaking for 5mins in 70%, then 95% and finally 100% ethanol solution before clearing in xylene and being cover-slipped with DPX mountant.

### 2.3.4 Quantification of striatal, lesion and graft volumes

Immuno-stained sections were visualised using a Leica DRMBE light microscope, Leica DFC420 camera with Leica Application Suite image analysis software.

Striatal volume and ventricle volume were calculated using a 1:6 series of Cresyl Violet stained sections. The dorsal striatal perimeter (see **Figure 2.3 A**) was traced in 5 sequentially anterior sections from ~bregma +0.00mm (or the most posterior section within which the two lateral ventricles remain distinct from each other) in the mice, and 9 anterior sections from ~bregma +0.60mm in the rats.

Volumes were calculated using the following formula: **Volume = ( $\sum a * M$ ) /  $f$** , where **a** = area ( $\mu\text{m}^2$ ), **M** = section thickness ( $\mu\text{m}$ ) and **f** = frequency of sampled sections.

Lesion and graft volumes were calculated in a similar way, by tracing DARPP-32 depleted regions within the striatum of all affected sections in a 1:6 series for lesions, and by tracing all GFP<sup>+</sup> staining in the striatum for grafts, **Figure 2.3 B & C** respectively.

### 2.3.5 Quantification of striatal and graft cell numbers

Estimates of striatal cell numbers were calculated by unbiased stereology using an Olympus C.A.S.T. grid system. A randomised sampling grid (inside the areas outlined previously) was used to position counting frames, within which all Cresyl Violet-stained cells were counted. In addition, measures of the cell diameter of 10 randomly selected cells for each animal were taken. The total number of cells within the striatal volume selected was calculated using the following formula: **Cell number =  $\sum c * (\sum A / \sum(a * n)) * f * (M / (M + D))$** , where **c** = number of cells counted, **A** = area outlined ( $\mu\text{m}^2$ ), **a** = sample frame area ( $\mu\text{m}^2$ ), **n** = number of sample frames, **f** = frequency of sampled sections, **M** = section thickness ( $\mu\text{m}$ ) and **D** = mean cell diameter ( $\mu\text{m}$ ).

The same method was used on NeuN-stained sections to calculate the number of cells within large grafts (i.e. containing approximately 1000 cells or more). For smaller grafts unbiased stereology would not yield accurate estimates and therefore cells within these grafts were manually counted directly from the microscope. In these cases, the following formula was used to estimate total grafted cell numbers: **Cell number =  $\sum c * (1 / f) * M$** .

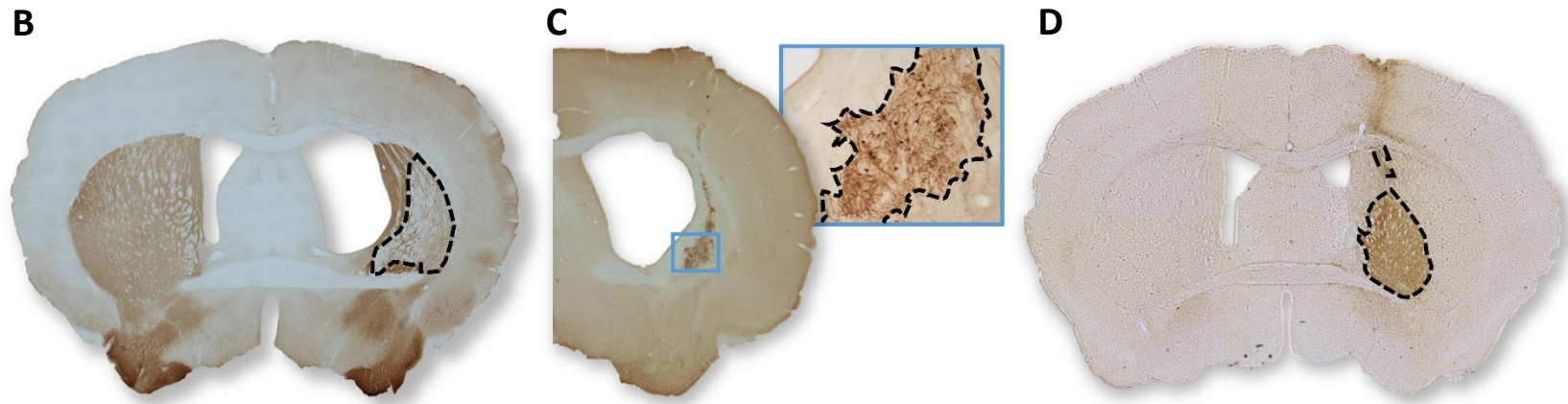
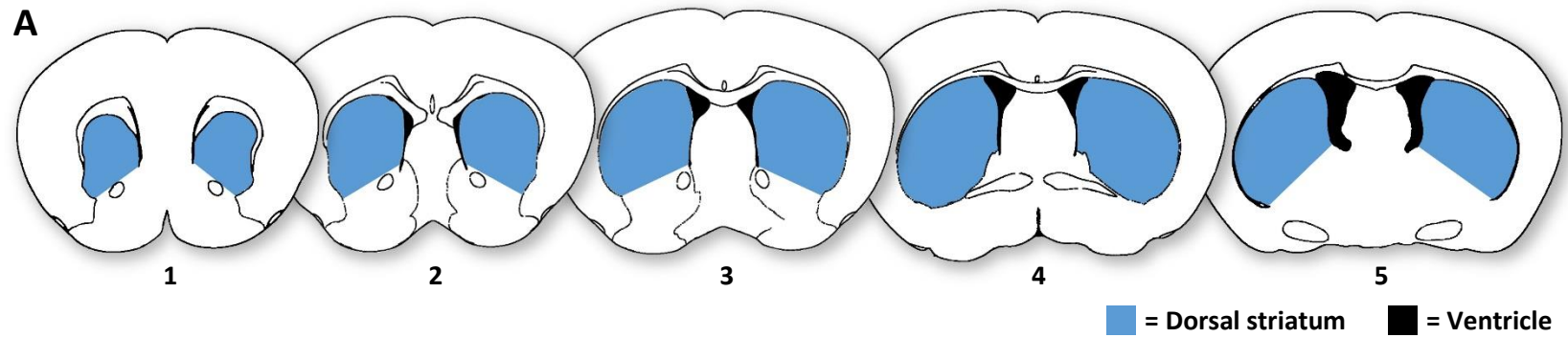


**Figure 2.3** **A** Schematic diagram (adapted from Paxinos and Franklin, 2004) to show the approximate sections from which volumetric measurements were taken, 1-5. **B** Lesioned area trace in a DARPP-32 labelled section. **C** Graft area trace in a GFP labelled section. **D** Activated microglia area trace in an Iba1 labelled section.

### 2.3.6 Quantification of host inflammatory response

The grading of the host inflammatory response was mostly focussed on the degree of microglial activation and was measured with both quantitative and semi-quantitative methods, each of which yield different benefits. A quantitative comparison of the total volume of the lesioned striatum containing dense Iba1 staining was performed in **Experiment 1** whereby clear regions of dense microglia were traced and the volume calculated in a similar way to that described for striatal volume in section 2.3.4, see **Figure 2.3 D**. This method was developed as a quick and easy way to quantify the microglial reaction where distinct regions of dense Iba1 staining are discernible. More detailed information on the quantity of infiltrating inflammatory cells was obtained through stereological counting of the microglia under higher power magnification, using the same method as for cell counting described in section 2.3.5. This provided accurate measures for microglial cell numbers and density, however, the stereological counting method is more laborious and time consuming, and as such was employed at just one critical time-point in **Experiment 1**, in addition to all groups in **Experiments 2 & 3**.

A semi-quantitative grading method was utilised in **Experiment 4**, adapted from Duan et al. (1995), whereby all sections from an Iba1 labelled series were categorised into grades ranging from 0 to 4 according to the degree of microglial activity observed, **Figure 2.4**. While this method is the simplest, it is the most open to subjectivity of the assessor, and therefore a random selection of sections was blindly evaluated by a second assessor to validate the sample categorisation. Despite the increased potential for subjective variation, it was found that the grading system was highly consistent.

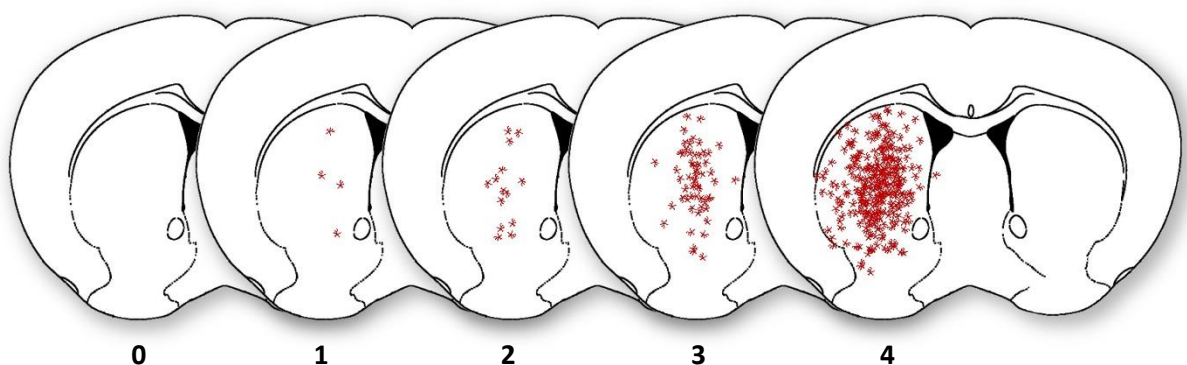


**Figure 2.4** Schematic diagram to represent the five grades of the microglial activation scale adapted from Duan et al. (1995). (0) No specific activated microglia in the graft area; (1) Low number of activated microglia, distributed as scattered single cells or clustered in a few small patches in or around the graft; (2) Several activated microglia distributed as single cells or clustered in multiple, prominent patches; (3) Dense immunostaining of the graft area and a large number of activated microglia in and around the graft; (4) Very dense immunostaining of the whole graft area and a very large number of activated microglia in and around the graft.

## 2.4 Cell culture procedures

### 2.4.1 *In Vitro* cell culture

For experiments in which cell suspensions were to be cultured *in vitro*, the cells were prepared as if for transplantation, as described in section 2.2.2. However, at the final stage, the cells were re-suspended in neuronal differentiation media (DMEM/F12 + 1% foetal calf serum + 2% B27 + streptomycin) and 30µl of cell suspension containing approximately 100,000 cells was transferred onto poly-L-lysine treated coverslips within a 24-well plate. After 1hr settling time, the wells were flooded with 500µl of differentiation media, and incubated at 37°C in humidified 5% CO<sub>2</sub> and 95% atmospheric air. Differentiation media was refreshed after 3 days in culture by removing half of the medium and pipetting 500µl of fresh media prepared at the same concentration described above. After 24 hrs or 7 days *in vitro*, 12 wells of each suspension were fixed with 4% PFA for 15mins, then washed three times in 1 x PBS (Phosphate buffered saline, pH7.4) before being stored at 4°C in PBS until immunocytochemical staining.

### 2.4.2 Immunocytochemistry

PBS was used to wash cultured cells before undergoing the basic protocol for immunocytochemical staining of cells listed in Table 2.4. The specific primary and secondary antibodies and associated blocking agents and concentrations are listed in Appendix 2. Following staining, the coverslips were mounted onto microscope slides using aqueous mountant, sealed with clear nail varnish and stored in the dark at 4°C.

### 2.4.3 Quantification

Labelled cells were imaged using AxioVision software with a Carl Zeiss fluorescent microscope. Positive immunolabelled cells were counted over five fields of view at 20x magnification, and percentages were calculated based on counts of live cells staining positive for Hoechst.

Solution	Duration
Quench/permeabilization (100% ethanol)	2 mins
PBS wash	x 3
Block (3% BSA + 1% serum in PBST)	1 hour at RT
Primary antibody* (in 1% BSA + 1% horse serum in PBST)	Overnight at 4°C
PBST wash	x 3
Fluorescent secondary antibody* (in PBS)	2 hours at RT in dark
PBS wash	x 3
Hoechst counterstain (1:10,000)	5 mins
PBS wash	x 3

**Table 2.4** Summarized protocol for immunocytochemical staining of fixed cultured cells. Recipes and protocols for solutions are listed in **Appendix 1**. \*Specific primary and secondary antibodies and associated blocking agents and concentrations are listed in **Appendix 2**. PBS = Phosphate buffered saline, PBST = 0.3% Triton X-100 in PBS.

## 2.5 Behavioural testing

### 2.5.1 Food and water restriction

For tests requiring motivation for a food reward, mice were maintained on either food- or water-restriction to maximise response levels depending on the task.

#### **Food restriction protocol**

Food was removed from the home cages and a once-daily schedule of food delivery was established. Mice were weighed daily, and the amount of food provided per mouse was reduced incrementally from excess (~3.5g) until a bodyweight of ~90% of free-feeding weight was reached. Mice were then fed as to maintain their weight between 85 and 90% for the duration of the testing period.

#### **Water restriction protocol**

A water restriction regime was implemented over the course of 5 days, with bottles removed from home cages for incrementally longer periods until access was restricted to 3hrs (2pm – 5pm) each day. Mice were weighed daily during the implementation period and weekly thereafter for the duration of the testing period.

### 2.5.2 Motor tests

#### **i) Locomotor activity**

Locomotor activity was measured by recording the movement of animals over a 32hr period. Movement was quantified by automated counting of the number of crosses per hour through infrared beams traversing a cage.

Equipment and set-up:

- A 4 x 4 rack of clear plastic cages each measuring 22 x 38 x 19cm (W x L x H), with a clear plastic lid perforated with air holes and 3 parallel infrared beams passing across the floor of each cage spaced 10cm apart.
- MED-PC IV software to record whenever a mouse within the cage crosses through an infrared beam.

- Enough lamps to light the room (angled away from the mice), set on a timer to replicate standard holding room conditions (i.e. on at 6am, off at 6pm).
- Standard food crushed to a powder placed on the floor at the end of each cage, ensuring that pieces are small enough not to disturb the infrared beams, and a drinking bottle of fresh water at the opposite end.

Protocol:

Mice were placed into the cages at approximately midday on the day of testing, thus allowing 6 hrs acclimatisation time before commencement of the dark phase of the light cycle. The total number of non-consecutive beam-breaks made during each 12hr light and dark phases were calculated.

### ii) Open field exploration test

Behaviour within an open field arena was used to explore general motor performance, as well as anxiety-related thigmotaxic behaviour.

Equipment and set-up:

- 80 x 80cm arena with white laminated wooden base and plastic walls.
- The arena is divided by a 4 x 4 grid, creating an inner square zone of 40 x 40cm at the centre, and a peripheral zone of width 20cm around the perimeter.
- Overhead camera connected to a PC running Ethovision software (Version 2.3.19, Noldus Information Technology, The Netherlands)).
- Dimly lit room.

Protocol:

The arena was cleaned with 70% ethanol and allowed to dry. Mice were placed into the arena in cage groups for a habituation period of 5mins. The following day each mouse was placed one at a time into the centre of the arena and tracked by the software for 15mins. The distance travelled, velocity, time spent moving, rearing, turning speed (not reported) and time spent within the centre or peripheral zones were calculated.

### iii) Rotations

Lateralised imbalance of striatal neurocircuitry was assessed by automated counts of spontaneous or drug-induced rotations made by mice.

Equipment and set-up:

- 8 X 500ml glass beakers.
- Clear acrylic sheet.
- Overhead infrared camera connected to a PC running Ethovision software (Version XT10, Noldus Information Technology, The Netherlands).
- Silhouette Tracker v0.11 post hoc video analysis software<sup>1</sup> (BH software services, Cardiff, UK).
- Dimly lit room.

Protocol:

Beakers were set within the camera's field of view. Mice were tested on four occasions after receiving intraperitoneal injections of either 0.9% saline, 2.5mgkg<sup>-1</sup> amphetamine, 1mgkg<sup>-1</sup> apomorphine or 2mgkg<sup>-1</sup> apomorphine at volume of 10mlkg<sup>-1</sup>, with at least two days left in between each test. Immediately following injection, mice were placed into the beakers, covered with the acrylic sheet and recorded for 1hr. The videos were subsequently processed using the Silhouette Tracking software<sup>§</sup> and the NET number of rotations per min calculated.

Assessment of activity levels over the 1hr period determined the peak period of drug activity. As such, the mean number of rotations were taken between 25 – 45mins post-injection for the spontaneous (saline) and amphetamine probes, and between 5 – 25mins post-injection for the apomorphine probes.

**iv) Gait analysis**

Changes in gait were assessed through stride length, fore and hind base width and the overlap of fore and hind paws by measurements of footprint tracks.

Equipment and set-up:

- Acrylic corridor 5 x 60 x 15cm (W x L x H) with a dark hide box at one end.
- Child-safe paints (red and blue).
- Small paintbrush.
- White paper cut to fit corridor base.
- Sharp pencil and ruler.

---

<sup>§</sup> Silhouette Tracker is custom-built software designed to track changes in orientation of rodents from pre-recorded video files frame by frame. Data was transformed to provide the NET number of clockwise and anticlockwise rotations per minute per animal. The software also provides a video file displaying the traced outline of each animal and associated cumulative counts, thus allowing for manual validation of the counts. Available from BH software services (benhavell@gmail.com).

**Protocol:**

The corridor was lined with white paper and the hide box with absorbent paper (blue roll). Prior to testing, each mouse was placed directly into the hide for 10secs before being removed and placed in the corridor just in front of the hide entrance and allowed to re-enter the hide for 10secs. The mouse was removed and placed at a successively further distance from the hide and allowed to return until it would run the entire length of the corridor directly to the hide. Once all mice were trained to run to the hide each was held by the scruff and a small amount of red paint applied to the forepaws and blue paint to the hind paws using a paintbrush. The mouse was then gently placed at the far end of the corridor and allowed to run to hide. Following a successful run (i.e. at least three unfaltering stride lengths) the paper was removed from the corridor and allowed to dry whilst the mouse was placed in a cage lined with wet blue roll to remove most of the remaining paint before being returned to its home cage.

Gait was analysed from the footprints by using a ruler to draw a straight line between the two most extreme digits of each paw and a line from the middle toe (hind-paws) or between the two middle toes (fore-paws) through the centre of the pad on each pawprint, **Figure 2.5 A**. A line was drawn between the intersection of these lines for each paw (i.e. left fore, right fore, left hind, right hind) for three stride-lengths (black arrows, **Figure 2.5 B**), and the mean distance taken to calculate left and right stride-length. Midway between steps, perpendicular lines were drawn across the stride-length lines at three points and the mean distance between the hind-paws and fore-paws calculated (purple and red arrows respectively, **Figure 2.5 B**). Overlap was measured as the mean distance between the lines drawn across the extreme digits of the hind- and fore-paws for three steps on each side (orange arrows, **Figure 2.5 B**).

**v) Balance beam**

Balance and motor coordination were assessed through the number of foot-slips and time to turn on the elevated balance beam.

**Equipment and set-up:**

- A 100cm long beam, 1.5cm wide at one end tapering to 0.5cm wide at the other. Wider end elevated 35cm above the base and rising to 50cm above the base at the narrower end. A dark hide box situated at the elevated narrow end of the beam. A ledge extending 5mm from the base runs the length of the beam.

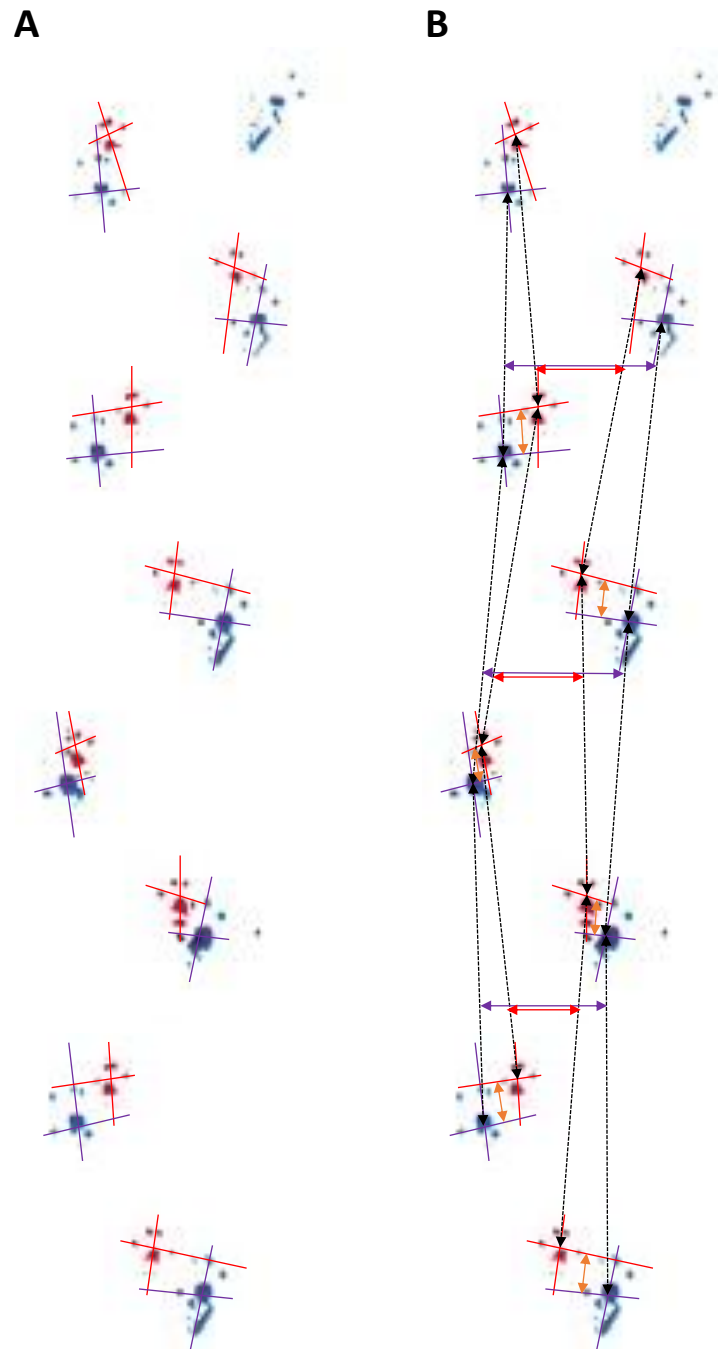


**Figure 2.5** Example of a footprint trace used for gate analysis. **A** Lines determining the centre point of each paw at the cross-section of medial-lateral and anterior-posterior bisections. **B** Lines determining the distances measured for each outcome; black arrows = stride length, purple arrows = hind base width, red arrows = fore base width and orange = overlap.

- Soft towels
- 2 x stopwatches
- 4 x clicker counters

Protocol:

The balance beam was placed on top of a trolley and a thick layer of towels placed around the base to protect mice in case of a fall from the beam. Prior to testing, each mouse was placed directly into the hide for 10secs before being removed and placed back in the home cage while the rest of the group were trained in the same way. Next, each mouse was placed on the beam, just in front of, and facing, the hide entrance and allowed to re-enter the hide for 10secs. Mice were placed at successively further distances from the hide until the entire length of the beam was run, and each time being returned to home. Finally, each mouse was placed at the far end of the beam facing away from the hide and allowed to turn and run to the hide.

Once all mice were trained, each mouse was placed in turn at the far end of the beam facing away from the hide and allowed to run to the hide. With one observer situated on each side of the beam, the first used a stopwatch to record the time taken for the mouse to turn from facing away from the hide to facing towards the hide and counted the number of times the left fore- or hind-paw slipped from the beam onto the underlying ledge during the run up the beam. Meanwhile the other observer timed the time taken for the mouse to run the length of the beam and counted the number of right fore- or hind-paw slips. This was repeated a second time with the observers swapping sides. The mean times and counts from both runs were taken as the final measure.

#### vi) Rotarod

Motor coordination was assessed by measuring the duration for which the mice could remain on the accelerating rotarod without slipping.

Equipment and set-up:

- Accelerating rotarod (Ugo Basil, Italy)
- Timer

Protocol:

Training session 1: Mice were placed onto rotarod turning at 4rpm for a total of 5mins and replaced back onto the equipment if they fell before that time.

Training session 2: Mice were placed onto the rotarod turning at 4rpm for 15secs before the speed was increased for 20secs. The rate was then held for 15secs before being increased again for a further 20secs. This was repeated for a total of 5mins. Mice were replaced onto the rotarod if they fell within the 5min period.

Training session 3 – 6: Mice were placed on the rotarod turning at 4rpm. The rate was accelerated to 44rpm max over 5mins. When a mouse fell for the first time the duration was recorded and the mouse replaced back until 5mins was completed. This was repeated daily until the duration for which they could remain on the rotarod plateaued.

Testing: Testing was performed in the same way as training sessions 3-6 but without replacement. Once a mouse fell it was returned to its home cage. Each mouse was tested twice per time-point on consecutive days, and the maximum latency to fall was used to calculate performance.

#### vii) Staircase

Custom-built staircase chambers as described by Baird et al., (2001) (Figure 2.6), were used to detect changes in skilled motor function and manual dexterity of the forelimbs.

Equipment and set-up:

- Staircase chambers
- 20mg sucrose reward pellets (5TUT, TestDiet, UK)

Protocol:

Mice were placed on a food restricted regime as described in Section 2.5.1 and sucrose pellets were introduced into home cages for 3 days prior to training.

Training session 1: (15mins) Mice were habituated to the chambers for 15mins with sucrose pellets freely available both in the chamber and on the reaching platform itself.

Training session 2: (15mins) Excess pellets placed into the staircase wells and a few along the platform

Training sessions 3-12: (15mins) Staircase wells each baited with 2 pellets

Test sessions 1-15: (30mins) Staircase wells each baited with 2 pellets.

The number of pellets remaining in each well at the end of the 30min test sessions was recorded. Data from the final five test sessions at each time-point was used in the analysis.

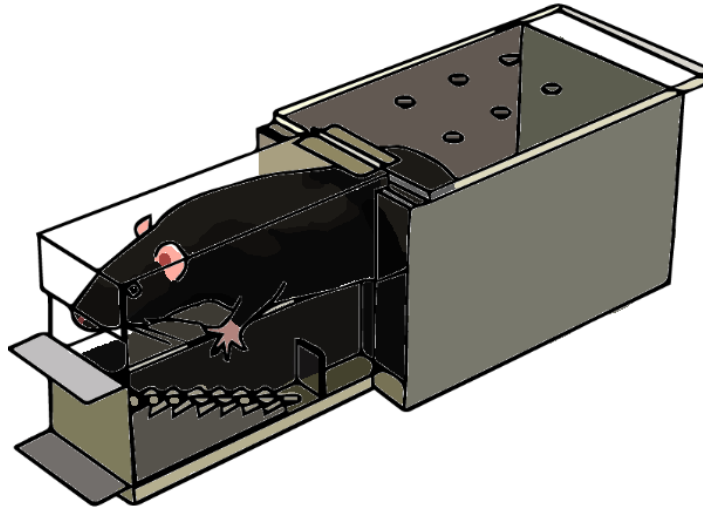


**Figure 2.6** Diagram to show a custom-built staircase chamber. Mice can only use their right paw to collect pellets from the right and their left to reach pellets from the left wells. Dropped pellets accumulate at the bottom of the stairwell.

### 2.5.3 Non-motor tests

#### i) Reward consumption

Reward value and a measure of motivation were assessed in consumption tests.

Equipment and set-up:

Sucrose consumption test:

- Clean, empty home cages with lids
- 35mm plastic petri-dish lids (430588, Appleton Woods, UK)
- Blutac
- 20mg sucrose reward pellets (5TUT, TestDiet, UK)
- Fine balance

Milkshake consumption test:

- Clean, empty home cages with lids
- 50ml falcon tubes (13065723, ThermoFisher, UK)
- Rubber bungs with drinking spouts
- Strawberry milkshake (Yazoo, Poundland, UK)
- Fine balance

Protocol:

Reward consumption was tested in four consecutive sessions following completion of rewarded behavioural tests. For each session mice were placed into an empty cage at 5pm with either ~5g of sucrose pellets in a low-rimmed petri-dish lid, or ~45ml of strawberry milkshake in a falcon tube sealed with a rubber bung with drinking spout, each weighed to an accuracy of 0.001g. At 9am the following day mice were removed, and the amount consumed was calculated by weight of the remaining reward. Consumption data used for analysis was calculated using the following formula: **Mean g consumed / mean bodyweight**.

## ii) Corridor

Lateralised bias in sensory-motor perception and neglect was assessed with the corridor test, first described by Dowd et al., (2005).

Equipment and set-up:

- 2x Opaque Acrylic corridor of dimensions 8.5 x 60 x 15cm (W x L x H)
- 40x 1.5ml microcentrifuge tube lids (TUL-800-190D, ThermoFisher)
- Strawberry milkshake (Yazoo, Poundland, UK)
- 1ml syringe
- Timer
- 2x clicker counters

Protocol:

Mice were placed on water restriction as described in [Section 2.5.1](#).

Habituation session: Animals were habituated to the equipment for 5mins with droplets of milkshake deposited randomly up and down the corridor for two sessions. Empty microcentrifuge tube lids were then fixed in pairs on either side along the length of the corridor at intervals of 5cm (see [Figure 2.7](#)) and mice left to explore for 5mins.

Test session: Immediately following habituation, mice were placed into one end of an identical corridor with ~0.1ml strawberry milkshake syringed into the lids and allowed to explore. Each time a reward was investigated by the mouse (i.e. nose into the lid) the visit was recorded as left- or right-sided, for a maximum of 20 times, or 5mins - whichever came sooner. The test was repeated on three consecutive days at each time-point and the mean number of visits for each side was used for analysis.

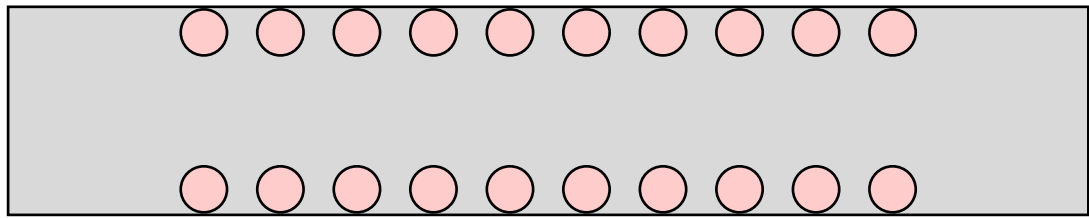


**Figure 2.7** Plan showing the distribution of lids in the corridor task.

---

### iii) Elevated plus maze

An elevated plus maze was used to measure anxiety-related behaviour.

Equipment and set-up:

- Elevated plus maze consisting of 2 'open' arms and 2 'closed' arms (6 x 42cm) enclosed by walls 1.7cm or 14.9cm in height respectively (**Figure 2.8**) and raised to a height of 72cm from the floor.
- Overhead camera connected to a PC running Ethovision software (Version 2.3.19, Noldus Information Technology, The Netherlands).
- Dimly lit room.

Protocol:

The maze was placed in the centre of the room directly beneath the overhead camera. Mice were placed in the centre of the of the plus maze and tracked for 15 minutes. The proportion of time spent and the number of entries into each arm was recorded and analysed.

---



**Figure 2.8** Image of an elevated plus maze.

---

#### iv) Spontaneous alternation

The inherent trend for rodents to spontaneously switch between left and right when exploring an environment was tested using the spontaneous alternation test.

Equipment and set-up:

- Opaque Acrylic T-maze of 12.8cm height, with a central arm (8.6 x 60cm) leading to a perpendicular pair of arms each 12.8 x 25.6cm, see **Figure 2.9**. Guillotine-style doors created an 8.6 x 10cm holding area at the end of the central arm and allowed the perpendicular arms to be closed off or opened as required.

Protocol:

Mice were placed into holding area for 10secs before the door was raised and they were allowed to explore the central arm. As soon as an arm was entered (whole body crossing into arm excluding tail) the door to the arm was lowered, holding the mouse for 20secs. The time taken for the mouse to cross into an arm and arm choice were recorded. The mouse was removed, the maze cleaned with 70% ETOH and the task immediately repeated. An entry into the opposite arm in the second trial was classed as an alternation. The test was repeated daily for three consecutive days and the proportion of alternation choices was used for analysis.

To maximise the exploratory behaviour of the mice, the context of the T-maze was altered at the second time-point by use of a different room, maze floor, wall colour and cleaning solution).



**Figure 2.9** Image of a T-maze.

### Novel object recognition

Short- and longer-term memory deficits were assessed using a novel object recognition task based on protocols adapted from McQuade et al., (2002).

Equipment and set-up:

- Acrylic arena 80 x 80cm
- 2x identical, easily cleanable objects plus 2 similarly sized but different shape and colour
- Timer

Protocol:

The mice were introduced to the arena for 10mins with two identical objects placed in opposite quadrants before being returned to their home cage. Following a 15min delay one object was replaced for a novel one of a different colour and shape but in the same position. The mice were reintroduced to the arena for 5mins and the time spent investigating each object was recorded before they were returned to their home cage. After 24hrs, the novel object was again replaced by a new novel object of different colour and shape, but same position and the mice allowed to explore for a further 5mins. The time spent on the familiar and novel objects was recorded.

### Operant tasks

Operant tests were performed in sixteen sound-attenuated automated chambers (Camden Instruments, Loughborough, UK), (**Figure 2.10**) in which mice were trained to respond to light stimuli by using their nose to poke into holes in the chamber wall. Correct responses were reinforced with strawberry milkshake (Yazoo, Poundland, UK) reward delivered into a magazine.

Operant chambers were controlled using a BehaviourNet Controller BNC MKII operating system (Camden Instruments, Loughborough, UK). The chambers of dimensions 140 x 135 x 35mm were constructed of four aluminium walls and a clear acrylic lid. One wall was curved and held an array of nine holes (**Figure 2.10 A**), each containing a bulb to illuminate the hole and an infrared sensor to detect nose entries into the hole. The opposing wall contained a magazine (**Figure 2.10 B**), also with a light bulb and infrared sensor, into which strawberry milkshake was dispensed via a peristaltic pump (**Figure 2.10 C**). Additional

holes with bulbs and sensors were located either side of the magazine (**Figure 2.10 D**), and two house-light bulbs were located at the top of the side wall panels to illuminate the chamber (**Figure 2.10 E**). Through blockading holes, different operational set-ups could be

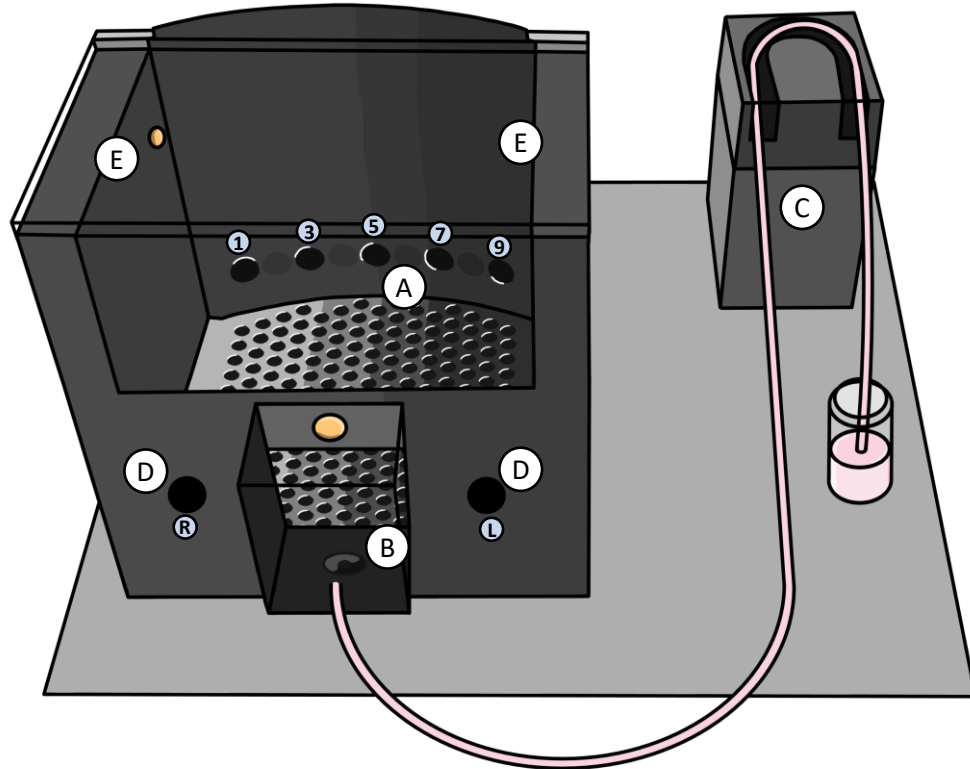


**Figure 2.10** Diagram to show an automated operant chamber. **A** 9-hole array (holes 1 -9 with holes 2, 4, 6 & 8 blockaded). **B** Reward magazine. **C** Peristaltic pump to dispense reward. **D** Nose-pokes to the left and right of the magazine (hole L and hole R respectively). **E** House lights.

applied, dependent on the task.

### General operant training

Mice were placed onto a water restriction schedule as described in **Section 2.5.1** one week prior to testing. For three days prior to introducing the mice to the operant chambers, strawberry milkshake was presented in their home cages to reduce any neophobic response to the reward.

Day 1 – Magazine training (20 minutes)

Mice were introduced to the chamber; the magazine light was illuminated and 500µl of milkshake was delivered. Mice were free to investigate and habituate to the chamber and magazine. The number of entries into the magazine was recorded.

### Day 2-3 – Magazine training (20 minutes)

Mice were introduced to the chamber; the magazine light was illuminated and 5 $\mu$ l of milkshake was delivered. Once the mouse entered the magazine to collect the milkshake its light would be extinguished. Upon leaving the magazine a 5sec inter-trial interval (ITI) began during which no lights were illuminated. Following the ITI the magazine light would once again be illuminated and a 5 $\mu$ l reward delivered. The number of magazine entries was recorded.

### Day 4-7 – Hole poke training (20 minutes)

Mice were trained to poke into the illuminated holes using a fixed ratio response program. Initially hole 5 is illuminated (for the delayed alternation task substitute ‘hole 5’ for ‘holes L and R’). The mouse is required to make a response into the hole, upon which the light is extinguished, the magazine light illuminated and a 5 $\mu$ l reward delivered. Upon collection of the reward, all lights are extinguished followed by an ITI of 5secs after which a new trial would begin, with hole 5 illuminated again. To encourage the mice to explore the illuminated hole, milkshake was painted around and into the back of hole 5. Once mice began initiating hole pokes by themselves no further ‘painting’ was needed. Initial training was considered complete once a minimum of fifty trials per session was attained. Once all mice were achieving the required level of responses, the whole group were moved on to specific tasks, as described below.

#### v) **Bilateral lateralised choice reaction time task**

Set-up: All holes were blockaded with the exception of the centre hole (5) of the nine-hole array, and one hole either side of the centre (3 and 7) which were left open, as illustrated in **Appendix 3 Figure 1**.

Training: After a 5sec delay, hole 5 was illuminated (S1). The mice were required to respond in hole 5, upon which the light would be extinguished and either hole 3 or hole 7 would light up (S2). Upon making a second response in the appropriate (i.e. illuminated) hole, that light would be extinguished, the magazine light would come on and a reward delivered. Following collection of the reward all lights were extinguished for an inter-trial interval (ITI) of 2secs before the next trial began. A response into the incorrect (i.e. unilluminated) hole for S2 would cause a time-out (TO) period of 5secs in which all hole and magazine lights were extinguished, and the house light illuminated. The task parameters would initially be set at a

simple level and gradually increased until enough responses were made at the testing standard (see **Appendix 3 Table 1**).

Testing: Mice were run for five consecutive days on test parameters and mean values taken for analysis of the following parameters; accuracy (correct/incorrect response to S2), reaction time (time taken to withdraw nose from S1 once S2 is illuminated), movement time (time taken between removing nose from S1 and poking in S2), number of usable trials (trials for which an S1 response was made), number of TO errors (number of trials for which no S2 response was made) and number of premature withdrawals (number of times that nose was removed from S1 before S2 was presented).

#### vi) Unilateral lateralised choice reaction time task

Set-up: All holes were blockaded with the exception of the centre hole (5) of the nine-hole array, and the two holes adjacent on the side contralateral to lesion (either holes 3 and 4 or holes 6 and 7 depending on the mouse being tested), as illustrated in **Appendix 3 Figure 2**.

Training: This task was performed following completion of the bilateral version described above and therefore no further training was required for this test. However, the task was changed so that the second stimulus light was pseudo-randomly presented in either 'near' (one hole adjacent to hole 5), or 'far' (two holes away from hole 5 in the same direction).

Testing: Mice were run for five consecutive days on same test parameters as for the bilateral task (**Appendix 3 Table 1**) and the following mean values taken for analysis; accuracy (correct/incorrect responses to S2 x 100), reaction time (time taken to withdraw nose from S1 once S2 is illuminated), movement time (time taken between removing nose from S1 and poking in S2), number of usable trials (trials for which an S1 response was made), number of TO errors (number of trials for which no S2 response was made) and number of premature withdrawals (number of times that nose was removed from S1 before S2 was presented).

#### vii) Delayed alternation

Set-up: All holes were blockaded with the exception of the left (L) and right (R) holes either side of the magazine which were left open, as illustrated in **Appendix 3 Figure 3**.

Training: At the start of each session the mice were presented with both L and R stimulus lights which remained illuminated until a response was made in either hole, at which time both were extinguished, and the magazine light illuminated. Following a response to the magazine a delay timer was started with a duration 'X' (listed in **Appendix 3 Table 2**), after

which both L and R stimuli were illuminated again. The mouse must poke in the opposite hole to that of the previous response in order to receive the reward. Following collection of the reward the next trial was initiated and the delay timer started again. If an incorrect response was made (i.e. into the same hole as the previous response), or no response was made, all lights were extinguished for a TO period of 2secs before both stimuli were re-presented. Initially the delay values were set to 0sec until the mice were able to perform the test to an accuracy of 85%, after which they were moved to the next stage of training. After having reached the final stage of training (delay times from 0 up to 10secs) and performance was ~85% at the shortest delays and ~50% at the longest delays, the mice were tested for a further five days.

Testing: The mean of the final five days testing values were taken for analysis of the following; total accuracy (total correct/total incorrect responses x 100), number of usable trials (number of trials in which a response was made before a time out was initiated), accuracy at each delay (correct/incorrect x 100) and reaction time (time taken to respond to the stimuli once presented).

#### viii) Five-choice serial reaction time task

Set-up: All holes were blockaded with the exception of the holes 1, 3, 5, 7, and 9 of the nine-hole array, as illustrated in **Appendix 3 Figure 4**.

Training: Mice were presented with a 10sec stimulus light in a randomly selected open hole. If a correct response was made (into the stimulus hole) within 10secs, a 50 $\mu$ l reward was delivered. Once the reward was collected, all lights were extinguished for the duration of a 2sec inter-trial interval, after which the next trial was started. If an incorrect response (poking into an unlit hole) or no response was made within 10secs, a TO period of 5secs was initiated whereby the house light would turn on and all other lights were extinguished. Following the TO period, the next trial would begin. After ten sessions at 10secs, the presentation of the stimulus light was reduced to 2secs for a further ten sessions, followed by a further reduction to 0.5secs. The time given before a TO was initiated remained at 10secs throughout the task.

Testing: The mean values of the final five days at each stimulus length were taken for analysis of the following; accuracy (correct/incorrect x100), response time (time taken to correctly respond to the stimulus), number of time outs (no response made during 10secs after stimulus presented), usable trials (trials in which a response was made). Following

completion of the tests, the mice were run on a one-session distraction probe test which used the same parameters as before except that milkshake was made freely available within the test chamber at all times.

# Chapter 3

## Exploring the effect of host in QA lesion models<sup>1</sup>

### 3 Chapter summary

Following a review of the literature ([Chapter 1.3.2](#)), and from observation of experiments conducted within the lab, the current most effective protocol for striatal transplantation of primary embryonic tissue in mouse to mouse models was determined to be Chrm-EGFP-CD1 donor tissue transplanted into unilaterally QA lesioned C57BL/6 hosts, seven to ten days post-lesion. The protocols use striatal progenitors of the whole ganglionic eminence (WGE) at age E14, dissected and prepared as a dissociated single-cell suspension, stored at room temperature and transplanted at a concentration of  $150,000 \text{ cell}\mu\text{l}^{-1}$  in two deposits totalling 300,000 cells.

The experiments described in this chapter compare different aspects of the host models chosen for transplantation studies in mice, and how alterations to this aspect of the protocol may improve graft outcome.

**Experiment 1** compared the C57Bl/6 mouse QA lesion model to the Lister Hooded rat model to determine if there were species specific differences which could explain the poorer graft outcomes observed in mouse studies. **Experiment 2** assessed how altering the time between lesion and transplantation might improve the quality of the resulting grafts by avoiding the post-lesion host inflammatory response. Finally, **Experiment 3** aimed to determine if the choice of mouse host and donor strains could affect graft outcome by comparing a range of strain combinations.

---

<sup>1</sup> Declaration

A subsection of rat brains were cut and stained by a visiting student Sarah Rollason as part of her student project, and a subsection of stereological counts of microglia was performed by master's student Katrin Wendrich.

## Experiment 1

### A species comparison of excitotoxic lesions

#### 3.1 Summary

The first experiment described in this chapter was designed to determine whether quinolinic acid (QA) lesions affect the physical and inflammatory environment of the striatum differently in rat and mouse brains. The aim was to identify potential explanations for the relatively poor transplantation outcomes observed in mice as compared to rats. To this end, four main questions were addressed: 1) Can we be sure the cells were transplanted into the striatum? The post-lesion collapse of the striatum may occur at an accelerated rate in the mice compared to rats, thereby reducing the accuracy of calculated transplantation coordinates and potentially resulting in mis-injection of cells. 2) Are there species differences in the density of the post-lesion striatum which could restrict the space available for transplanted cells to develop? 3) Are we transplanting at the right time? Differences in the way the striatal inflammatory environment develops post-lesion could mean that the timing of transplantation is sub-optimal in the mouse model. 4) Could differences in the intensity of inflammatory response result in a more hostile striatal environment in mice?

To address these questions, Lister Hooded rats and C57Bl/6 mice received a unilateral QA lesion and were perfused for histological analysis at time-points up to 90 days post-lesion. Immunohistochemical staining was used to assess changes in striatal and ventricular structure and inflammatory cell numbers, including measures of microglial activation and astrogliosis.

The results show that it is unlikely that cells are mis-injected in the mice due to changes in the striatal and ventricular volumes following lesioning since the transplantation co-ordinates remain well within the mid-striatum throughout the typical transplantation time window. A greater increase in cell density of the lesioned striatum was observed in the mice compared to the rat model, highlighting a difference which could potentially adversely affect cell survival in the mice. Labelling of microglia revealed that a peak inflammatory response occurs during the post-lesion time window standardly used for transplanting into the QA models, and that this inflammatory response is more exaggerated in the mouse model.

## 3.2 Introduction

### Rats and mice are different models

Historically it has been assumed that a mouse is simply smaller version of a rat, and that disease models in these species will function in a similar way to each other. However, there are clear differences in size, behaviour (Frick *et al.*, 2000) and developmental rate (Butler and Juurlink, 1987), as well as how the peripheral immune system and CNS macrophage cells respond to insult (Smialowicz, 1994; Loveless *et al.*, 2008; Wei *et al.*, 2013). Smialowicz demonstrated that following administration of the toxin 2,3,7,8-Tetrachlorodibenzo-p-dioxin, CD8+ T cell counts were reduced in mice, yet enhanced in rats. Furthermore, Loveless *et al.* showed that after toxic doses of ammonium perfluorooctanoate, mice and not rats exhibited a suppressed antibody immune response. Therefore, assumptions that the standard protocols and temporal design of lesioning and transplanting would be the same in both species warrants testing, particularly because striatal embryonic transplants into QA lesion mouse models of HD appear to survive less well, are smaller and generally more ‘pencil-like’ than those transplanted under similar conditions in rats (Watts, Dunnett and Rosser, 1997; Kelly *et al.*, 2007; Klein, Lane and Dunnett, 2013; Robertson *et al.*, 2013; Lelos *et al.*, 2016).

### Striatal collapse

Following administration of QA, the structure of the lesioned striatum changes over time, with the macrostructure of the striatum collapsing laterally due to the loss of cells, and consequently causing an increase in ventricular volume (Duan *et al.*, 1998; Shear *et al.*, 1998). As the same stereotaxic co-ordinates are utilised for both the lesion and transplantation sites, it is critical that any changes that occur before the point of transplantation do not shift the anatomical structure of the striatum away from the targeted co-ordinates and onto the ventricular space, as proposed in **Figure 3.1**.

The standard transplantation time-frame of 2 – 10 days post-lesion does not appear to interfere with cell placement in rats since most studies report near 100% presence of grafts in the striatum. However, if an increased rate of collapse were to be apparent in mice, this could provide an explanation for the reduced number of remaining grafts observed from transplants in mouse models, particularly if rapid changes were to occur around the time of

transplantation. It is also worth noting that the amount of QA used in the basic protocols (1.5 $\mu$ l total for rats (Kelly *et al.*, 2007; Precious, 2010), 0.75 $\mu$ l for mice (Brooks, Trueman and Dunnett, 2007; Döbrössy *et al.*, 2011)) equates to approximately 0.08 $\mu$ l and 0.14 $\mu$ l per mm<sup>3</sup> striatum in the rat and mouse respectively, based on the contralateral striatal volume measures described in this chapter. The higher relative amount of QA used in the mouse models could therefore exacerbate the collapse of the striatum compared to the rats, despite the dose being relatively high in comparison to that used in many rat studies (Dunnett *et al.* 2013; Watts *et al.* 2000, each 1.0 $\mu$ l), and the mouse dose being about average for mouse studies (Mazzocchi-Jones *et al.* 2011; Hargus *et al.* 2008, 0.48 $\mu$ l and 1.0 $\mu$ l respectively).

Without the use of imaging to track labelled cells post-transplantation it is not possible to confirm the fate of the cells over time *in vivo*. Instead their fate is assessed using the snapshot of time at perfusion, typically 12 weeks after transplantation. Therefore, in the absence of a graft, it is difficult to determine if there was once a graft present that had since been rejected completely, or indeed, if the cells were ever placed in the striatum in the first place. By assessing the post-lesion structure of the two models longitudinally, it is possible to determine the extent to which striatal collapse is likely to be contributing to the problem and hence if mis-injection of cells is likely.

In addition, a change in the cell density of the striatum is likely following the QA injection. The reduction in MSN cell number, influx of immune cells and the collapse of the striatum will disturb the composition of the cells at the site of transplantation (Roberts *et al.*, 1993), and this could affect the ability of transplanted cells to grow and thrive.

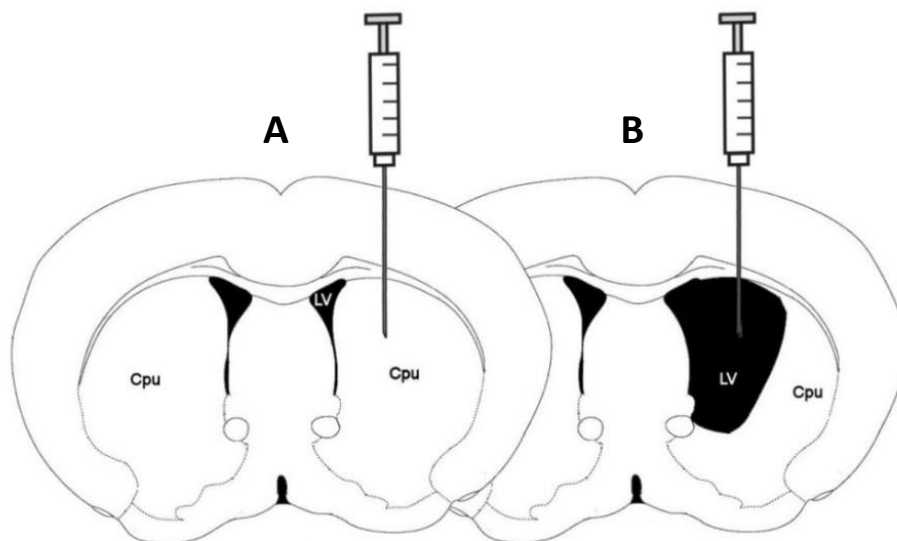


**Figure 3.1** Diagram to show how a target based on stereotaxic coordinates could change between injecting an excitotoxin **A** and injecting a cell suspension **B**. While the coordinates for the lesion are clearly in the striatum (Cpu), after the striatum has collapsed the same coordinates could deliver cells into the ventricle (LV) where they would not be effective in restoring cell loss.

## Immune response

Despite the persistence of the common perception that the brain is an immune-privileged site, there is an increasing body of evidence to counteract this idea, at least in any absolute form. Rejection of transplanted tissue and acute inflammatory responses in the brain show that, at best, the blood brain barrier is leaky, particularly following surgery or in disease states (Drouin-Ouellet *et al.*, 2015). In addition, the brain's own immune response can create a very hostile environment to foreign cells (Kraft and Harry, 2011). By injecting the QA toxin into the striatum an inflammatory response is triggered in the brain, potentially priming the environment into which vulnerable cells will be transplanted.

Differences in the way that the peripheral immune system of rats and mice deal with the same toxin have been demonstrated (Smialowicz, 1994), and the extent of response of cultured microglia to stimuli has been shown to be greater in mice than rats (Wei *et al.*, 2013). In addition, the use of immune suppression and desensitisation techniques to reduce graft rejection have been shown to be less effective in mice than rats (Robertson *et al.*, 2013). If the inflammatory response to QA is more exaggerated in mice, then it is possible that the cells are being transplanted into a more hostile environment than those in rats. In turn this could limit the survival, proliferation and integration of any potential grafts in the mouse model and exacerbate any immune response to the transplanted cells.

This study used both a rat and mouse QA lesion model of HD to track and compare the progression of morphological changes and inflammatory response around the lesioned striatum of each species. The objective was to determine if the intensity or rate of change in response to the QA lesions at the target site could offer insight into why the rat might yield a better transplantation environment than the mouse model. The study examined the progression of the lesion response longitudinally to identify a point at which the balance of factors favours a supportive rather than a hostile environment for transplanted cells.

### 3.3 Methods

#### 3.3.1 Experimental design

Male C57BL/6J mice (25-30g, n=42) and Lister Hooded rats (400-500g, n=42) (Charles River, UK) were housed under standard conditions. Animal numbers were calculated based on data from previous experiments and confirmed using sample size analysis software G\*Power. The animals were left to acclimatise for at least 1 week prior to the commencement of the study. Food and water were available at all times *ad libitum*.

Mice and rats received unilateral mid-dorsal striatal QA lesions as described in methods section 2.2.1, with the intact side acting as a within subject control. Surgeries took place over 3 days (14 animals per day). Animals were assigned to one of 7 experimental groups (n=6) per species, counterbalanced to include individuals from each surgical day to be perfused at the following post-lesion time-points: 4, 8, 12, 16, 20, 28 or 90 days (Figure 3.2). Following surgery all animals were returned to their home cages and were unhandled except for routine cleaning until the end of the experiment.

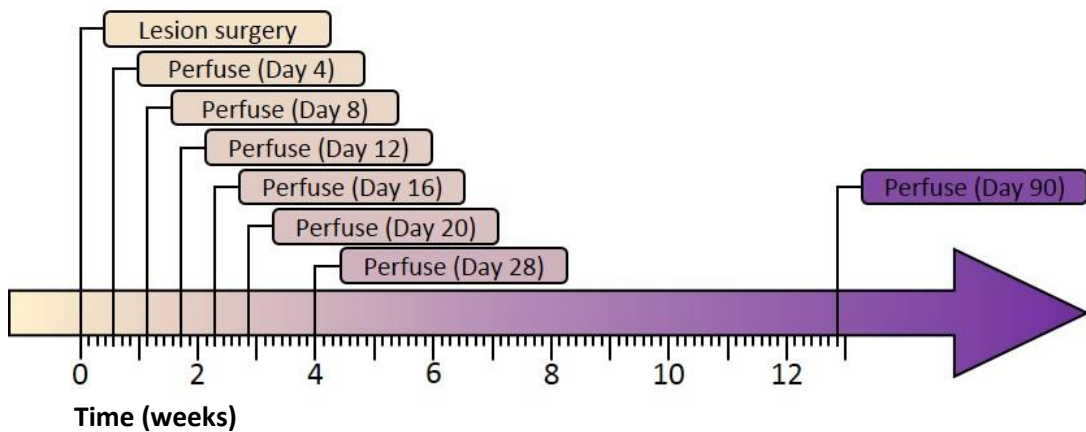


Figure 3.2 Experimental timeline indicating the progression of the experiment in weeks.

### 3.3.2 Immunohistochemical analysis of lesions

Animals were perfused, and brains were sectioned into 40µm slices as described in methods section 2.3.1. Cresyl violet staining was used to label Nissl bodies in a series of 1:6 sections. Bright-field microscopy was used to measure the striatal and ventricle areas in five sequentially anterior sections from ~bregma +0.26mm (or the most posterior section within which the two lateral ventricles remain distinct from each other) in the mice, and nine anterior sections from ~bregma +0.60mm in the rats, and the striatal and ventricle volumes calculated as described in methods section 2.3.4. The proportional change in the volume of the lesioned (ipsilateral) striatum and ventricle compared to the intact contralateral side was calculated using the following formula: **% change =  $(I_v / C_v) \times 100$** , where  $I_v$  = Ipsilateral volume and  $C_v$  = Contralateral volume.

Unbiased stereology was used to estimate the number of all Nissl<sup>+</sup> cells in each hemisphere within the area defined by the criteria above, as described in methods section 2.3.5. The proportional change in cell number of the ipsilateral striatum compared to the contralateral side was calculated using the following formula: **% change =  $(I_c / C_c) \times 100$** , where  $I_c$  = Ipsilateral cell count and  $C_c$  = Contralateral cell count. Striatal cell density in the ipsilateral side was calculated using the following formula: **Density =  $(I_c / I_v)$** . Proportional change in density of the ipsilateral side was calculated by the following formula: **% change =  $(I_c / I_v) / (C_c / C_v)$** .

To calculate mean cell diameter, one striatal cell per section (total of 210 cells for mice and 378 cells for the rats) was randomly selected and the average width of the widest and narrowest diameter recorded. To ensure that a truly random sample was taken, the unbiased random placement of the stereology counting frame was utilised, with the cell closest to the top right corner of the first counting frame per sample being selected.

Further stains of DARPP-32, Iba1 and GFAP were performed from sections of frequency 1:12 as described in [Table 3.1](#).

Lesion placement was assessed in DARPP-32 stained sections, with the lesioned area identified through ablation of positive staining within the ipsilateral striatum.

Iba1 staining of microglia was used to assess the inflammatory response to the lesion. Regions of dense staining incorporating activated microglia were measured and volumes determined in a similar method to the volumetric measures detailed above, see methods

section 2.3.6. The degree of inflammation was determined by calculating the proportion of ipsilateral striatal volume containing regions of activation by using the following formula: **% volume =  $(I_{mv} / I_v) \times 100$** , where  $I_{mv}$  = Volume of microglial activation and  $I_v$  = ipsilateral striatal volume.

Antibody	Marker for
Cresyl violet	Nissl bodies / anatomical measurements
DARPP-32	MSNs / lesion identification
Iba1	Microglia
GFAP	Astrocytes

**Table 3.1** List of immunohistochemical stains and associated targets.

Using unbiased stereology, the number of microglial cells in the ipsi- and contralateral striatum at Day 8 were calculated. The increase in microglia in the lesioned striatum was calculated using the following formula: **% increase =  $(I_{mc} / C_{mc}) \times 100$** , where  $I_{mc}$  = Ipsilateral microglia count and  $C_{mc}$  = Contralateral microglia count. Ipsilateral density of microglia cell was calculated using the following formula: **Density =  $(I_{mc} / I_v)$** , where  $I_{mc}$  = Ipsilateral microglia count and  $I_v$  = Ipsilateral striatal volume.

A measure for astrogliosis was taken using GFAP stained sections. Since the identification of individual astrocytes within the lesioned striatum was not possible, an unbiased stereology setup was utilised to quantify the response. Using a x40 objective, the number of individual fibres or cell bodies crossing into a sampling frame were counted using a setup similar to that used for cell counting. A measure of the response was then calculated using the following formula: **% increase =  $(I_{ac} / C_{ac}) \times 100$** , where  $I_{ac}$  = Ipsilateral GFAP fibre count and  $C_{ac}$  = Contralateral GFAP fibre count. GFAP fibre density was calculated using the following formula: **Density =  $(I_{ac} / I_v)$** , where  $I_{ac}$  = Ipsilateral GFAP fibre count and  $I_v$  = Ipsilateral striatal volume.

### 3.3.3 Statistical analysis

One mouse assigned to the 8-day post-lesion group died before the brain was able to be recovered leaving that group as n=5. In addition, a small number of individual sections were damaged beyond use or were only partially stained during processing, and as a result some counts were performed on a reduced group size, as indicated in the statistical figures presented.

All statistical analysis was performed using Genstat (18<sup>th</sup> edition). ANOVAs or student t-tests were performed to compare within-species experimental groups across all time-points. Sidak's post hoc pairwise comparisons were performed to analyse significant interactions, correcting for multiple comparisons. Additional analysis of data from Day 8 was undertaken separately to probe the conditions in the two species at the standard time for transplantation (7-10 days) using a t-test. Significance was taken as  $p \leq 0.05$ .

Post-hoc power analysis based on final animal numbers was calculated using G\*Power software and was estimated to be 100% for large effect sizes and 99% for medium effect sizes.

## 3.4 Results

### Lesion placement

Areas of depleted DARPP-32 staining confirmed that the mid-dorsal striatal placement of the lesions was consistent throughout the groups, **Figure 3.3 A**. Lesioned regions were less discernible in the mouse striatum at the early time-points but became more obvious by Day 12. Clear areas of lesioning were evident in the rats from the first time-point onwards. From Day 16 onward the lesions incorporated the majority of the ipsilateral striatum in both species.

### Striatal morphological changes

Measures taken from cresyl violet staining (**Figure 3.3 B**) showed that the ipsilateral striatal volume decreased over time in both species with respect to the contralateral side (Time:  $F_{6,69}=14.83$ ,  $p < 0.001$ ), **Figure 3.4 A**. The ipsilateral striatum contracted to  $58.8\% \pm 5.3$  of the contralateral side in the mice and  $61.9\% \pm 5.9$  in the rats by 90 days post-lesion. The size of the ipsilateral ventricle increased in comparison to the contralateral side in both species (Time:  $F_{6,69}=4.09$ ,  $p = 0.001$ ) with ipsilateral ventricle volume increasing by  $62\% \pm 25.2$  and  $74.2\% \pm 15.7$  in the mice and rats respectively by Day 90, **Figure 3.4 B**. It was observed that whilst the rat ipsilateral ventricle volume increased gradually from Day 8, the mouse ventricle retained its size until Day 20 when a rapid enlargement occurred (from  $\sim 100\%$  of contralateral size to  $\sim 160\%$ ). Although there was no significant statistical interaction to allow this to be tested, the change is interesting because the expansion of the ventricle seems to correspond to the perceived development of the lesion in the mouse model. However, no

difference in proportional changes in either the striatal or ventricle volume between the rat and mouse models was found, (Species:  $F_{1,69}=2.84$ , ns; and Species:  $F_{6,69}=3.47$ , ns respectively). Around the time at which transplantation would occur (Day 8) there were no differences between species in the amount of change in either striatal or ventricle volume (Day 8:  $t_9=1.55$ , ns; and Day 8:  $t_9=1.24$ , ns respectively). In addition, when the target grafting coordinates are applied to the lesioned sections, all fall within the striatum including at 90 days post-lesion (see Xs in **Figure 3.3 B**).

The relative ipsilateral neuronal cell counts reduced over time in both mouse and rat models, with no difference found between the mice and rats (Time:  $F_{6,68}=3.07$ ,  $p=0.01$ , Species:  $F_{1,68}=2.83$ , ns), **Figure 3.4 C**. There was no difference at Day 8 in the proportion of cell loss between species ( $t_8=1.21$ , ns).

The number of cells per  $\mu\text{m}^3$  in the ipsilateral striatum increased over time in both species, however the increase was greater in the mouse model compared to the rat (Time:  $F_{6,68}=7.11$ ,  $p<0.01$ , Species:  $F_{1,68}=39.40$ ,  $p<0.001$ ), **Figure 3.4 D**. Cell density was also significantly higher in the mouse model at Day 8 when compared to the rat ( $t_8=6.53$ ,  $p<0.001$ ). The proportional change in cell density of the lesioned striatum increased over time, seemingly driven by an increase at Day 90, but no difference was found between species (Time:  $F_{6,68}=2.51$ ,  $p<0.05$ , Species:  $F_{1,68}=0.20$ , ns), **Figure 3.4 E**.

There was no significant difference in Nissl<sup>+</sup> cell size between the two species ( $t_{1124}=1.63$ , ns), **Figure 3.4 F**.

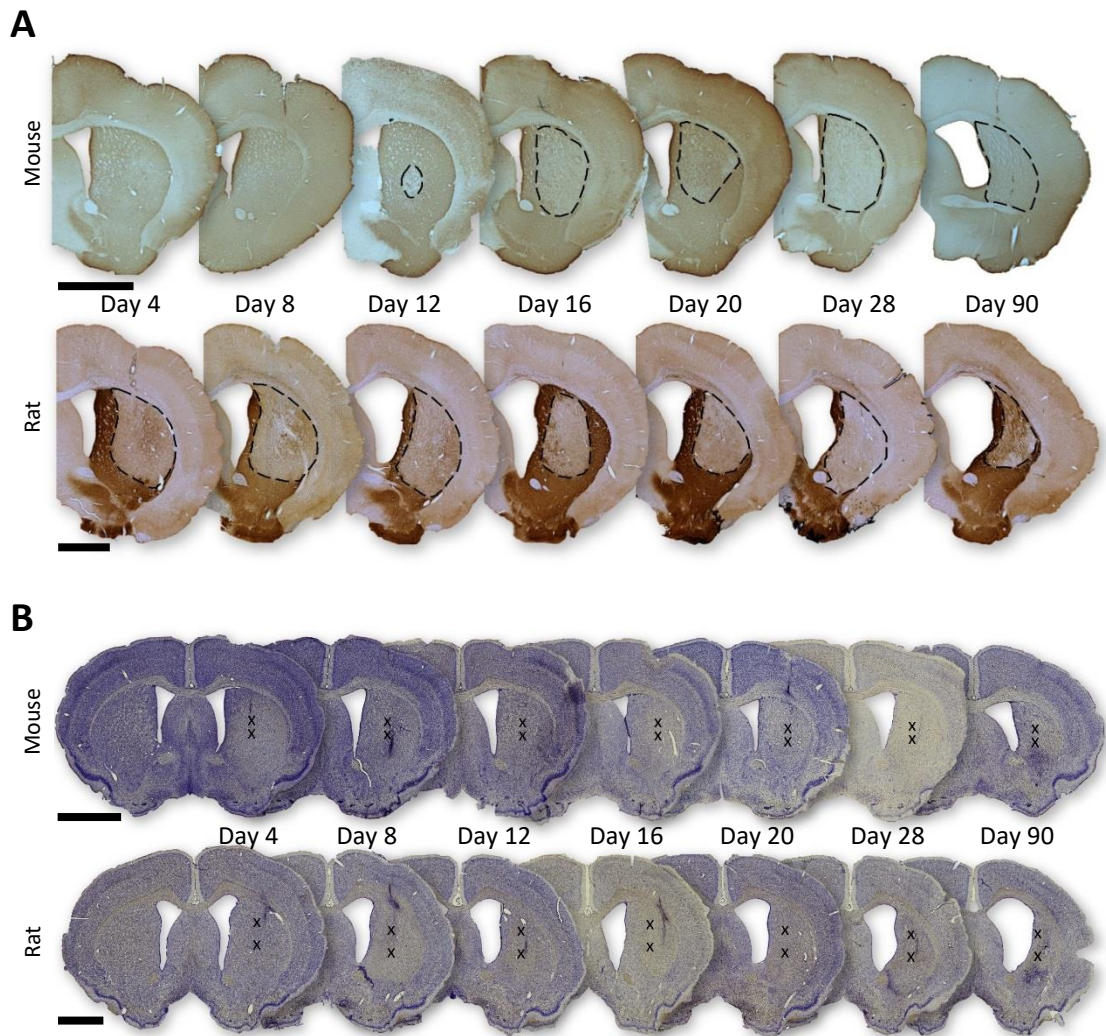


**Figure 3.3** **A** DARPP-32 staining in the mouse (top) and rat (bottom) models labelling MSNs in the ipsilateral striatum. Areas of reduced staining within the striatum (black dashed line) highlight the lesioned area. Clear lesioned regions were apparent in the mice from Day 12, and from Day 4 in the rat. Lesions developed over time to incorporate the majority of the dorsal striatum in both species. **B** Cresyl violet staining in the mouse (top) and rat (bottom) models labelling Nissl bodies in all neurons for striatal and ventricle measurements. X represents the medial-dorsal and dorso-ventral coordinates used in the grafting protocols. Scale bars represent 2mm.

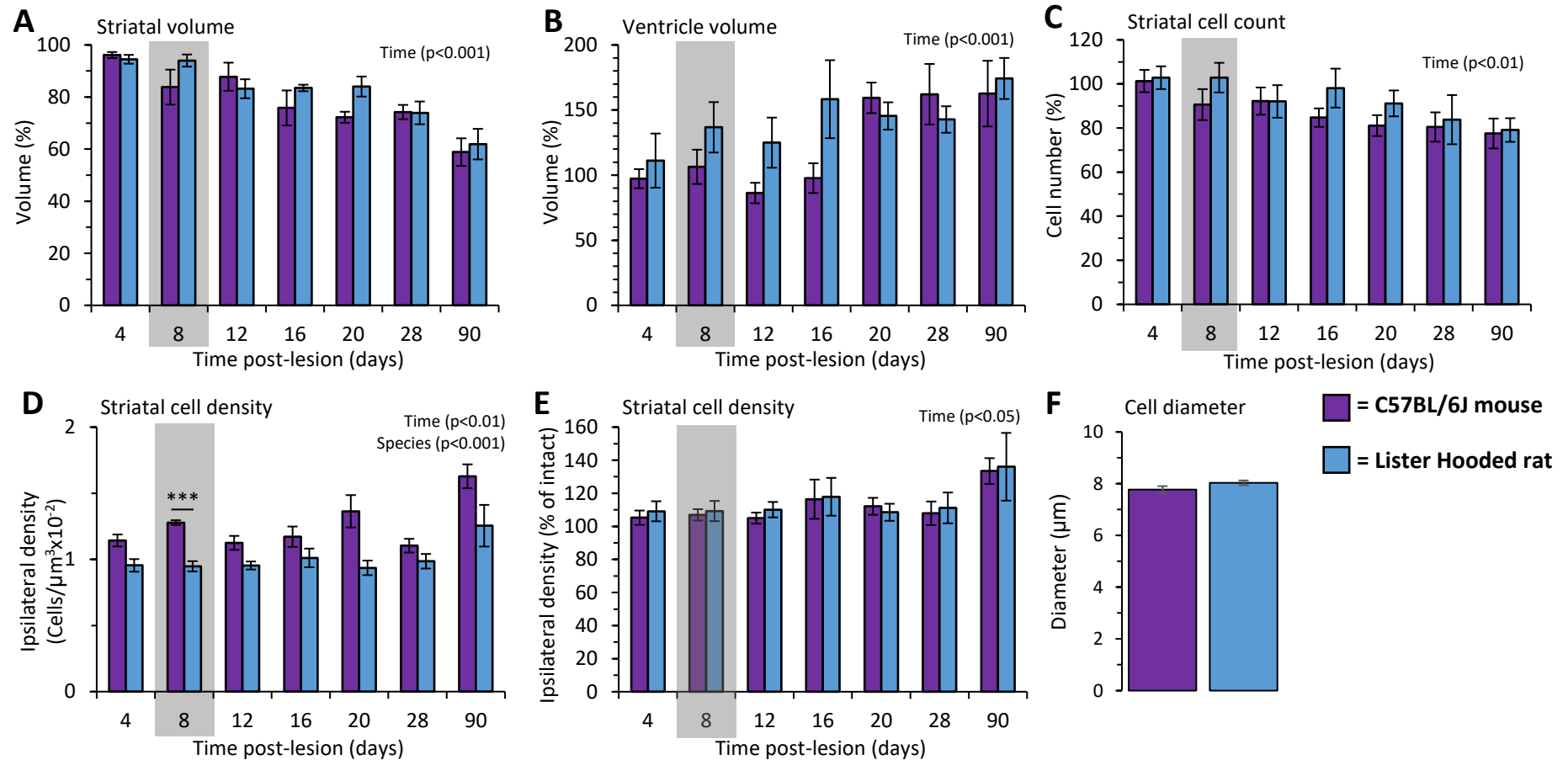


**Figure 3.4** **A** Ipsilateral striatal volume expressed as a percentage of contralateral volume. Striatal volume was reduced over time ( $p < 0.001$ ). No difference was found between species. **B** Ipsilateral ventricular volume expressed as a percentage of contralateral volume. Ventricular volume increased over time ( $p < 0.001$ ). No difference was found between species. **C** Ipsilateral striatal cell number expressed as a percentage of contralateral counts. Striatal cell number was reduced over time ( $p < 0.01$ ). No difference was found between species. **D** Ipsilateral striatal cell density. Striatal cell density increased over time ( $p < 0.01$ ) and was more dense in the mouse striatum than the rat ( $p < 0.001$ ). At day 8 the mouse striatum had a higher cell density than the rat (\*\*\*) ( $p < 0.001$ ). **E** Ipsilateral striatal cell density expressed as a percentage of contralateral density. Ipsilateral striatal density increased over time ( $p < 0.05$ ). No difference was found between species. **F** Mean striatal cell diameter. No difference was found between species. Grey shaded bars highlight representative time-point for transplantation under standard protocols. Error bars represent SEM.

### Inflammatory response to QA lesioning

Iba1 staining of microglia revealed intense staining in the lesioned striatum in both the mice and rats from the first time-point, which persisted up to 90 days post-lesion, **Figure 3.5**. Uniformly distributed microglia extending multiple branched processes were observed in the contralateral striatum (**Figure 3.6 A & B**), in contrast to the densely packed cells with retracted processes in the ipsilateral side, **Figure 3.6 C & D**.

The proportion of ipsilateral striatum containing intense staining of the activated microglia changed over time (Time:  $F_{6,67}=9.42$ ,  $p<0.001$ ). Both species exhibited a rapid increase in activated volume up to Day 8, followed by a lull and a second peak of activity at Day 16, **Figure 3.7 A**. Subsequently, inflammation tended to decrease and, though much reduced, was still present after 90 days post-lesion. A greater proportion of the striatum was incorporated in the region of inflammation in the mouse model including at Day 8 (Species:  $F_{1,67}=4.47$ ,  $p<0.05$ ; Day 8:  $t_9=2.61$ ,  $p<0.05$ ). Microglial cell counts at Day 8 showed that the number of microglia in the lesioned side, compared to the intact side, increased to a significantly higher degree in the mouse model ( $t_9=9.57$ ,  $p<0.001$ ), with ipsilateral microglial density also greatest in the mouse ( $t_9=6.31$ ,  $p<0.001$ ), **Figure 3.7 B**.

A clear difference could be seen in GFAP staining of astrocytes between the intact and lesion sides, **Figure 3.6 E-F**. Astrocytes in the contralateral striatum appeared to be more sparsely distributed, with individual cells and processes distinctly identifiable, whereas many more inter-tangled fibres could be seen in the lesioned side making it impossible to discern individual cells. It was also noticeable that the intact striatum (used as baseline) of the rats contained a greater number of astrocytes than that of the mice, **Figure 3.6 E & F**. The proportion of ipsilateral astrogliosis compared to the contralateral side, as measured by GFAP<sup>+</sup> fibre density, was increased by the greatest amount in the mice (Species:  $F_{1,68}=62.39$ ,  $p<0.001$ ), **Figure 3.7 C**. This difference was evident at Day 8 ( $t_9=2.68$ ,  $p<0.05$ ). No significant change in the proportion of astrogliosis over time was observed (Time:  $F_{6,68}=1.63$ , ns), and no difference in ipsilateral GFAP fibre density between the species was observed at Day 8 ( $t_9=1.28$ , ns). However, there was an effect of time on ipsilateral GFAP fibre density (Time:  $F_{6,68}=3.84$ ,  $p<0.01$ ), **Figure 3.7 D**. The trend of fibre density in the mice followed a similar pattern to that seen in microglial activation, with an early increase up to Day 8 followed by a dip and a second peak at Day 16 before gradually decreasing. The same measure in the rat did not follow this pattern and seemed to maintain a more constant density over time. This observation was probed through correlation analysis of GFAP fibre

density and proportion of microglial activation (**Figure 3.7 E**), which revealed a very highly significant correlation in the mice ( $r=0.95$ ,  $p<0.001$ ), however no significance was found for the rat model.

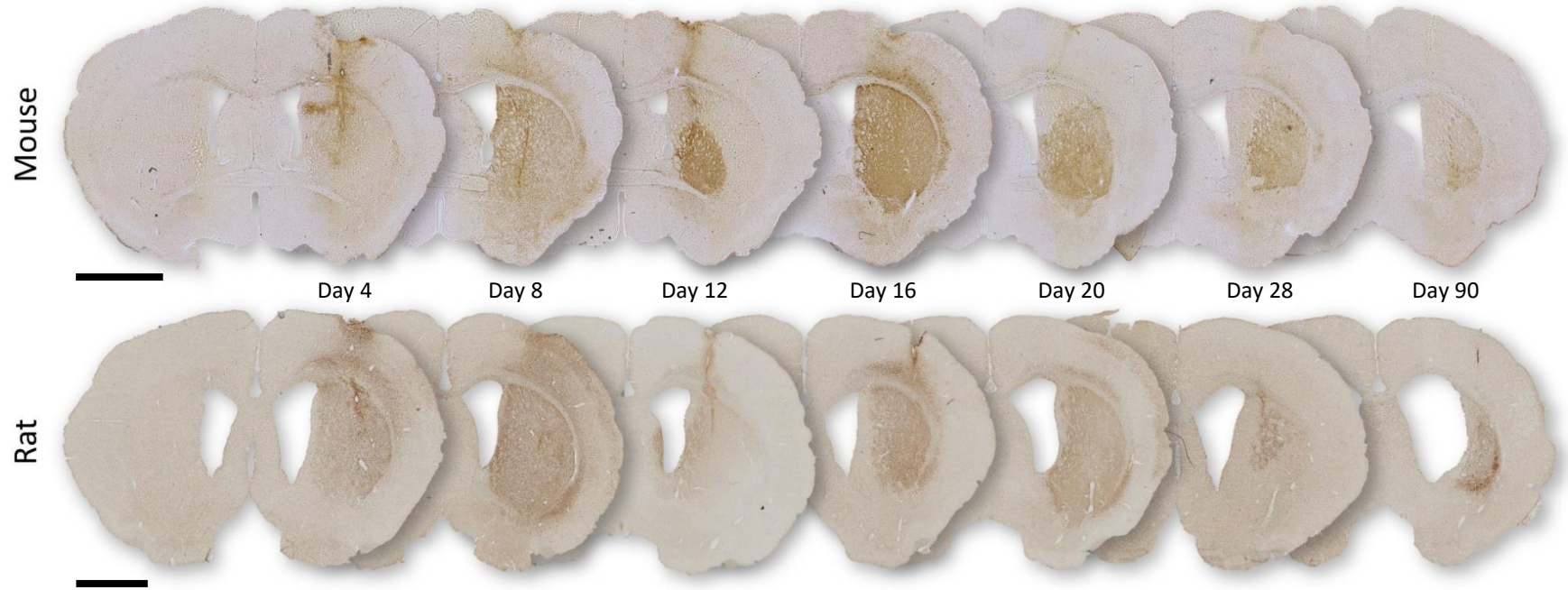


**Figure 3.5** Iba1 staining in the mouse (top) and rat (bottom) with representative examples from each time-point. Resting-state ramified microglia can be observed in the contralateral side (Day 4), with clear regions of activated microglia in the ipsilateral striatum. Scale bars represent 2mm.

---

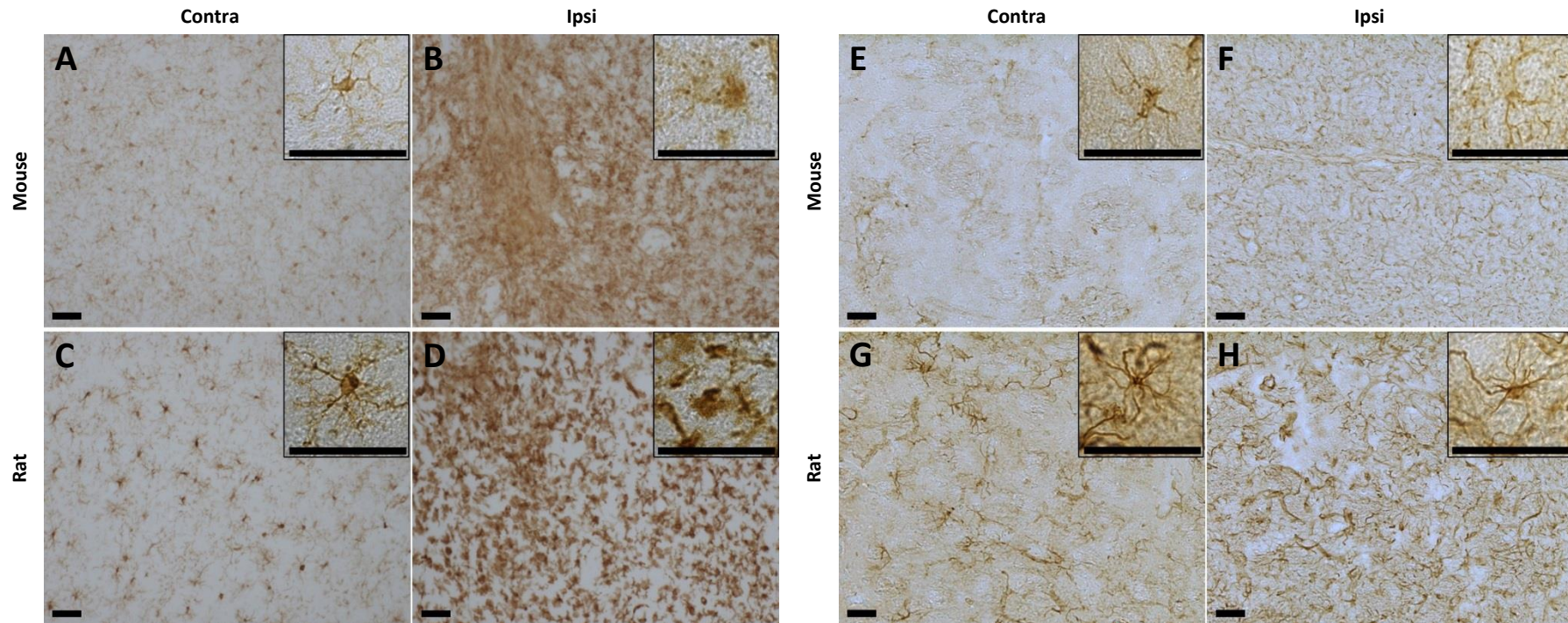


**Figure 3.6** **A & B** Iba1 staining of microglia in the contra- and ipsilateral mouse striatum respectively. **C & D** Iba1 staining of microglia in the contra- and ipsilateral rat striatum respectively. Uniformly distributed ramified microglia are seen in the contralateral side, whilst densely packed microglia with processes withdrawn are observed in the ipsilateral striatum. **E & F** GFAP staining of astrocytes in the contra- and ipsilateral mouse striatum respectively. **G & H** GFAP staining of astrocytes in the contra- and ipsilateral rat striatum respectively. Sparse cells are seen in contralateral mouse striatum, with more observed in the rat model, each with multiple long processes. On the ipsilateral side the staining is denser, with an increased number of fibres and shorter processes. All images taken from Day 8 post-lesion group. Main pictures x10 magnification, inset pictures x40 magnification. Black scale bars represent 50 $\mu$ m.

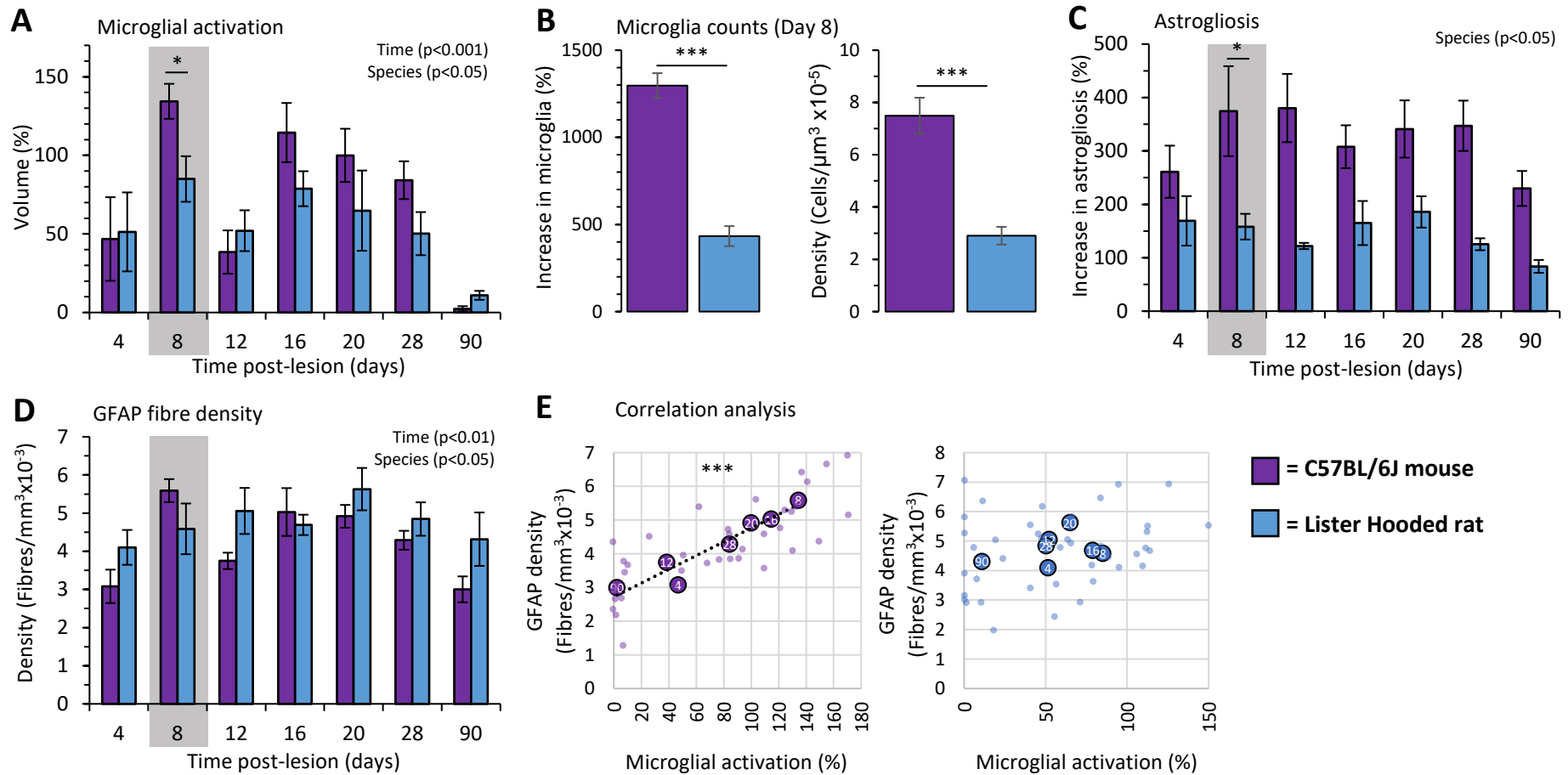


**Figure 3.7** **A** Ipsilateral volume of activated microglia expressed as a percentage of total ipsilateral striatal volume. The percentage volume of activated microglia was higher in the mouse than the rat ( $p < 0.05$ ). At day 8 the mice had a significantly higher percentage volume of activated microglia ( $* p < 0.05$ ). A main effect of time was observed ( $p < 0.001$ ). A biphasic peak was observed in both species first at day 8, then again at day 16. **B** Microglia counts from Day 8 time-point presented as a proportion of ipsilateral compared to contralateral counts, and density of microglia in the ipsilateral striatum. There was a greater increase in microglia number in the mouse model than the rat ( $*** p < 0.001$ ) and density of microglia cells was greatest in the mouse ( $*** p < 0.001$ ). **C** Increase in astroglialosis presented as the proportion of ipsilateral compared to contralateral fibre counts. The increase in astroglialosis was greater in the mouse model ( $p < 0.05$ ). At day 8 the mice had a significantly higher percentage increase in astroglialosis ( $* p < 0.05$ ). **D** Density of GFAP<sup>+</sup> fibres in the ipsilateral striatum. Fibre density was greatest in the rat model ( $p < 0.05$ ). A main effect of time was observed ( $p < 0.01$ ). **E** GFAP<sup>+</sup> fibre density plotted against proportion of microglial activation for the mouse (purple) and rat (blue) models. Small dots represent individual animals. Large dots represent the group mean with the post-lesion time-point labelled in white. There was a significant correlation between the GFAP fibre density and microglial activation in the mouse model ( $*** r = 0.95$ ,  $p < 0.001$ ), however no correlation was detected in the rat model. Error bars represent SEM.

### 3.5 Discussion

The purpose of this experiment was to determine if the way the striatum reacts following a QA lesion differs between mouse and rat models to highlight parameters which may be detrimentally affecting the success of transplantation in mice. Animals of the two species were lesioned and the striatal tissue analysed at time-points spanning up to 90 days post-surgery to answer four main questions: 1) Can we be sure the cells are being transplanted into the striatum? The post-lesion collapse of the striatum may occur at an accelerated rate in the mice compared to rats, thereby reducing the accuracy of calculated transplantation coordinates and potentially resulting in mis-injection of cells. 2) Are there species differences in the density of the post-lesion striatum which could restrict the space available for transplanted cells to develop? 3) Are we transplanting at the right time? Differences in the way the striatal immunological environment develops post-lesion could mean that the timing of transplantation is sub-optimal in the mouse model. 4) Could differences in the intensity of immune response result in a more hostile striatal environment in mice?

#### 1) Changes in striatal and ventricle volume following QA lesioning are not sufficient to affect atlas-based coordinates for transplantation in mice

The structural changes that occur in the striatum following a QA lesion followed a similar pattern in the mice and rats. Both had a relative decrease in striatal volume and an increase in ventricle volume similar to that observed in a study of QA lesioned Sprague-Dawley rats (Martínez-Serrano and Björklund, 1996) which saw an 15% decrease after 28 days post-lesion. Others have reported a 95% decrease in neuronal content after 14 days (Roberts *et al.*, 1993), however these counts were restricted to the lesion itself rather than in the striatum as a whole. No apparent differences between rats and mice in the amount of structural change were found at the time-point reflecting the time of grafting (Day 8), and it was shown that the relative grafting coordinates were consistently well within the dorsal striatum up until at least Day 90. In fact, judging by the delay in ventricular expansion, it was the physical structure in the mouse brain which appeared to retain its integrity for longer compared to the rats. It was not until Day 12 that the appearance of a definable lesion in the mice was observed, and the apparent collapse of the supporting parenchyma (and subsequent expansion of the ipsilateral ventricle) was only evident from Day 20. This suggests that intraventricular placement of transplanted cells due to a physical distortion of

the striatum is not a likely factor contributing to the comparatively lower yields of grafts in the mouse model.

### 2) The post-lesion striatum in the mouse has a greater cell density than the rat

Whilst there was no difference between species in the proportional increase of lesioned striatum cell density compared to the intact side, the cell density of the ipsilateral striatum, and striatum in general was significantly greater in the mice compared to the rat. This difference was evident at the standard time for transplantation (Day 8). A higher density of cells could leave less physical space for transplanted cells to grow and thrive in mice. The effect of density on graft survival and quality could be probed by comparing transplants in standard cell density (Day 7 post-lesion) and an increased density environment (Day 90+ post-lesion). A study which incorporates transplanting into animals after a prolonged period after lesioning is describe in [Experiment 2](#).

### 3) Transplantation occurs at a time of peak inflammatory activity

An intense microglial reaction was seen from the first time-point up to 28 days post-lesion in both rats and mice, with some animals still exhibiting areas of inflammation even after 90 days. The density of astrocyte fibres in the lesioned mouse striatum was also increased although this was more sustained. Inflammatory microglial response is known to begin within hours of insult with cells migrating to the site of injury (Duan *et al.*, 1998), and previously, high numbers of infiltrating macrophages have been observed up to 70 days post-lesion in a longitudinal study of QA lesioned Wistar rats (Shemesh *et al.*, 2009).

The biphasic pattern in microglia reactivity seen in both mice and rats with an initial peak at Day 8, followed by a secondary peak a week later reflects a similar pattern of microglial activation markers seen following a facial nerve cut (Raivich *et al.*, 1999) and could indicate secondary recruitment of microglia into the region of damage. A study in QA lesioned Wistar rats which followed microglia expression up to 90 days also saw a peak in microglial activity 14 days post-lesion (Arlicot *et al.*, 2014), although in this case by 90 days baseline levels were restored.

At the time at which transplantation is performed the microglial response observed was particularly marked, corresponding to other studies which observed peak microglial activity at 7-8 days post-insult (Janeczko, 1989; Barker *et al.*, 1996; Moresco *et al.*, 2008). This would indicate that this is not the ideal time to introduce transplanted cells. Johann *et al.* (2007), described an experiment in which they transplanted C57BL6/J mice at 2, 7, or 14 days

post-lesion and demonstrated that those transplanted at 2 days post-lesion yielded a larger graft volume compared to the later time-points in which they also observed an increase in microgliosis. Hence it would seem that transplanting before the peak in microglial activity is beneficial. However, since the cells transplanted 2 days post-lesion must have had to survive throughout the increased microglial activation period, the number of microglial cells cannot be the sole factor for any detrimental effects. It is known that the process of lesioning could 'prime' the microglia (Perry and Teeling, 2013) turning them from helpful contributors to homeostasis to activated pro-inflammatory cells. It is possible that the priming process has not peaked by the early period but had reached deleterious levels at the later time-points. Therefore, it is possible that placing cells into the activated microglial environment causes detrimental effects to the grafts. If this is the case then it could be that we have picked a poor time to transplant our cells, and perhaps it would be better to transplant earlier or to wait until all residual activation has dissipated. An experiment designed to test this hypothesis by transplanting into animals lesioned 12 months previously is described later (**Experiment 2**). It is important to note that microglial activation can be increased in HD mouse models (Ma, Morton and Nicholson, 2003), and patients with HD (Sapp *et al.*, 2001; Crotti *et al.*, 2014) and is therefore a problem worth considering for transplantation as a therapy.

#### 4) The microglial and astrocyte reactions are more exaggerated in the mouse than the rat

The pattern of inflammation was superficially similar in mice and rats. However, the proportion of microgliosis and astrogliosis in the lesioned striatum is significantly higher in the mice compared to the rats. At the times post-lesion at which transplantation would conventionally have been planned, the reaction in the mice observed here is massively exaggerated when compared to rats in terms of microglial number and density

Studies utilising microglial cultures have shown that stimulated mouse microglia will produce a greater number of pro-inflammatory markers, such as interleukin-6 (IL-6), tumour necrosis factor- $\alpha$  (TNF- $\alpha$ ), interleukin 1 $\beta$  (IL-1 $\beta$ ) and inducible nitric oxide synthase (iNOS), than those derived from rats (Wei *et al.*, 2013). Activated microglia can also produce QA (Heyes *et al.*, 1996; Espey *et al.*, 1997), which, in addition to its excitotoxic effects, has been implicated in immune cell signalling and, thus the exacerbation of inflammatory processes (Moffett *et al.*, 1993). This could indicate that there are not only greater numbers of cells in the inflamed mouse striatum, but they are also releasing a greater number of inflammatory compounds. Differences in the way that the peripheral immune system of

rats and mice deal with the same toxin have been demonstrated (Smialowicz, 1994), so it is likely that the immune system of the CNS could also respond differently. In fact, differences reported in two rodent models (rat and gerbil) demonstrate that the microglia of rats produce significantly less QA in response to ischemic brain injury (Heyes *et al.*, 2002).

In this experiment, we found a close correlation between the microglia activity measures and the astrocyte measures in the mice, but this was absent in the rats. This would imply that either the way in which one of these cell types reacts to the lesioning is different, or the way one of these cell types interacts with the other is different. Human astrocytes have been shown to be neuroprotective whilst in their resting state, producing beneficial neuroprotective factors such as dizocilpine (MK-801, a glutamate receptor antagonist) which can reduce susceptibility to excitotoxins (Giulian, 1993), as well as forming beneficial glial scars which can aid CNS recovery (Liddelow *et al.*, 2017). However, in the presence of activated microglia, astrocytes may lose their ability to protect neurons thus inciting neuronal death, or become detrimentally reactive themselves (Liddelow *et al.*, 2017). In addition, the microglia will metabolise kynurenine produced by the astrocytes to form QA (Guillemin *et al.*, 2001), which has been shown to upregulate chemokines and stimulate astrocytes in culture (Guillemin *et al.*, 2003), potentially leading to an escalating inflammatory loop. The greater density of resting state astrocyte fibres in the contralateral striatum of rats could be indicative of a more protective baseline which might attenuate inflammation (Kim *et al.*, 2010), whereas in mice the exaggerated microglia response and corresponding astrogliosis could intensify the inflammatory process.

Whilst it has been argued that this inflammation in itself is not necessarily detrimental to any cells being transplanted (Duan *et al.*, 1998) these studies were conducted only in rats. In addition, the same authors report that if the immune system is sufficiently stimulated then rejection is more likely to occur (Duan, Brundin and Widner, 1997). Since the immune reaction has been shown to be more exaggerated in mice, then it is possible that the threshold of stimulation to initiate rejection is more easily passed in this species. The escalation of inflammation is likely to create a detrimental environment for transplantation of cells which, as well as potentially being recognised as foreign bodies, could also be targeted due to damage via the process of dissection and suspension (Perry and Teeling, 2013).

Notably, it took longer before a lesion could be visualised through DARPP-32 staining in the mice than in the rats, **Figure 3.3 A**. There was a steady decline in ipsilateral cell numbers, so

it could be that the supporting parenchyma could only withstand a certain loss before it collapsed. This could explain why there was a delay in the expansion of the ventricle in the mice. The fact that the lesion seems to manifest earlier in the rats highlights a potential difference in the species in the way that MSNs succumb to QA and the cells are destroyed. Additionally, it could mean that the injected QA is not processed as quickly in the mice and remains for longer at the injection site. This, in addition to the QA potentially being produced by the reactive microglia, could have an unfavourable impact on cells being transplanted into the region, especially considering that under normal conditions there is virtually no QA to be found in the brain parenchyma (at least in rats) (Moffett, Espey and Namboodiri, 1994). A comparative longitudinal quantitative assay of striatal QA content would be able to determine at which time the exogenous QA has dissipated, for example by gas chromatography-mass spectrometry (Smythe *et al.*, 2002; Ghosh *et al.*, 2012).

### 3.6 Conclusions and future work

The aim of this experiment was to determine if there were differences between the rat and mouse QA lesion model which could explain why transplants in the mouse model are small in comparison and do not survive as well as those seen in rats.

The results show that mice exhibited an exaggerated reaction to lesioning compared to rats in terms of microglial and astrocytic response, which could lead to a more hostile striatal environment into which cells are transplanted.

To examine the details of the immune response it is necessary to determine the phenotype of the cells observed. The assessment of levels of pro-inflammatory cytokines and QA within the models at each time-point is necessary to pin down the beneficial or detrimental nature of the response. A replicated experiment in which tissue is dissected and qPCR used to analyse the level of toxins (QA) or inflammatory factors (e.g. IL-6, TNF- $\alpha$ ) could help to determine the type of environment the cells are subjected to.

To avoid transplanting into a primed environment, an extended post-lesion period could be left. Even though the very process of inserting the grafting cannula may once again trigger a response, this would not be exacerbated by the presence of QA. This hypothesis forms the basis of **Experiment 2**.

Whilst the C57BL/6 mice used in this experiment have a highly exaggerated immune response compared to the Lister Hooded rats, it is unclear if this is representative of all mice. In addition, it is not known what effect this response could have on the survival of transplanted cells. **Experiment 3** investigates the how the choice of host mice, and the donor strain choice could alter the graft outcome.

## Experiment 2

### Extending the post-lesion period and the effect of host age<sup>§</sup>

#### 3.7 Summary

The previous experiment determined that under standard protocols, cells are transplanted into a very reactive inflammatory post-lesion environment. The following experiment was designed to test if extending the time between lesioning and transplantation, to a point beyond which any residual inflammatory response was detectable, could lead to increased graft survival and improved neuronal count. The study described compared grafts in mice transplanted 7 days post-lesion with those transplanted after 12 months. In addition, it was necessary to include an age-matched older control group which were transplanted 7 days post-lesion, thus allowing for the separation of transplantation timing and age-related effects.

Graft survival, volume and cell counts were used to evaluate the grafts and inflammatory response was assessed through quantification of microglia in the grafted region.

The results show that neither graft survival or graft volume were improved when the post-lesion period prior to transplantation was extended to 12 months.

---

<sup>§</sup> Declaration

Lesion surgery was shared with PhD student Victoria Robertson. Tissue dissection was performed by Ngoc Nga Vinh.

### 3.8 Introduction

#### QA lesions invoke an intense immune response in mice

**Experiment 1** demonstrated that following QA lesioning there was an intense microglial and astrocytic reaction which lasted at least until 28 days post-lesion, and some residual activity even after 90 days. It was hypothesised that transplanting into this inflammatory situation would mean delivering donor cells into a hostile environment, and thus impact on the success of the grafts. By increasing the time between lesion surgery and transplantation surgery it was suggested that the reactive and primed microglial environment could be avoided, and the graft outcome improved.

#### The immune system changes in aged mice

As people age there is an increase in microglial activation and dysfunction, as well as a reduced ability to suppress inflammation (Franceschi et al., 2007; Mosher and Wyss-Coray, 2014; Sapp et al., 2001). Increases in microglial activation and dysfunction have also been reported in the aging rodent brain (Godbout et al., 2005; Perry et al., 1993), although others report contrary evidence (Ma et al., 2003). By leaving an extended time between lesioning and transplanting the mice will necessarily be more aged at the time of transplantation. To separate the effects of extended inter-surgery time and age, an additional experimental group of animals was included in the comparison which were aged but transplanted at the standard 7 days post-lesion. This addresses an important issue relevant to the clinical application of cell transplantation since those patients most likely to receive the treatment will be at least in their forties (Foroud et al., 1999), while most preclinical transplantation studies are performed in young adult animals.

This experiment compares transplants performed at the standard 7 days post-lesion in young mice (Y7D group) with those carried out one year after lesioning (O12M group), once all traces of lesioning would presumably have dissipated. In addition, an age matched 12-month-old control group was transplanted 7 days after lesioning (O7D group). The success of the grafts was assessed on graft survival, volume and neuronal cell numbers, and the microglial response was quantified to address the following questions:

- 1) Does transplanting after the post-lesion inflammatory period increase the survival and growth of grafts?
- 2) Is the immune response to transplantation affected by the age of the host?
- 3) Does the age of the host affect the survival and growth of the transplants?

### 3.9 Methods

#### 3.9.1 Experimental design

Male C57BL/6J mice (n=40, bred in-house) were weaned from litters born in two batches. The first batch were divided into two groups with half receiving unilateral mid-dorsal striatal QA lesions at 8 weeks old ('O12M' group, n=14, ~25g bodyweight), as described in methods section 2.2.1, and returned to their home cages whilst the others ('O7D' group, n=14) remained in their home cages (Figure 3.8). The second batch of mice, born a year later from the same breeding colony, received a similar lesion at 8 weeks old ('Y7D', n=12, ~25g bodyweight), at which point the O7D group were also lesioned at 51 weeks old (~35g bodyweight).

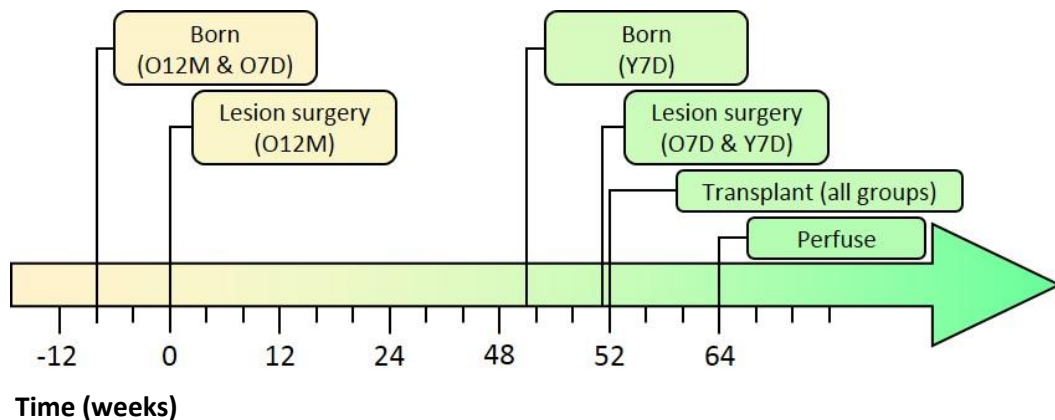


**Figure 3.8** Experimental timeline. **Y7D** = young mice lesioned 1 week prior to transplantation, **O7D** = old mice lesioned 1 week prior to transplantation and **O12M** = old mice lesioned 52 weeks prior to transplantation. Between surgeries mice remained in their home cages until they were perfused.

### Transplantation surgery

At 7 days post-lesion (O7D and Y7D groups) and 52 weeks post-lesion (O12M group) mice received a unilateral transplant of Chrm4-EGFP-CD1 WGE tissue into the lesioned striatum, as described in methods section 2.2.3. Each mouse received 300,000 cells in total, delivered in two 1 $\mu$ l deposits of 150,000 cell $\mu$ l<sup>-1</sup> cell suspension, at two depths within the same tract at the lesion site. A summary of groups can be found in Table 3.2.

A total of 34 E14 pups from three pregnant Chrm4-EGFP-CD1 dams were dissected on 3 consecutive days prior to transplantation. Animals from each group were counter-balanced between surgery sessions. The medial transplantation coordinates for the O12M group were adjusted to -2.4 (rather than the standard -2.0) to account for striatal collapse and ensure striatal placement of cells.

Group name	Lesioned age (weeks)	Transplanted age (weeks)	Transplant time (weeks post-lesion)
O12M	8	60	52
O7D	59	60	1
Y7D	8	9	1

**Table 3.2** Summary of experimental groups. O12M = old mice lesioned 12 months prior to transplantation, O7D = old mice lesioned 7 days prior to transplantation and Y7D = young mice lesioned 7 days prior to transplantation.

### 3.9.2 Immunohistochemical analysis of the grafts and microglia

At 12 weeks post-transplantation all mice were transcardially perfused, as described in methods section 2.3.1, and brains transferred to sucrose solution for 48 hours.

Fixed brains were sectioned at 40 $\mu$ m. GFP, NeuN and Iba1 immunohistochemical DAB staining was performed on free floating sections. Graft survival was assessed based on GFP<sup>+</sup> staining, with those not exhibiting any positive staining deemed to have no surviving grafts. Graft volume measures were calculated by measuring cross-sectional areas of GFP<sup>+</sup> staining across 1:12 series and using the formula:  $Volume = (\Sigma A * M) / f$ , where A = area of graft ( $\mu$ m<sup>3</sup>), M = section thickness ( $\mu$ m) and f = section frequency) and NeuN<sup>+</sup> grafted cell numbers were manually counted. Graft cell density was calculated from the cell count and volume data.

Iba1 antibody was used to stain microglia within the sections. Unbiased stereology was used to calculate the number of Iba1<sup>+</sup> cells in the contra- and ipsilateral striatum in one section per brain at the level of the site of transplantation, including those with no surviving grafts. Density calculation of cells/ $\mu\text{m}^3$  were used rather than absolute cell counts to account for the collapse of the ipsilateral striatum in the O12M group, thus allowing for comparison between groups regardless of striatal volume.

Proportional changes in microglial density in the ipsilateral striatum were calculated using the following formula: % **increase** =  $(I_{\text{md}} / C_{\text{md}}) \times 100$ , where  $I_{\text{md}}$  = Ipsilateral microglia density and  $C_{\text{md}}$  = Contralateral microglia density.

### 3.9.3 Statistical analysis

Four mice from the Y7D group and one mouse from each of the O7D and O12M groups were culled due to ill health prior to transplantation. Therefore, the final group sizes were as follows: Y7D n=8, O7D n=13 and O12M n=13.

All statistical analysis was performed using Genstat (18<sup>th</sup> edition). ANOVAs or student's t-tests were performed to compare experimental groups and between hemispheres where appropriate. Newman-Keuls' post-hoc pairwise comparisons were performed to analyse significant interactions, correcting for multiple comparisons. Significance was taken as  $p \leq 0.05$ .

Post-hoc power analysis based on final animal numbers was calculated using G\*Power software and was estimated to be 100% for large effect sizes and 98% for medium effect sizes.

### 3.10 Results

#### Graft survival and placement

GFP staining confirmed that grafts had survived in each group, with survival rates summarised in **Table 3.3** and **Figure 3.10 A**. Surviving grafts were located within the dorsal striatum (**Figure 3.9 A - C**), and NeuN<sup>+</sup> grafted cells could be identified within regions of relative neuronal depletion. Non-specific staining associated with dead or rejected cells were found within the striatum of brains with no surviving cells, as well as within some of the surviving grafts **Figure 3.9 D**.

#### Graft volume and cell counts

Graft size was generally small although there was large variability within groups and some grafts with less than 100 surviving cells. Mean graft volumes and NeuN<sup>+</sup> cell counts are summarised in **Table 3.3**. There was no difference in the GFP<sup>+</sup> volume, NeuN<sup>+</sup> cell counts or NeuN<sup>+</sup> cell density between the three groups (Group:  $F_{2,20}=0.29$ , ns;  $F_{2,20}=0.64$ , ns and  $F_{2,20}=1.7$ , ns respectively), **Figure 3.10 B - D**.

Group	Number of surviving grafts	Mean graft volume ( $\times 10^5 \mu\text{m}^3$ )	Graft volume range ( $\times 10^5 \mu\text{m}^3$ )	Number of NeuN <sup>+</sup> cells ( $\times 10^2$ )
Y7D	5 of 8 (63%)	97.3 $\pm$ 57.9	9.5 - 323.5	14.9 $\pm$ 8.9
O7D	10 of 13 (77%)	101.1 $\pm$ 34.8	2.4 - 261.4	6.6 $\pm$ 1.6
O12M	8 of 13 (62%)	149.5 $\pm$ 84.8	0.4 - 583.3	12.1 $\pm$ 8.1

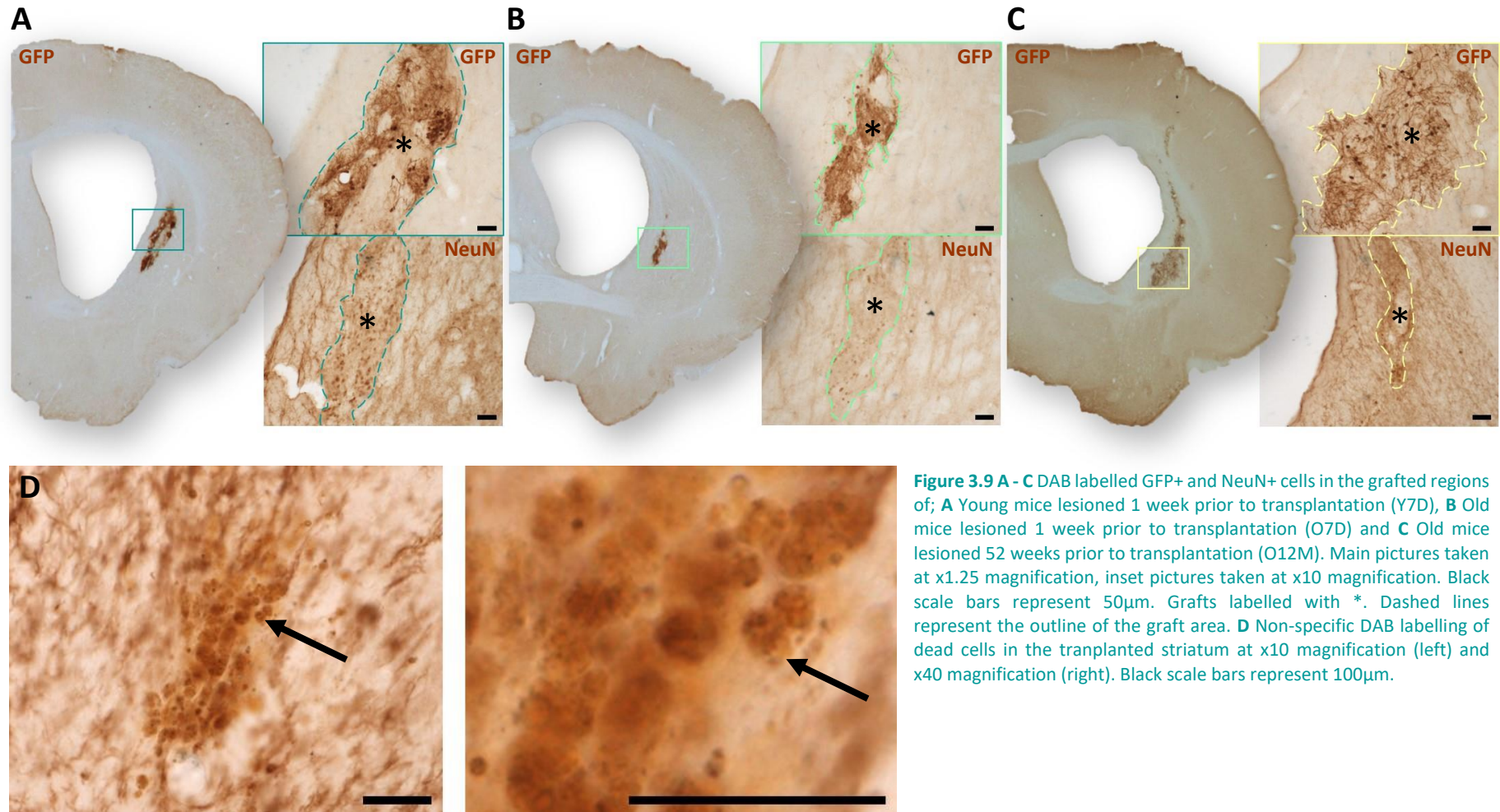
**Table 3.3** Summary of graft survival, GFP<sup>+</sup> graft volume and NeuN<sup>+</sup> cell counts. Y7D = young mice lesioned 7 days prior to transplantation, O7D = old mice lesioned 7 days prior to transplantation and O12M = old mice lesioned 12 months prior to transplantation.

#### Immune response to grafting

Iba1 labelling of microglia showed marked ipsilateral activation in all surviving graft groups, as well as in the O7D mice with no surviving grafts, **Figure 3.11**. Microglial density was significantly higher in the ipsilateral compared to the contralateral striatum in groups with surviving grafts (Side:  $F_{2,20}=105.98$ ,  $p<0.001$ ), **Figure 3.12 A**, however there was no difference between these groups (Group:  $F_{2,20}=0.38$ , ns). When the proportional increase in ipsilateral microglial density was compared, there was a significant effect of group, and a trend towards the O12M having a smaller increase when compared to the Y7D and O7D groups, however

no significant difference between any group could be determined in the post hoc analyses. (Group:  $F_{2,20}=5.12$ ,  $p<0.05$ ; O12M and Y7D  $t_{20}=2.71$ , ns; O12M and O7D  $t_{20}=2.83$ , ns respectively), **Figure 3.12 B**.

In those groups with no surviving grafts there was still a significant increase in microglial density on the ipsilateral side, driven by a significant increase in the O7D group (Group\*Side:  $F_{2,7}=14.51$ ,  $p<0.01$ ; Side (Y7D):  $t_7=0.60$ , ns; Side (O7D):  $t_7=7.90$ ,  $p<0.01$ ; Side (O12M):  $t_7=2.38$ , ns), **Figure 3.12 C**. The ipsilateral density was higher in this group than in either the Y7D or O12M groups ( $t_7=6.71$ ,  $p<0.01$  and  $t_7=4.84$ ,  $p<0.05$  respectively), however there was no difference in the contralateral side between any group. The proportional increase in microglia density was elevated in the O7D group compared to the Y7D and O12M groups (Group:  $F_{2,7}=20.69$ ,  $p<0.001$ ;  $t_7=6.28$ ,  $p<0.01$  and  $t_7=4.39$ ,  $p<0.05$  respectively), **Figure 3.12 D**, but no difference was found between the O12M and Y7D groups ( $t_7=1.89$ , ns).



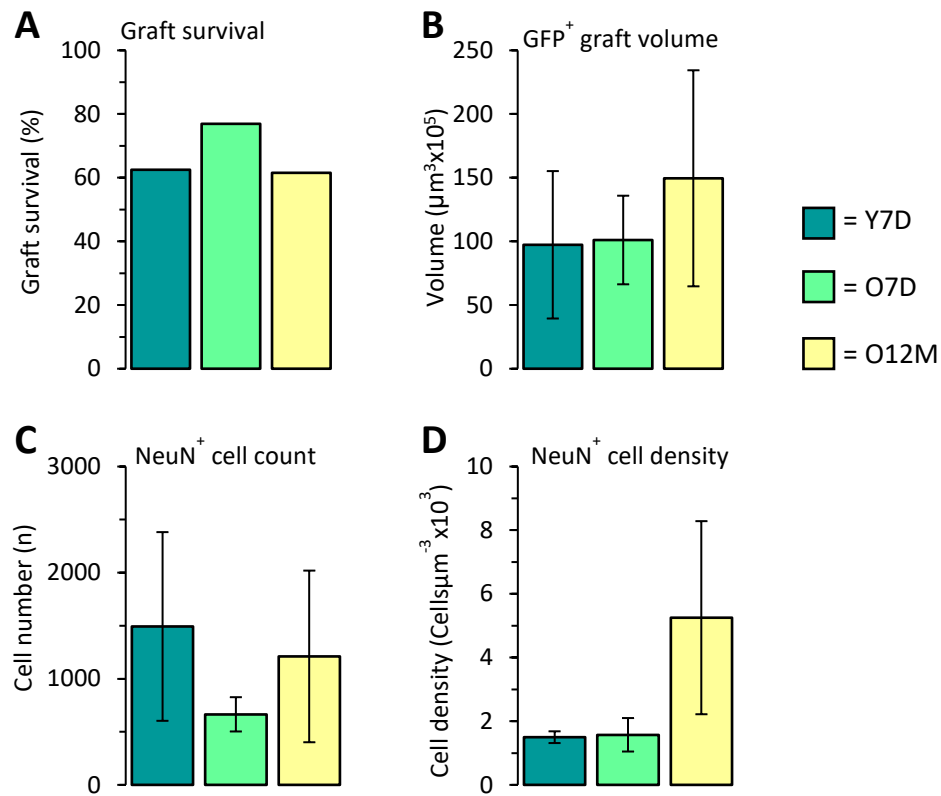


**Figure 3.10** Y7D = young mice lesioned 1 week prior to transplantation, O7D = old mice lesioned 1 week prior to transplantation and O12M = old mice lesioned 52 weeks prior to transplantation. **A** Percentage of mice with surviving cells 12 weeks post-transplantation (Young mice transplanted 1 week post-lesion (Y7D) 5 of 8; old mice transplanted 1 week post-lesion (O7D) 10 of 13; old mice transplanted 52 weeks post-lesion (O12M) 8 of 13). **B** GFP<sup>+</sup> graft volume. No difference was found between groups. **C** NeuN<sup>+</sup> cell counts within the graft. No difference was found between groups. **D** NeuN<sup>+</sup> cell density within the graft. No difference was found between groups.

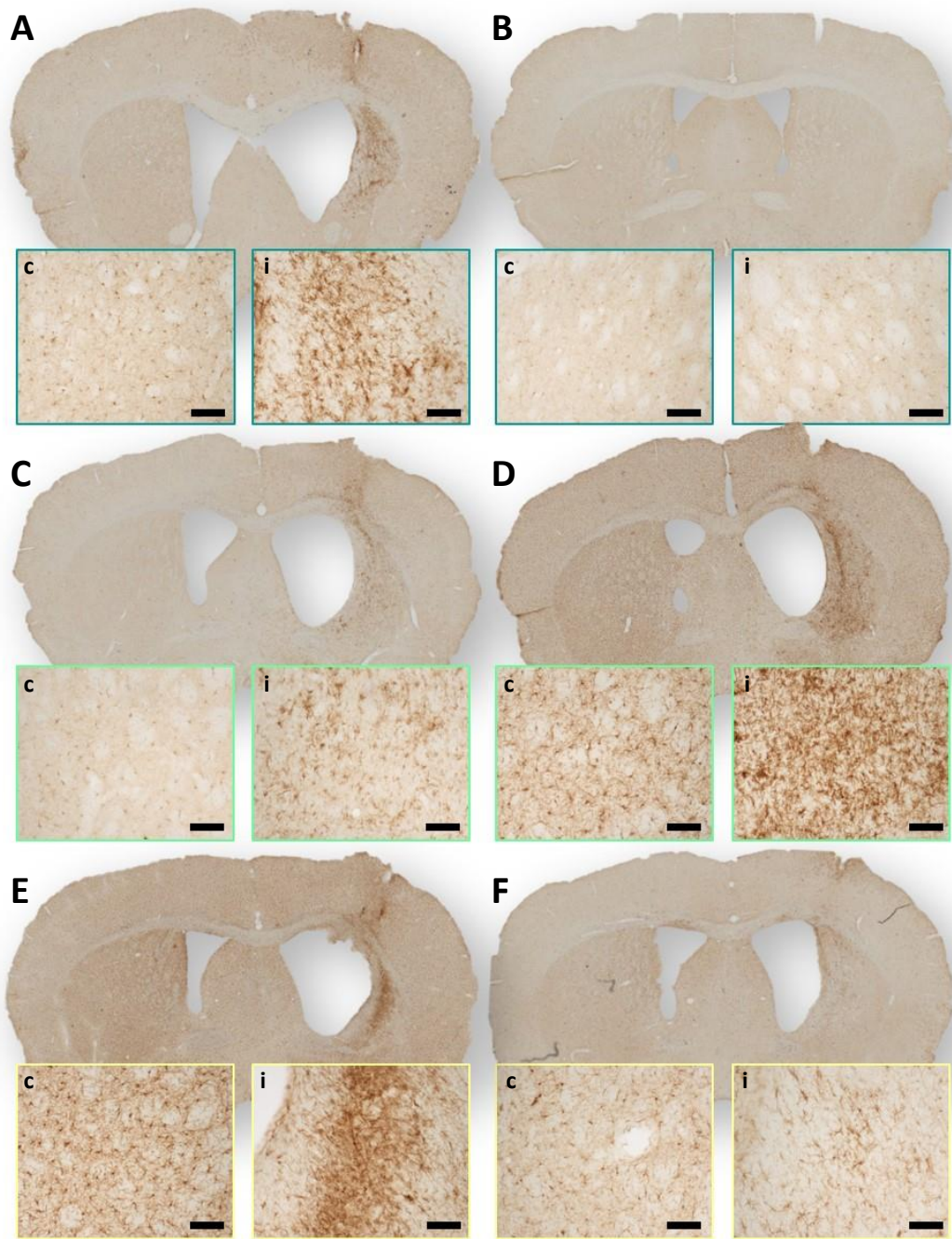


**Figure 3.11** DAB labelled Iba1+ cells in the contra- and ipsilateral striatum at transplantation site. **A** Young mice lesioned 1 week prior to transplantation (Y7D) with surviving grafted cells and **B** no surviving grafted cells. **C** Old mice lesioned 1 week prior to transplantation (O7D) with surviving grafted cells and **D** no surviving grafted cells. **E** Old mice lesioned 52 weeks prior to transplantation (O12M) with surviving grafted cells and **F** no surviving grafted cells. Main pictures taken at x1.25 magnification, inset pictures taken at x10 magnification, c = contralateral side, i = ipsilateral side. Black scale bars represent 100µm.

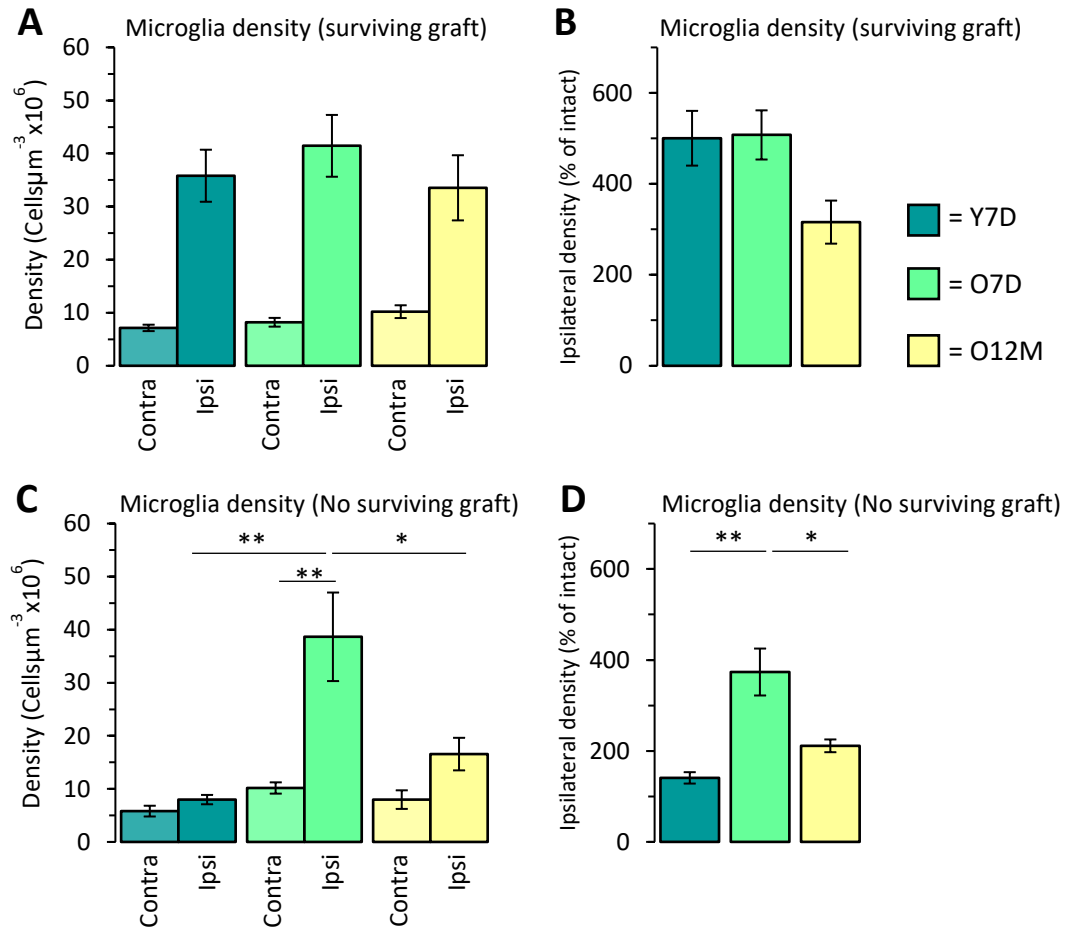


**Figure 3.12** Y7D = young mice lesioned 1 week prior to transplantation, O7D = old mice lesioned 1 week prior to transplantation and O12M = old mice lesioned 52 weeks prior to transplantation. **A** Microglia cell density in the contra- and ipsilateral side in animals with surviving grafts. Microglia density was increased in the ipsilateral side compared to the contralateral ( $p < 0.001$ ). No difference was found between groups. **B** Ipsilateral density of microglia in animals with surviving grafts expressed as a percentage of contralateral density. There was a main effect of group ( $p < 0.05$ ), and a trend towards the increase in microglial density being less severe in the O12M mice compared to the Y7D or O7D groups, although this trend was not statistically significant. **C** Microglial density in the contra- and ipsilateral side in animals with no surviving grafts. An increase in microglia density in the ipsilateral side was observed in the O7D group (\*\*  $p < 0.01$ ), but not the Y7D or O12M groups. The density of microglia was significantly higher in the ipsilateral side of the O7D group when compared to the Y7D and O12M groups (\*\*  $p < 0.01$  and \*  $p < 0.05$  respectively). No difference in the contralateral density was found between groups. **D** Ipsilateral density of microglia in animals with no surviving grafts expressed as a percentage of contralateral density. The increase in microglial density was greatest in the O7D mice compared to either the Y7D or O12M groups (\*\*  $p < 0.001$  and \*  $p < 0.05$  respectively).

### 3.11 Discussion

The aim of this study was to assess whether graft outcome in the QA mouse model of HD could be improved by transplanting into the striatum after all immune reaction to lesioning had dissipated. This was achieved by comparing grafts of cells transplanted during a time of high post-lesion microglial activation and those transplanted once all traces of the initial response to lesioning were deemed to have completely dissipated. In addition, the effect of transplanting into aged mice compared to young animals was considered. Three groups were transplanted; standard young mice transplanted 7 days post-lesion, mice transplanted 12 months post-lesion and age-matched older mice transplanted 7 days post-lesion. The following questions were addressed: 1) Does survival and growth of grafts improve if mice are transplanted after the post-lesion inflammatory period? 2) Is the immune response to transplantation affected by the age of the host? 3) Does the age of the host affect the survival and growth of the transplants?

#### 1) Delaying transplantation beyond the post-lesion inflammatory response does not improve graft survival or content

Delaying transplantation for 12 months after lesioning had no effect on the proportion of surviving grafts, the volume of the grafts or the number of surviving cells within the grafts. In addition, no difference in the ipsilateral density of microglia between groups with surviving grafts 12 weeks after transplantation was found, however, all groups exhibited a profound increase compared to the contralateral baseline. This suggests that the microglia response to the transplanted cells could supersede, or ‘top up’ any residual response related to lesioning. It was originally hypothesised that the microglia following a lesion were primed and as such would result in a more detrimental environment for cells to be transplanted into, and these results could suggest that might not be the case. However, it has been shown that the activation of microglia begins within hours of trauma (Duan et al., 1998) and so the act of inserting the transplantation cannula could in itself initiate priming of microglia in the area, in addition to the presence of the transplanted cells themselves.

The collapse of the striatum in the mice lesioned 12 months previous was pronounced, however, the adjusted transplantation coordinates compensated for this. The fact that there was no significant difference in graft volume or cell number in the short and long post-lesion time groups would suggest that the increased ipsilateral striatal cell density in the 12M groups did not have an increased detrimental effect on the grafts as was previously

postulated in **Experiment 1**. Whilst the analysis included only data of graft volume and cell counts from those animals in which surviving grafts were detected, it is noted that even when all animals were included, with graft volume / cell counts given as 0 where no detectable grafts were observed, still no significant differences are identified. However, this does not preclude to possibility that the increased density of the mouse striatum in general, compared to rats, could influence the ability of the transplanted cells to thrive.

Poor graft size, cell survival and continued intense microglial activity 12 weeks post-transplant in all groups with surviving cells, and the presence of dead or rejected cells in most animals, might indicate that immune response and graft rejection is an ongoing process in all groups. This suggests that any effect of transplanting at a later post-lesion time could be lost as soon as the transplantation surgery occurs since the presence of the cells triggers an inflammatory process, whether new or ongoing. A previous study assessed the effect of transplanting earlier, at 2 days post-lesion, and also found no difference in graft outcome (Robertson, 2014), despite some reports that transplanting at this stage, prior to peak immune response, improves graft survival (Johann et al., 2007).

## 2) The immune response to transplantation is affected by the age of the host

No difference between contralateral baseline levels of microglia density were found between the aged and young mice. Others report an increase in the number of activated microglia and increased release of pro-inflammatory cytokines in older animals (Njie et al., 2012; Norden and Godbout, 2013), although not necessarily an increase in number or density of microglia in general. There was a trend towards an increased baseline density in the O12M group and it is possible that this would become significant if a larger group size was used. The comparative ipsilateral increase in microglia density was significant in all groups, with a trend towards the Y7D and O7D mice yielding a greater proportional increase. This was in part due to the trend towards an increased contralateral density in this group, rather than a lower ipsilateral microglia density. In fact, the O12M group was the only one to demonstrate a significant correlation between the microglial density in the two hemispheres ( $r=0.76$ ,  $p<0.05$ ), which could suggest that the activity of microglia in response to the transplantation is more global in those animals that were lesioned a long time before rather than being restricted to the ipsilateral side. One hypothesis could be that this is a result of a priming mechanism induced by the original insult, which means subsequent insults induce a greater reaction, and further experiments would be able to test this.

Dead cells and cell debris were identified within the transplanted striatum of animals with no surviving grafts, indicating that the cells had been rejected at some point prior to the 12-week post-transplantation perfusion time, rather than having been mis-injected. In contrast to the brains with surviving grafts, there was a difference detected between groups in microglial density changes in animals with no surviving grafts. In groups which were transplanted 7 days post-lesion, young animals with no grafts had microglial numbers equivalent to contralateral baseline levels, whilst older mice exhibited an increase in microglial density. It is possible that the cells were rejected early in the young animals and the striatum is in a post-reactive phase. Whereas in the older animals, either the rejection was delayed, or the microglial response had taken longer to dissipate. In support of the latter, studies have shown a prolonged and exacerbated microglial-related neuroinflammation in aged mice compared to younger (Huang et al., 2008; Perry et al., 1993).

Whilst there was a trend towards the O12M group with no surviving grafts having an elevated change in microglial density compared to the Y7D mice, this increase was certainly not as marked as in the O7D group, therefore this difference can be assumed to be a consequence of either the greater gap between surgeries, or the age at which they were lesioned, although it is unclear what the mechanism could be. One possible explanation could be that an escalated inflammatory process due to the recent lesioning is less able to be dampened in older animals, whereas in those aged mice who have had time to recover from the lesion effects are able to manage their response to the new insult more effectively, although not as effectively as the younger animals.

A progressive increase in reactive microglia is often seen in patients with HD (Sapp et al., 2001; Tai et al., 2007a, 2007b). These findings highlight an important consideration for transplantation in patients since not only their age but also the inflammatory processes of the disease lead to an increase in microglial activation, which could confound the success of transplants in clinical trials. In addition, the hyperactivity of microglia in HD mouse models (Björkqvist et al., 2008; Ma et al., 2003) could confound preclinical assessment of the treatment.

### 3) Transplanting into aged mice did not affect graft survival or cell number

The age of the host mouse did not affect the survival, size or cell number within the grafts, however the size and quality of the grafts was poor in all groups. Despite the data from the animals with no surviving grafts suggesting that age may exacerbate the innate immune response and *ex vivo* studies demonstrating that microglia from aged animals secrete more

pro-inflammatory cytokines than younger animals (Njie et al., 2012), this does not appear to relate to how well the grafts survive in this case. The intense microglial response within the grafted striatum in all groups may suggest that a ceiling level has been reached, after which any further release of cytokines due to age has no effect, which would also reflect the poor quality of the grafts.

### 3.12 Conclusions and future work

Delaying transplantation until well past the time any immune response from lesioning has returned to normal did not improve the survival or quality of graft outcome. The effect of microglia within the grafted site cannot easily be negated since the process of transplantation and the presence of the cells themselves are both likely to maintain the activated reaction.

Preventing the activation of microglia in the host could be a potential solution. Studies in HD and other disease models have reported reduction of microglial inflammation, and a subsequent improvement in disease features, through the use of drugs such as minocycline (Sriram et al., 2006) or cox-2 inhibitors (Casolini et al., 2002; Kalonia and Kumar, 2011; Sánchez-Pernaute et al., 2004; Vijitruth et al., 2006) which can prevent the switching of microglia to their activated state.

It is also possible that the response seen in the experiments so far are specific to, or more exaggerated in, the C57BL/6 strain used. This hypothesis is probed in **Experiment 3** which compares transplants in three different mouse strains.

## Experiment 3

### The effect of host and donor strains

#### 3.13 Summary

As shown previously, the C57BL/6 mice show a marked immune response to lesioning compared to the Lister Hooded rats. Transplanting Chrm4-EGFP-CD1 tissue into this strain after any expected lesion-induced inflammation had dissipated neither improved the graft outcome, nor mediated the microglial response to the transplanted tissue.

To determine if the intense immune response is an intrinsic characteristic of either the C57BL/6 hosts, or the Chrm4-EGFP-CD1 tissue specifically, the following experiment examined the effects of transplanting tissue from, and into, multiple donor/host combinations.

Chrm4-EGFP-CD1, C57BL/6 or CD1 tissue was transplanted into hosts of each of the three strains and the grafts assessed after twelve weeks. Graft survival, volume and cell number were compared to establish the effect of host and donor, as well as the effect of transplanting within the same strain or between different strains. The number of microglia and dead cells found within the grafted striatum were used as markers of immune response and rejection and compared between the different groups.

The data did not show a significant difference between the inflammatory response of the C57BL/6 hosts and the other strains examined, neither was it shown that the Chrm4-EGFP-CD1 neural tissue triggered a greater inflammatory response than that from the other strains. Conclusions drawn for the present experiment are cautious since a low graft survival rate resulted in very small group sizes which may not be sufficient to demonstrate statistically relevant differences.

### 3.14 Introduction

**Experiment 1** demonstrated an exaggerated immune response to QA lesioning in the C57BL/6 mice compared to that observed in the Lister Hooded rat, and **Experiment 2** showed that there is a significant microglial reaction to transplanted cells in this strain. However, it remains unclear if the magnitude of this response is unique to the C57BL/6 strain or whether alternative strains might offer a more receptive environment for cell transplantation. Similarly, it is not known if the Chrm4-EGFP-CD1 in itself is more immunogenic than striatal progenitors from other mouse strains.

#### Different mouse strains can exhibit different immunological responses

Studies of immunogenicity in mice have demonstrated a differential response to viral challenges among different mouse strains (Herath et al., 2016; Kaba et al., 2008). Whilst some have shown the C57BL/6 strain to mount a weaker response to virally transfected transgenes compared to other mice (Michou et al., 1997), another study demonstrated that injury to the CNS in the C57BL/6 triggers an increased number of inflammatory cells to the site when compared to BUB/BnJ mice (Luchetti et al., 2010).

Genetic background has also been shown to influence the susceptibility of striatal cells to excitotoxins, with C57BL/6 mice demonstrating a reduced sensitivity to QA than the other mouse strains that were compared, (McLin et al., 2006). In addition, the R6/1 HD mouse line bred on a CBAXC57BL/6 background, has shown resistance to QA lesioning (Hansson et al., 1999). These experiments were conducted in adult mice and it is unknown if these differences extend to the developing primary tissue in the various strains, however, it is possible that transplanted cells derived from donors of these backgrounds could be more resilient to the hostile environment into which they are being placed, particularly if, as was proposed in **Experiment 1**, QA dissipates from the lesion site at a slower rate in the mouse lesion model.

#### Different tissues can have different immunogenic effects

Transplants of peripheral organs in inbred and outbred mice show that outcome success was dependent on the genetic background of the donor, with inbred strains having an improved outcome over outbred (Reichenbach et al., 2013). However, this was not true of the background status of the host. Species differences in the amount of graft outgrowth have been shown (Kelly et al., 2007), and it is possible that a between-strain effect could also be

seen, albeit to a lesser extent since the disparity in immunogenicity between strains is smaller than between species.

Additionally, the Chrm4-EGFP-CD1 donor used throughout this thesis was chosen because observations from within the lab suggested that this strain produced the most substantial grafts of those used for mouse transplantation. However, some reports suggest that the enhanced green fluorescent protein (EGFP) used to label the cells may aggravate host response to the transplants. Stripecke et al., (1999), reported that EGFP was immunogenic in Balb/c mice, and later determined that its immunogenicity is strain dependent (Gambotto et al., 2000; Skelton et al., 2001). However, further investigations by the same lab, in agreement with Denaro et al., (2001), determined that EGFP is not inherently immunogenic in C57BL/6 models.

The differences described highlight the variability between donor strain tissues and the need to establish the most appropriate models for use in preclinical transplantation studies.

#### Matching and mismatched tissue can influence graft survival

The major histocompatibility complex (MHC) are the genes which encode for surface proteins recognised by the immune system. The less closely related individuals are, the more dissimilar the proteins are, and therefore the greater the intensity of the host immune response to the transplanted tissue. MHC mismatch between host and donor reduces graft cell counts and differentiation, and increases microglial activation compared to matched pairings (Chen et al., 2011), with the immunogenic effect increasing with the degree of mismatch from genetically identical (isogenic) host/donor combinations up to strongly mismatched xenografts (Duan et al., 1995). Transplants between outbred strains have been shown to have reduced survival in comparison to those between the more genetically similar inbred strains (Chen et al., 2011), however the subtle effects of MHC incompatibility and chronic immune activation are not well defined. Of the strains most commonly used within the lab, the Chrm4-EGFP-CD1 is most closely related to CD1 strain, although the two lines originate from separate colonies. The C57BL/6 strain, which is used as the host species in the previous experiments and as the background strain of many genetic models of HD and most behavioural studies in mice, could be presumed to be more strongly mismatched to the Chrm4-EGFP-CD1 donor tissue than the CD1 hosts, the strain used in many histology-based transplantation studies (Kelly, 2005; Kelly et al., 2007; Robertson, 2014).

The following experiment aimed to examine the effect of host and donor choice on graft outcome, in a counter-balanced study involving transplanting tissue derived from each of three different mouse strains, C57BL/6, CD1 and Chrm4-EGFP-CD1, into hosts of each of the same three strains. Graft survival, volume and cell number were compared for each host and donor strain, as well as between matched and mismatched strain combinations. The microglial response was also assessed as an indication of inflammatory reaction in the hosts.

### 3.15 Methods

#### 3.15.1 Experimental design

##### Host animals

Male C57BL/6J (n=12, 25-30g), CD1 (n=12, 35-45g), and Chrm4-EGFP-CD1 (n=12, 35-45g) mice were bred from an in-house colony (originally purchased from Harlan, Bicester, UK (C57BL/6J & CD1) and MMRRC, City, USA (Chrm4-EGFP-CD1)) and assigned to age-matched groups, **Table 3.4**. At age ten weeks all mice received unilateral mid-dorsal striatal QA lesions (**Figure 3.13**), counter-balanced over four daily surgery sessions, and were returned to their home cages. The same stereotaxic coordinates were used for all strains.

Host	Donor		
	C57BL/6J	CD1	Chrm4-EGFP-CD1
C57BL/6J	4	4	4
CD1	4	4	4
Chrm4-EGFP-CD1	4	4	4

**Table 3.4** Summary of planned experimental group numbers.

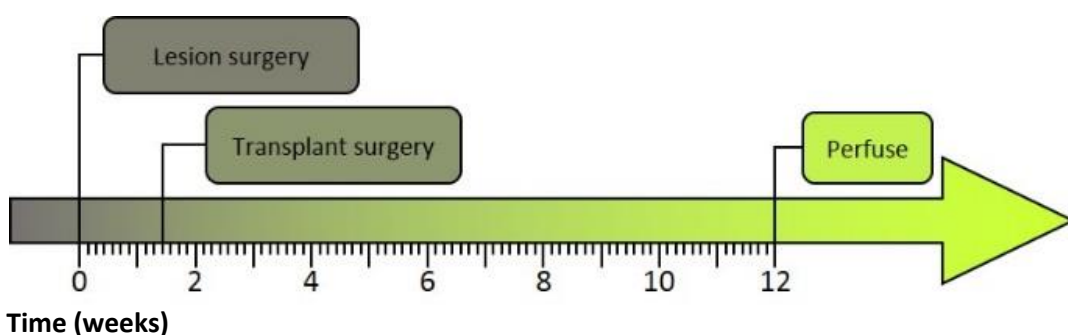


**Figure 3.13** Experimental timeline.

### Transplantation surgery

From ten days post-lesion animals received a unilateral transplant into the lesion site as described in methods section 2.2.3. Surgery sessions were planned to be split over four days with a counter-balanced number of animals from each group receiving transplants on each day, i.e. one of each strain receiving tissue from one of three dissections, **Figure 3.14**. Therefore, for each donor strain, four different suspensions were made (one for each day of surgery) thus reducing any effect of any one suspension being of a reduced quality.

One pregnant female of each strain was dissected each day prior to surgery, and the WGEs dissected from E14 embryos and made into single-cell suspensions of  $150,000 \text{ cells}\mu\text{l}^{-1}$  as described in methods section 2.2.2.

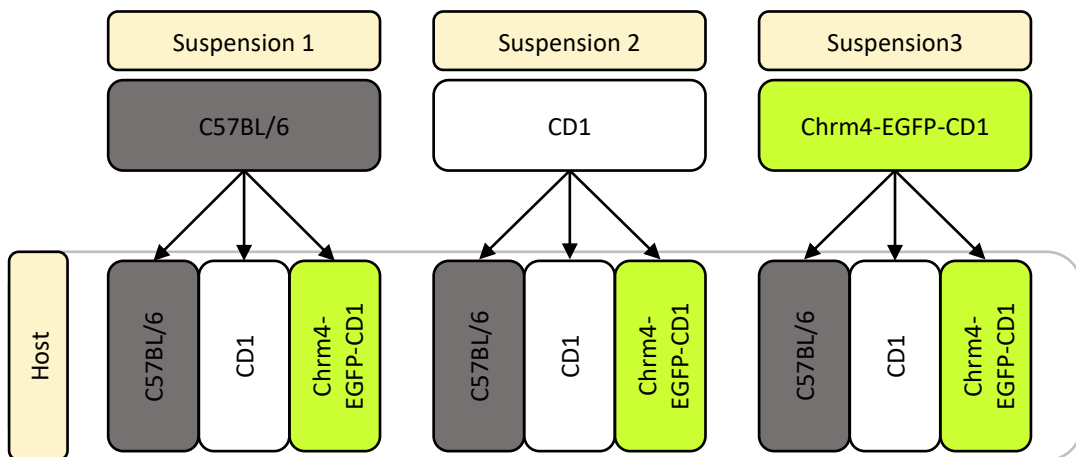


**Figure 3.14** Schematic depicting how groups were counter-balanced for each surgery day.

Due to problems obtaining pregnant Chrm4-EGFP-CD1 females, one batch of this suspension was transplanted on a separate day, and another set was not able to receive transplants at all, **Table 3.5**.

Each mouse received a total of 300,000 cells split between two  $1\mu\text{l}$  deposits of cell suspension at two depths within the same tract at the lesion site.

### 3.15.2 Immunohistochemical analysis of the grafts and microglia

At 12 weeks post-transplantation all mice were transcardially perfused as described in methods section 2.3.1, and brains transferred to sucrose solution for 48 hrs.

Brains were sectioned on a freezing-stage microtome into 40µm thick sections and stored in anti-freeze at -20°C. Cresyl violet (CV) staining was performed on 1:12 sections as described in section 3.3.2, and immunohistochemical staining was performed on free-floating sections using GFP, NeuN and Iba1 antibodies.

Graft location was determined by observing areas of altered parenchyma structure on the CV stained sections and graft survival was verified by the presence of cells within the relatively NeuN<sup>+</sup> depleted lesion at this site. Graft volume and cells counts were measured on NeuN<sup>+</sup> stained sections, and microglial density from Iba1 stained sections were calculated as describe in section 3.9.2.

The number of dead or rejected cells was assessed in all animals by attributing semi-quantitative grading scores (adapted from (Duan et al., 1995) between 0 and 6 according to the following criteria; (0) No visible dead cells, (1) < 5 dead cells, (2) one group of 5+ dead cells, (3) two or more groups of 5+ dead cells, (4) large region with dead cells, (5) multiple large regions of dead cells, or (6) dead cells throughout entire grafted region.

### 3.15.3 Statistical analysis

In the 12-week period between transplantation and perfusion, one CD1 mouse transplanted with C57BL/6 tissue, one C57BL/6 mouse transplanted with CD1 tissue and one Chrm4-EGFP-CD1 mouse transplanted with CD1 tissue became unwell and were euthanised before the end of the experiment. The final experimental group numbers are therefore summarised in **Table 3.5**.

Host	Donor		
	C57BL/6J	CD1	Chrm4-EGFP-CD1
C57BL/6J	4	3	3
CD1	3	4	3
Chrm4-EGFP-CD1	4	3	3

**Table 3.5** Summary of final group numbers.

Statistical analysis was performed using Genstat (18<sup>th</sup> edition) or IBM SPSS Statistics 23. ANOVAs, Kruskal-Wallis or student's t-tests were performed to compare experimental groups and between hemispheres where appropriate.

Newman-Keuls' post hoc pairwise comparisons were performed to analyse significant interactions, correcting for multiple comparisons. Significance was taken as  $p \leq 0.05$ .

Post-hoc power analysis based on final animal numbers was calculated using G\*Power software and was estimated to be 99% for large effect sizes and 83% for medium effect sizes.

Whilst descriptive data of individual groups was informative, statistical comparisons between these groups was not viable since some groups had just two surviving grafts to analyse. However, it was possible to analyse main effects of host and donor in the combined groups.

### 3.16 Results

#### Graft survival and placement

Densely stained areas of parenchymal disruption were observed in the CV-stained sections signifying the transplanted region, **Figure 3.15 A**. Grafted cells were identified in the corresponding NeuN<sup>+</sup> stained sections, **Figure 3.15 B - D**. Surviving grafts were located centrally within the lesioned striatum in all groups and survival rates are summarised in **Table 3.6** and **Figure 3.16 A**. No effect on graft survival of host strain or donor strain was found (Host:  $F_{2,6}=0.29$ , ns; Donor:  $F_{2,6}=0.61$ , ns), **Figure 3.16 B - C**. Fewer grafts survived in the mismatched donor/host combinations than in those which were matched (Strain:  $t_6=3.80$ ,  $p<0.01$ ), **Figure 3.16 D**.

#### Graft volume and cell counts

While grafts still appeared small and narrow in comparison to those described in rat studies, they were generally larger than in the previous experiment, including those transplanted under the same conditions **Table 3.6**. Graft volumes of each group are summarised in **Figure 3.16 E**. There was no effect of host on the volume of the grafts (Host:  $F_{2,21}=2.97$ , ns), **Figure 3.16 F**. A main effect of donor on graft volume was observed, however, although there was a trend towards the Chrm4-EGFP-CD1 tissue yielding a greater graft volume, no significant differences between the Chrm4-EGFP-CD1 and the C57BL/6 or CD1 groups was shown in post hoc analyses (Donor:  $F_{2,21}=4.53$ ,  $p<0.05$ ;  $t_{21}=2.24$ , ns and  $t_{21}=2.86$ , ns respectively), **Figure 3.16 G**. There was a trend for the between-strain transplants to produce larger grafts than the within-strain transplants, however, this was not significant (Strain:  $t_{23}=1.65$ , ns), **Figure 3.16 H**.

NeuN<sup>+</sup> cell counts from each group are summarised in **Figure 3.17 A**. Whilst a main effect of host on cell number was observed, the trend towards CD1 hosts yielding lower counts was not statistically different to either the C57BL/6 or Chrm4-EGFP-CD1 group (Host:  $F_{2,21}=4.55$ ,  $p<0.05$ ;  $t_{21}=2.67$ , ns;  $t_{21}=2.55$ , ns respectively), **Figure 3.17 B**. There was no effect of donor on cell number (Donor:  $F_{2,21}=2.45$ , ns), **Figure 3.17 C**. There was a trend for the between-strain transplants to yield a greater number of cells than the within-strain transplants, however, this was not significant (Strain:  $t_{23}=1.81$ , ns), **Figure 3.17 D**.

**Figure 3.17 E** summarises the cell density within the grafts for each group. There was no effect of host on graft cell density (Host:  $F_{2,21}=3.02$ , ns), **Figure 3.17 F**, and no effect of donor

strain (Donor:  $F_{2,21}=3.20$ , ns), **Figure 3.17 G**. Neither was there a difference in cell density in grafts in the between-strain and within-strain models (Strain:  $t_{23}=0.62$ , ns), **Figure 3.17 H**.

### Dead cell grading

Dead cells were observed in all groups, examples of which are shown in **Figure 3.18 A - B**, and each mouse was assigned a grade based on how many dead cells were found within the grafted region. No difference in grade was found between host strains, donor strains or between mismatched groups ( $\chi^2(2)=0.15$ , ns;  $\chi^2(2)=1.70$ , ns and  $\chi^2(1)=0.07$ , ns respectively), **Figure 3.19 A - C**.

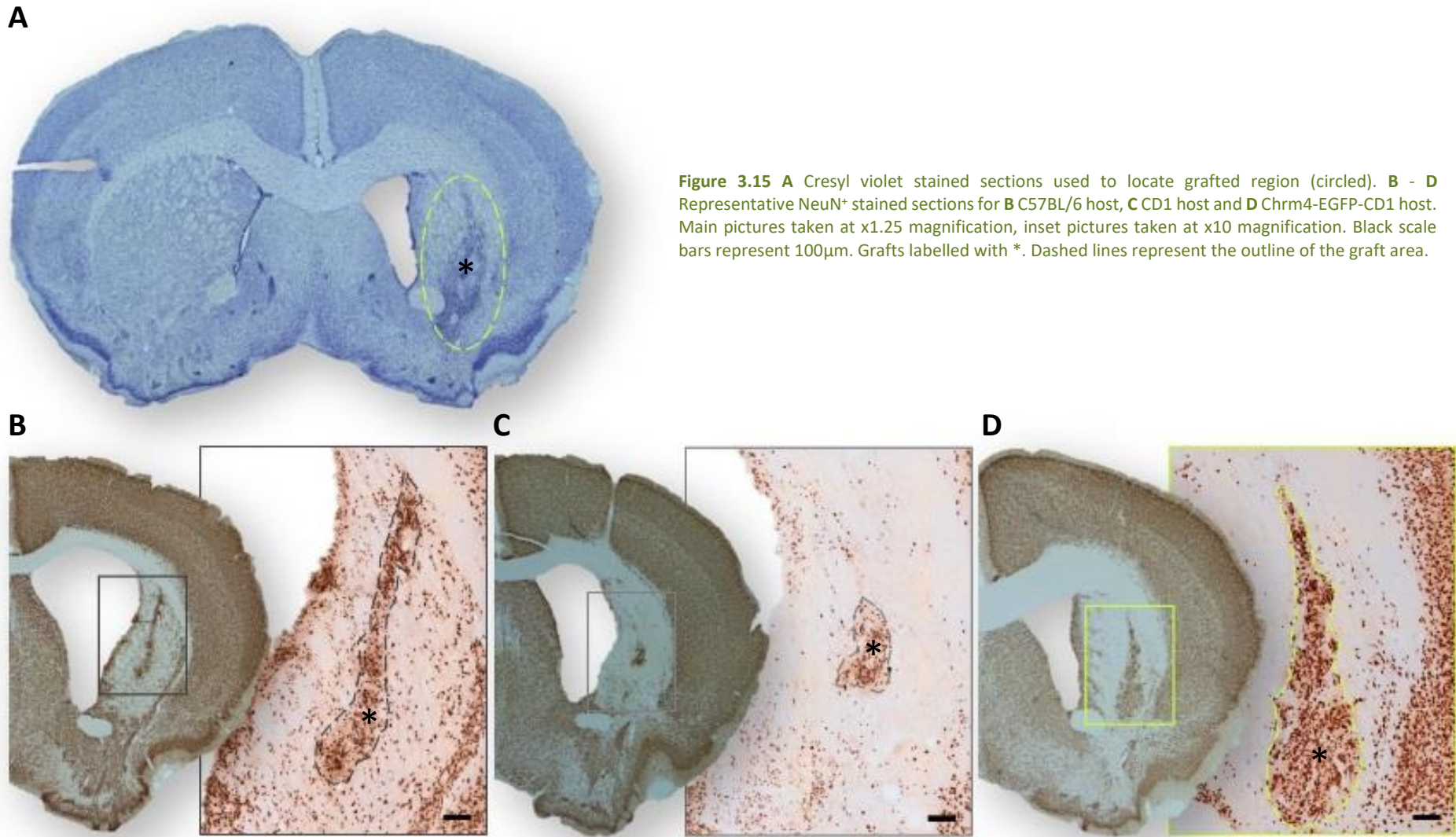
### Inflammatory response to grafting

Activated microglia were seen in the ipsilateral striatum in all host strain groups, **Figure 3.20**. Microglia density was significantly greater in the ipsilateral side compared to the contralateral side, (Side:  $F_{2,16}=166.26$ ,  $p<0.001$ ), however no effect of host or donor strain was seen (Side\*Host:  $F_{2,2}=1.24$ , ns; Side\*Donor:  $F_{2,2}=1.33$ , ns), **Figure 3.21 A - B**. Neither was there an effect of between- and within-strain donor/host combinations (Side\*Strain:  $F_{1,1}=0.32$ , ns), **Figure 3.21 C**.

There was no effect of host or donor strain on the proportional change in microglial density on the lesioned side (Host:  $F_{2,16}=2.51$ , ns; Donor:  $F_{2,16}=1.25$ , ns), nor of between- and within-strain combinations (Strain:  $t_{23}=0.43$ , ns), **Figure 3.21 D-F**.

Host	Donor	Number of surviving grafts	Mean graft volume ( $\times 10^5 \mu\text{m}^3$ )	Graft volume range ( $\times 10^5 \mu\text{m}^3$ )	Number of NeuN <sup>+</sup> cells ( $\times 10^2$ )
	C57BL/6	4 of 4 (100%)	189.3 $\pm$ 39.6	100.6 - 266.6	102.5 $\pm$ 11.1
C57BL/6	CD1	2 of 3 (67%)	163.6 $\pm$ 113.1	50.5 - 276.6	87.4 $\pm$ 66.4
	M4	2 of 3 (67%)	420.3 $\pm$ 322.2	98.1 - 742.5	129.1 $\pm$ 62.1
	C57BL/6	2 of 3 (67%)	41.8 $\pm$ 26.31	15.5 - 68.1	29.0 $\pm$ 8.5
CD1	CD1	4 of 4 (100%)	35.0 $\pm$ 21.4	8.4 - 98.8	16.14 $\pm$ 6.5
	M4	2 of 3 (67%)	329.4 $\pm$ 12.1	317.3 - 341.5	137.6 $\pm$ 6.7
	C57BL/6	3 of 4 (75%)	276.9 $\pm$ 140.9	128.8 - 558.4	112.2 $\pm$ 59.1
M4	CD1	3 of 3 (100%)	277.6 $\pm$ 65.1	148.3 - 355.5	124.5 $\pm$ 15.7
	M4	3 of 3 (100%)	231.1 $\pm$ 52.6	122.0 - 304.4	87.7 $\pm$ 16.6

**Table 3.6** Summary of graft survival, NeuN<sup>+</sup> graft volume and cell counts. M4 = Chrm4-EGFP-CD1.



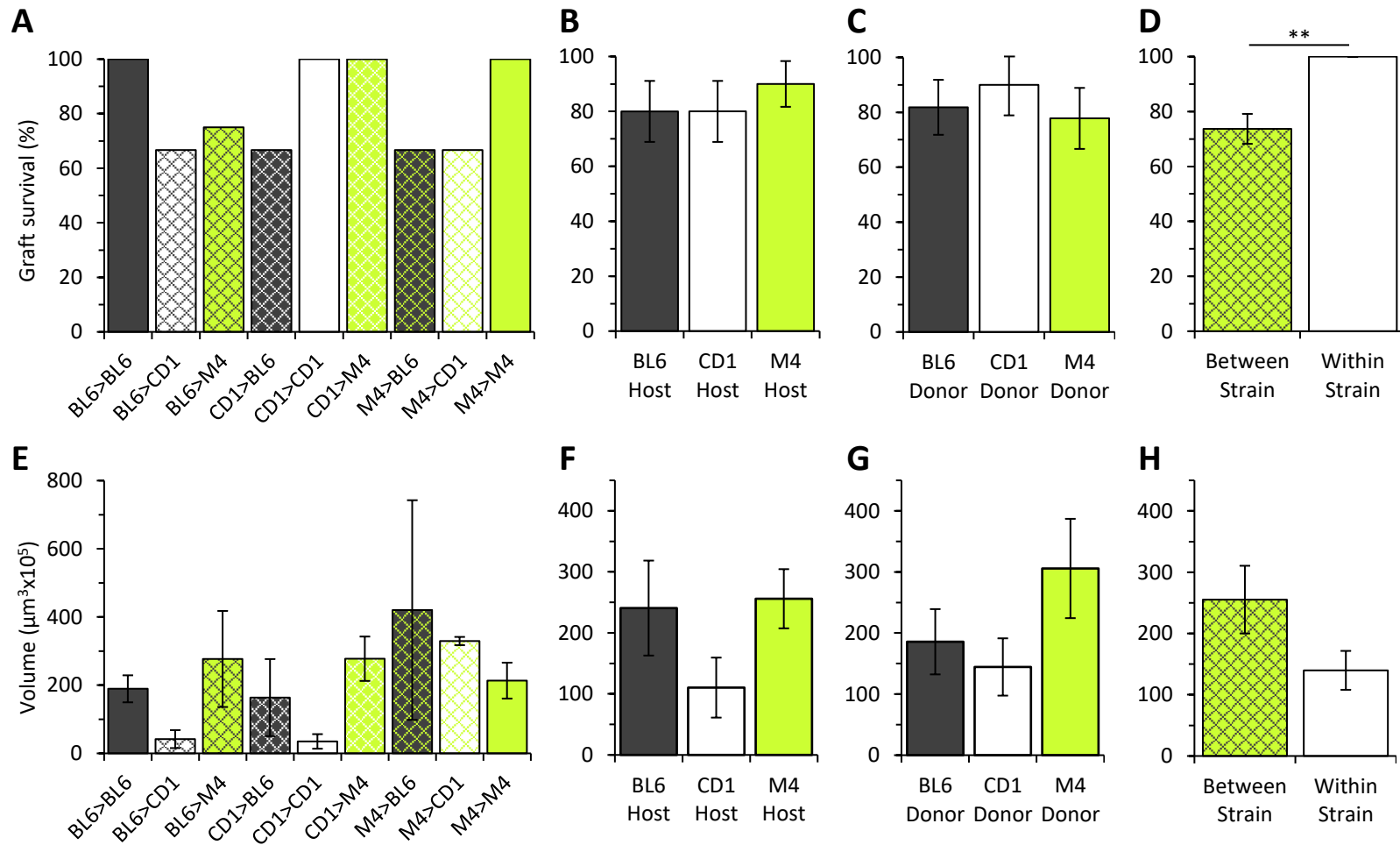


**Figure 3.16** **A** Graft survival in each group (number of surviving grafts / number animals transplanted). **B** Graft survival grouped by host strain. There was no effect of host on graft survival. **C** Graft survival grouped by donor strain. No effect of donor was found. **D** Graft survival grouped by between- and within-strain donor/host pairing. 100% of within-strain grafts survived whilst ~74% of between-strain grafts survived (\*\*  $p < 0.01$ ). **E** NeuN<sup>+</sup> volume of grafts in each group. **F** NeuN<sup>+</sup> volume of grafts grouped by host strain. There was no effect of host. **G** NeuN<sup>+</sup> volume of grafts grouped by donor strain. No statistical difference between donor groups was found. **H** NeuN<sup>+</sup> volume of grafts grouped by between- and within-strain donor/host pairing. No effect of strain was found. BL6 = C57BL/6, M4 = Chr4-EGFP-CD1.

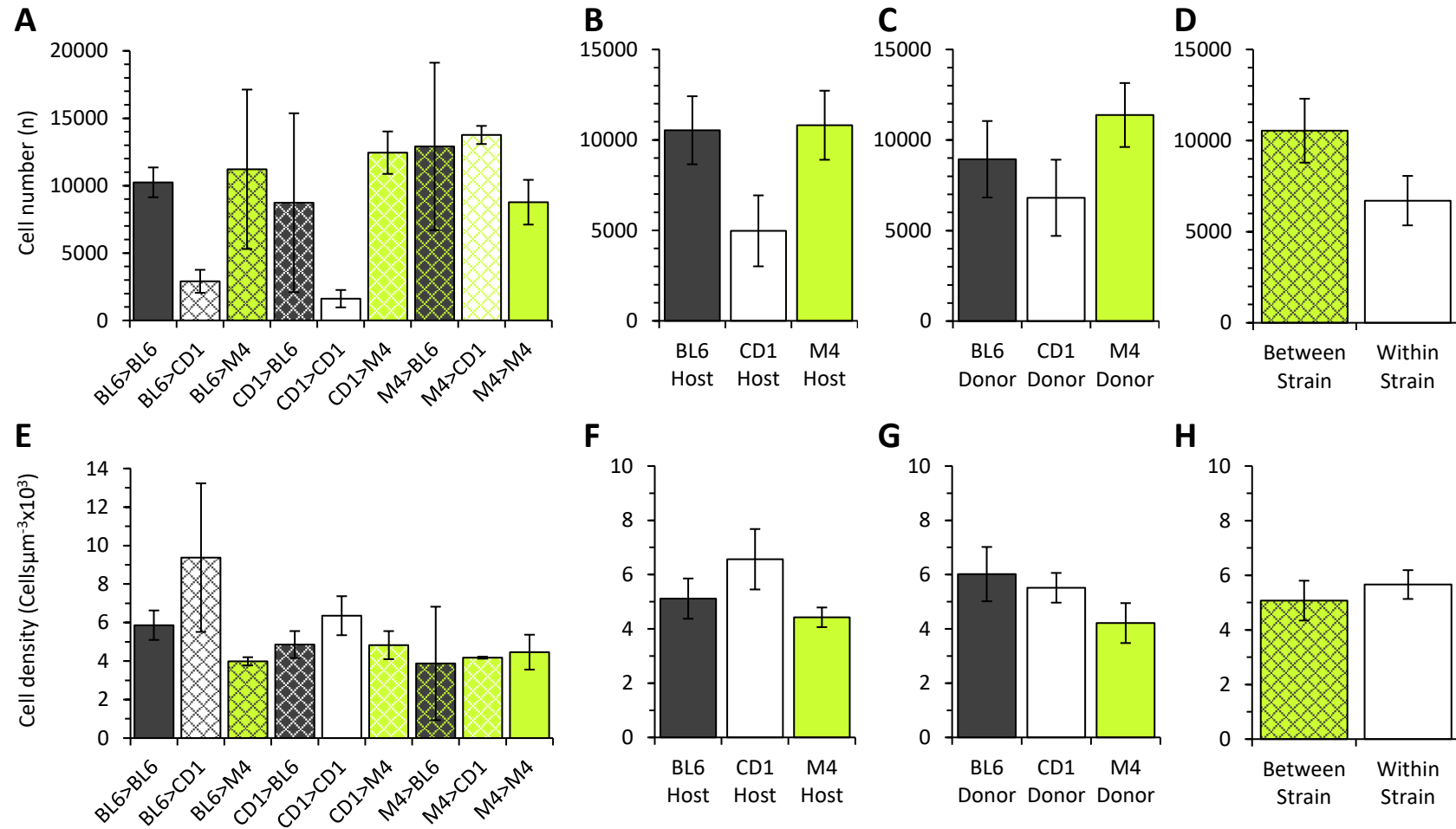


**Figure 3.17** A NeuN<sup>+</sup> cell count of grafts in each group. B NeuN<sup>+</sup> cell count of grafts grouped by host strain. There was a main effect of group ( $p < 0.05$ ), however, post-hoc analysis was unable to detect a statistical difference between any group pair. C NeuN<sup>+</sup> cell count of grafts grouped by donor strain. No effect of donor was found. D NeuN<sup>+</sup> cell count of grafts grouped by between- and within-strain donor/host pairing. No difference was found. E NeuN<sup>+</sup> cell density in grafts in each group. F NeuN<sup>+</sup> cell density in grafts grouped by host strain. No effect of host on graft cell density was found. G NeuN<sup>+</sup> cell density in grafts grouped by donor strain. No effect of donor was detected. H NeuN<sup>+</sup> cell density in grafts grouped by between- and within-strain donor/host pairing. No effect of strain mismatching was found. BL6 = C57BL/6, M4 = Chr4-EGFP-CD1.

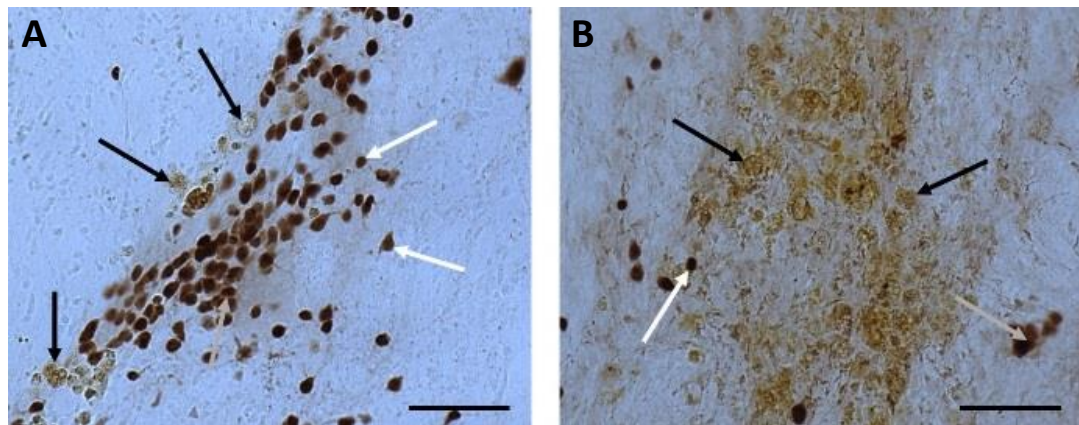


**Figure 3.18** NeuN<sup>+</sup> stained sections showing examples of healthy-looking grafted cells (white arrows), dead cells (black arrows) and cell which look unhealthy (grey). **A** An example of a graft scoring 3 in grading scale. **B** An example of a graft scoring 6 in grading scale. Images taken at x20 magnification. Black scale bars represent 100µm.

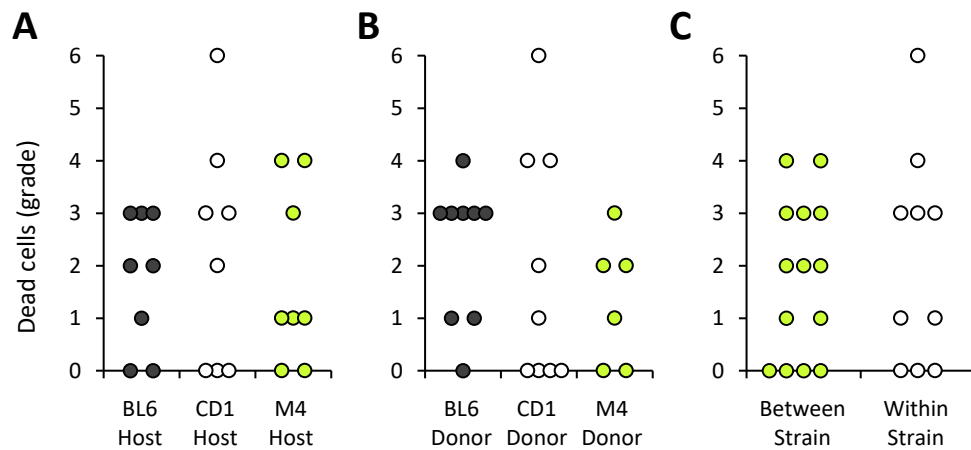


**Figure 3.19** Grade assigned for number of dead cells found within the grafted region of each animal, grouped by **A** host strain, **B** donor strain and **C** as between- or within-strain donor/host pairing. No effect of host, donor or strain combination was found. BL6 = C57BL/6, M4 = Chr4-EGFP-CD1.

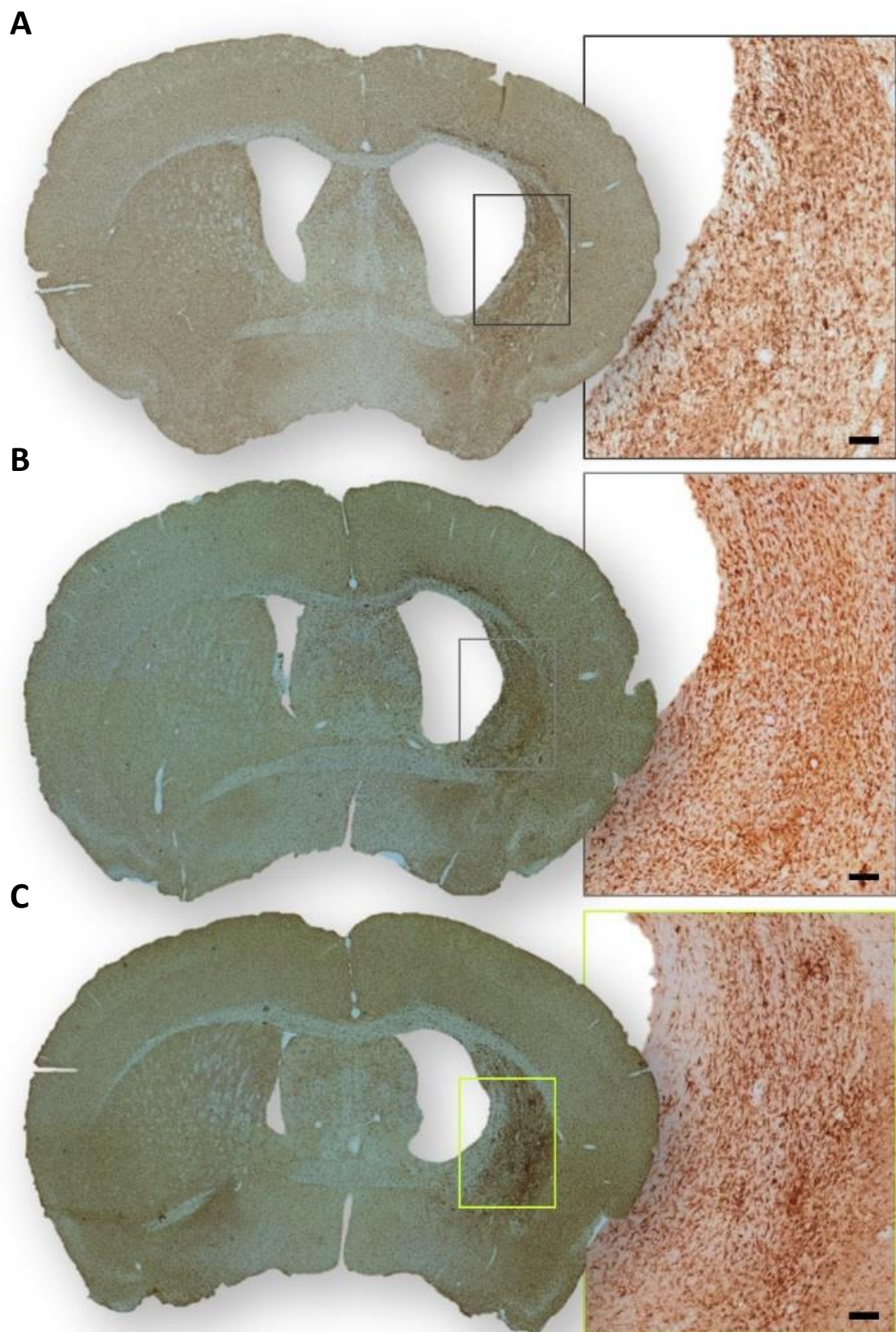


**Figure 3.20** Iba1 staining of microglia in a representative example **A** C57BL/6 host, **B** CD1 host and **C** Chrm4-EGFP-CD1 host. Main pictures taken at x1.25 magnification. Inset pictures of ipsilateral side taken at x10 magnification. Black scale bars represent 100µm.

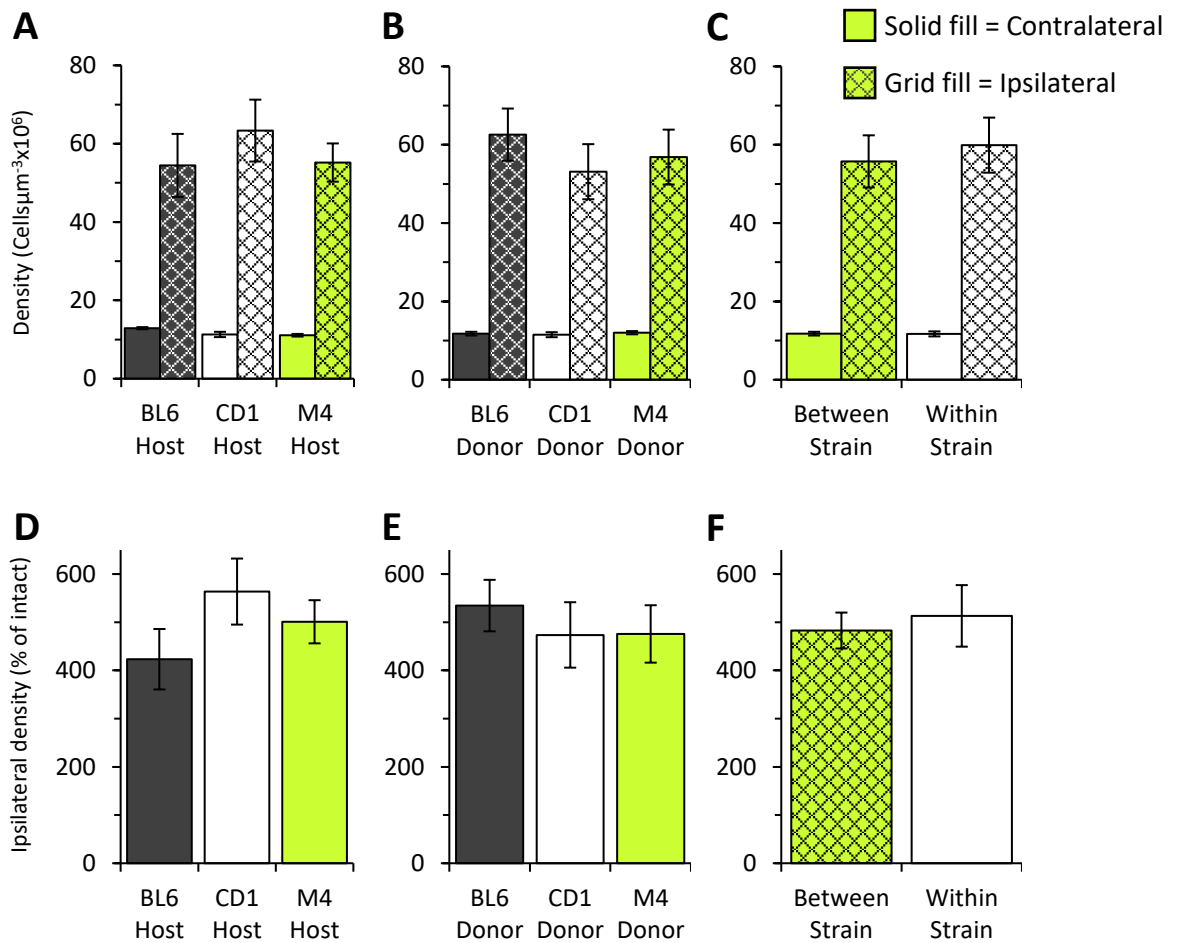


**Figure 3.21** **A** Ipsi- and contralateral microglial cell density in hosts with surviving grafts grouped by host strain. Ipsilateral density was greater than the contralateral density ( $p < 0.001$ ). No difference between groups was found. **B** Ipsi- and contralateral microglial cell density in hosts with surviving grafts grouped by donor strain. There was no effect of donor. **C** Ipsi- and contralateral microglial cell density in hosts with surviving grafts grouped by between- and within-strain donor/host pairing. No effect of strain mismatching was found. **D** Change in microglia density in hosts with surviving grafts as a proportion of contralateral side grouped by host strain. No difference between groups was found. **E** Change in microglia density in hosts with surviving grafts as a proportion of contralateral side grouped by donor strain. There was no effect of donor. **F** Change in microglia density in hosts with surviving grafts as a proportion of contralateral side grouped by between- and within-strain donor/host pairing. No effect of strain mismatching was found. BL6 = C57BL/6, M4 = Chrm4-EGFP-CD1.

### 3.17 Discussion

This experiment aimed to separate the effects of mouse host and donor strains on graft survival and morphology by transplanting tissue derived from three different donor strains into three host strains. The resultant grafts were compared and analysed for size, cell content and degree of inflammatory response observed. The effect of the matched and mismatched tissue combinations was also evaluated.

#### C57BL/6 hosts do not have an exaggerated immune response compared to other mouse strains

Very few significant differences or consistent trends were found for a beneficial effect of one host strain over another. It is possible that this is due to underpowered tests since individual groups were very small once non-surviving grafts had been removed from analysis. A study that used increased groups sizes and less comparisons may well give a clearer result, but any strain differences that are present are likely to be modest.

The number of dead cells found in each group was not significantly different, regardless of host strain, suggesting that the problem of poor grafts extend beyond an exaggerated response from the C57BL/6 strain, but again this interpretation is suggested with the caveat that the study is the constrained by small group sizes.

#### Chrm4-EGFP-CD1 neural tissue is not more immunogenic compared to neural tissues of other mouse strains

No effect of strain was found in the microglial response to transplanted tissue, and there was no consistent difference in graft outcome. However, there was trend towards the Chrm4-EGFP-CD1 tissue producing larger grafts than the CD1 or C57BL/6 strains and this is certainly suggestive that Chrm4-EGFP-CD1 tissue does not induce a greater inflammatory response, nor that these cells are more susceptible to rejection. However, stem cells isolated from different strains of mice have shown differences in proliferation rates and differentiation potential (Peister et al., 2004), and the inherent strain differences in the phenotype of the cells transplanted were not probed in this study. Therefore, it is unknown if a particular strain was more proliferative, but subsequently had less cells survive up to the 12-week time-point. The properties of the progenitor cells of the three strains could be assessed by culturing the cell suspensions *in vitro* before quantifying proliferation and differentiation though immunocytochemical stains, such as the mature neuronal marker

$\beta$ -tubulin and early markers of MSN fate CTIP2 and FOXP1. Alternatively, a repeated *in vivo* experiment with groups taken at different time-points during graft development could also provide evidence for this.

#### Matching donor/host strains increased survival but did not improve graft content

Whereas graft survival was consistent with the previously described experiment for those derived from mismatched donor and host strain, there was improved survival in those from matched strains, in fact, matched combinations showed a 100% rate of survival in this experiment. However, no improvement in the size or cell numbers within the grafts was identified, nor was there any apparent difference in the host microglial response to the transplanted tissue. While the greater survival rates might be expected in those transplanted between animals of the least MHC disparity (Chen et al., 2011), it would also be expected that improved cell survival and graft volume would be observed. It is possible that mismatching strains might influence the speed of graft rejection rather than improving the conditions for the transplanted cells. Since all were taken at the same time-point it is not possible to say whether the matched strain grafts may have undergone a slow rejection process later.

These data should be interpreted with care since, although suggestive, the small group sizes mean that a small loss in graft survival creates a large difference in the percentage score. In fact, of the mismatched groups, only one graft for each did not contain any surviving cells. While there is some evidence here to suggest that the matched strains would lead to improved survival, it is necessary for a larger experiment to be carried out to verify the observations.

#### Graft outcome was inconsistent under similar transplant conditions

The cells transplanted under the standard conditions in this experiment resulted in a larger mean graft volume than those seen in the previous experiment (Experiment 2: M4 tissue into BL6 host mean graft volume =  $97.3 \pm 51.9 \times 10^5 \mu\text{m}^3$ ; Experiment 3: M4 tissue into BL6 host mean graft volume =  $420.3 \pm 322.29 \times 10^5 \mu\text{m}^3$ ). This could be explained by a number of reasons: (a) the cell suspensions, despite having a similar viability score upon dissection, may have been from higher quality embryos or dissected in a slightly different way, or, alternatively, (b) the host animals may have been exposed to fewer pathogens which are known to exacerbate inflammation within the CNS (Combrinck et al., 2002; Perry and Teeling, 2013). However, it is unlikely that these conditions would have changed significantly within

the time-course of the experiments. A further difference that could potentially have had an effect is (c), that fewer mice were transplanted from each cell suspension in the current experiment. Only three mice were transplanted per suspension here, whereas up to fourteen were for **Experiment 2**. It is possible that repeated extraction of cells from the aliquot could be detrimental to the remaining cells over time, or that more cells are taken up during earlier surgeries leaving fewer left in the suspension for subsequent transplantations. Since the timing of transplantation surgeries are counter-balanced between groups and across days, this should not affect the results of individual comparisons within experiments, providing that the groups are large enough. However, it could be a problem in general and be contributing to lower success rates in the mice. Surviving cell numbers from the previous two experiments, and **Experiment 4**, is assessed with respect to the order of surgery at the beginning of **Experiment 5** in the next chapter.

#### Differences in NeuN<sup>+</sup> grafted cell morphology

It is interesting to note that a different NeuN antibody was used in this study, one which was raised in rabbit rather than mouse. The resultant immunological stains contained far less non-specific staining, possibly previously linked to immunoglobulins released at the site of surgery. Therefore, the new antibody allowed for very clear identification of the grafts and brought attention to morphological differences between some NeuN<sup>+</sup> cells within the grafts. While most cells had crisp edges and dark staining, and obviously dead cells were orange-coloured and spherical, a few cells seemed to be slightly larger, have a slightly paler brown staining and a fluffiness to their edges. While these cells were counted in the surviving cell counts, it is proposed that these cells may be in the process of undergoing rejection, however, it was not possible to confirm this within the scope of the present experiment.

### 3.18 Conclusions and future work

As a pilot study, this experiment was able to show there may be differences to graft outcome driven by donor and host choice in mouse striatal transplantation, such as higher survival in within-strain transplants and possible trends that individual combinations may be unsuited. However, the group sizes became too small to analyse with statistical confidence. Through comparing too many strains, and therefore complicating any donor or host effects, and counterbalancing the design across surgery days, potential interactions were lost. A greater

number of transplants could have been completed from each suspension if one donor strain type had been used each day, however the risk of a poor cell preparation affecting any particular group would then be increased.

A study design with a greater group size and a simplified model comparison is discussed in **Experiment 4**, which was completed in collaboration with another PhD student (VHR) and enabled a greater number of surgeries of each type to be completed on each day.

# Chapter 4

## Exploring the effects of donor tissue and cell preparations

### 4 Chapter summary

The experiments of the previous chapter predominantly concentrated on the host effects on transplantation outcome in lesion models of HD. The next set of experiments will examine another part of the equation, the donor tissue. **Experiment 3** considered the effect of strain choice; however, it is important to also consider the procedural parameters of the cell preparation, and how the quality of the suspension, prior to transplantation, may change over the surgical period.

Therefore, the experiments in this chapter aimed to determine how changes to the cell preparation protocols, specifically, the effects of donor age and dissociation technique, can affect graft outcome (**Experiment 4**). In addition, the characteristics of single-cell suspensions were examined for changes in viability and homogeneity which could impact the graft outcome (**Experiment 5**).

## Experiment 4

### The effect of tissue preparation and donor age<sup>§</sup>

#### 4.1 Summary

The first experiment of this chapter re-examines the effects of altering some of the fundamental components of the standard transplantation protocols established in the rat model; donor age and tissue dissociation.

Transplants of WGE tissue of donor age E12 and E14 were compared in combination with different degrees of tissue dissociation, either through triturating to a single-cell suspension or by processing with minimal dissociation to leave a tissue-piece style preparation. Cells were transplanted in two donor/host paradigms; the between-strain Chrm4-EGFP-CD1 tissue into C57Bl/6 mice, as predominantly used for the previous experiments in this thesis; and the CD1 into CD1 within-strain model<sup>§</sup>.

Grafts were analysed after twelve weeks and assessed in terms of volume, cell number, DARPP-32<sup>+</sup> content and parvalbumin<sup>+</sup> interneuron content. The content of the grafts was considered in more detail than in previous chapters to establish the effects of treatment on the critical MSN content. The host immune response to the transplants was gauged based on the severity of microglial response.

Furthermore, cells from each donor age were assessed *in vitro* for differences in proliferation and differentiation.

---

<sup>§</sup> Declaration.

This experiment was conducted in collaboration with another PhD student; Victoria Robertson, who discussed the data relating to the CD1 mice in her thesis (Robertson, 2014). Tissue dissections were performed by Ngoc Nga Vinh. Data from this experiment was published in Cell Transplantation (2017), **Appendix 4**.

## 4.2 Introduction

### Rat transplantation protocols need to be reassessed for translation to mice

Protocols have been optimised and are well established for rat to rat striatal transplants, with extensive preclinical literature showing consistent large and functional grafts from E14-E16 WGEs (Fricker et al., 1997; Schmidt et al., 1981). Rat protocols have been refined over many years, with donor age and tissue preparation identified as critical factors affecting graft survival, morphology and function of rat to rat striatal transplants (Björklund and Stenevi, 1984; Kromer et al., 1983; Watts et al., 2000a), however, these factors have not been systematically investigated in mice. It is evident throughout the literature (Cisbani et al., 2014; El Akabawy et al., 2012; Johann et al., 2007; Kelly et al., 2007; Robertson et al., 2013), and from the data presented in the preceding experiments, that the direct translation of these protocols to mice results in considerable graft variability.

### The influence of donor age on graft outcome

Studies in rat to rat transplants have shown that the optimal donor age varies depending on tissue type used, and more specifically on the developmental stage of those particular neuronal types (Torres et al., 2007; Kromer et al., 1983). The most effective age is considered to be when the precursor cells are at the stage of proliferation and final mitotic division *in vivo*, with survival of cells after this time significantly reduced (Björklund and Stenevi, 1984). Rat studies comparing grafts of different neural tissue found that early differentiating tissues, such as brainstem and spinal cord were more successful when tissue of early stage embryos (E15 – E17) was transplanted, whereas those tissues of later stage development, such as hippocampus, were more successful using later stage embryos of E20 – E22, as measured by graft volume (Kromer et al., 1983). This accords well with the viability of different populations cultured *in vitro*, explored systematically by Olson et al., (1983).

When donor age for striatal transplantation of WGE in rats was investigated specifically, it was found that the largest grafts, greatest number of MSNs and most improved behavioural recovery were generated from tissue taken closest to the time of striatal neurogenesis (Fricker et al., 1997; Schackel et al., 2013; Watts et al., 1997).

Striatal neurogenesis in the rat typically first occurs between E12.5 and E14.5 (Bayer, 1984). The majority of rat transplantation studies use tissue at age E14 and produce large, functional and DARPP-32<sup>+</sup> rich grafts (Döbrössy and Dunnett, 1998; Dunnett and White,

2006; Mazzocchi-Jones et al., 2009). In mice the lateral ganglionic eminence (LGE), the source of striatal progenitors (Deacon et al., 1994), is visible by E12, while the medial ganglionic eminence (MGE), where interneurons are born, is visible as early as E11 (Olsson et al., 1998; Smart and Sturrock, 1979). To obtain the neural diversity in grafts closest to that seen in the adult striatum, it is necessary to transplant both the LGE and MGE (the whole ganglionic eminence – WGE) (Olsson et al., 1998; Watts et al., 2000a), indicating that E12 might be the earliest time point for obtaining all the necessary cell types in mice. This is supported by comparing the Carnegie stages of development in the mouse and rat, given that age E14 in the rat relates to approximately age E12.5 in the mouse (Butler and Juurlink, 1987), **Figure 4.1**.

The different developmental rates seen between the species may suggest that an earlier donor of E12 may be more comparable for seeing similar results in the mice.



**Figure 4.1** The relationship between embryonic age and Carnegie stage of the rat and mouse. Adapted from (H. and B.H.J. 1987).

#### The influence of tissue preparation on graft outcome

Historic clinical trials of striatal cell replacement in Parkinson's disease (PD) and HD patients have typically transplanted suspensions of tissue pieces (A.-C. Bachoud-Lévi et al., 2000; A. Bachoud-Lévi et al., 2000; Kopyov et al., 1998), although others have employed dissociated single cell suspensions (Rosser, 2002). The effect of the tissue processing and preparation methods used prior to implantation is a vital consideration for graft survival and development.

There are potential benefits of delivering the transplant as tissue pieces, rather than triturated cell suspensions. Limiting the manipulation of the tissue can reduce disruption and death of neuronal populations within the preparation, and the retention of the extracellular

matrix may protect cells during transplantation (Thomas et al., 1999) and in the initial post-graft period. However, it has been suggested that the transplantation of whole tissue pieces may induce a stronger immune response due to the presence of the intact donor vasculature and antigen presenting cells (Chen et al., 2011; Redmond et al., 2008). Although the use of non-immunogenic bio-engineered scaffolds could avoid this issue (Newland et al., 2015; Wang et al., 2016), protocols generally require dissociation of cells prior to seeding into a scaffold, therefore still posing a risk to neuronal populations. Preparing tissue as partly digested tissue pieces without trituration (Rath et al., 2012; Watts et al., 2000b) may prevent disruption to MSN precursors prior to transplantation and thus improve graft survival.

The development of trypsinised single cell suspensions provided an advantage over solid pieces of tissue by potentially allowing transplanted cells access to the host capillary network more easily. The necessity of establishing contact in order to nourish the grafted tissue was demonstrated early on in studies implanting on vessel-rich and vessel-poor microenvironments (Stenevi et al., 1976). Rat to rat grafts derived from transplantation of single-cell suspensions have been shown to produce a greater proportion of striatal-like tissue, and larger DARPP-32 expressing cell populations than those of tissue pieces, as well as providing greater innervation of the host parenchyma (Watts et al., 2000b), however tissue pieces wielded the larger overall graft volume.

#### Different tissue preparations could induce different immunological responses

As highlighted in the previous experiments, mice express an acute microglial inflammatory response to lesions, as well as a chronic response to transplanted tissue. The severity of this response appears to be unaffected by the timing of the transplantation after lesioning or the age or strain of the host, or the between-strain or within-strain combination. However, it remains unclear if the immunogenicity of the transplant could be affected by the developmental age of the tissue, or by altering the treatment of the cell suspension. Differences in the host response to kidney transplants suggest that older tissues elicit a greater inflammatory response in humans and rats (Reutzel-Selke et al., 2007; Tasaki et al., 2014), therefore, reducing the age of the donor tissue may have a beneficial effect in the mice.

Dissociated cell suspensions are also thought to provoke less of a host immune response when transplanted because the immunogenic donor vasculature is destroyed prior to implantation (Baker-Cairns et al., 1996; Chen et al., 2011). Further benefits include the ability to screen the cells for counts, viability and health in advance of implantation, thus allowing

an extra quality control. However, the process of trypsinisation and manual trituration involved in preparing a dissociated suspension could cause physical damage to the cells and reduce the population viability, whereas preparation of tissue pieces is far less disruptive.

The current study aimed to examine the resulting phenotypes of striatal grafts of mouse primary embryonic tissue prepared under a variety of conditions to determine how current standard protocols of transplantation could be adapted to produce more reliable and effective grafts in mouse models.

Grafts derived from the most commonly used donor age (E14) were compared with an earlier gestation (E12) to determine whether survival and morphology of primary foetal striatal transplants in mice could be improved by using younger tissue. In addition, the effect of cell suspension preparation was explored by comparing standard dissociated single cell suspensions (CS) with non-triturated partially digested tissue piece suspensions (TP), to establish whether reducing the amount and severity of tissue manipulation could improve the resultant grafts of the transplanted tissue. Both donor ages were compared using each preparation method to ascertain the most appropriate method of preparing tissue.

These conditions were tested in two strain paradigms to determine how the choice of model could affect the experimental outcome. Between-strain and within-strain conditions were compared using Chrm4-EGFP-CD1 tissue transplanted into C57BL6/J hosts and CD1 donor tissue transplanted into CD1 hosts respectively. To elucidate some of the findings discussed in **Experiment 3**, larger group sizes and a simplified donor/host combination were used, and the graft cellular composition was explored in more detail. The host response to transplantation, including the disparity in immunological background between donor and host, and the preparation of transplanted cells, was also considered.

## 4.3 Methods

### 4.3.1 Experimental design

#### Host animals

Young adult male C57BL6/J (n=33) and CD1 (n=33) mice (20-30g, Harlan, Bicester, UK) were used in this experiment. Thirty mice of each strain received unilateral QA Lesions to the mid-dorsal striatum (methods section 2.2.1), with three mice of each strain retained as intact controls. The same stereotaxic coordinates were used for both strains.

#### Donor tissue

Two transplant paradigms were used; a within-strain (W-S) model with CD1 tissue transplanted into CD1 hosts, and a between-strain (B-S) model with Chrm4-EGFP-CD1 tissue transplanted into C57BL/6J hosts.

E12 or E14 embryos were dissected from time-mated CD1 and Chrm4-EGFP-CD1 mice from an in-house colony (originally purchased from Harlan, Bicester, UK and MMRRC, City, USA respectively). Four transplant preparations were made for each donor strain: 1) E12 single cell (CS); 2) E12 tissue pieces (TP); 3) E14 CS; and 4) E14 TP. Transplantation surgery was spread across multiple days with fresh suspensions made each morning for each group.

#### Transplantation surgery

Approximately 10 days post-lesion mice were randomly assigned to experimental groups with 20 C57BL6/J and 27 CD1 mice receiving primary tissue transplants (n=6-7 per group) as described in methods section 2.2.3, Figure 4.2. In addition, a group of mice from each strain were retained as lesion-only controls (C57BL6/J n=2, CD1 n=3).

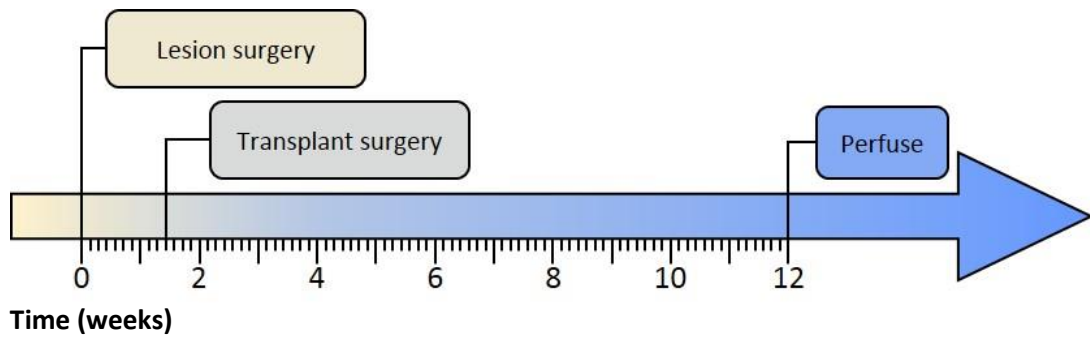


Figure 4.2 Experimental timeline.

### Single cell preparations

CS preparations consisted of pooled E12 or E14 WGEs for each strain prepared as described in methods section 2.2.2. Cells were concentrated at 250,000 cells/ $\mu$ l for transplantation. 1 $\mu$ l of suspension was injected at each of two depths, depositing approximately 500,000 cells in total into the lesioned striatum over 2 min.

### Tissue piece preparations

For TP preparations, no cell counts could be conducted directly from non-dissociated tissue, therefore WGE units equating to approximately 500,000 cells (the number of cells transplanted in the CS groups) were transplanted. Cell counts calculated from the CS dissections showed this to equal approximately a pair of WGEs for E12 tissue and a single WGE for E14, see Table 4.1. Each preparation was treated as with CS, however, after gentle washing, tissue was transferred directly into  $\sim$ 4 $\mu$ l DMEM/F12 for transplantation, with no trituration and minimal mechanical manipulation to maintain integrity of the tissue pieces. TP preparations were injected as above, at a rate of 1 $\mu$ l/min over 4 min (2min at each depth). Mice were monitored daily until full recovery.

### *In vitro* primary cultures

Time-mated CD1 dams were sacrificed at E12 or E14 (n=3 per group), and WGEs dissected as previously described. Tissue from each litter was pooled to prepare three separate suspensions for each embryonic age and plated down for *in vitro* culturing as described in methods section 2.4.1. After 24 hrs and 7 days *in vitro*, 12 wells of each suspension were fixed with 4% PFA and stored at 4°C until immunocytochemical staining.

### 4.3.2 Immunohistochemistry and immunocytochemistry

At 12 weeks after transplantation surgery, mice were perfused, and the brains processed for histological analysis of the grafts, as described in methods section 2.3.1. Brains were cut at 40µm on a freezing microtome, and sections stored in anti-freeze at -20°C until immunohistochemical analysis. 1:12 series were incubated as free-floating sections with primary antibodies for NeuN, Iba1, parvalbumin or anti-GFP and labelled with DAB. Parvalbumin series were double-stained with DARPP-32 and Vector SG kit.

Cultured cells were labelled with the following pairs of primary antibodies, as described in methods section 2.4.2.;  $\beta$ -tubulin and GFAP or early MSN markers FoxP1 and CTIP2 and labelled with the following fluorescent secondary antibodies; Alexa594 (red) for  $\beta$ -tubulin and CTIP2 and Alexa488 (green) for GFAP and FoxP1. All cells were counter-stained with Hoechst (blue) before being mounted onto microscope slides. Cell counts were conducted under fluorescent microscopy with five regions per coverslip counted, and the mean count from each suspension recorded.

Donor strain	Embryonic age	Preparation	Cells per WGE	Proportion WGE transplanted	Number cells transplanted
Chrm4-EGFP-CD1	E12	CS	180,769	2.77	500,000
Chrm4-EGFP-CD1	E12	TP	180,769	2.00	361,538
Chrm4-EGFP-CD1	E14	CS	577,273	0.87	500,000
Chrm4-EGFP-CD1	E14	TP	577,273	1.00	577,273
CD1	E12	CS	357,143	1.40	500,000
CD1	E12	TP	357,143	2.00	714,286
CD1	E14	CS	1,041,667	0.48	500,000
CD1	E14	TP	1,041,667	1.00	1,041,667

**Table 4.1** CS = single cell preparation; TP = tissue piece style preparation. The number of cells per WGE was estimated based of the mean cell counts of the CS preparations. The number of WGEs used in the TP preparations was adjusted based on the mean number of cells in the WGE for each particular donor strain and age with the aim of transplanting a similar number of cells in each group. Since it was only possible to use whole WGE units in the non-dissociated TP preparations, the number of cells transplanted could not be exactly matched but was kept as close to 500,000 as possible. Subsequently the proportion of WGE transplanted was used to transform the data to account for the differences in proliferative potential of the cells transplanted.

### 4.3.3 Analysis of grafts and microglia

The location of grafts in the C57BL6/J hosts was identified through immunohistochemical labelling of the transplanted Chrm4-EGFP-CD1 tissue using an anti-GFP antibody. The presence of fully differentiated adult neurons (NeuN<sup>+</sup> cells) within the grafted area was used to determine graft survival in all groups, and grafts with no positive NeuN staining excluded from analyses. These non-surviving transplants were retained in the analysis of microglial immune response.

Volumes were calculated by measuring cross-sectional areas of NeuN<sup>+</sup> (total graft volume) and DARPP-32<sup>+</sup> graft regions (P-zones) across 1:12 series and using the formula:  $Volume = (\Sigma A * M) / f$ , where A = area of graft ( $\mu\text{m}^2$ ), M = section thickness ( $\mu\text{m}$ ) and f = section frequency).

For smaller grafts, total cell numbers were counted manually using Image J software following imaging of grafted sections, however, this was not feasible for larger grafts, therefore these were calculated by unbiased stereology. Mean cell diameter was obtained for NeuN<sup>+</sup>, DARPP-32<sup>+</sup> and parvalbumin<sup>+</sup> cells by measuring the minimum and maximum diameters of ten cells per graft using Image J.

Iba1 labelled series were used to grade the host microglial response in the grafted area using an established semi-quantitative rating scale (Duan et al., 1995). Each section was graded 0-4 according to the following categories; (0) No specific activated microglia in the graft area; (1) Low number of activated microglia, distributed as scattered single cells or clustered in a few small patches in or around the graft; (2) Several activated microglia distributed as single cells or clustered in multiple, prominent patches; (3) Dense immunostaining of the graft area and a large number of activated microglia in and around the graft; (4) Very dense immunostaining of the whole graft area and a very large number of activated microglia in and around the graft. Activated microglia were easily identified by their darker staining and morphological appearance (Boche et al., 2013). The highest grade given to any section for each animal was the grade assigned to that animal.

As TP were not dissociated, transplants were prepared by WGE units rather than by cell number. Embryos used for CS and TP were collected from the same litters, so although cell number could not be determined, an estimate of the number of cells per WGE at each age was calculated using total counts from the CS and dividing by the total number of WGEs dissociated, see [Table 4.1](#). Since E12 WGE contained approximately half the number of cells

of E14 WGE, a pair of E12 WGEs were transplanted for each E14 WGE to maintain a consistent total cell number, as close to 500,000 as possible. However, transplanting different proportions of WGE raises the issue that the E12 TP grafts of two WGEs may have twice the proliferative potential of the single WGE E14 TP. As it is not possible to control for both cell number and quantity of WGE transplanted, graft outcome measures were subsequently transformed to account for the proportion of WGE transplanted as described below;

Cell counts and volume data were corrected for the proportion of WGE transplanted, to yield values per unit WGE at each age, using the following transformations;  $Tn = n / \text{proportion of WGE transplanted}$  and  $Tvol = vol / \text{proportion of WGE transplanted}$ , where  $\text{proportion of WGE transplanted} = \text{number of cells transplanted} / \text{mean number of cells in WGE}$ ,  $Tn$  = corrected cell count,  $n$  = actual cell count,  $Tvol$  = corrected volume and  $vol$  = actual volume.

#### 4.3.4 Statistical analysis

After accounting for loss of animals due to ill health, the final group sizes are summarised in **Table 4.2**.

Transformed data from successful grafts in all groups were analysed together using ANOVAs using Genstat (18<sup>th</sup> edition) or Kruskal-Wallis tests as appropriate. Between-strain and within-strain groups were subsequently analysed in separate ANOVAs. For immune response data, transplanted mice with no detectable surviving grafts, as well as lesion only controls were also included in the analyses.

Sidak's post hoc pairwise comparisons were performed to analyse significant interactions, correcting for multiple comparisons. Significance was taken as  $p \leq 0.05$ .

Post-hoc power analysis based on final animal numbers was calculated using G\*Power software and was estimated to be 99% for large effect sizes and 83% for medium effect sizes.

<b>Group</b>	<b>C57BL6/J</b>	<b>CD1</b>
Intact control	3	3
Lesion only control	2	3
E12 CS	5	6
E12 TP	5	7
E14 CS	4	7
E14 TP	6	7

**Table 4.2** Summary of final group numbers.

## 4.4 Results

### Graft survival and placement

The presence of DAB-labelled GFP<sup>+</sup> Chrm4-EGFP-CD1 donor cells corresponded with areas of NeuN<sup>+</sup> and DARPP-32<sup>+</sup> staining in the C57BL6/J hosts, confirming the donor origin of the cells, **Figure 4.3 A - B**. Transplanted cells could be clearly identified within the lesioned host striatum on NeuN stained sections. The proportion of surviving grafts for each group, and raw untransformed data for surviving grafts are shown in **Table 4.3**. A high proportion of grafts survived in all groups (80 – 100%) except for E14 TP, of which only 5 out of 13 (38%) transplanted mice had NeuN<sup>+</sup> cells in the grafted region after 12 weeks, **Figure 4.4 A**. There was no difference in graft survival between the between-strain (Chrm4-EGFP-CD1 tissue into C57BL6/J hosts; B-S) and within-strain (CD1 tissue into CD1 hosts; W-S) groups ( $t_6=0.20$ , ns). Graft volumes varied both within and between groups, ranging from just  $12 \times 10^6 \mu\text{m}^3$  up to  $588 \times 10^6 \mu\text{m}^3$ .

### Graft volume and cellular composition

**Figure 4.4 B** shows the volumes of NeuN<sup>+</sup> tissue in the surviving grafts for each group and a comparison of mean graft volume of the B-S and W-S groups. Grafts from the W-S group were significantly larger than those observed in the B-S group (Strain:  $F_{1, 27}=19.08$ ,  $p<0.001$ ). E14 tissue yielded larger graft volume than the E12 in both the B-S and W-S groups (Age:  $F_{1, 11}=4.90$ ,  $p<0.05$  and  $F_{1, 16}=12.21$ ,  $p<0.01$  respectively). CS yielded larger graft volume than TP in the W-S groups only (B-S Preparation:  $F_{1, 11}=0.03$ , ns; W-S  $F_{1, 16}=15.68$ ,  $p<0.001$ ). Preparations of E14 CS yielded significantly larger grafts than E14 TP in the B-S model, while the younger E12 tissue produced larger grafts when prepared as TP than as CS (Age\*Preparation:  $F_{1, 11}=16.93$ ,  $p<0.01$ ; E12 (Preparation):  $t_{11}=2.79$ ,  $p<0.05$ ; E14 (Preparation):  $t_{11}=3.04$ ,  $p<0.05$ ). In the W-S model, E14 CS also yielded significantly larger grafts compared to E14 TP, however there was no significant difference between grafts derived from different preparations of E12 tissue (Age\*Preparation:  $F_{1, 16}=12.21$ ,  $p<0.001$ ; E12 (Preparation):  $t_{16}=0.13$ , ns; E14 (Preparation):  $t_{16}=5.73$ ,  $p<0.001$ ).

Distinct regions of DARPP 32<sup>+</sup> staining were observed within all surviving grafts (**Figure 4.3 C**). The volume of DARPP-32<sup>+</sup> patches (P-zones) within each graft is shown in **Figure 4.4 C**. W-S transplants yielded significantly larger total P-zone volumes than B-S (Strain:  $F_{1, 27}=6.50$ ,  $p<0.05$ ). There was no main effect of Age on DARPP-32<sup>+</sup> in either B-S or W-S groups although

in both cases this approached significance (B-S Age:  $F_{1, 11}=4.66$ ,  $p=0.054$ ; W-S  $F_{1, 16}=4.12$ ,  $p=0.059$ ). No main effect of preparation on DARPP-32<sup>+</sup> volume was seen in either the B-S or W-S groups (B-S Preparation:  $F_{1, 11}=0.86$ , ns; W-S  $F_{1, 16}=0.00$ , ns). B-S transplants contained larger P-zone volumes when transplanted as CS than TP at E14, while the reverse was true for E12 tissue (Age\*Preparation:  $F_{1, 11}=21.30$ ,  $p<0.001$ ; E12 (Preparation):  $t_{11}=2.61$ ,  $p<0.05$ ; E14 (Preparation):  $t_{11}=3.93$ ,  $p<0.01$ ). A similar trend was observed in the W-S groups; however, a statistically significant interaction was not found (Age\*Preparation:  $F_{1, 16}=4.06$ , ns).

There were no differences in the proportion of DARPP-32<sup>+</sup> P-zone volume in B-S and W-S groups (Strain:  $F_{1, 27}=0.05$ , ns), **Figure 4.4 D**. There was no effect of Age in either the B-S or W-S groups (Age:  $F_{1, 11}=0.50$ , ns;  $F_{1, 16}=2.18$ , ns respectively), and TP yielded a higher proportion of DARPP-32<sup>+</sup> tissue than CS in the W-S group only (B-S Preparation:  $F_{1, 11}=0.92$ , ns; W-S  $F_{1, 16}=13.88$ ,  $p<0.01$ ). B-S transplants showed a trend towards higher proportion of P-zones in E14 CS compared to E14 TP, although this was not statistically significant (Age\*Preparation:  $F_{1, 11}=1.84$ , ns). No trend in the B-S E12 preparations was observed. W-S E12 groups again showed a tendency for higher proportions of P-zone tissue from E12 transplants as TP rather than CS. At E14, TP tended towards a larger DARPP-32<sup>+</sup> proportion compared to CS (Age\*Preparation:  $F_{1, 16}=0.27$ , ns).

There was no difference between B-S and W-S transplants in the total number of mature NeuN<sup>+</sup> neurons within the grafts (Strain:  $F_{1, 27}=0.18$ , ns), **Figure 4.5 A**. No main effects of Age or Preparation were found in the B-S groups (Age:  $F_{1, 11}=0.37$ , ns; Preparation:  $F_{1, 11}=0.14$ , ns), however, for the W-S groups, E14 tissue and TP yielded a greater cell number than E12 and CS respectively (Age:  $F_{1, 16}=7.68$ ,  $p<0.05$ ; Preparation:  $F_{1, 16}=12.22$ ,  $p<0.01$ ). Cell counts reflected the data patterns observed in graft volume, with E14 CS yielding more cells than E14 TP and E12 TP yielding more cells than E12 CS in both strain types, however despite a significant Age\*Preparation interaction in the B-S group, the post hoc comparisons did not reach significance (B-S Age\*Preparation:  $F_{1, 11}=10.23$ ,  $p<0.01$ ; E12 (Preparation):  $t_{11}=2.53$ , ns; E14 (Preparation):  $t_{11}=2.01$ , ns). (W-S Age\*Preparation:  $F_{1, 16}=13.08$ ,  $p<0.01$ ; E12 (Preparation):  $t_{16}=0.09$ , ns; E14 (Preparation):  $t_{16}=5.03$ ,  $p<0.001$ ).

The W-S grafts contained more DARPP-32<sup>+</sup> cells than B-S (Strain:  $F_{1, 27}=21.43$ ,  $p<0.001$ ), **Figure 4.5 B**. Grafts of E14 tissue contained more DARPP-32<sup>+</sup> cells than those of E12 origin in both B-S and W-S groups (Age:  $F_{1, 11}=7.83$ ,  $p<0.05$  and  $F_{1, 16}=13.60$ ,  $p<0.01$  respectively), although there was no effect of preparation (B-S Preparation:  $F_{1, 11}=3.82$ , ns; W-S

$F_{1, 16}=3.03$ , ns). E14 tissue yielded higher DARPP-32<sup>+</sup> content when transplanted as CS than TP, while there was a trend for E12 to produce more as TP in both the B-S (Age\*Preparation:  $F_{1,11}=20.11$ ,  $p<0.001$ ; E12 (Preparation):  $t_{11}=1.79$ , ns; E14 (Preparation):  $t_{11}=4.56$ ,  $p<0.01$ ) and W-S groups (Age\*Preparation:  $F_{1,16}=8.94$ ,  $p<0.01$ ; E12 (Preparation):  $t_{16}=0.88$ , ns; E14 (Preparation):  $t_{16}=3.34$ ,  $p<0.01$ ).

Parvalbumin<sup>+</sup> cells constituted  $6.2\pm 0.79$  of the NeuN<sup>+</sup> cell population, with significantly more parvalbumin<sup>+</sup> cells found in W-S transplants compared to B-S ( $F_{1, 27}=20.67$ ,  $p<0.001$ ), **Figure 4.5 C**. In addition, E14 generated more parvalbumin<sup>+</sup> cells than E12 tissue in both B-S and W-S groups (Age:  $F_{1, 11}=16.50$ ,  $p<0.01$  and  $F_{1, 16}=19.39$ ,  $p<0.001$  respectively), and CS yielded more than TP preparations (Preparation:  $F_{1, 11}=9.39$ ,  $p<0.05$  and  $F_{1, 16}=4.49$ ,  $p<0.05$  respectively), although this effect was mostly due to very high numbers in the E14 CS groups compared to all other combinations. E14 CS grafts contained significantly more parvalbumin<sup>+</sup> cells than E14 TP in both the B-S and W-S groups and there was a trend for E12 TP to yield more than E12 CS but this did not reach significance (B-S Age\*Preparation:  $F_{1, 11}=11.81$ ,  $p<0.01$ ; E12 (Preparation):  $t_{11}=0.26$ , ns; E14 (Preparation):  $t_{11}=4.61$ ,  $p<0.001$ ) (W-S Age\*Preparation:  $F_{1, 16}=18.40$ ,  $p<0.001$ ; E12 (Preparation):  $t_{16}=1.54$ , ns; E14 (Preparation):  $t_{16}=4.54$ ,  $p<0.001$ ).

#### Microglial response

Iba1 labelling revealed dense areas of microglial activation, not only within the grafted area, but extending beyond the transplant boundaries to the host striatum in all mice except for intact control animals **Figure 4.3 D**. Numerous dead cells and cellular debris were observed within most grafts and needle tracts, visible in sections stained with DAB as spherical clusters of paler staining.

**Figure 4.6** shows the graded microglial response for each group, including the lesion only and intact control animals. Activation of microglia within grafted groups was significantly higher in B-S than W-S groups ( $\chi^2(1)=22.53$ ,  $p<0.001$ ). There was no difference in the microglial reaction in response to preparation type ( $\chi^2(1)=0.09$ , ns), or donor age ( $\chi^2(1)=1.38$ , ns).

There was no difference in the degree of microglial activation within the B-S grafted groups ( $\chi^2(3)=0.73$ , ns), or the W-S groups ( $\chi^2(3)=7.38$ , ns).

The intact control did not exhibit any signs of microglial activation, whereas the lesion only controls presented a moderate degree of activation which was not significantly different to

the grafted animals (Surgery:  $\chi^2(2)=58.00$ ,  $p<0.001$ ; Intact-Lesioned:  $\chi^2=28.90$ ,  $p<0.05$ ; Intact-Grafted:  $\chi^2=29.0$ ,  $p<0.001$  and Lesioned-Grafted:  $\chi^2=0.11$ , ns).

#### Differentiation *in vitro*

To investigate the development and maturation of cells from E12 and E14 donor embryos independently of the host environment, CS from CD1 embryos were prepared as described for transplantation and cultured for 24hrs and 7 days *in vitro*, **Figure 4.7**. As TP preparations were not dissociated, it was not possible to culture these comparably. Cell counts from primary cultures are shown in **Figure 4.8**. There was no difference in the proportion of  $\beta$ -Tubulin<sup>+</sup> cells across any age or time-point (DIV:  $F_{1,8}=2.09$ , ns; Age: ( $F_{1,8}=4.04$ , ns). Very few GFAP<sup>+</sup> cells were found in any group, however there were significantly more after 7 days compared to 24 hours *in vitro* (DIV:  $F_{1,8}=16.99$ ,  $p<0.01$ ), but no effect of donor age was found (Age: ( $F_{1,8}=1.37$ , ns). There was a significant increase in the proportion of CTIP2<sup>+</sup> cells at 7 DIV compared to 24 hrs (DIV:  $F_{1,8}=44.52$ ,  $p<0.001$ ) but no effect of embryonic age (Age: ( $F_{1,8}=1.88$ , ns). FoxP1<sup>+</sup> MSN precursor cells also accounted for a higher proportion of the population at 7 DIV compared to 24 hrs (DIV:  $F_{1,8}=78.21$ ,  $p<0.001$ ) with no effect of embryonic age (Age: ( $F_{1,8}=4.84$ , ns).

Host strain	Group	Number of surviving grafts	Graft volume (x10 <sup>6</sup> μm <sup>3</sup> )	Number of NeuN <sup>+</sup> cells (x10 <sup>3</sup> )	P-zone volume (x10 <sup>6</sup> μm <sup>3</sup> )	Number of DARPP-32 <sup>+</sup> cells (x10 <sup>3</sup> )	% DARPP-32 <sup>+</sup> patches
C57BL6/J	E12 CS	4 of 5 (80%)	110.3±52.4	11.1±5.1	61.2±42.4	1.4±0.7	51.0%
C57BL6/J	E12 TP	5 of 5 (100%)	301.6±88.5	28.4±8.0	180.6±67.7	2.5±0.8	55.5%
C57BL6/J	E14 CS	4 of 4 (100%)	188.9±32.7	12.9±4.1	127.6±5.7	2.4±0.4	74.4%
C57BL6/J	E14 TP	2 of 6 (33%)	97.0±16.3	6.8±0.5	44.7±3.7	0.8±0.5	48.1%
CD1	E12 CS	5 of 6 (83%)	226.0±52.9	11.1±2.4	91.1±31.1	2.1±0.5	34.0%
CD1	E12 TP	6 of 7 (86%)	335.6±46.5	16.4±2.8	237.5±66.4	4.2±0.7	68.4%
CD1	E14 CS	6 of 7 (86%)	194.0±21.6	9.6±1.4	84.3±16.9	2.3±0.4	44.3%
CD1	E14 TP	3 of 7 (43%)	146.9±36.8	6.6±1.6	119.0±25.6	2.5±0.3	89.9%

**Table 4.3** CS = single cell preparation; TP = tissue piece preparation. Untransformed data presented ±SEM. High graft survival rates were seen in most groups with the exception of those derived from E14 TP. Large differences in graft volume and cell numbers were observed within groups.

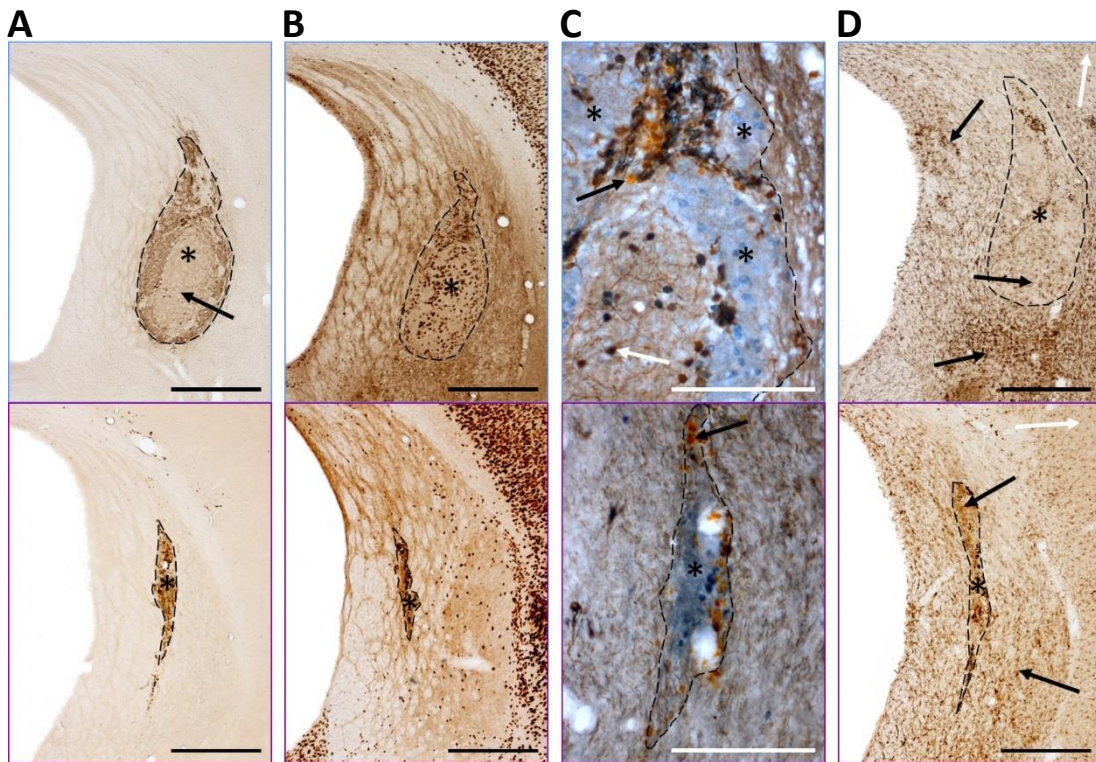


**Figure 4.3** Photomicrographs of typical large and smaller grafts (top and bottom row respectively). **A** GFP<sup>+</sup> staining identifying Chrm4-EGFP-CD1 grafted tissue (\*) within the host parenchyma. Paler areas of non-MSN cell types are seen within the graft (indicated by arrow). Black scale bar represents 500µm. **B** NeuN<sup>+</sup> staining of mature neurons. Areas of grafted cells can be clearly identified within the lesioned striatum (\*). Black scale bar represents 500µm. **C** DARPP-32<sup>+</sup> staining (blue) shows distinct P-zones within the grafts (indicated by \*). Parvalbumin<sup>+</sup> interneurons (brown stain) (white arrow) are present throughout the grafts. Black arrows highlight the non-specific orange-coloured staining of spherical dead cells. White scale bar represents 100µm. **D** Iba1<sup>+</sup> staining of microglia. Resting-state ramified cells (white arrow) can be seen on the peripheral cortex areas. Clusters of darker, amoeboid activated cells (black arrow) can be seen within the grafts (\*) and the surrounding striatum. Black scale bar represents 500µm.

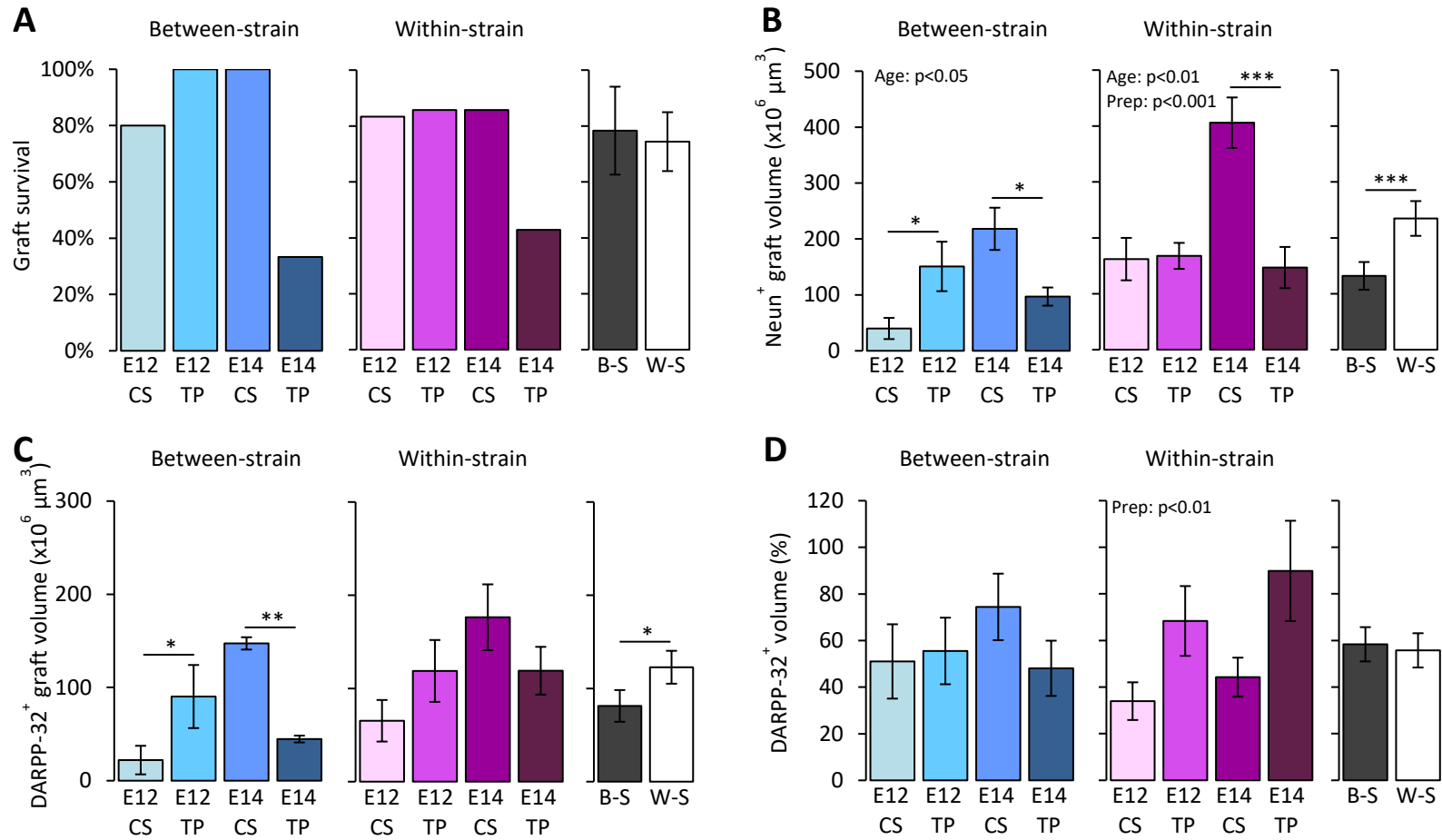


**Figure 4.4** **A** Graft survival (number of surviving grafts / number of animals transplanted). The E14 TP transplants had the lowest survival rates in both the B-S and W-S groups. **B** NeuN<sup>+</sup> graft volumes. W-S transplants were larger than the B-S (\*\*\*)  $p < 0.001$ ). E14 tissue produced larger grafts than E12 in the B-S ( $p < 0.05$ ) and W-S ( $p < 0.01$ ) groups. E14 tissue yielded a larger volume than E12 tissue when transplanted as CS in both the B-S ( $* p < 0.05$ ) and W-S strain (\*\*\*)  $p < 0.001$ ) models. E12 tissue yielded a larger volume when transplanted as TP than CS in the B-S model only ( $* p < 0.05$ ). **C** DARPP-32<sup>+</sup> graft volumes. W-S transplants contained a larger volume of DARPP-32<sup>+</sup> tissue than the B-S ( $* p < 0.05$ ). E14 tissue yielded a larger volume when transplanted as CS than TP (\*\*  $p < 0.01$ ). E12 tissue yielded a larger volume when transplanted as TP than CS ( $* p < 0.05$ ). **D** Proportion of DARPP-32<sup>+</sup> graft tissue. There was no difference in the proportion of DARPP-32<sup>+</sup> tissue in the different models, however, TP yielded a higher proportion of DARPP-32<sup>+</sup> tissue than CS in the W-S group ( $p < 0.01$ ). All data presented **B - D** is adjusted for proportion of WGE transplanted.

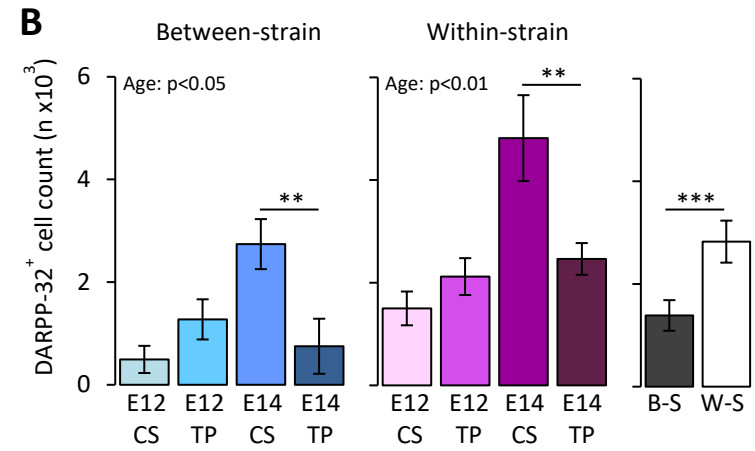
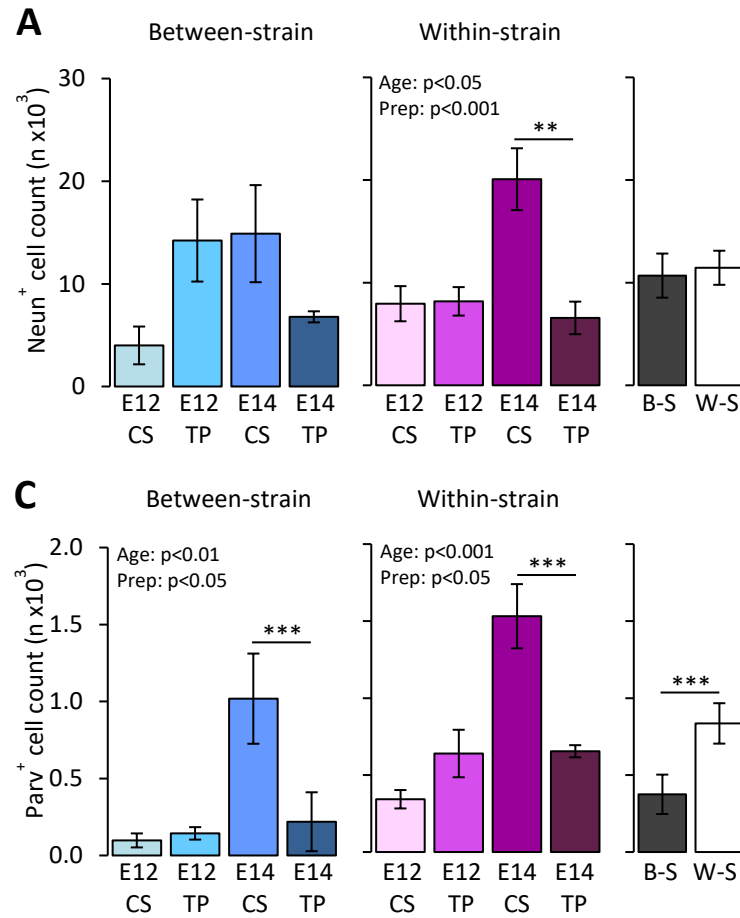


**Figure 4.5** **A** NeuN<sup>+</sup> graft cell counts. No effect of model on neuronal cell counts was detected. E14 tissue yielded a greater number of neurons when transplanted as CS than as TP in the W-S group (\*\* p<0.01). **B** DARPP-32<sup>+</sup> cell counts. More DARPP-32<sup>+</sup> cells were present in the W-S grafts than the B-S (\*\*\* p<0.001). E14 tissue produced more DARPP-32<sup>+</sup> cells than E12 in both the B-S (p<0.05) and W-S (p<0.01) models. E14 tissue yielded a higher DARPP-32<sup>+</sup> cell count when transplanted as CS than TP in the B-S (\*\* p<0.01) and W-S (\*\* p<0.01). **C** Parvalbumin<sup>+</sup> cell counts. A greater number of parvalbumin<sup>+</sup> interneurons were present in the W-S model than the B-S (\*\*\* p<0.001). E14 tissue yielded a greater number of parvalbumin<sup>+</sup> interneurons than E12 in both the B-S (p<0.01) and W-S (p<0.001) models. TP produced more interneuron than CS in the B-S (p<0.05) and W-S (p<0.05) groups. E14 tissue yielded a higher parvalbumin<sup>+</sup> cell count when transplanted as CS than TP in the B-S (\*\*\* p<0.001) and W-S (\*\*\* p<0.001) models. All data presented is adjusted for proportion of WGE transplanted.



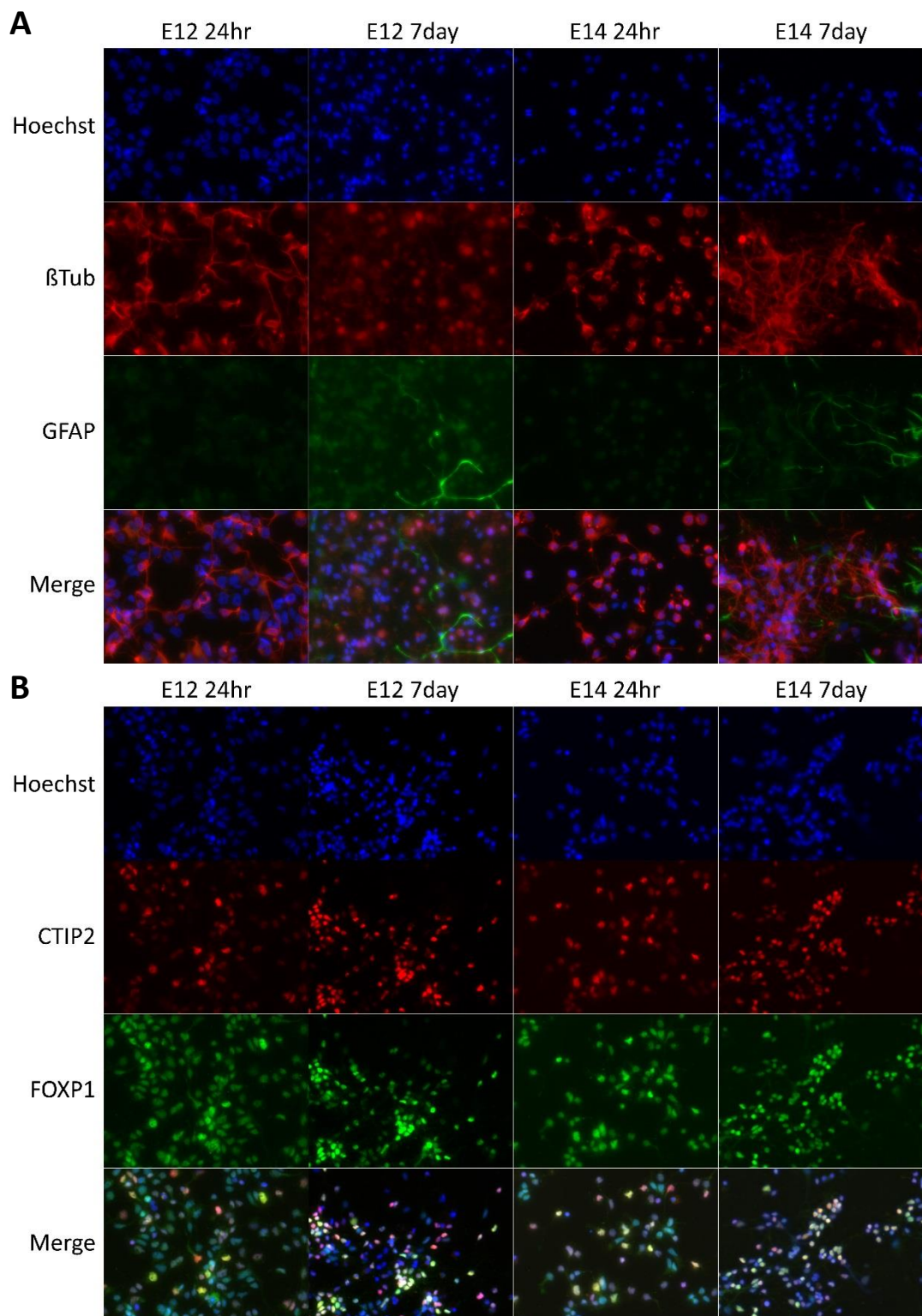


**Figure 4.7** Immunofluorescent photomicrographs of E12 and E14 WGE cells cultured for 24 hours or 7 days. **A** Cells labelled for mature neuronal marker  $\beta$ -Tubulin (red), astrocyte marker GFAP (green) and nuclear counter-stain Hoeschst (blue). **B** Cell labelled for MSN precursor markers CTIP2 (red), FOXP1 (green) and Hoeschst (blue).

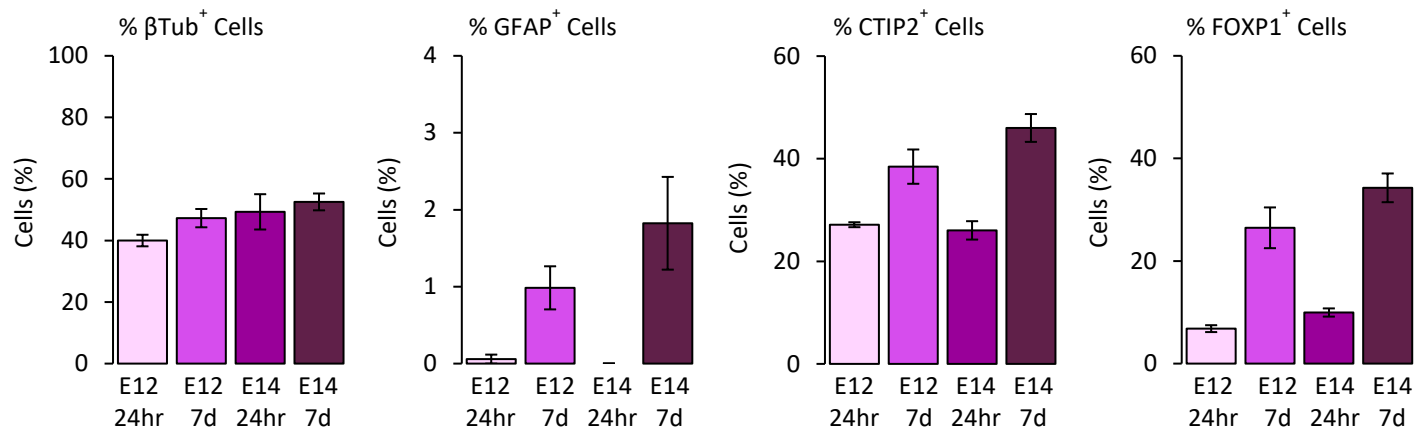


**Figure 4.8** Cell counts from plate-downs of 100,000 cells from E12 and E14 single cell suspensions after 24hrs and 7 days *in vitro*. No differences were observed in the number of mature neurons across groups ( $\beta$ Tub<sup>+</sup> staining). Compared to 24hrs, the cultures at 7DIV contained a significantly higher percentage of astrocytes (\*\* GFAP<sup>+</sup>,  $p < 0.01$ ) and MSN precursors (\*\* CTIP2<sup>+</sup>,  $p < 0.001$ ; \*\* FOXP1<sup>+</sup>,  $p < 0.001$ ). However, no effect of donor age was found.

## 4.5 Discussion

The effect of donor age, cell preparation and donor/host strain combination on primary embryonic striatal graft development, and the host microglial response were investigated. Preparation as a CS is the method most routinely used, with trituration following enzymatic digestion to form a quasi-single cell suspension. The tissue-piece style of preparation used in this study, although not an identical treatment to other chopped tissue piece preparations (A.-C. Bachoud-Lévi et al., 2000; Redmond et al., 2008), provides a less severe treatment than standard CS protocol (Rath et al., 2012; Watts et al., 2000b). Cells underwent the same enzymatic digestion to aid in the transplantation process, but did not undergo manual trituration, thus leaving the tissue relatively intact, thus theoretically reducing cell stress. To provide information on how model selection could affect the host response to transplants and subsequent graft survival/development, two different donor/host strain combinations were used; a between-strain (B-S) model transplanting Chrm4-EGFP-CD1 tissue into C57BL6/J hosts, and a within-strain (W-S) model with CD1 tissue transplanted into CD1 mice.

A high percentage of graft survival was found across all groups, except for E14 TP in both strains, which was the least effective transplant protocol in terms of graft survival, see **Table 4.3**. These data show that transplanted cells can survive under a variety of protocol conditions, yet survival rates were still not as high as usually seen in rat studies, and considerable variation in graft volume and content was seen within experimental groups. Graft cells were analysed for the expression of the mature neuron marker NeuN, MSN marker DARPP-32 and the interneuron marker parvalbumin. Some NeuN<sup>+</sup> cells did not appear to express either DARPP-32 or parvalbumin, and could be either immature cells, non-striatal neural cells, non-parvalbumin interneurons or a non-neuronal tissue type.

### Donor age

In general, E14 tissue produced grafts containing a higher number of mature neurons, DARPP-32<sup>+</sup> MSN cells and parvalbumin<sup>+</sup> interneurons compared to preparations transplanted using E12 tissue after considering the number of progenitor cells transplanted. Neural graft volume was larger for E14 preparations than E12 in both the W-S and B-S groups. CS preparations produced more NeuN<sup>+</sup> cells, larger graft volumes, and more DARPP-32<sup>+</sup> and interneuron content when harvested at E14 than at E12. Additionally, B-S transplants of E14 CS produced a higher proportion of P-zone tissue than E12 CS. In contrast, there was no

effect of age on TP in any of the above measures, although a consistent trend was apparent showing the opposite effect, with TP yielding better grafts at E12 than at E14. Striatal transplants of E14 preparations in rats have been shown to produce larger grafts and DARPP-32<sup>+</sup> P-zones within the graft compared to older tissue, as well as the greatest functional recovery (Fricker et al., 1997; Schackel et al., 2013; Watts et al., 1997). Given that the developmental stage at E14 in rats is equivalent to age E12.5 in mice, by comparing the Carnegie stages of development (Butler and Juurlink, 1987), it would be expected that E12 TP in mice should reflect the results seen in E14 TP rat studies. It is possible that the digestion process and trituration of the mouse CS has more of a detrimental effect on the cells at this younger age than at E14, or that mouse CSs are less tolerant to the treatment than rat cells. This could lead to a reduced capability of mouse E12 CS cells to survive and develop post-transplantation.

No effect of donor age was found in the *in vitro* measures investigated, including numbers of mature neurons ( $\beta$ -tubulin), early MSNs (FoxP1, CTIP2), and astrocytes (GFAP). E12 and E14 cells were equally viable at the time of transplantation/cell plating. However, these conditions do not match those seen *in vivo* since the cells are maintained in an optimised environment and supported through culture media, separate from any host interaction. In addition, it is possible that the Carnegie stages are not perfectly translated from rat to mouse and E12 could be more representative of a younger stage than the estimated E14 rat stage. This could have important implications for foetal age selection in primary human tissue transplants. The differences seen *in vivo* may suggest that it is the interaction of cells with the host environment affecting the apparent differences in development. It has been shown that neuronal cells under stress are more likely to be destroyed by the host (Brown and Neher, 2014), therefore if younger cells are more susceptible to stress, they may be more susceptible to the host immune response. The high levels of activated microglia seen within the grafted regions, and even in the lesion only controls, confirm that the immune response could play a critical role in the long term survival of cells (Robertson et al., 2013).

Parvalbumin<sup>+</sup> cells were more abundant in grafts derived from E14 CS than those from any other, an indication that these grafts may contain a greater interneuron population than the other groups, thereby presenting a cell population more characteristic of the normal striatum (Fentress et al., 1981). To obtain the neural diversity in grafts closest to that seen in the adult striatum, it is necessary to transplant both the lateral ganglionic eminence (LGE) and the medial ganglionic eminence (MGE) (Olsson et al., 1998; Watts et al., 2000a). In mice, the LGE, the source of striatal progenitors (Deacon et al., 1994), is visible by E12, while the

MGE, where interneurons are born, is visible as early as E11 (Olsson et al., 1998; Smart and Sturrock, 1979), indicating that E12 might be the earliest time point for obtaining all the necessary cell types in mice. It is known that interneuron populations contribute to normal striatal function and development (Olsson et al., 1998) and these may be playing a supportive role in the development of the MSNs within the graft (Gerfen et al., 1985). The MGE is much larger at E14 than at E12, and as the origin of interneuron progenitors would most likely contribute a greater proportion of interneurons to the transplanted population (Anderson et al., 1997; Campbell et al., 1995). In turn, this may have resulted in the improved development of E14 grafts (Olsson et al., 1998; Watts et al., 2000a). The relative contribution of MGE to the cell population within the suspension could be defined through sectioning of the dissected WGEs at each age and labelling the tissue for relatively LGE and MGE specific markers, such as *Gsh2* and *Nkx2.1* respectively (Corbin et al., 2003; Yun et al., 2003). This would allow for the topographic proportion of each within the E12 and E14 WGE to be compared.

### Cell preparation

The results show a significant difference in the effect of preparation type on graft morphology depending on the age of the tissue used. E14 tissue prepared as CS produced grafts that are phenotypically superior to those transplanted as TP in almost all parameters, including graft survival. Previously studies suggest this could be a result of the immunogenic donor vasculature in single-cell preparations being at least partially destroyed prior to implantation (Baker-Cairns et al., 1996; Chen et al., 2011). In addition, CS preparations could have an advantage over solid pieces of tissue through improved access to the host capillary network (Stenevi et al., 1976). Rat to rat grafts from CS transplants have also produced a greater proportion of striatal-like tissue, with more DARPP-32 expressing cell populations than those from TP, as well as providing greater innervation of the host parenchyma (Watts et al., 2000b). Cells transplanted as TP within a surrounding matrix may be restricted in terms of migration and integration into the host brain. The present study suggests the benefits of transplanting dissociated cell suspensions may outweigh those of a supportive matrix provided by TP transplants, and that the trituration process is not too harsh to affect survival of the transplant at E14.

Conversely, E12 tissue produced larger grafts with greater striatal-like content when prepared as TP over CS. Previous studies in rats have shown that, for transplants of TP, older donor tissue is tolerated less and that younger tissue has a better chance of survival (Björklund and Stenevi, 1984; Kromer et al., 1983; Stenevi et al., 1976) corresponding to what we find in mouse TP transplants. It is unclear why the dissociation processes involved in CS preparation would reverse this trend, although, as discussed above, it seems that mouse WGE tissue is better able to withstand dissociation when processed at E14 than at E12 as evidenced through E14 CS transplants yielding improved long-term graft survival and larger grafts. Studies have suggested that different sub-populations of rat neurons are more sensitive to trypsinisation than others (Björklund and Stenevi, 1984). Mouse cells may also be more sensitive, particularly at different developmental stages, warranting a systematic study of the effect of trypsinisation on mouse precursors.

E12 TP survived transplantation with an improved capacity to produce successful grafts, although it is unclear why the same results are not reflected with E14 TP. Potentially, the less mature cells within the E12 TP are more proliferative and migratory at this early stage of development, therefore not restricted by the surrounding matrix. The particularly low survival rate in E14 TP preparations may indicate that TP at this age are not as amenable to

integration as those at E12, possibly due to an increased potential of their vasculature and antigen presenting cells (APCs) to induce an immune response in the host (Chen et al., 2011). Whilst this was not demonstrated through the quantification of microglial response, other immune responses, such as T cell activation, were not investigated in the current experiment. In addition, following expulsion from the graft cannula, cells within the E14 TP might be more densely packed within the host striatum than single cells which could impede diffusion and timely integration with the capillary (Baker-Cairns et al., 1996; Cisbani et al., 2014).

### Strain effects

The two most commonly used transplantation paradigms within the host laboratory were selected for the purposes of this study, with the aim of determining how the choice of these models could affect the graft outcome.

The use of the different W-S and B-S models did not affect the number of surviving grafts. However, the transplants in the W-S model yielded the largest grafts in terms of neuronal volume compared to the B-S paradigm and had a higher number and proportion of DARPP-32<sup>+</sup> cells. The CD1 grafts also contained more interneuron cells. A previous study using the same Chrm4-EGFP-CD1 donor tissue observed much larger grafts and survival (Döbrössy et al., 2011), although notably this CD1 derived tissue was transplanted into CD1 hosts, rather than the C57BL/6.

In contrast, grafts of CD1 tissue into CD1 hosts observed in **Experiment 3** appeared smaller than those seen in the Chrm4-EGFP-CD1 in the C57BL/6 hosts. The results from this experiment provide clearer evidence to suggest that the choice of strain and matching of donor and host animals for transplantation studies, in particular for mice, could be critical in achieving robust results, possibly due to simplifying the number of strain comparisons and the larger group sizes. Iba1 staining revealed a significant amount of microglial activation within the grafted areas of all mice except the intact controls, including those in the lesion only group and those with no detectable surviving grafts, although a significantly higher grading of activated microglia was found in the B-S than the W-S groups. Allografts are known to elicit a greater immune response than isogenic tissue, and whilst neither of the models investigated here are inbred strains, it is clear that the response is increased when immunological disparity is greater (Chen et al., 2011). This, in turn, can be linked to reduced transplant survival. Since the CD1 hosts received tissue derived from the same strain and cohort, it is likely that this was tolerated more than the tissue in the mismatched B-S groups. Some studies have shown that the GFP marker associated with the Chrm4-EGFP-CD1 donor

tissue could in itself be immunogenic (Stripecke et al., 1999), although this did not appear to be the case when the Chrm4-EGFP-CD1 tissue was compared in **Experiment 3**. It might also be plausible that the C57BL/6 strain is inherently more prone to an exaggerated inflammatory response compared to the CD1 mice since the strain has been shown to have a strong bias to M1 inflammatory reaction, whereas other strains, such as Balb/c, tend towards a more supportive M2 response (Mills et al., 2000). However, this also was not seen when the C57BL/6 hosts were compared in **Experiment 3**.

The higher levels of activated microglia in the C57BL6/J hosts could explain the lower surviving cell number and graft volume (Perry and Teeling, 2013; Raivich et al., 1999). It was noted that the area of activation exceeded the area of transplantation, suggesting secondary activation or recruitment of microglia to the site of transplantation. In agreement with observations made in **Experiment 2**, the glial response appeared reduced in individuals with rejected grafts, presumably because the transplanted cells had already been subjugated and the immune response had entered a post reactive phase. The ongoing proliferation of activated glial cells in and around the grafts is suggestive of ongoing reactivity with the surviving implanted cells. This could be an indication that the grafts surviving to 12 weeks may be hampered long-term by the immune response of the hosts. Therefore, the study of immunosuppressive regimes in mouse to mouse transplantation could be a key to resolving the less than optimum quality of the grafts seen, as immunosuppression is generally only considered to be required for xenotransplant models.

## 4.6 Conclusions and future work

Both donor age and tissue preparation technique were shown to be important factors affecting the morphology of mouse primary foetal grafts. The data from this study suggest that more successful grafts are derived from single cell preparations of E14 tissue or from less-dissociated tissue pieces at E12. Across all measures assessed it appears that the E14 CS is the best combination of age and cell preparation to use in mouse transplants.

However, a large variation was observed in grafts across all the experimental groups, which implies the influence of other factors that may be more fundamental than the methodological modifications investigated in this study. Any impact of changes in cell preparation or donor age may be reduced by other more influential factors in the mouse to mouse model, highlighted by the differences between the strains investigated here. High levels of activated microglia in the grafted zones, particularly in the between-strain transplants, and the presence of dead cells in all groups suggest that further investigation into immune response of mouse hosts to specific tissues is warranted.

The grafts observed in the preceding experiments have shown a large degree of variation within experimental groups, from few or no obvious surviving cells to large grafts with thousands of cells. The fact that the conditions in which these cells were transplanted was consistent suggests that a possible source of the variation comes from changes in the cell preparation itself. The experiments described in the next part of this chapter will investigate how changes in the quality of the cell suspension may vary over time, and potentially impact on graft outcome.

## Experiment 5

### The viability of cell suspension during the surgery period<sup>1</sup>

#### 4.7 Summary

The previous *in vivo* experiments have demonstrated a variability in graft outcome, often observed even within experimental groups. The purpose of the final experiment of this chapter was to determine if any of these differences may be accounted for by variability in cell suspensions within the surgical period.

Cells were prepared as if for transplantation and the qualities of the suspension examined over time. Measures of viability and the number of live cells taken up by the surgical cannula, as well as the numbers left within the cannula following a deposit, were each measured for eight hours after the cells were prepared. The homogeneity of the suspension, in addition to the susceptibility of cells to cell death, were also assessed.

Furthermore, a study trialling an alternative method of aliquoting cell preparations for surgery was considered, with the aim of improving the loss of cell numbers from preparations over time.

The results indicate that trypan blue viability staining may not be the most reliable method for assessing cell preparations prior to surgery since it cannot accurately measure the health of the cells in the suspension. Furthermore, the data suggest that cells suspensions do not remain homogenous for the duration of a surgical period, potentially providing an explanation of the variability seen in graft size and cell counts within experimental groups *in vivo*. It was shown that a significant number of cells remain within a transplantation cannula after expulsion of preparation, suggesting that these cells should be considered when estimating the number of cells being transplanted.

The susceptibility of cells to death was not shown to increase with age of suspension, although trypan blue may not be considered the optimum technique for testing this. Finally, the variability of the number of cells taken up in successive samples was not improved by preparing individual preparations.

---

<sup>1</sup> Declaration – Dissection of tissue for cell suspensions performed by Ngoc Nga Vinh

## 4.8 Introduction

### Meta-analysis of previous data

The results of the transplantation experiments discussed in [Experiments 2 - 4](#), show a large variation in graft cell counts transplanted under the same conditions, with very large and very small grafts found within experimental groups. The range in cell number for some of the groups is presented in [Figure 4.9 A](#), where range is the difference between the largest and smallest grafts within a group, excluding those with no detectable graft. In some cases, there were discrepancies of over 20,000 cells. Given that all other variables were kept constant, this could suggest that factors outside the independent variables that were explicitly investigated may be affecting the graft outcome. One potential source for this variation, other than inherent differences between individual animals, may come from variability in the cell suspension itself.

To probe this further, NeuN<sup>+</sup> cells counts from the transplantations from [Experiments 2 - 4](#) which used the standard transplantation protocols were collated. Cell counts were ranked in the order in which the mice were transplanted for each cell preparation used, and the effect of surgery order on graft cell number was analysed using the Kendall's tau correlation test in the IBM SPSS 23 statistics program. There was a significant correlation between surgical order and cell count ( $\tau = -.32, p < 0.05$ )

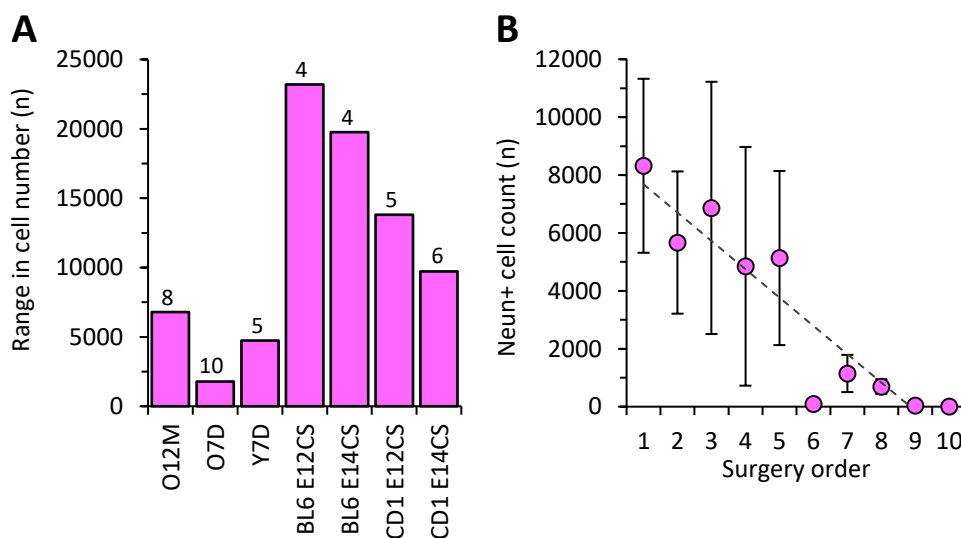


**Figure 4.9 A** Graph to illustrate the range in graft cell counts within experimental groups from a selection of experiments. (Range = greatest number – smallest number (excluding animals with no graft survival)) Numbers above each column represent the number of animals in each group. **B** Mean cell counts from animals ranked in surgical order from Experiments 2 - 4.

This data indicates that there could be a reduction in cell suspension viability over time, or that the number of cells being taken up for transplantation is reducing over time. Potential explanations for this could be that more cells are being removed in the first few extractions during a surgical period leaving fewer for the subsequent surgeries, or the suspension is becoming more clumped over time with the larger clumps not being taken up the syringe cannula as the suspension ages, or both.

#### Does viability screening represent the suspension quality?

Even though cells to be transplanted are screened for greater than 80% viability prior to surgery, it was noted that, even for the first few surgeries from a preparation, there was a wide variation in graft size, **Figure 4.9 B**. Trypan blue viability tests determine the proportion of alive and dead cells as snapshots at the beginning and end of surgery, however, at least for murine striatal cells, it is also not known how the viability measure changes over time. Time-course studies of the viability of neuronal tissue preparations at room temperature have shown that rat CNS neurons can remain viable for several hours, although this timeframe was dependent on both the age of the donor tissue and the brain region of origin (Brundin et al., 1985).

Since dead cells can only be identified for a limited period before cytolysis removes them from the sample, we cannot necessarily know the proportion of cells which have died. Furthermore, we determine if a cell is alive, but not how healthy it is. Cells that are in perfect condition are counted along with those struggling, therefore, assessing the viability longitudinally could help determine if the viability measure is accurate for the duration of its use. If viability declines significantly during the time-course of surgery, it would be expected that those animals transplanted later in the day would have reduced-quality graft outcome.

#### Could the homogeneity of the cell suspension change over time?

Standardly, one suspension is utilised for at least half a day's surgery, possibly up to eight hours, and sometimes incorporating 10 or more animals. Despite the preparation being triturated into a "single-cell" suspension prior to surgery, cells tend to settle to the bottom of the aliquot quickly and may become clumped together. While the suspension is agitated between surgeries to re-suspend the cells, this is kept to a minimum to avoid damage and may not be sufficient to fully re-dissociate the cells. In addition, the primary tissue preparations are kept at room temperature, so it's possible some dehydration could occur, thereby increasing the viscosity of the preparation. In fact, it was noted during

transplantation that despite trituration between surgeries, cell suspensions sometimes seem to become more glutinous and clumped throughout the day. These factors could contribute to a non-homogenous suspension and result in an uneven allocation of cells between animals, or cause cells to stick within the transplantation cannula. In either case it is unclear how many cells each animal would receive during transplantation and could explain why there are such differences in graft outcome within groups.

#### Are older cell suspensions more susceptible to cell death than fresh?

The robustness of cells, in terms of how easily damaged or susceptible to cell death they are, is another factor which could determine how well they survive *in vivo*. The conditions within the suspension media presumably become less ideal the longer that it is supporting cells. Therefore, we might expect the cells towards the end of surgery to be in a poorer condition to cope with the process of transplantation than those from a fresh nutrient-rich preparation. As discussed above, while trypan blue viability measures can tell us the proportion of alive and dead cells, it cannot tell us the condition of the cells.

The following experiment aimed to establish if the quality of the cell suspension changes detrimentally over the duration of a surgical period, and if the single cell preparations remain homogenous during this time.

Cell suspensions were prepared, and a transplantation cannula was used to withdraw samples in a way similar to surgical conditions. Measures of cell number and viability were taken each hour for eight hours and the number of cells deposited from the cannula, and the number of residual cells left in the cannula were counted. The number of clumping cells was also quantified. In addition, since it is known that the trypan blue stain is cytotoxic and will rapidly cause cell apoptosis (Awad et al., 2011), samples of the fresh and aged suspension were left in the stain for a prolonged period to assess if either was more susceptible to cell death.

To investigate if the problem of dwindling cells numbers in successive cell extractions during a surgical period could be avoided, an additional experiment was performed. A standard pooled suspension providing multiple aliquots was compared to a series of individual preparations made to provide a single aliquot. Viability and cell counts were again measured hourly over an 8-hour period.

## 4.9 Methods

### 4.9.1 Experimental design

#### Cell suspension viability and cell counts

A total of twelve pups at age E14 were dissected from two female Chrm4-EGFP-CD1 mice and three single-cell suspensions prepared as described in methods section 2.2.2. Preparation one constituted of WGE's from pups taken from the first litter, preparation two was a mixture from both litters and preparation three was derived solely from the second litter to provide suspensions from a mix of different donor animals. Each suspension was made up to a concentration of 250,000 cells $\mu\text{l}^{-1}$  and stored at room temperature in the dark, the same conditions as if for transplantation. The cells were gently triturated every 15 minutes with a 10ml SGE transplantation syringe to imitate the conditions of surgery. In addition, every hour, from 0hr until +8hr, a 1 $\mu\text{l}$  sample was removed for analysis using the transplantation syringe and slowly expelled from a vertical position into 100 $\mu\text{l}$  of DMEM-F12 media. After gently mixing, 10 $\mu\text{l}$  was transferred into 10 $\mu\text{l}$  of 0.4% trypan blue. 10 $\mu\text{l}$  of this suspension was taken and viewed under a microscope using a haemocytometer and viability and cell count recorded. In this way the number of cells, which in surgical conditions would have been transplanted, could be calculated.

#### Counting residual cells

Once the test sample had been collected, 3 x 10 $\mu\text{l}$  of DMEM-F12 media was used to flush out the syringe and 10 $\mu\text{l}$  of this transferred into 10 $\mu\text{l}$  of trypan blue to count the number of residual cells remaining within. This was used to approximate the number of cells which may be left in a syringe after surgical deposits have been made.

#### Quantifying clumpiness

Photographs of the five counting grid squares of the haemocytometer for each sample were taken to quantify cell clumping. The cells seen in each grid photo were counted and recorded depending on how many cells were in each clump with eight categories defined as follows; single cell, or group of 2, 3, 4, 5, 6, 7 or 8+. Cell in groups much larger than 8 were recorded as multiples based on estimated size, **Figure 4.10**. Subsequently the categories were simplified to either dissociated cells (1-3 cells) or clumped cells (4+ cells).

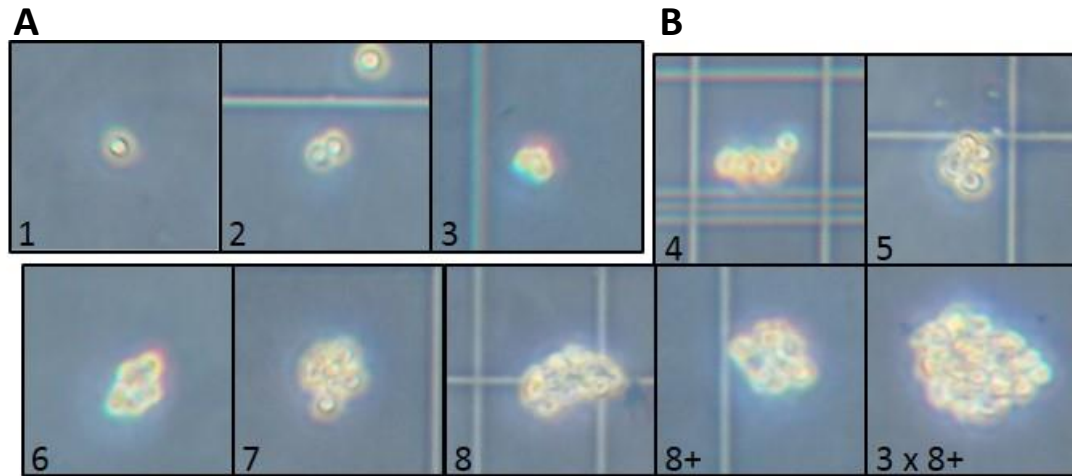


**Figure 4.10** Photographs of cells on haemocytometer. **A** Cells in groups of 1 – 3 were classed as 'dissociated'. **B** Cells in groups of 4 or more were classed as 'clumped'.

#### Assessing cell susceptibility

The rate at which cell death occurs after being stained with trypan blue was used as an indirect measure of cell susceptibility. The three samples of cell suspension taken at 0hr and 5hr above, were retained within the haemocytometer in trypan blue solution. Photographs of the counting grid were taken every 30 seconds for 5 minutes for analysis later. The number of live cells within the grid were counted in the 0hr images and tracked through each photo, **Figure 4.11**. The proportion of original cells surviving at each time-point was calculated.

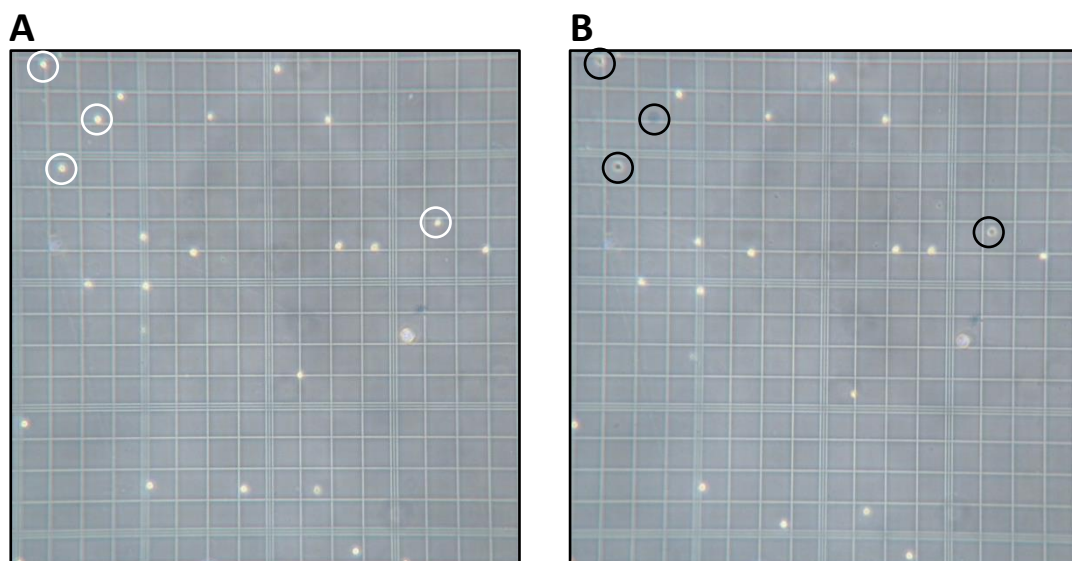


**Figure 4.11** **A** Photograph of cells on haemocytometer taken immediately after suspension was made and **B** five minutes later. Circles indicate cells that have undergone cell death in the time between the photos were taken.

Following on from the experiment described, the problem of reduced live cell concentrations in repeatedly sampled suspensions was investigated. The standard pooled WGE cell suspensions, for transplanting multiple surgeries, were compared with preparations made from individual WGE suspensions allocated to one surgery per preparation.

For this, a total of twenty-three pups at age E14 were dissected from two female Chrm4-EGFP-CD1 mice. Four or five embryos were pooled together for each of three single cell suspensions of  $150,000 \text{ cells}\mu\text{l}^{-1}$ , each of which was stored in the dark at room temperature and sampled every hour for 8 hours. The remaining nine embryos were individually processed into separate suspensions and stored in the same conditions, with one suspension being sampled for each time-point. To sample, the suspension was gently triturated using a  $200\mu\text{l}$  pipette tip before a  $10\mu\text{l}$  sample was taken for trypan blue exclusion counting as described in methods section 2.2.2.

#### 4.9.2 Statistical analyses

Unless otherwise stated, all statistical analysis was using GenStat (18<sup>th</sup> edition). One-way ANOVAs were performed to analyse the effect of time on cell suspension measures. Significance was taken as  $p \leq 0.05$ .

## 4.10 Results

### Viability and cell counts

The initial viability of the three suspensions was  $94.7\% \pm 2.3$  which was consistent with the level considered appropriate for transplantation (80%+). The viability of the samples decreased with time although there was no significant change until 7 hours after the preparations were made (Time:  $F_{8,16}=3.59$ ,  $p < 0.05$ ), **Figure 4.12 A**. Even after 8 hours the viability remained above 80%.

The number of live cells deposited from the syringe in the first samples ( $349,333 \pm 81,258$  cells  $\mu\text{l}^{-1}$ ) was higher than the calculated cell concentration ( $250,000$  cells  $\mu\text{l}^{-1}$ ) but declined with time (Time:  $F_{8,16}=5.54$ ,  $p < 0.01$ ), **Figure 4.12 B**. After just 2 hours the number of live cells deposited was below that which was expected and after 8 hours was reduced to just  $61,133 \pm 7,249$  cells  $\mu\text{l}^{-1}$ . The number of dead cells was also greatest in samples taken just after the preparation, although no effect of time was found (Time:  $F_{8,16}=1.41$ , ns), **Figure 4.12 C**.

The total number of cells remaining within the syringe following sample expulsion was between approximately 5,000 and 20,000 and did not change significantly for the duration of the experiment (Time:  $F_{8,16}=0.88$ , ns), **Figure 4.12 D**.

### Cell dissociation and clumping

The number of ‘dissociated’ cells counted within the haemocytometer grid decreased with suspension age (Time:  $F_{8,16}=6.95$ ,  $p < 0.001$ ), and whilst there was a trend for the number of ‘clumped’ cells to decrease, this was not found to be significant (Time:  $F_{8,16}=2.41$ , ns), **Figure 4.13 A**. Approximately 20% of the cells within the samples deposited were found to be clumped in groups of 4 or more and this was not affected by age of suspension (Time:  $F_{8,16}=0.29$ , ns), **Figure 4.13 B**.

### Trypan blue cell death

The proportion of cell death that occurred after exposure to trypan blue did not differ between the fresh preparations and those which were 5 hours old (Age:  $F_{10,22}=0.91$ , ns), **Figure 4.13 C**. Neither was there significant cell death over the 5-minute observations (Time:  $F_{10,20}=1.59$ , ns).

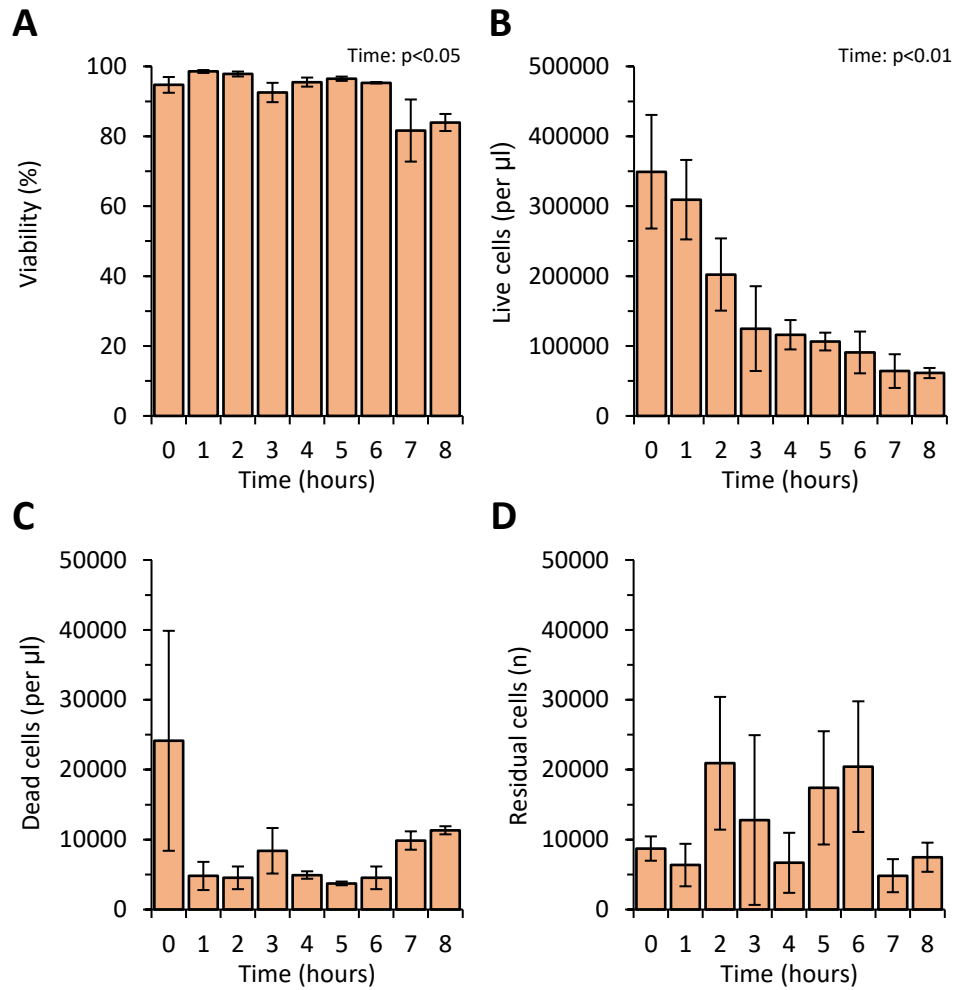


**Figure 4.12** **A** Viability of preparations over time. Viability decreased over time ( $p < 0.05$ ). **B** Number of alive cells per  $\mu\text{l}$  in the preparation sample over time. The number of alive cells in the samples declined over time ( $p < 0.01$ ) **C** Number of dead cells per  $\mu\text{l}$  in the preparation sample over time. No difference in the number of dead cells was found. **D** Number of residual cells flushed from syringe over time. No difference was found in the number of residual cells found.

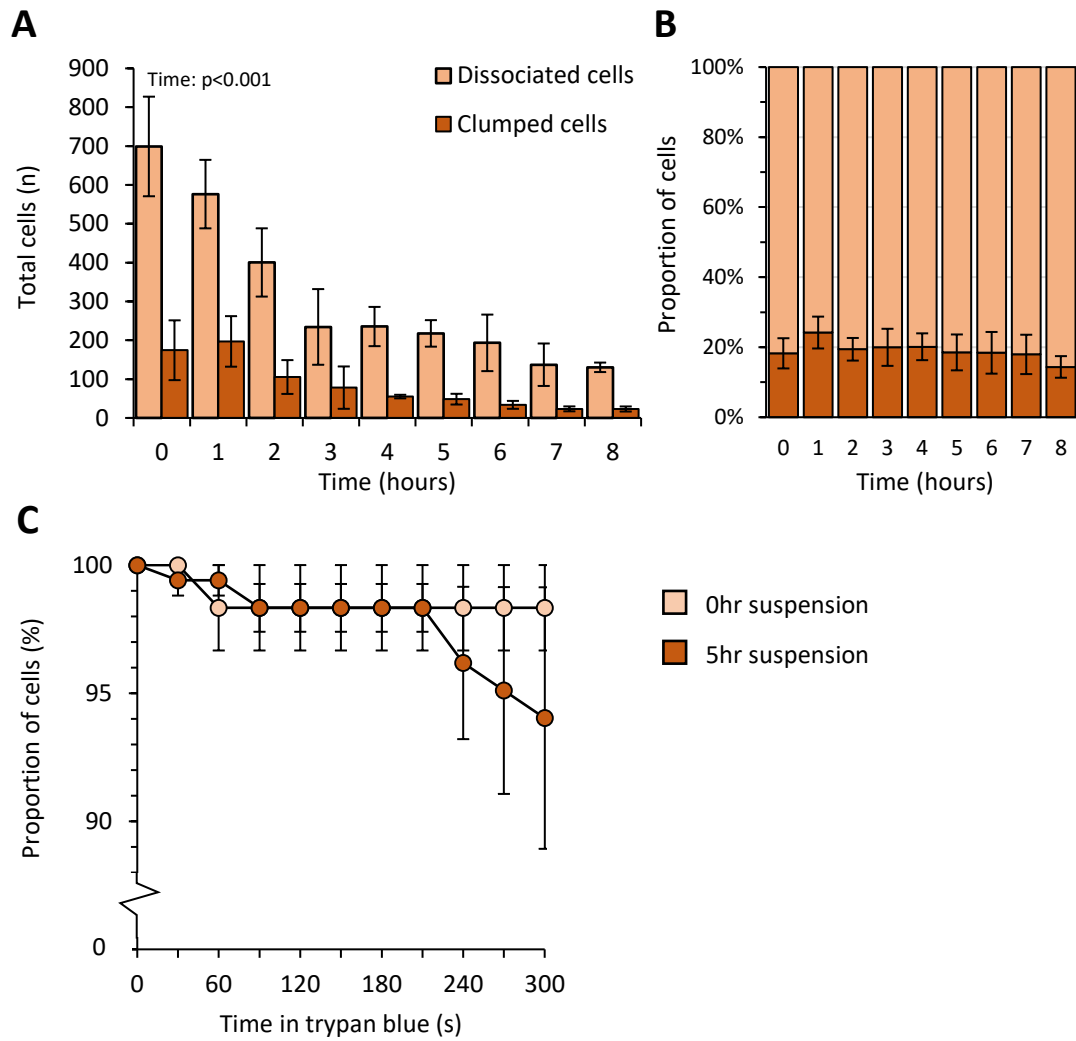


**Figure 4.13** **A** Total number of dissociated and clumped cells counted within the suspensions over time. The number of dissociated cells reduced over time ( $p < 0.001$ ), however, no change in clumped cells was detected. **B** Proportion of dissociated and clumped cells within the preparation over time. There was no change in the proportion of clumped and dissociated cells over time. **C** The proportion of alive cells within the haemocytometer counting grid compared to in the fresh trypan blue solution (0s) for fresh (0hr) preparation and an older (5hr) preparation. No effect of sample age or time was seen.

For the second part of the experiment in which the pooled and individual suspension were compared, there was no difference in the viability of the pooled suspension over time (Time:  $F_{8,16}=0.59$ , ns), **Figure 4.14 A**. As before, the number of live cells  $\mu\text{l}^{-1}$  declined over time (Time:  $F_{8,16}=3.22$ ,  $p<0.05$ ), but no change in the number of dead cells was detected (Time:  $F_{8,16}=0.46$ , ns), **Figure 4.14 B - C**.

Since only one individual preparation was measured at each time-point, it was not possible to perform statistical analysis with the data. However, it was observed that all but the first viability scores were approximately 80%, **Figure 4.14 D**. The sample taken immediately after the suspension was prepared had the lowest viability measure. The number of live cells counted in each of the suspensions varied between approximately 200,000 and 500,000 cells  $\mu\text{l}^{-1}$ , and the number of dead cells ranged from 100,000 to 30,000 cells  $\mu\text{l}^{-1}$ , but neither seemed to relate to the age of the preparation, **Figure 4.14 E - F**.

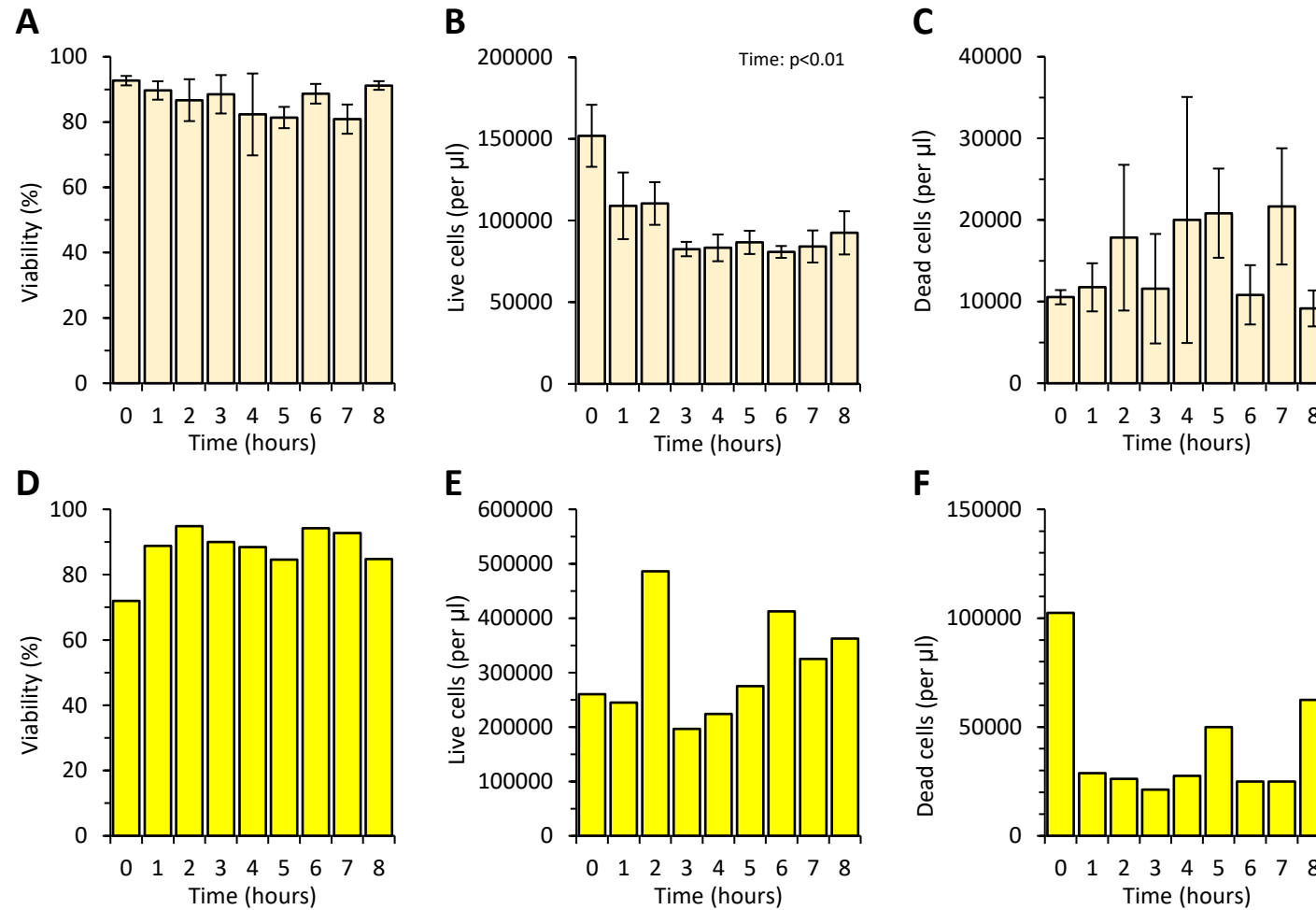


**Figure 4.14** **A** Viability of the pooled suspensions over time. No change in viability was observed. **B** Number of live cells  $\mu\text{l}^{-1}$  in the pooled suspensions over time. The number of live cells reduced over time ( $p < 0.05$ ). **C** Number of dead cells  $\mu\text{l}^{-1}$  in the pooled suspensions over time. No difference was found over time. **D** Viability of each individual preparation measured at different time-points. Only the first sample had a low viability count. **E** Number of live cells  $\mu\text{l}^{-1}$  in each individual preparation measured at each time-point. Some preparations appeared to contain more live cells  $\mu\text{l}^{-1}$  than other but did not seem to be related to age of suspension. **F** Number of dead cells  $\mu\text{l}^{-1}$  in each individual preparation measured at each time-point. The number of dead cells in each preparation did not seem to be related to the age of the suspension.

## 4.11 Discussion

### Graft cell count is correlated to surgery order

The meta-analysis of the grafts from previous experiments demonstrated the variability of graft outcome within experimental groups and showed that the number of cells counted within surviving grafts was correlated to the order in which they were transplanted. Those transplanted earliest end up with a greater number of surviving cells.

This was further investigated by assessing the viability and cell counts within cell suspensions over a time equivalent to a reasonable surgical period. Three suspensions composed of dissections from E14 embryos were treated as they would be in a surgical situation. Each hour over an eight-hour period, a sample was withdrawn using a surgical syringe cannula and the number of cells deposited was counted, as well as the number of residual cells left within the cannula. The susceptibility of the cells to the trypan blue toxin and the homogeneity of the suspensions was also measured.

### Trypan blue viability measures are not reflective of the quality of the cell suspension

Currently, viability of a cell preparation is typically calculated using a simple trypan blue stain to highlight dead and alive cells within the suspensions prior to being used in surgery. Any suspension falling below 80% viability would lead to the suspension being rejected. All suspensions used in this experiment were above this criterion, and in fact retained a high viability throughout the eight hours of sampling. However, over time there was a clear reduction in the number of live cells in the preparations. Since the number of dead cells counted did not rise correspondingly, it might be assumed that as the cells died, they underwent degeneration (cytolysis) and after a while did not appear in the cell counts at all. Therefore, despite still having a high live:dead viability ratio, the number of viable cells in the suspensions was depleted. Whilst trypan blue staining has been adopted as a relatively quick and easy method for assessing preparation viability, historically the acridine orange / ethidium bromide method was used (Dunnett and Bjorklund, 1992; Shiigi and Mishell, 1996), which was able to classify both live and dying or unhealthy cells. Given the results discussed here, the benefits of the simplicity of the trypan blue stain might need to be reconsidered against the potentially more reliable acridine orange / ethidium bromide measure.

In addition, some of the ‘missing’ cells could still be present within the preparation but were not sampled. Despite the regular agitation of the cells, it was possibly not sufficient to completely re-dissociate the cells. The cells were withdrawn from the preparations using a transplantation cannula, rather than a pipette tip as they might be usually when calculating cell counts and viability, and since this has a finer bore, any cells which may have clumped together up to a certain size may not be withdrawn so easily into the cannula. This could mean that only those more dissociated cells were being sampled, and hence not a reflection of the true number of cells in the preparation, but perhaps a more accurate representation of that which would actually be transplanted.

The counts of dissociated and clumped cells seem to support this hypothesis. When the cell counts were broken down into the type of cell in the sampled suspension (i.e. dissociated or clumped), it was still evident that the number of dissociated cells was reducing. This could be a result of cells clumping together in larger groups as the age of the suspension increased. An increase in the proportion of clumped cells was not observed, however, as discussed above, larger clumps would be less able to be withdrawn into the cannula and therefore not counted. This could be tested by also sampling the suspension with a 1ml pipette tip and observing under the microscope for large groups of cells. In any case, the number of cells actually being taken up for the hypothetical transplants was significantly reduced over time and thus providing an explanation for the decline seen in association with surgery order.

Overly manipulating the suspension is avoided to cause minimal disruption of the cells, however, if the suspension is not fully dissociated then cells could remain in small clumps. If these clumps are small enough to fit into the cannula lumen then any given quantity of suspension with these clumps in would contain a disproportionately higher concentration of cells than the intended concentration. If these smaller clumps of cells are taken up each time an animal is transplanted, then the pool of cells left subsequently is depleted. It is possible that a combination of these events may be impacting on those grafts occurring later in the surgery order.

#### Cells are left within the surgical cannula after deposits have been expelled

By rinsing the cannula after each deposit was counted, the number of residual cells remaining in the syringe were able to be counted. While this did not change significantly over the eight-hour period, there was quite a substantial number left behind. At the later time-points, residual cells accounted for a higher proportion of cells taken up into the cannula. While it

may be difficult to change this when in a surgical situation, it is worth considering when calculating how many cells are required for any transplantation protocol.

#### Cells in an older suspension were not more prone to cell death from trypan blue than those from fresh

Since trypan blue is known to be toxic to cells, exposure to it was used as a proxy measure for the susceptibility to cell death of cells within the suspensions. During the five-minute exposure period observed, there was no more cell death in suspensions which were five hours old compared to fresh preparations. This could imply that the reason for smaller cell numbers in those animals transplanted later is more likely to be due to non-homogeneity of the cell suspensions as discussed above, rather than the cells having increased susceptibility to apoptosis. It is worth noting however that this test was conducted over just five minutes, whereas once transplanted, cells may be under more chronic stress from their environment. The trend observed at the end of the five-minute period may suggest that if the cells were left for longer in the trypan blue, a difference in the rate of cell death could have become apparent.

Alternatively, other methods of determining cell viability may provide a more useful insight on the condition of the cells. Rather than simply seeing if cells are alive or dead, assays such as the LIVE/DEAD Cell vitality Assay Kit (Hu et al., 2002), enabled a graded labelling of cells which convey their metabolic state, and therefore their state of health. Decisions on the suitability of suspension for surgery could then be assessed on the proportion or number of healthy cells to give a more accurate representation of how many might be more likely to survive.

#### Preparing individual suspensions did not improve variability between samples

The pooled preparations measured in the second part of the experiment demonstrated the same cell loss pattern as previously, with a consistently high viability measure and a cell number declining over time. The individual preparation samples typically had a higher cell number than the pooled, and did not appear to decline over time, thereby indicating that successive sampling of a suspension has a greater impact on subsequent samples than the effect of time *per se*. However, the disparity between counts was noticeable. This is likely due to individual differences between the embryos, or their dissections, an effect which, in a pooled suspension, would be reduced since tissue is shared between samples. The first sample taken had the lowest viability and highest dead cell count. This could be because the

sample was examined while the cells were still undergoing cell death due to the recent dissociation process or could have just been a poor-quality embryo. This experiment would need to be repeated with a greater number of samples to test this.

The disparity between individual embryos could easily be overcome by creating a pooled preparation as normal and apportioning the suspension into individual aliquots immediately after. This would remove the chances of surgical order affecting the number of cells transplanted due to unequal distribution of cells between animals. It would also be useful if the aliquots to be transplanted were at the correct volume required per animal, since then the entire fraction could be drawn up to ensure that all cells were used.

During clinical application of cell replacement therapy, the suspension is drawn up in a single dose and held within the cannula for depositing. This could last for several hours and it could be important to understand what happens to the cells within the cannula, since this is likely to have a different impact than keeping them in Eppendorf tubes. Studies exploring the behaviour of cells within cannula show that they can settle within the lumen and consequently, are expelled in an uneven distribution (Torres et al., 2015). In the preclinical experiments conducted here, the suspension remains in the cannula for just two minutes, so within-cannula settling is less likely to be so much of a problem, however clinical surgeries often take hours to complete. Therefore, the settling of cells, and potential changes to its viscosity and clumpiness could be major factors in graft outcome in clinic.

## 4.12 Conclusions and future work

**Experiment 5** investigated how the state of cell suspension changed over time and how this might impact on the graft outcome. It was found that the number of cells within samples withdrawn from the preparations decreased with time, and this corresponded to the observed pattern of cell numbers within surviving grafts *in vivo*.

The decline in cell numbers seems likely to be caused by incomplete dissociation of cells into a single cell suspension, or a re-aggregation of cells over time. This could potentially be resolved through retaining DNase in the media, more thorough trituration of the suspensions prior to each surgery, perhaps with a wider bore pipette tip, or through aliquoting the cells out for each surgery at the time at which they are prepared. However,

the balance between the potential damage caused by the extra manipulation or through being stored in smaller aliquots of media would need to be investigated since previously excess dissociation has been shown to detrimentally affect cells (Fricker et al., 1996).

Another aspect of the cell preparations which should be considered is the media in which they are dissociated and stored. It might be possible to improve the cell survival by adding beneficial factors into the media, such as free radical-inhibiting lazaroids (Nakao et al., 1994) or growth factors such as GDNF (Brundin et al., 2000).

Finally, a comparison of the trypan blue method of assessing viability and other more graded assays and the graft outcome could be beneficial by potentially avoiding the transplantation of cells which would otherwise have appeared healthy.

In conclusion, the proposed optimal parameters for mouse donor cells in future experiments are:

- Use single-cell suspensions of donor tissue aged E14.
- Calculate suspension viability based on cell 'health' rather than by trypan blue exclusion.
- Increase the number of cells to be transplanted by ~5% to account for residual cells in the transplantation cannula.
- Retain DNase in the suspension to reduce clumping of cells.
- Aliquot separate cell suspensions for each individual prior to surgery.

# Chapter 5

## The functional assessment of the quinolinic acid lesioned mouse model<sup>§</sup>

### 5.1 Summary

The experiments described in this chapter aim to determine the most effective behavioural tests for assessing functional changes in the QA lesion mouse model of HD ready for cell transplantation. A comprehensive battery of tests describing the behavioural deficits of this commonly used model has not been previously identified, therefore the object of this study was to identify clear and stable deficits in the lesioned animals against which potential functional recovery could be evaluated in future experiments.

Behavioural changes induced from unilateral lesions of the dorsolateral striatum, and from bilateral lesions of the dorsomedial striatum were assessed, designed to represent disruption to the motor and non-motor pathways of the basal ganglia respectively.

Following initial behavioural training, mice received QA lesions to the striatum and were tested at an early (from 1-week post-lesion) and late (from 16 weeks post-lesion) time-point in a broad selection of motor and cognitive behavioural assays. Brain tissue was collected and processed to assess the characteristics of the lesions and compare with the associated behaviour observed.

Tests were considered appropriate for use in assessment of cell transplantation therapy if a significant deficit was determined compared to sham treated controls, which was sustained throughout the late time-point. Transient deficits were not deemed apposite since spontaneous recovery or compensation later on could mask or mimic potential graft-induced recovery which may not be seen until the maturation and / or integration is complete.

---

<sup>§</sup> Declaration

A subset of non-licenced behavioural tests described in this chapter were carried out by undergraduate student Harry Potter and submitted as his professional training year project report.

## 5.2 Introduction

### Therapeutic studies require an outcome measure

The results for the previous experiments within this thesis show that the methods and models used for striatal transplantation in mice can be optimised and adapted to improve the size and cell survival of grafts. While this information can give an indication that changes to protocols are moving in a beneficial direction, ultimately, we need to know if these changes translate to effective reduction of disease symptoms. If transplantation is to be used as a therapeutic strategy, efficacy of grafts in improving function and behaviour must be demonstrated, and in order to show an improvement, a deficit must first be detected.

Whilst the rat QA models have been extensively characterised and show many measurable deficits (Dunnett et al., 1999; Eagle et al., 1999; Shear et al., 1998) there are fewer behavioural outcome measures defined for the QA mouse model, with transplantation studies almost exclusively focussing on morphology or a few token motor tests such as rotarod performance (Gharaibeh et al., 2016; Lin et al., 2011), rotations (Bernreuther et al., 2006), open field (Ma et al., 2012) or less often, gait analysis (Zimmermann et al., 2016). Results from a single behavioural test could be open to many interpretations, but by incorporating a larger battery of tests, the observations made can be more accurately attributed to specific behavioural deficits. In addition, many of the tests performed using striatal lesions are within just a few weeks of the lesion surgery with no long term assessment of the deficits (Brown and Robbins, 1989; Hauber and Schmidt, 1994). The expertise and time required to train animals and run behavioural tests are potential reasons for this lack of testing, but additionally, a lack of systematic investigations of appropriate assays for mouse QA models is also a problem.

Any behavioural test must detect appropriate HD related motor or cognitive deficits in the mice, and these deficits must be stable in the long-term to enable adequate measures of potential therapeutic recovery. A comprehensive guide to the tests that reveal HD relevant deficits would be an incredibly useful tool in all areas of testing HD therapeutics in these models.

### Behaviour is affected by lesion position

Typical non-behavioural grafting experiments target the mid-striatum as the site for lesion and graft placement because the histological experimental outcomes will not be affected by the precise position within the striatum. However, if behavioural outcome measures are to be examined then specific lesion placement becomes an essential consideration. Studies of QA lesioned rats have shown that the mediolateral position of the lesion within the striatum is critical in relation to the resultant behavioural outcomes observed (Brown and Robbins, 1989; Devan and White, 1999; Hauber and Schmidt, 1994). The dorsal striatum is organised with a mediolateral gradient of afferent connections, with the lateral aspect receiving most input from the sensorimotor cortex and affecting motor aspects of performance measures, and the medial regions receiving more inputs from the prefrontal cortex and involving more cognitive components of behaviour (Voorn et al., 2004).

This experiment set out to characterise two QA lesion mouse models, one directed towards a motoric deficit, through targeting of the unilateral dorsolateral striatum (DLS), and the other focussing on cognitive deficits through lesioning of the bilateral dorsomedial striatum (DMS). Unilateral rather than bilateral lesions were utilised in the DLS groups primarily for animal welfare reasons. It has been previously observed that bi-lateral QA lesions in this region can cause severe weight loss and poor recovery rates in the days following surgery. This is likely caused through disruption of the regions responsible for eating, chewing and swallowing – signs often apparent in HD patients. This effect is reduced if one hemisphere is left intact. A further benefit to the lateralised nature of the lesion is that the ipsilateral side acts as a within-subject control, with many deficits in motor performance restricted to the contralateral side of the body. Therefore, contralateral deficits displayed by individuals in many tasks can be directly compared to or expressed as a proportion of performance of the ipsilateral side. In contrast, bilateral lesions to the dorsomedial striatum do not present such a severe detriment to the general health of the animals. Furthermore, it has been shown that bilateral disruption of cortico-striatal circuitry is required in order to confer cognitive losses (White and Dunnett, 2006).

For this study two experiments were performed, the first using the unilateral DLS lesion model and the second using the bilateral DMS lesion model, to establish an effective battery of behavioural tests against which different aspects of graft-mediated functional recovery could be judged.

## Experiment 6

### Characterisation of deficits in a unilateral dorsolateral QA lesion mouse model

The first experiment described in this chapter utilised unilateral DLS lesions designed to elicit motoric deficits in the QA mouse model of HD. A battery of motor and non-motor behavioural tests was employed at an early and late time-point post-lesion to establish if stable deficits could be detected.

#### 5.3 Methods

##### 5.3.1 Experimental design

Thirty-two six-week-old C57/BL6J mice (Harlan Laboratories, Bicester, UK) were used in this study, housed under standard conditions. Animal numbers were calculated based on data from previous experiments and confirmed using sample size analysis software G\*Power. On arrival mice were left to acclimatise for one week prior to testing. Animals were initially housed in groups of eight, however, following the lesion surgery the groups had to be separated due to severe fighting and from one-week post-lesion all animals were housed individually.

Behavioural tests were selected based on those most commonly used in rat QA lesion / transplant behavioural studies and which reflect aspects of HD, see **Table 5A**.

Mice were sorted into experimental groups based on their performance in the pre-lesion lateralised choice reaction time task (LCRTT). Inherent side-bias, number of trials completed, and accuracy were used to rank the mice and allocate them into one of two counter-balanced groups; lesion (n=20) and intact sham-lesion controls (n=12). To eliminate side-bias as a confounding factor when assessing the effect of the lesion, animals were split into left- and right-hand surgery groups, with half of the left- or right-side biased animals being allocated to each group.

### 5.3.2 Pre-lesion training

All mice were placed on a food restricted feeding schedule and maintained at ~90% of free-feeding body weight before commencing training in both the staircase reaching task (methods section 2.5.2 vii) and LCRTT in operant 9-hole boxes (methods section 2.5.3 vi). From commencement of operant training to completion of the full LCRTT was approximately eight weeks. During this time pre-lesion baseline performance was recorded and mice were returned to free-food for one week prior to undergoing surgery, at which time the mice were sixteen weeks of age.

### 5.3.3 Lesion surgery

Surgery was performed using the standard protocols described (Methods section 2.2.1), with the stereotaxic co-ordinates adapted for a lateralised placement for the purpose of this experiment.

The lesioned mice received 0.2µl 0.9M QA at two sites using the following coordinates: AP = +1.2, ML = +2.4 (for left) or -2.4 (for right), DV = -2.4 and AP = +2.2, ML = +1.8 (for left) or -1.8 (for right), DV = -2.4. The sham lesion animals received injections of 0.2µl 0.9% saline at the same coordinates.

### 5.3.4 Post-lesion testing

Following a one-week post-surgery recovery period, mice were tested in non-food restricted tests before being returned to food restriction for reward dependent tasks, as listed in **Table 5.1**. These ‘early time-point’ tests were complete within a post-lesion time of 1-7 weeks, (17 to 23-week age range), before mice were returned to *ab lib* feeding.

Four months following surgery, the testing schedule was repeated with the addition of rotational behaviour measures. This ‘late time-point’ comprised post-lesion times of 16-23 weeks, and an age range of 32 to 39 weeks old.

The complete experimental timeline is shown in **Figure 5.1 A**. All behavioural protocols are described in methods section 2.5.

Behavioural test	Measure
Locomotor activity	General activity levels
Open Field	Anxiety, speed
Spontaneous rotations	Dopamine receptor loss
Amphetamine-induced rotations	Dopamine receptor loss
Apomorphine induced rotations	Dopamine receptor loss
Footprint analysis	Gait
Balance beam	Balance
Rotarod	Motor coordination
Staircase test (FR)	Manual dexterity
Sucrose consumption test	Reward value perception
Corridor test (FR)	Lateralised neglect
LCRTT (FR)	Visuospatial processing
Elevated plus maze	Anxiety

**Table 5.1** Complete list of all behavioural tests performed in the DLS mice and the behavioural measure they probe. (FR) indicates tests requiring mice to be food restricted, all other tests were performed under an *ab lib* feeding regime.

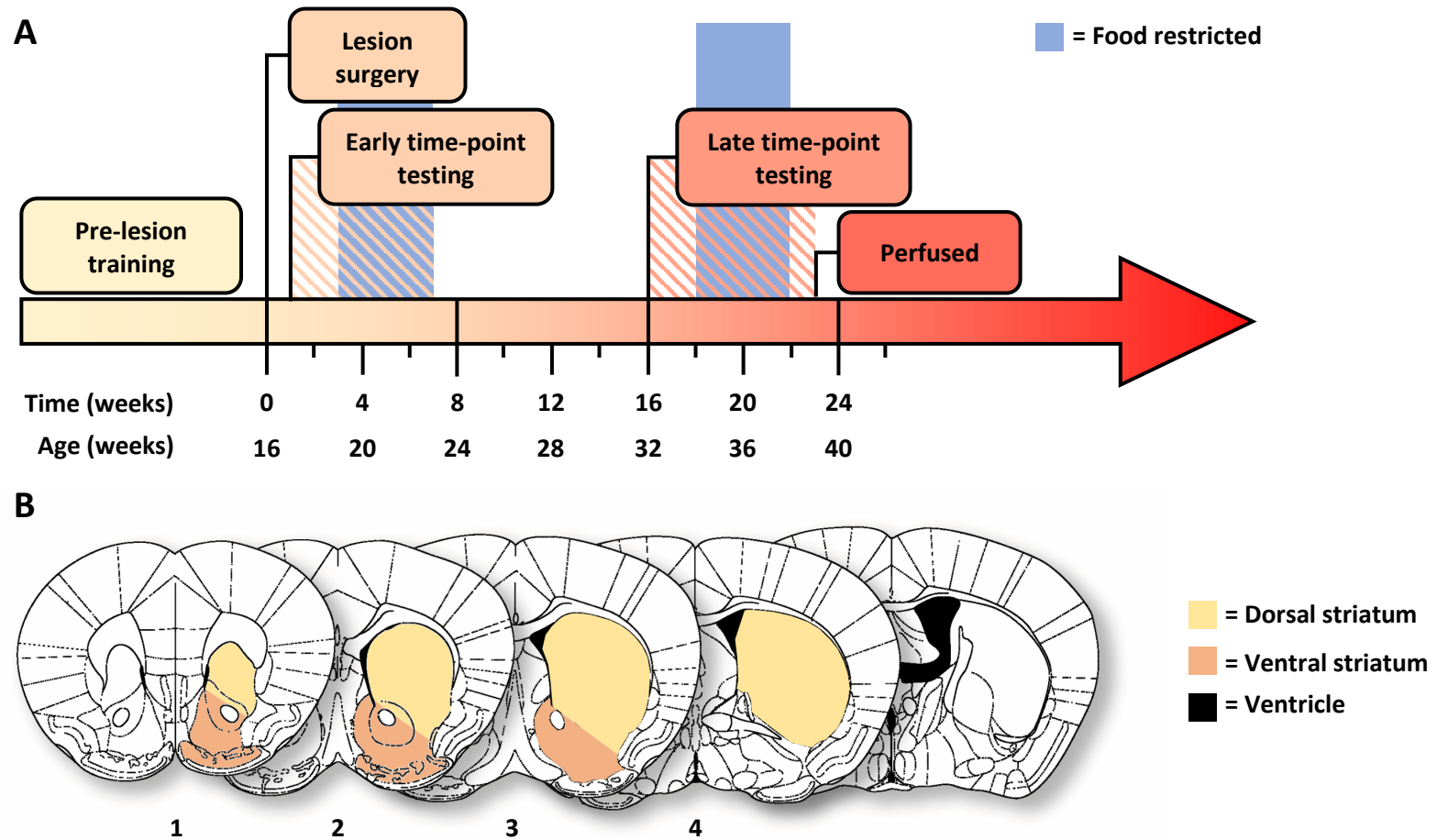


**Figure 5.1** **A** Experimental timeline. The diagonally shaded regions span the duration of all behavioural tests for each time-point. The blue filled regions represent the time for which animals were food restricted. **B** Schematic diagram (adapted from Paxinos and Franklin, 2004) to show the approximate sections from which volumetric measurements were taken, 1-4.

### 5.3.5 Immunohistochemical analysis of lesions

Following completion of all behavioural tests, mice were perfused, and brains cut into 30 $\mu$ m sections as described in methods section 2.3.1. Immunohistochemical stains of MSN marker DARPP-32 and neuronal marker NeuN were applied to 1 in 6 sections.

Bright-field microscopy of the DARPP-32<sup>+</sup> labelled tissue was used to identify the location and volume of the lesions within the striatum. Ipsi- and contralateral dorsal DARPP-32<sup>+</sup> striatal volume, as well as ventricular and ventral striatal volume were measured, see **Figure 5.1 B**. Volumetric measures were recorded from four sequentially anterior sections from ~ bregma +0.26mm (or from the most posterior section within which the two lateral ventricles remain distinct from each other).

### 5.3.6 Statistical analysis

Two mice from the lesioned group died following surgery and were excluded from the experiment completely. Five mice became ill and were perfused prior to completion of the late time-point and have been included in analysis for only those tests that were completed. Following histological examination, one animal was removed retrospectively from all behavioural analyses due to very small lesion size (less than 2 standard deviations from the mean, and no behavioural deficits observed). Consequently, the final group sizes for behavioural analyses were; control group n=12, and lesion group n= 14 to 17 (dependant on the task).

Of the prematurely terminated mice, one brain was not able to be recovered prior to perfusion, and therefore could not be included in lesion and volumetric analyses.

All statistical analysis was performed using Genstat (18<sup>th</sup> edition). ANOVAs were performed to compare experimental groups and either contra- and ipsilateral measures, or early and late time-points. Sidak's post hoc pairwise comparisons were performed to analyse significant interactions, correcting for multiple comparisons. Correlation analysis was used to identify significant correlations between behavioural data and lesion volume. Only those that reached significance are presented. Significance was taken as  $p \leq 0.05$ .

Post-hoc power analysis based on final animal numbers was calculated using G\*Power software and was estimated to be 97% for large effect sizes and 69% for medium effect sizes.

## 5.4 Results

### Histological analyses

DARPP-32 staining revealed a loss of DARPP-32<sup>+</sup> striatal cells in the lateral region of the lesioned striatum, with relative sparing to the medial striatum, see **Figure 5.2 A - B**. Minimal lateralised sparing was seen in the mid to anterior striatum (Bregma +1.70 to +0.26mm) with greater sparing seen in general towards the more posterior regions of the striatum (Bregma +0.26 to -0.70mm).

The QA injections resulted in a mean lesion volume of  $0.81 \pm 0.06 \text{ mm}^3$ , with a range of 0.25 - 1.21  $\text{mm}^3$ , **Figure 5.2 C**. Following the removal of the animal with the smallest lesion from the group (as discussed above) the mean lesion volume was  $0.84 \pm 0.05 \text{ mm}^3$ , with a range of 0.45 - 1.21  $\text{mm}^3$ . These lesions equated to an ipsilateral loss of 78.2%  $\pm 2.7$  DARPP-32<sup>+</sup> striatal volume in the DLS group, with no changes detected in the sham animals (Surgery\*Side:  $F_{1, 24}=400.56$ ,  $p<0.001$ ; Sham (Side):  $t_{24}=1.16$ , ns; Lesion (Side):  $t_{24}=27.15$ ,  $p<0.001$ ), **Figure 5.3 A**. The lesions produced an increase of 99.7%  $\pm 18.6$  in ipsilateral ventricle volume, when compared to the intact contralateral side with no changes observed between the hemispheres in the sham lesion group (Surgery\*Side:  $F_{1, 24}=50.12$ ,  $p<0.001$ ; Sham (Side):  $t_{24}=1.05$ , ns; Lesion (Side):  $t_{24}=11.05$ ,  $p<0.001$ ), **Figure 5.3 B**.

Measures of the ventral striatum showed no difference in DARPP-32<sup>+</sup> volume between the ipsi- and contralateral hemispheres, confirming that the lesions were correctly placed in only the dorsal region of the striatum, with the nucleus accumbens remaining unaffected, **Figure 5.3 C**.

There was a significant inverse correlation between the volume of remaining ipsilateral DARPP-32<sup>+</sup> tissue and the volume of the lesion,  $r=-0.64$ ,  $p<0.01$ , and a significant positive correlation between lesion volume and the ipsilateral ventricle,  $r=0.64$ ,  $p<0.05$ , see **Figure 5.3 D - E**.

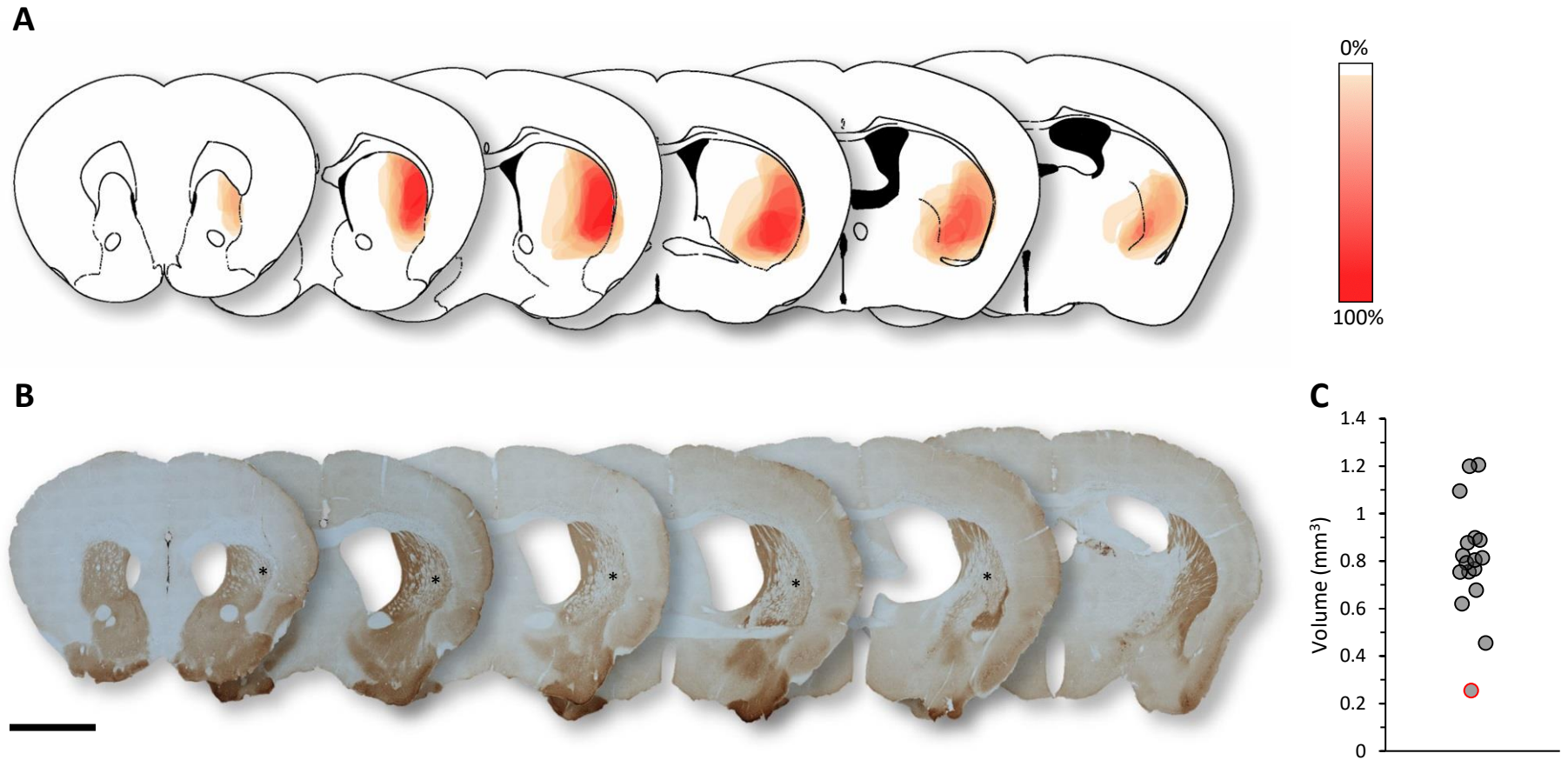


**Figure 5.2** **A** Graphical representation of the size and position of each unilateral QA lesion of mice included in the results. The scale represents the proportion of animals with lesions in the coloured area. **B** Photomicrographs of a typical cross section of a lesioned brain labelled with DARPP-32. Lesions are clearly visible through lack of DAB staining (\*) in the striatum. **C** Graph representing lesion volume and group spread, as measured on DARPP-32 labelled brain sections. The red dot represents the animal which was removed from the behavioural analyses due to inadequate lesion volume. Scale bar represents 2mm.

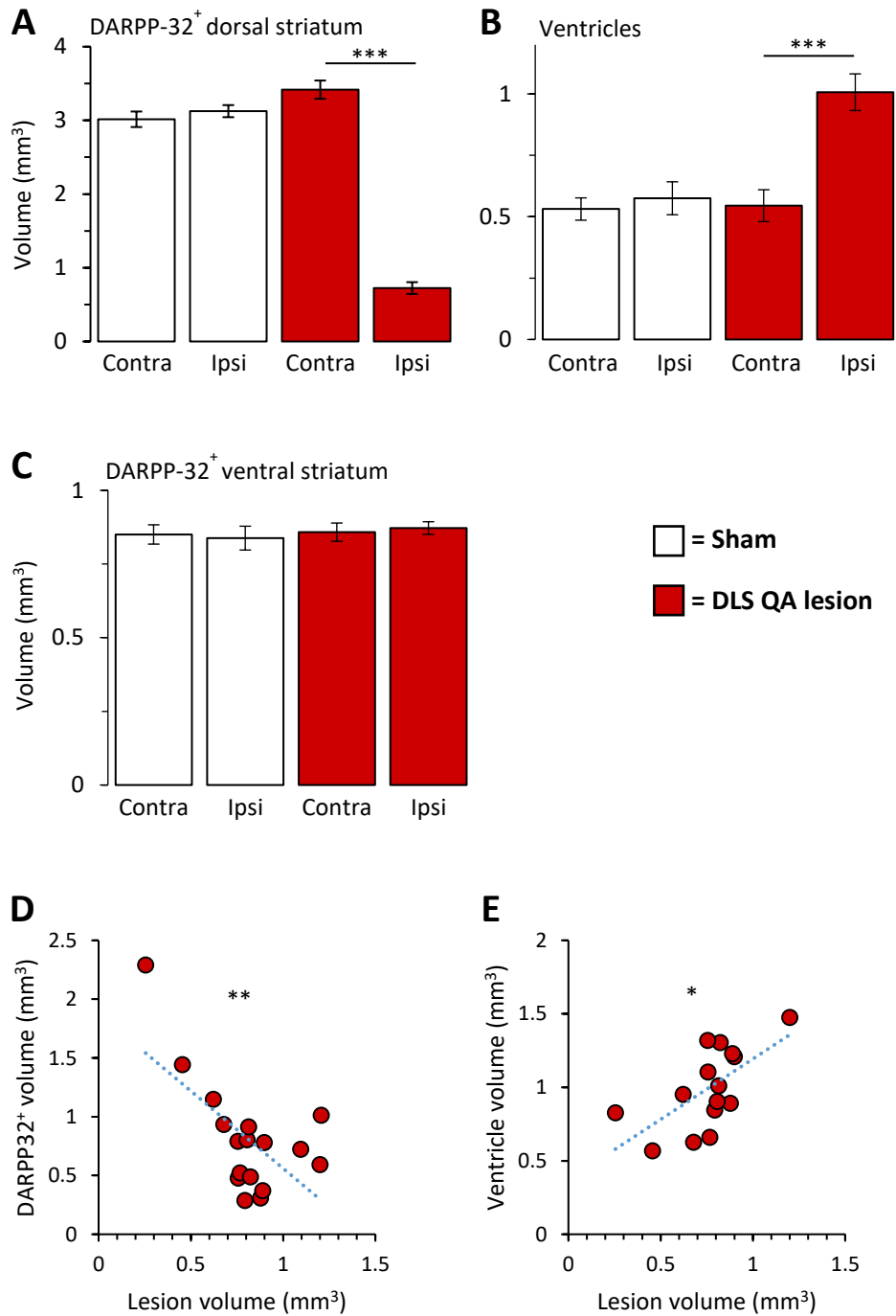


**Figure 5.3** **A** Volume of the contra- and ipsilateral dorsal striatum as measured by DARPP-32<sup>+</sup> staining. The ipsilateral dorsostriatal volume was reduced in the QA lesioned group compared to the contralateral side (\*\*\*)  $p < 0.001$ , whilst there was no difference between the sides of the sham animals. **B** Contra- and ipsilateral ventricle volume. The ipsilateral ventricle volume was increased in the QA lesioned group compared to the contralateral side (\*\*\*)  $p < 0.001$ . No difference was seen in the sham group. **C** Volume of the contra- and ipsilateral ventral striatum as measured by DARPP-32<sup>+</sup> staining. No significant differences were found. **D** Plot showing the correlation between ipsilateral dorsostriatal volume and lesion volume. DARPP-32<sup>+</sup> volume decreased as lesion size increased, \*\*  $r = -0.64$ ,  $p < 0.01$ . **E** Plot showing the correlation between ipsilateral ventricle volume and lesion volume. Ventricle volume increased proportionally to lesion volume, \*  $r = 0.64$ ,  $p < 0.05$ .

### Weight

Following surgery the sham group maintained a stable body weight, however the DLS lesion group saw a gradual decline of nearly 2% of their pre-surgery weight over seven days and had a higher proportion of bodyweight loss than the sham group from days 4 to 6 post-lesion (Surgery\*Time:  $F_{7, 189}=10.51$ ,  $p<0.001$ ; Surgery (Day 1):  $t_{82}=1.80$ , ns; Surgery (Day 2):  $t_{82}=1.20$ , ns; Surgery (Day 3):  $t_{82}=1.67$ , ns; Surgery (Day 4):  $t_{82}=3.65$ ,  $p<0.01$ ; Surgery (Day 5):  $t_{82}=4.16$ ,  $p<0.01$ ; Surgery (Day 6):  $t_{82}=4.84$ ,  $p<0.01$ ; Surgery (Day 7):  $t_{82}=3.95$ ,  $p<0.01$ ),

#### Figure 5.4 A.

This difference was transitory, and no significant difference was observed between the free-feeding body weights of the sham and lesion groups during the testing period ( $t_{27}=1.58$ , ns). During food-restriction however, despite both groups maintaining just over 90% of their free-feeding weight, the QA lesion group weighed less than the sham group, ( $t_{27}=2.36$ ,  $p<0.05$ ), see **Figure 5.4 B.**

### Motor tests

#### Locomotor activity

The number of beam breaks during the dark (i.e. active) period between 6pm and 6am was significantly increased in the QA lesioned group compared to the sham control group, indicating hyperactivity in the lesioned group, (Surgery:  $F_{1, 27}=15.23$ ,  $p<0.001$ ), **Figure 5.5 A.** Activity levels were significantly greater at the late time-point compared to the early time-point (Time:  $F_{1, 27}=15.17$ ,  $p<0.001$ ).

#### Open field

The total distance moved, velocity and movement time during the open field test was greater in the DLS lesion group (Surgery:  $F_{1, 27}=15.99$ ,  $p<0.001$ ,  $F_{1, 27}=16.00$ ,  $p<0.001$  and  $F_{1, 27}=14.27$ ,  $p<0.001$  respectively), **Figure 5.5 B - D.** The distance moved, and velocity increased at the late time point (Time:  $F_{1, 27}=13.79$ ,  $p<0.001$  and  $F_{1, 27}=13.77$ ,  $p<0.001$  respectively), however there was no change in time spent moving between the two time-points (Time:  $F_{1, 27}=1.32$ , ns). There were significantly fewer bouts of movement (movement frequency) in the QA lesion group (Surgery:  $F_{1, 27}=18.59$ ,  $p<0.001$ ), and a decrease in the number of bouts at the late time point (Time:  $F_{1, 27}=7.14$ ,  $p<0.05$ ), **Figure 5.5 E.**

### Rotations

Neither the sham nor the QA lesion group exhibited any spontaneous rotation behaviour, however, during the amphetamine drug probe the QA lesion group performed a higher net rotation rate than the sham group (Surgery:  $t_{23}=2.36$ ,  $p<0.05$ ), **Figure 5.6 A**. In the probes using both the low ( $1\text{mgkg}^{-1}$ ) and higher ( $2\text{mgkg}^{-1}$ ) dose of apomorphine the QA lesion group rotated at a higher rate than the sham controls (Surgery:  $t_{22}=3.65$ ,  $p<0.001$  and  $t_{22}=5.08$ ,  $p<0.001$  respectively). A significant correlation between lesion volume and net rotations during the higher apomorphine dose was noted ( $r=0.56$ ,  $p<0.05$ ), **Figure 5.6 B**, although no correlation could be made at the lower dose, nor with amphetamine induced rotations.

### Gait

Footprint analysis revealed a trend towards a reduced stride length in the QA lesioned animals, however this result was not statistically significant (Surgery:  $F_{1, 27}=3.83$ ,  $p=0.06$ ). Stride length was increased at the late time-point compared to the early time-point (Time:  $F_{1, 48}=105.06$ ,  $p<0.001$ ), but there was no difference between ipsi- and contralateral stride length in either group (Side:  $F_{1, 27}=0.28$ , ns), **Figure 5.6 C**.

There was no difference between the QA lesion and the sham controls in either hind- or forelimb base-width, (Surgery:  $F_{1, 27}=0.14$ , ns, and  $F_{1, 27}=0.00$ , ns, respectively), although hind limb base-width was increased at the late time-point (Time:  $F_{1, 24}=11.39$ ,  $p<0.01$ ), see **Figure 5.6 D**. A similar change was not seen for forelimb base width (Time:  $F_{1, 24}=0.59$ , ns).

A significant reduction in the amount of overlap between the placement of the fore- and hind paws was observed in the QA lesion group when compared to the sham controls, (Surgery:  $F_{1, 27}=5.12$ ,  $p<0.05$ ), **Figure 5.6 E**. At the late time-point the degree of overlap increased overall compared with the early time-point (Time:  $F_{1, 48}=7.66$ ,  $p<0.01$ ), but there was no effect on side (Side:  $F_{1, 51}=0.66$ , ns).

### Balance beam

The time taken to turn around on the balance beam task was increased in the DLS lesion group compared to the sham controls (Surgery:  $F_{1, 27}=8.05$ ,  $p<0.01$ ), however this effect was driven by the difference at the early time-point only, and no difference was seen between the groups at the late time-point (Surgery\*Time:  $F_{1, 25}=7.62$ ,  $p<0.01$ ; Surgery (Early):  $t_{47}=3.90$ ,  $p<0.001$ ; Surgery (Late):  $t_{47}=0.63$ , ns), **Figure 5.7 A**. There was no difference between groups on time to cross the beam (Surgery:  $F_{1, 27}=0.05$ , ns), and both took longer to traverse the beam at the late time-point (Time:  $F_{1, 25}=29.34$ ,  $p<0.001$ ), **Figure 5.7 B**.

No difference in the number of foot-slips was found between the DLS lesion and sham groups (Surgery:  $F_{1,27}=3.30$ , ns), **Figure 5.7 C**. The number of foot-slips increased between the early and late time-points (Time:  $F_{1,25}=34.27$ ,  $p<0.001$ ), and although there was a trend indicating a more extreme increase in the QA lesion group, this did not reach significance (Time\*Surgery:  $F_{1,25}=3.78$ ,  $p=0.06$ ).

### Rotarod

The QA lesioned mice fell from the rotarod earlier than the sham controls (Surgery:  $F_{1,27}=18.66$ ,  $p<0.001$ ), **Figure 5.7 D**. This deficit was maintained through both the early and late time-points (Time\*Surgery:  $F_{1,27}=7.44$ ,  $p<0.05$ ; Surgery (Early):  $t_{38}=2.80$ ,  $p<0.05$ ; Surgery (Late):  $t_{38}=5.05$ ,  $p<0.001$ ). The sham group were able to improve performance at the late point (Time (Sham):  $t_{27}=3.06$ ,  $p<0.05$ ), however, no improvement was seen in the QA lesion group (Time (Lesion):  $t_{27}=0.77$ , ns).

### Staircase

No lateralised bias was observed in the staircase task in either group (Side:  $F_{1,27}=1.11$ , ns), although an overall deficit in the total number of pellets retrieved was seen in the QA lesion group compared to the sham animals (Surgery:  $F_{1,27}=5.92$ ,  $p<0.05$ ), **Figure 5.8 A**. Both groups saw an increase in the total number of pellets obtained from the early to the late time-point (Time:  $F_{1,48}=51.28$ ,  $p<0.001$ ).

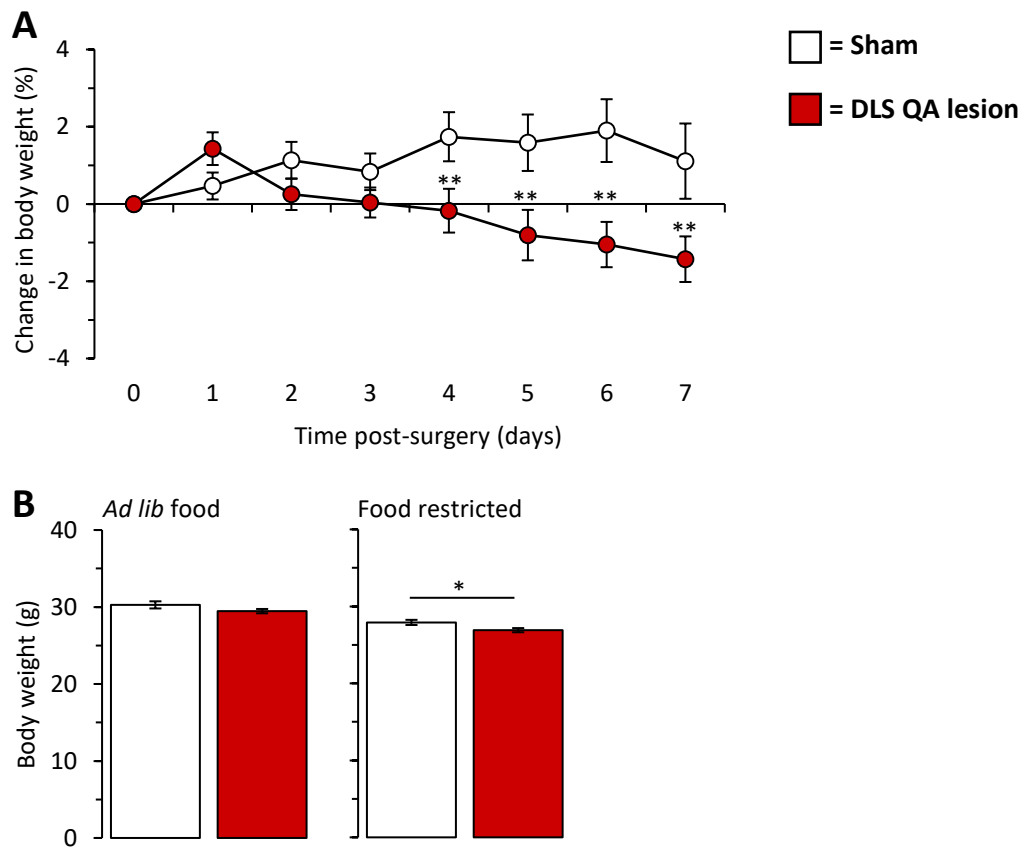


**Figure 5.4** **A** Mean daily body weights of the mice in the week following surgery. The DLS QA lesion group had a higher proportion of bodyweight loss than the sham group from days 4 to 6 post-lesion (\*\*  $p < 0.01$ ). **B** Mean body weights during *ad-lib* feeding and during food restriction periods. There was no difference between groups during free food phases, however the QA lesion group weighed less than the sham group during food restriction periods (\*  $p < 0.05$ ).

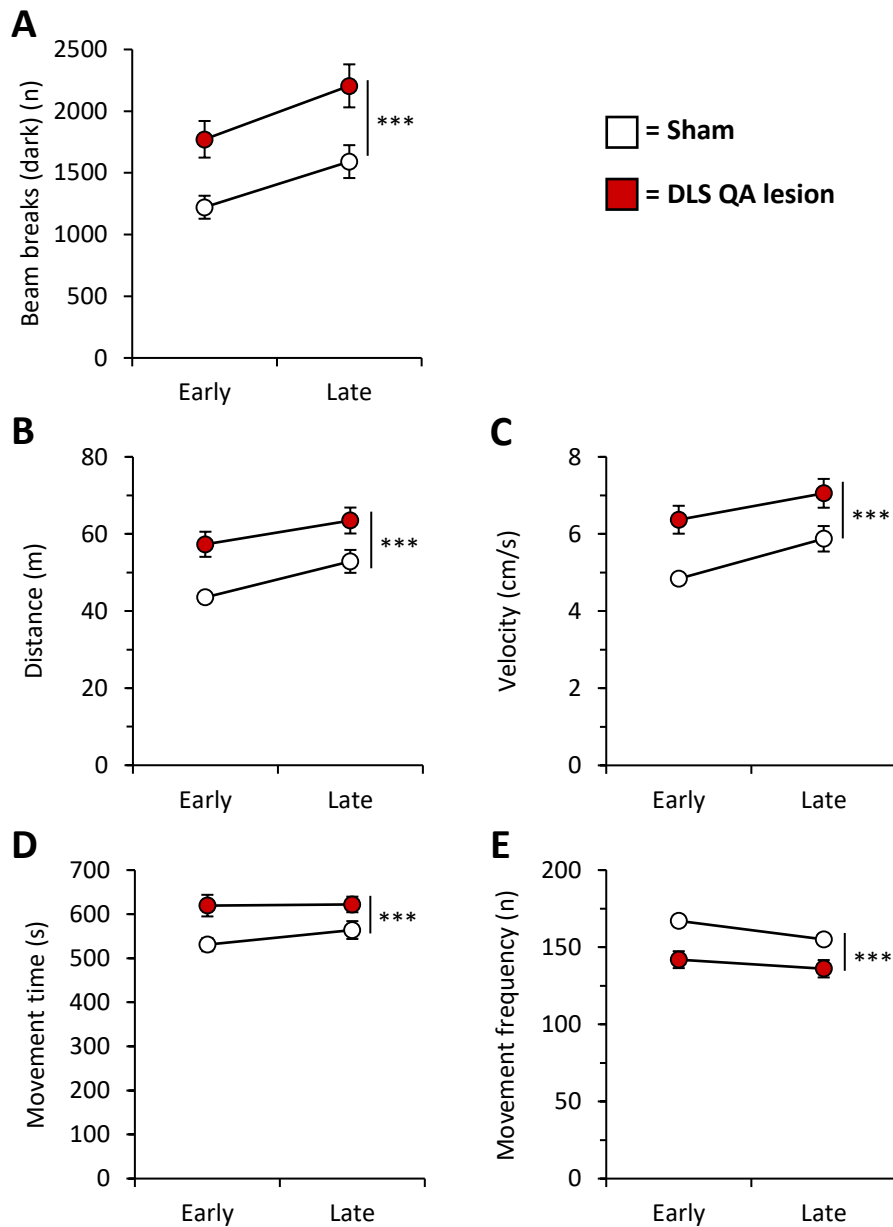


**Figure 5.5** **A** Number of beam breaks during the dark phase of locomotor activity test. DLS lesioned animals were significantly more active compared to the shams (\*\* $p < 0.001$ ). Activity levels increased at the late time-point compared to the early time-point ( $p < 0.001$ ). **B** Distance travelled in open field. The DLS lesioned group travelled a greater total distance than the sham (\*\* $p < 0.001$ ). Distance travelled increased in the late time-point compared to the early time-point ( $p < 0.001$ ). **C** Velocity in open field. DLS lesioned animals moved faster than the sham (\*\* $p < 0.001$ ). Animals moved at a greater speed in the late time-point compared to the early time-point ( $p < 0.001$ ). **D** Time spent moving in open field. The DLS lesioned animals were moving for a greater length of time than the shams (\*\* $p < 0.001$ ). There was no difference in time spent moving between the early and late time-points. **E** Number of bouts of movement in open field. The DLS lesioned mice had fewer separate bouts of movement time than the shams (\*\* $p < 0.001$ ). The number of bouts decreased between the early and late time-points ( $p < 0.05$ ).

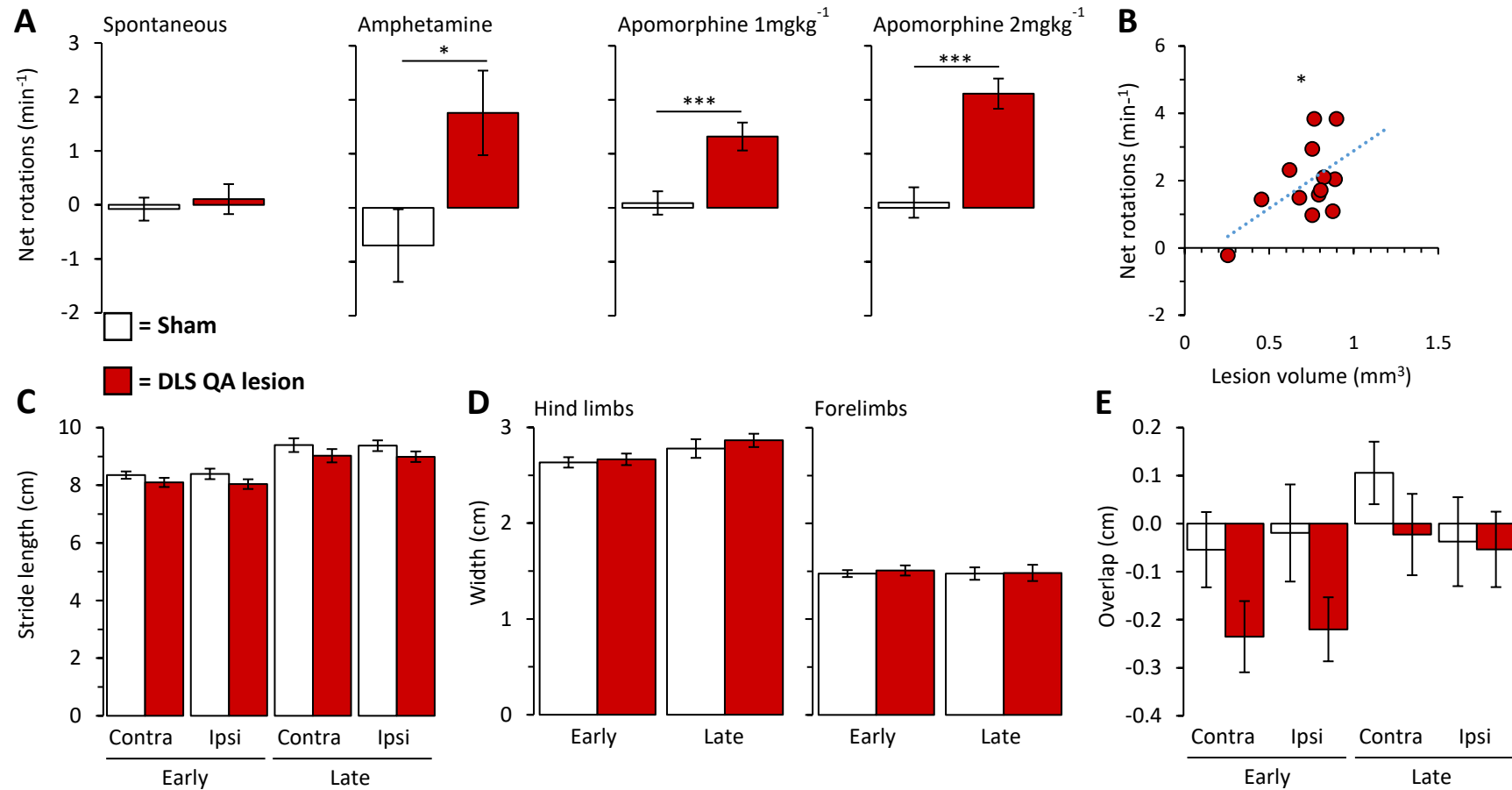


**Figure 5.6** **A** Net clockwise rotations (towards ipsilateral side) under spontaneous conditions plus amphetamine and apomorphine drug probes. No spontaneous rotation behaviour was observed. The DLS mice rotated more than the sham animals during the amphetamine probe (\*  $p < 0.05$ ). Lesioned mice also rotated more in the  $1\text{mgkg}^{-1}$  apomorphine probe (\*\*\*  $p < 0.001$ ) and the  $2\text{mgkg}^{-1}$  apomorphine probe (\*\*\*  $p < 0.001$ ). **B** Plot showing the correlation between net rotations during  $2\text{mgkg}^{-1}$  apomorphine drug probe and lesion volume. Net rotations per minute were proportional to lesion volume, \*  $r = 0.56$ ,  $p < 0.05$ . **C** Mean stride length of contra- and ipsilateral side at the early and late time-points as measured by footprint analysis. No effect of lesion on stride length was found. Stride length increased at the late time-point ( $p < 0.001$ ). No difference was found between ipsi- and contralateral sides. **D** Mean base width of the hind and fore paws. No effect of surgery was seen on either hind- or forelimb base-width. An increase in base-width at the later time-point was seen in hind limbs ( $p < 0.01$ ), but not forelimbs. **E** Mean overlap of the placement of hind and fore paws. A positive measure represents the placement of the hind paw in front of the fore paw when taking a step. There was a reduction in the amount of overlap in the DLS mice compared to sham ( $p < 0.05$ ). There was an increase in overlap at the late time-point ( $p < 0.01$ ), but there was no difference between ipsi- and contralateral overlap.

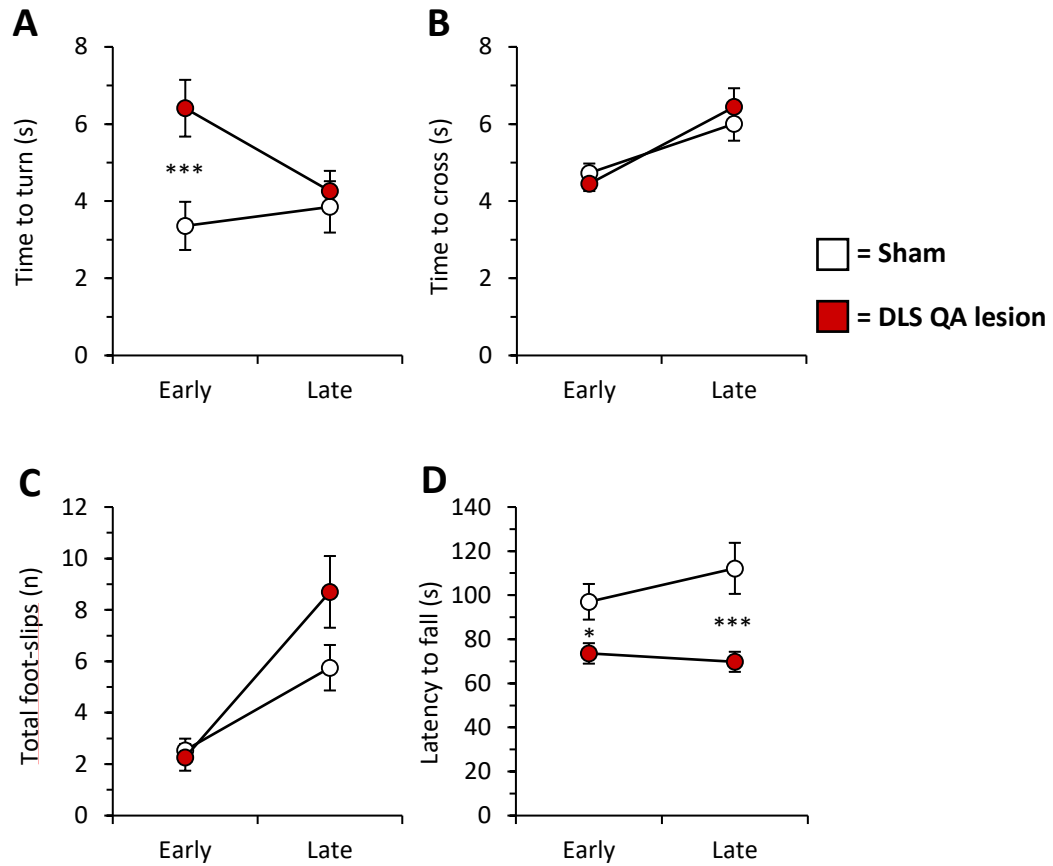


**Figure 5.7** **A** Mean time to turn around after placement on the elevated balance beam. The DLS lesioned mice took longer to turn than the sham group at the early time-point (\*\* $p < 0.001$ ). **B** Mean time to cross the balance beam. No effect of surgery was detected on the time taken to cross. Time to cross increased at the late time-point compared to the early time-point ( $p < 0.001$ ). **C** Total foot-slips made whilst crossing the balance beam. No effect of surgery on the total number of foot-slips was found. The number of foot-slips increased at the late time-point ( $p < 0.001$ ). **D** Latency to fall from the accelerating rotarod. The DLS lesioned groups had a reduced latency to fall compared to the shams at both the early and late time-points (\*  $p < 0.05$ ; \*\* $p < 0.001$ ).

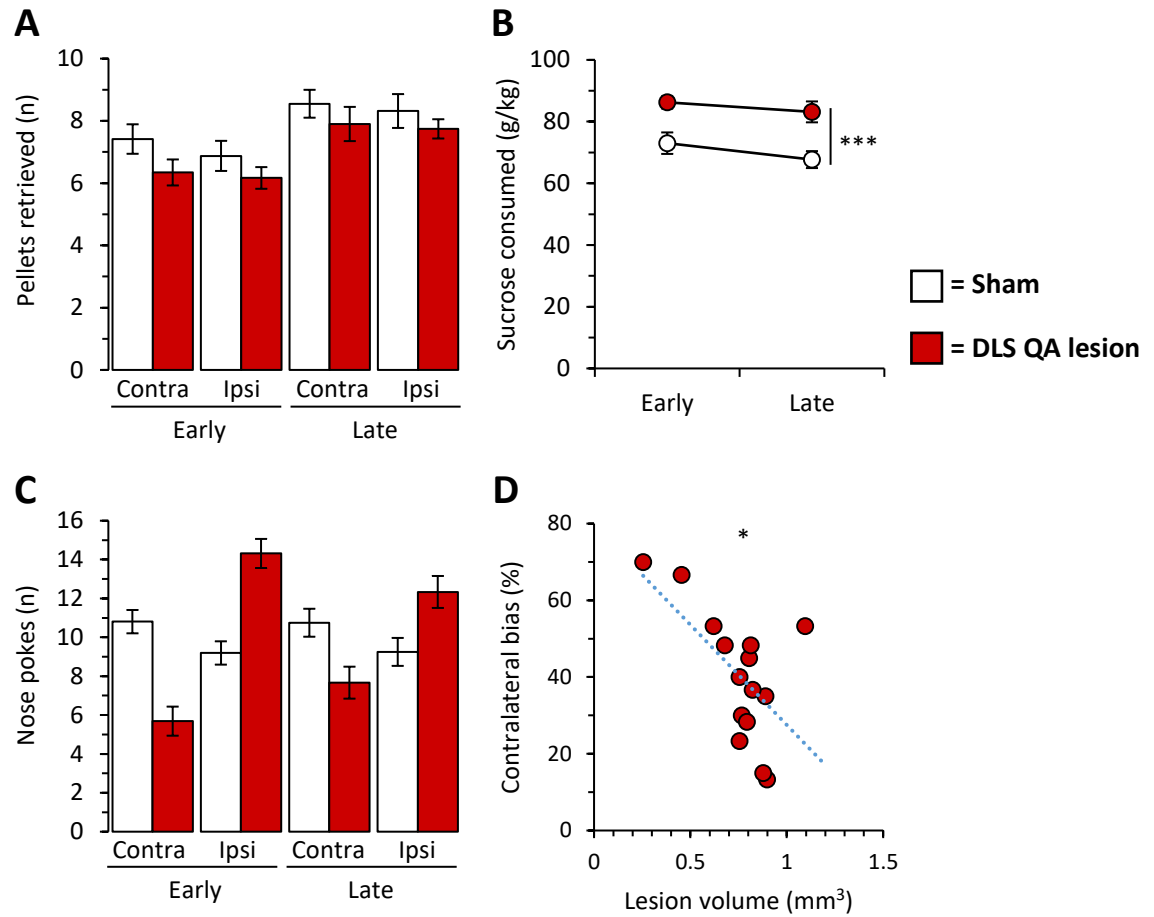


**Figure 5.8** **A** Mean number of pellets retrieved in the staircase task. The DLS lesioned mice retrieved fewer pellets than the sham group ( $p < 0.05$ ). No effect of side was seen. The number of pellets retrieved increased at the late time-point ( $p < 0.001$ ). **B** Amount of sucrose consumed per gram of bodyweight. The DLS lesioned group consumed a great amount of sucrose per kg bodyweight than the sham animals ( $*** p < 0.001$ ). There was no difference in the amount consumed between the late and early time-points. **C** Mean number of exploratory nose pokes into lateral wells in the corridor task. An ipsilateral bias was observed in the DLS animals ( $p < 0.001$ ) but not the shams. **D** Plot showing the correlation between contralateral bias in the corridor task and lesion volume. Contralateral bias was inversely proportional to lesion volume,  $* r = -0.61$ ,  $p < 0.01$ .

## Non-Motor tests

### Reward consumption

The amount of sucrose consumed per kg was increased in the QA lesion group compared to the sham controls in the consumption test (Surgery:  $F_{1, 27}=29.09$ ,  $p<0.001$ ), **Figure 5.8 B**.

### Corridor

In the corridor task the DLS lesion group made significantly more nose pokes on their ipsilateral side compared to the contralateral side, while sham animals did not exhibit any bias toward contra- or ipsilateral nose pokes (Surgery\*Side\*Time:  $F_{1, 48}=6.48$ ,  $p<0.05$ ; Side (Sham):  $t_{48}=2.18$ , ns; Side (Lesion):  $t_{48}=9.62$ ,  $p<0.001$ ), **Figure 5.8 C**. There was a significant correlation between lesion volume and contralateral side bias, with the proportion of bias away from the contralateral side increasing as lesion volume increased ( $r=-0.61$ ,  $p<0.05$ ), **Figure 5.8 D**.

### Bilateral lateralised choice reaction time task (BLCRTT)

The QA lesion mice were less accurate in the BLCRTT than the sham group (Surgery:  $F_{1, 26}=14.59$ ,  $p<0.01$ ), **Figure 5.9 A**. Reduced accuracy on the contralateral side was observed at the early time-point, driven by a deficit in the QA lesioned group's contralateral performance (Time\*Side:  $F_{1, 48}=14.16$ ,  $p<0.001$ . Early (Side):  $t_{33}=2.66$ ,  $p<0.05$ ). Due to a reduction in ipsilateral performance at the late time-point in both groups, the trend for the lesioned group to perform worse on the contralateral side did not reach significance (Late (Side):  $t_{33}=0.12$ , ns). A Side\*Surgery interaction was not quite significant (Side\*Surgery:  $F_{1, 26}=4.04$ ,  $p=0.055$ ), so the trend for contralateral deficits in accuracy in the DLS lesioned animals could not be tested post hoc, although it is likely that with improved numbers there would be a significant ipsilateral bias in these animals.

No difference was observed in the reaction time between the groups, nor between contra- and ipsilateral sides (Surgery:  $F_{1, 27}=0.62$ , ns; Side:  $F_{1, 25}=0.92$ , ns), **Figure 5.9 B**.

Movement time was increased in the QA lesioned group in comparison to the sham group (Surgery:  $F_{1, 27}=35.93$ ,  $p<0.001$ ), **Figure 5.9 C**. The movement time was greater for ipsilateral responses; however, this was driven by a transitory increase in ipsilateral response time in the QA group at the early time-point, (Time\*Surgery\*Side:  $F_{1, 45}=11.53$ ,  $p=0.001$ ; Early Lesion (Side):  $t_{51}=5.29$ ,  $p<0.001$ ); Late (Lesion (Side):  $t_{51}=0.73$ , ns).

The total number of usable trials (TTUs) generated was greater in the sham animals compared to the QA lesion group (Surgery:  $F_{1, 27}=35.38$ ,  $p<0.001$ ), **Figure 5.9 D**. The sham animals generated fewer TTUs at the late time-point than at the early time-point, however the DLS lesion group maintained the number of trials generated (Time\*Surgery:  $F_{1, 25}=7.36$ ,  $p<0.05$ ; Sham (Time):  $t_{25}=3.62$ ,  $p<0.01$ ; Lesion (Time):  $t_{25}=0.21$ , ns).

A greater proportion of the QA lesion group's usable trials resulted in a time-out (TO) error than the sham group (Surgery:  $F_{1, 27}=23.78$ ,  $p<0.001$ ). There was no difference between the groups in the number of premature withdrawals made (Surgery:  $F_{1, 27}=1.21$ , ns). A significant correlation between the total number of usable trials (TTU) and lesion volume was observed, with TTU decreasing as lesion volume increased at both the early and late time-points ( $r=-0.54$ ,  $p<0.05$  and  $r=-0.51$ ,  $p<0.05$  respectively), **Figure 5.9 E**.

### Unilateral lateralised choice reaction time task (ULCRTT)

Both groups were able to respond accurately to the near contralateral hole in the ULCRTT but were significantly less accurate in the far contralateral hole (Hole:  $F_{1, 21}=626.60$ ,  $p<0.001$ ) at both the early and late time-points, **Figure 5.10 A**, however there was no effect of lesioning (Surgery:  $F_{1, 25}=0.52$ , ns).

Reaction time was unaffected by surgery (Surgery:  $F_{1, 25}=2.28$ , ns), but was higher in response to the furthest hole compared to the near hole (Hole:  $F_{1, 20}=17.90$ ,  $p<0.001$ ), **Figure 5.10 B**.

Movement time to the far contralateral hole was greater than to the nearer hole (Hole:  $F_{1, 20}=34.11$ ,  $p<0.001$ ), **Figure 5.10 C**. The QA lesion group took longer to move to the holes than the sham group (Surgery:  $F_{1, 25}=18.60$ ,  $p<0.001$ ).

The sham group generated a greater number of TTUs than the QA lesion group (Surgery:  $F_{1, 27}=28.00$ ,  $p<0.001$ ), **Figure 5.10 D**, and both groups generated more trials at the late time-point compared to the early time-point (Hole:  $F_{1, 24}=33.64$ ,  $p<0.001$ ). The percentage of TTU resulting in a TO error was greater in the QA lesion group compared to the sham animals (Surgery:  $F_{1, 27}=37.04$ ,  $p<0.001$ ), with the lesion group, but not the shams, reducing the proportion of TO errors in the late time-point compared to the early time-point (Time\*Surgery:  $F_{1, 24}=5.07$ ,  $p<0.05$ ; Time (Sham):  $T_{24}=1.59$ , ns; Time (Lesion):  $T_{24}=4.76$ ,  $p<0.001$ ). There was no difference in the number of premature withdrawals between the groups (Surgery:  $F_{1, 27}=0.04$ , ns). A significant correlation between the total number of usable trials (TTU) and lesion volume was observed, with TTU decreasing as lesion volume increased at the early time-point ( $r=-0.51$ ,  $p<0.05$ ), **Figure 5.10 E**.

### Elevated plus maze

The QA group spent less time in the closed arm of the elevated plus maze compared to the sham group (Surgery:  $F_{1,27}=4.69$ ,  $p<0.05$ ), **Figure 5.11 A**, choosing instead to explore the open arms or be in the centre of the maze investigating the entrance to the open arms. While there was no difference in the total number of entries made into the arms of the maze (Surgery:  $F_{1,27}=2.38$ , ns), the QA group entered into open arms more frequently than the sham group (Surgery:  $F_{1,27}=4.57$ ,  $p<0.05$ ). However, there was no difference between groups in the number of entries into the closed arms (Surgery:  $F_{1,27}=0.13$ , ns), **Figure 5.11 B**.

### Open field

During the open field test, the DLS lesioned animals crossed into the central zone more frequently than the sham group, and spent more time there (Surgery:  $F_{1,27}=10.91$ ,  $p<0.01$  and  $F_{1,27}=6.65$ ,  $p<0.05$  respectively), **Figure 5.11 C**. Fewer entries into the central zone were made at the late time-point compared to the early time-point (Time:  $F_{1,27}=27.26$ ,  $p<0.001$ ), however a greater amount of time was spent there (Time:  $F_{1,27}=13.12$ ,  $p<0.001$ ). There was no difference in rearing frequency between groups (Surgery:  $F_{1,27}=0.00$ , ns), however the sham group reared more in the late time-point compared to the early time-point whereas the QA lesion group did not (Time\*Surgery:  $F_{1,27}=4.75$ ,  $p<0.01$ ; Sham (Time):  $T_{27}=3.37$ ,  $p<0.01$ , Lesion (Time):  $T_{24}=0.40$ , ns), **Figure 5.11 D**.

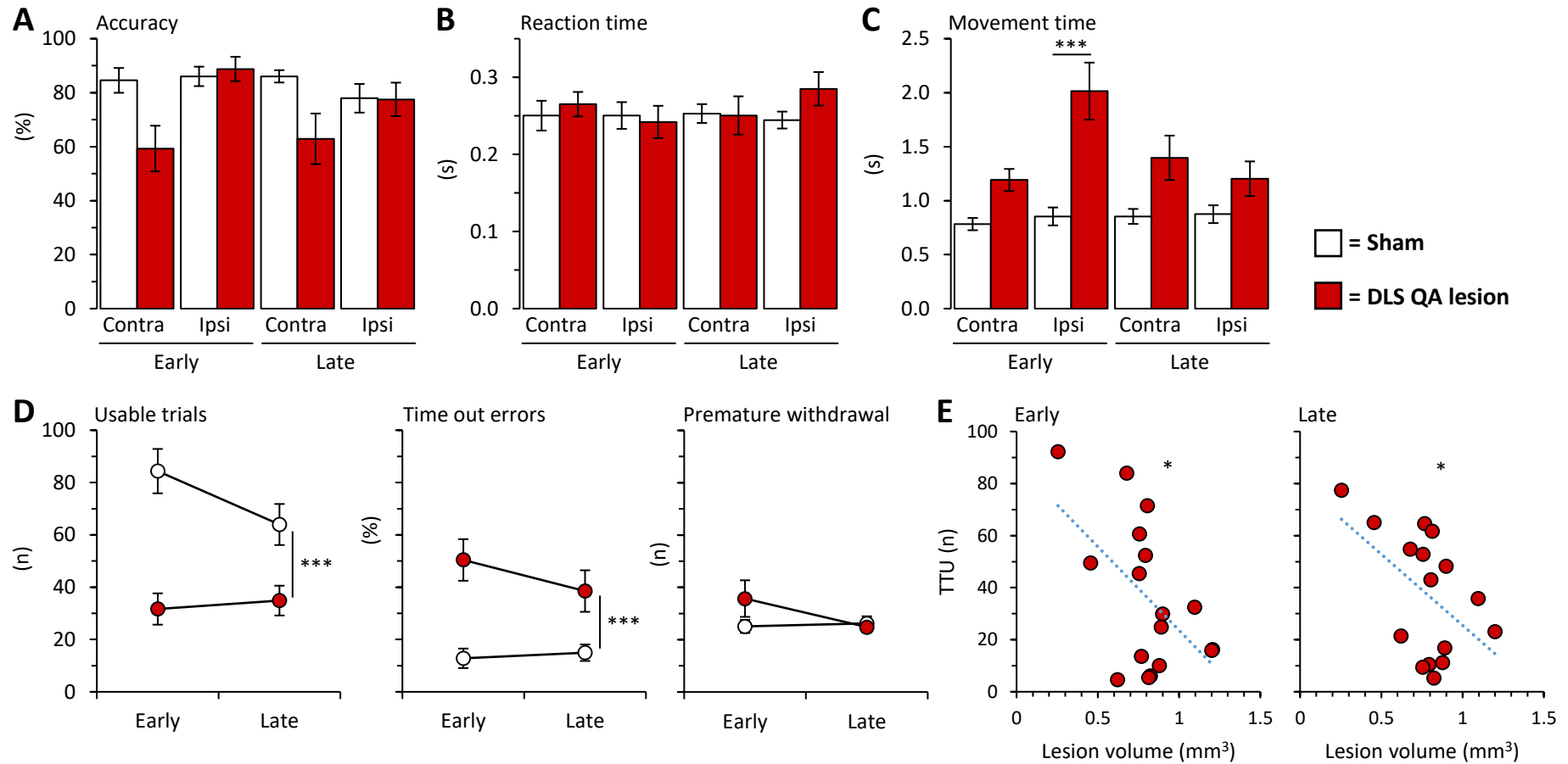


**Figure 5.9** **A** Mean accuracy in the bilateral lateralised choice reaction time task (BLCRTT) (correct/(correct + incorrect)). DLS lesioned mice were less accurate compared to the sham animals ( $p < 0.01$ ). Contralateral accuracy was reduced in the early time-point ( $p < 0.05$ ) but not at the late time-point. **B** Mean reaction time in the BLCRTT. No difference in reaction time between groups or between side were observed. **C** Mean movement time in the BLCRTT. The DLS group had an increased movement time compared to the shams ( $p < 0.001$ ). Ipsilateral movement time was increased compared to the contralateral in the DLS lesioned group in the early time-point ( $***p < 0.001$ ), but not the late time-point. **D** Total usable trials achieved in BLCRTT, percentage of usable trials resulting in a time out error and number of premature withdrawals per usable trial. The DLS lesion mice initiated fewer usable trials than the shams ( $*** p < 0.001$ ). Sham animals generated fewer usable trials at the late time-point than at the early time-point ( $p < 0.01$ ), whereas the lesioned animals maintained their trial number. A greater proportion of time-out errors were made by the lesioned group ( $*** p < 0.001$ ). No difference in the number of premature withdrawals was seen between groups. **E** Plot showing the correlation between the total usable trials in the BLCRTT and lesion volume at the early and late time-point. The number of usable trials was inversely proportional to lesion volume at both the early and late time-points,  $* r = -0.54$ ,  $p < 0.05$  and  $* r = -0.51$ ,  $p < 0.05$  respectively.

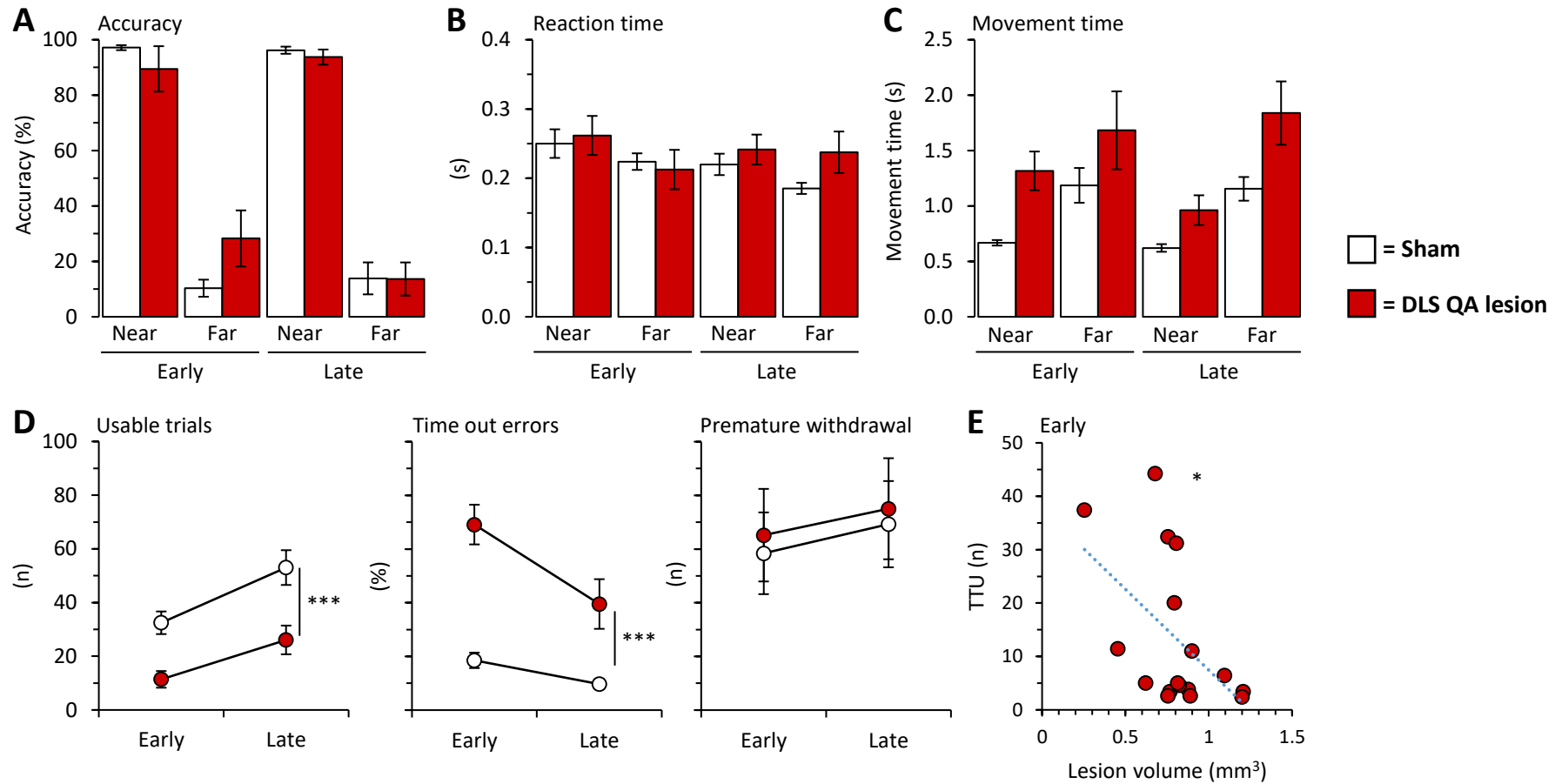


**Figure 5.10** **A** Mean accuracy in the unilateral lateralised choice reaction time task (ULCRTT) (correct/(correct + incorrect)). Accuracy in responses to the far hole was lower compared to the near hole ( $p < 0.001$ ). No effect of lesioning was detected. **B** Mean reaction time in the ULCRTT. Reaction time to the far hole stimulus was reduced compared to the near hole ( $p < 0.001$ ). No difference was detected between groups. **C** Mean movement time in the ULCRTT. The DLS lesioned mice took longer to move to the holes than then the sham group ( $p < 0.001$ ). Movement time to the far hole was greater than to the near hole ( $p < 0.001$ ). **D** Total usable trials achieved in ULCRTT, percentage of usable trials resulting in a time out error and number of premature withdrawals per usable trial. The DLS lesion group generated fewer trials than the sham animals ( $*** p < 0.001$ ). More trials were generated at the late time-point than the early time-point ( $p < 0.001$ ). A higher proportion of trials resulted in a time-out in the DLS lesion group than the shams ( $*** p < 0.001$ ). The proportion of time-outs from DLS lesion animal trials was reduced at the late time-point ( $p < 0.001$ ) but was maintained in the sham animals. No difference in premature withdrawals was found between groups. **E** Plot showing the correlation between the total usable trials in the ULCRTT and lesion volume at the early time-point. The number of usable trials was inversely proportional to lesion volume,  $* r = -0.51$ ,  $p < 0.05$ .

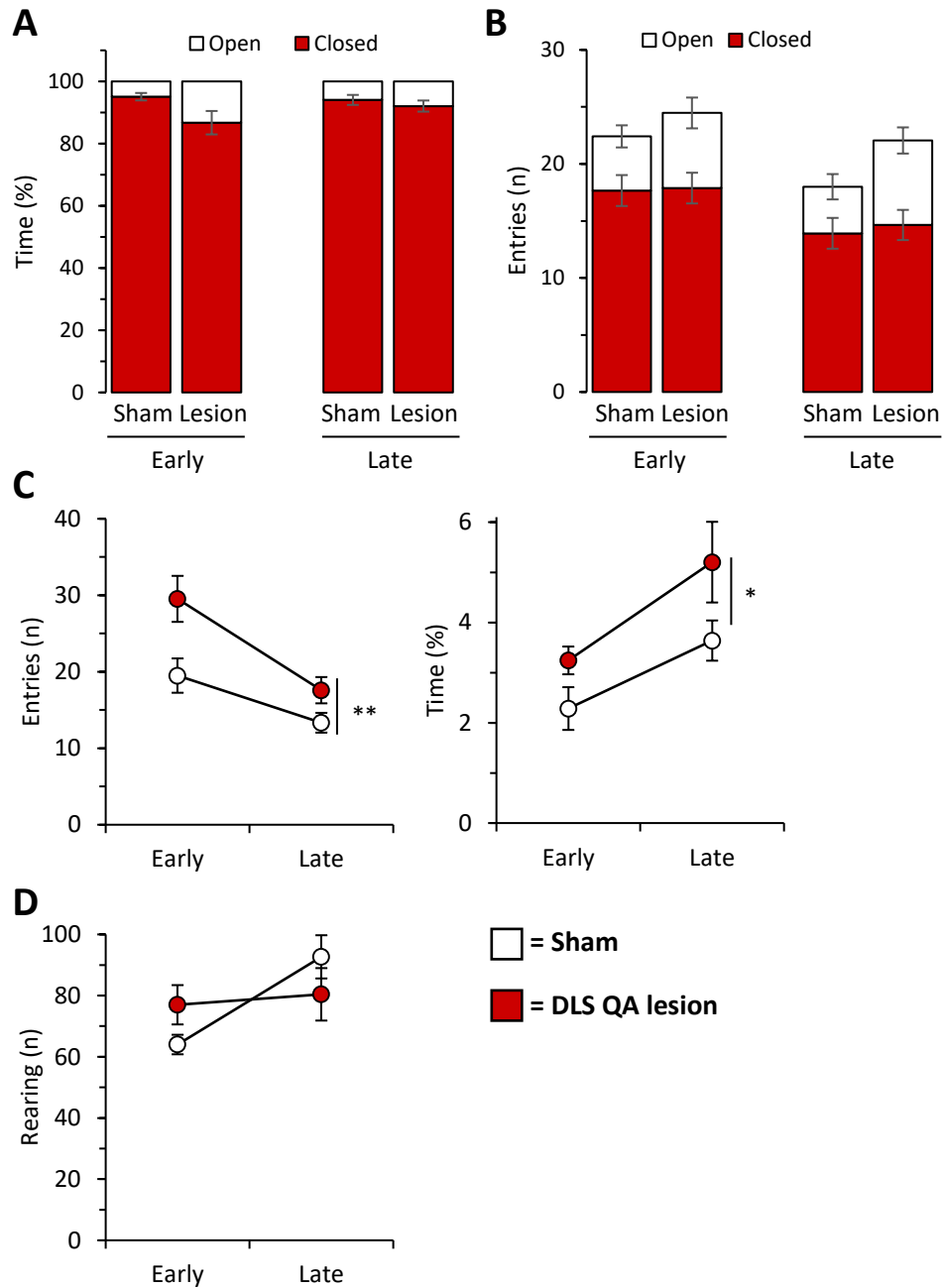


**Figure 5.11** **A** Proportion of time spent in each arm of the elevated plus maze. DLS lesioned mice spent a greater proportion of time in the open arms compared to the sham group ( $p < 0.05$ ). **B** Number of entries made into each arm of the elevated plus maze. The lesioned mice made a greater number of entries into the open arms than the shams ( $p < 0.05$ ), but there was no difference in number of crosses into the closed arms. **C** Number entries made into the central zone of the open field arena and the percentage of time spent within the central zone. The DLS lesioned animals crossed into the central zone more often than the shams (\*\*  $p < 0.01$ ). Less entries to the central zone were made at the late time-point than the early time-point ( $p < 0.001$ ). The lesioned animals also spent a larger proportion of their time in the central zone compared to shams (\*  $p < 0.05$ ). More time was spent in the central zone at the late time-point compared to the early time-point ( $p < 0.001$ ). **D** Frequency of rearing behaviour in the open field test. No effect of surgery was observed.

## 5.5 Experiment Discussion

The objective of this study was to establish a battery of apposite tests able to detect long-term lesion-induced deficits in a QA mouse model of HD designed to illicit motoric deficits through lesions of the DLS. The purpose of this was to enable their use in future investigations to efficiently test for functional improvements brought about by cell transplantation studies or other therapeutic interventions.

### Lesion quality

The immunohistological staining results show that the unilateral lesions were located within the DLS and were of a sufficient volume to elicit behavioural deficits in many of the tests implemented. One mouse was excluded which had a lesion volume of just  $0.25\text{mm}^3$ , equating to just under 20% loss of DARPP-32<sup>+</sup> volume. No behavioural deficits were detected in this individual, suggesting that a loss of more than 20% DARPP-32<sup>+</sup> dorsal striatal volume at least was required in order to elicit detectable behavioural disturbances in the tests used.

The direct correlation between lesion volume and ventricle volume implies that the lesion induced not only loss of DARPP-32<sup>+</sup> from the striatum, but also induced cell loss and collapse of the parenchyma on the ipsilateral side, as observed in [Chapter 3](#). Therefore, volumetric measures of DARPP-32<sup>+</sup> loss cannot relate an absolute measure of lesion size, since the parenchyma collapses and reduces the volume of the affected tissue. It can be assumed then that the actual extent of the lesion would be larger than that measured. Nevertheless, the fact that there was a direct correlation between the measured lesion volume and spared DARPP-32<sup>+</sup> volume, and to many behavioural deficits, demonstrates that measures taken in this way are adequate in assessing the magnitude of lesions.

DLS QA lesions had no effect on volumetric measures of DARPP-32<sup>+</sup> staining in the ventral striatum, demonstrating the sparing of damage in this region. The assertion that the ventral striatum was not disturbed removes the implication that damage directly to the nucleus accumbens could have directly affected aspects of reward motivation (Saddoris et al., 2015) or its control in modulating activity levels (Kalivas et al., 1984).

## Weight

The QA-lesioned animals exhibited a transitory free-feeding weight loss in the week following surgery that was not seen in the sham group, however, there was no difference in weight at the time of testing in non-restricted tasks. Since weight can influence performance in tests such as rotarod, balance beam and footprint, it is important to note that this was not a factor in this case. During periods of food restriction, the QA group weighed less than the control animals, however, bodyweight has less influence on those tasks for which food restriction was required.

It is important to note that seven mice of the twenty mice receiving the DLS lesion died or were culled in the post-surgical period. Of these, five were critically injured due to increased aggression and fighting within the home cages. This behaviour was sustained and led to the animals being housed individually from one week post-surgery. Irritability and aggressive behaviour in people with HD has been reported previously (Shiwach and Patel, 1993), as well as in some genetic HD mouse models, particularly in males (Shelbourne et al., 1999), and should be a consideration when designing studies in these models. It would be interesting to include tests of aggression, such as the resident intruder test, in cell replacement therapy behavioural studies since few non-motor deficits have been shown to be resolved pre-clinically.

## The effect of unilateral DLS lesions

The outcome of the tests explored is summarised in **Table 5.2**. Those tests which were able to detect a sustained deficit across the two time-points are marked.

Behavioural results are discussed in detail at the end of this chapter.

Test	Long-term deficits	Measure observed
Locomotor activity	✓	Hyperactivity
Open Field	✓	Increased distance, velocity & duration of movement Increased time in central zone
Spontaneous rotations	✗	No effect
Amphetamine-induced rotations	✓	Dopamine receptor loss
Apomorphine induced rotations	✓	Dopamine receptor loss
Footprint analysis	✓	Reduced overlap
Balance beam	✗	Early effect only on time to turn
Rotarod	✓	Reduced motor co-ordination
Staircase test	✓	Reduced manual dexterity
Sucrose consumption test	✓	Increased consumption
Corridor test	✓	Lateralised visuospatial bias
BLCRTT	✓	Lateralised visuospatial deficit & usable trials Increase in movement time & time-out errors
ULCRTT	✓	Reduction in usable trials Increase in movement time & time-out errors
Elevated plus maze	✓	Increased entry into open arms

**Table 5B** Summary assessment of tests performed. ✓ indicates a test was able to demonstrate stable DLS lesion-induced deficit, ✗ indicates either no detectable deficits or transient deficit.

## Experiment 7

### Characterisation of deficits in a bilateral dorsomedial QA lesion mouse model

The second experiment described in this chapter used bilateral DMS lesions designed to elicit non-motor deficits in the QA mouse model of HD. A battery of non-motor and motor behavioural tests were employed at an early and late time-point post-lesion to establish if stable deficits could be detected.

## 5.6 Methods

### 5.6.1 Experimental design

Thirty-two six-week old C57/BL6J mice (Harlan Laboratories, Bicester, UK) were used in this study, housed under standard conditions. Animal numbers were calculated based on data from previous experiments and confirmed using sample size analysis software G\*Power. On arrival mice were left to acclimatise for one week prior to testing. Animals were initially housed in groups of eight, however, following the lesion surgery the groups had to be separated due to severe fighting and from one-week post-lesion all animals were housed individually.

Behavioural tests were selected based on those most commonly used in rat QA lesion / transplant behavioural studies and which reflect aspects of HD, see [Table 5.3](#).

Mice were allocated into one of two counter-balanced experimental groups based on pre-lesion accuracy performance in the DA task; DMS lesion (n=20) or intact sham-lesion controls (n=12).

### 5.6.2 Pre-lesion training

All mice were placed on a water restriction protocol with access to three hours of water per day and trained in the delayed alternation (DA) task in skinner-style operant boxes (methods section 2.5.3 vi). Initiation of training to completion of the full DA task lasted approximately 15 weeks. During this time the pre-lesion baseline performance was recorded, and mice were returned to free-water for one week prior to undergoing surgery, at which time the mice were twenty-two weeks of age.

### 5.6.3 Lesion surgery

Surgery was performed using the standard protocols described in methods section 2.2.1, with the stereotaxic coordinates adapted for bilateral dorsomedial placement of the lesion.

The DMS lesioned mice received 0.1µl 0.9M QA at eight sites (four per hemisphere) at the following coordinates from bregma: AP = +1.2, ML = ±1.4, DV = -3.0/-2.0 and AP = +2.2, ML = ±1.2, DV = -2.8/-2.2. The sham lesion animals received injections of 0.1µl 0.9% saline at the same coordinates.

### 5.6.4 Post-lesion testing

Following a one-week post-surgical recovery period, mice were tested in the non-water restricted tests before being returned to water restriction for the reward dependant tasks, as listed in Table 5.3. These ‘early time-point’ tests were complete within a post-lesion time period of 1-7 weeks, (23 to 29-week age range), and mice returned to *ad lib* water access.

Four months following surgery, the testing schedule was repeated. This ‘late time-point’ comprised post-lesion times of 16 to 27 weeks (38 to 49 weeks of age).

The complete experimental timeline is shown in Figure 5.12. All behavioural protocols are described in methods section 2.5.

Behavioural test	Measure
Delayed alternation (WR)	Working memory, rule learning
5CSRTT (WR)	Attention
Milkshake consumption test	Reward value perception
Novel object recognition	Short & long-term memory
Elevated plus maze	Anxiety
Open Field	Anxiety, speed
Nest building	Natural behaviour
Locomotor activity	General activity levels
Footprint analysis	Gait
Balance beam	Balance
Rotarod	Motor coordination
Corridor test (WR)	Lateralised neglect

**Table 5.3** Complete list of all behavioural tests performed in the DMS mice and the behavioural measure they probe. (WR) indicates tests requiring mice to be water restricted, all other tests were performed under an *ab lib* water regime.

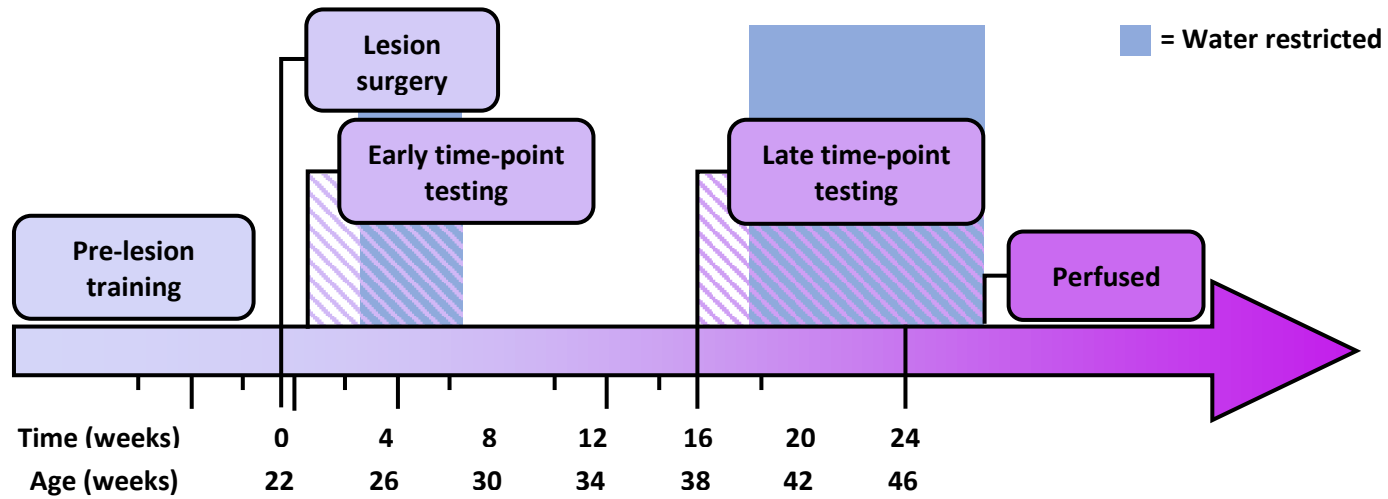


**Figure 5.12** Experimental timeline indicating the progression, in weeks, of the experiment. The diagonally shaded regions span the duration of all behavioural tests for each time-point. The blue filled regions represent the time for which animals were water restricted.

### 5.6.5 Immunohistochemical analysis of lesions

Following perfusion, the tissue was processed as described in section 5.3.5.

### 5.6.6 Statistical analysis

Three mice from the DMS lesioned group died following surgery and were excluded from the experiment completely. Following histological examination, a further seven mice were removed retrospectively from all behavioural analyses due to having no detectable lesion in either one or both hemispheres. Consequently, the final group sizes for behavioural analyses were; sham control group n=12, and DMS lesion group n=10.

All statistical analysis was performed using Genstat (18<sup>th</sup> edition). ANOVAs were performed to compare experimental groups and early and late time-points. For tests in which complex comparisons were made, i.e. delayed alternation, 5CSRTT and novel object recognition tasks, the early and late time-points were analysed in separate ANOVAs to simplify the interpretation of data. Sidak's post hoc pairwise comparisons were performed to analyse significant interactions, correcting for multiple comparisons. Correlation analysis was used to identify significant correlations between behavioural data and lesion volume. Only those that reached significance are presented. Significance was taken as  $p \leq 0.05$ .

Post-hoc power analysis based on final animal numbers was calculated using G\*Power software and was estimated to be 95% for large effect sizes and 61% for medium effect sizes.

## 5.7 Results

### Histological analyses

Lesions were identified through loss of DARPP-32<sup>+</sup> staining in the medial striatum, with sparing of tissue in the lateral regions observed, **Figure 5.13 A & B**. Spread of the lesion into more lateral areas was observed within the anterior striatum (Bregma +1.70 to +1.18mm) and some sparing of tissue at the striatal-ventricle margin, and in the most dorsal aspect of the medial striatum was seen in more posterior areas (Bregma +0.74 to -0.58mm). Some lesions were observed extending posteriorly to parts of the globus pallidus.

The bilateral QA injections resulted in a mean total lesion volume of  $0.73 \pm 0.10 \text{ mm}^3$ , with a range of  $0.23 - 1.35 \text{ mm}^3$ , **Figure 5.13 C**. These lesions equated to a loss of  $34.5\% \pm 6.24$  total DARPP-32<sup>+</sup> striatal volume compared to the shams (Surgery:  $t_{20}=3.73$ ,  $p<0.001$ ) and affected an increase of  $47.0\% \pm 14.0$  in ventricle volume when compared to the mean sham measurements (Surgery:  $t_{20}=2.73$ ,  $p<0.05$ ), **Figure 5.14 A - B**.

Measures of the ventral striatum showed no difference in DARPP-32<sup>+</sup> volume between the sham and DMS lesioned groups, confirming that the lesions were correctly placed in only the dorsal region of the striatum, with the nucleus accumbens remaining unaffected by the lesion (Surgery:  $t_{20}=0.20$ , ns), **Figure 5.14 C**.

There was a significant inverse correlation between the volume of remaining DARPP-32<sup>+</sup> tissue and the volume of the lesion,  $r=-0.72$ ,  $p<0.001$ , and a significant positive correlation between lesion and ventricle volume,  $r=0.57$ ,  $p<0.05$ , see **Figure 5.14 D - E**.

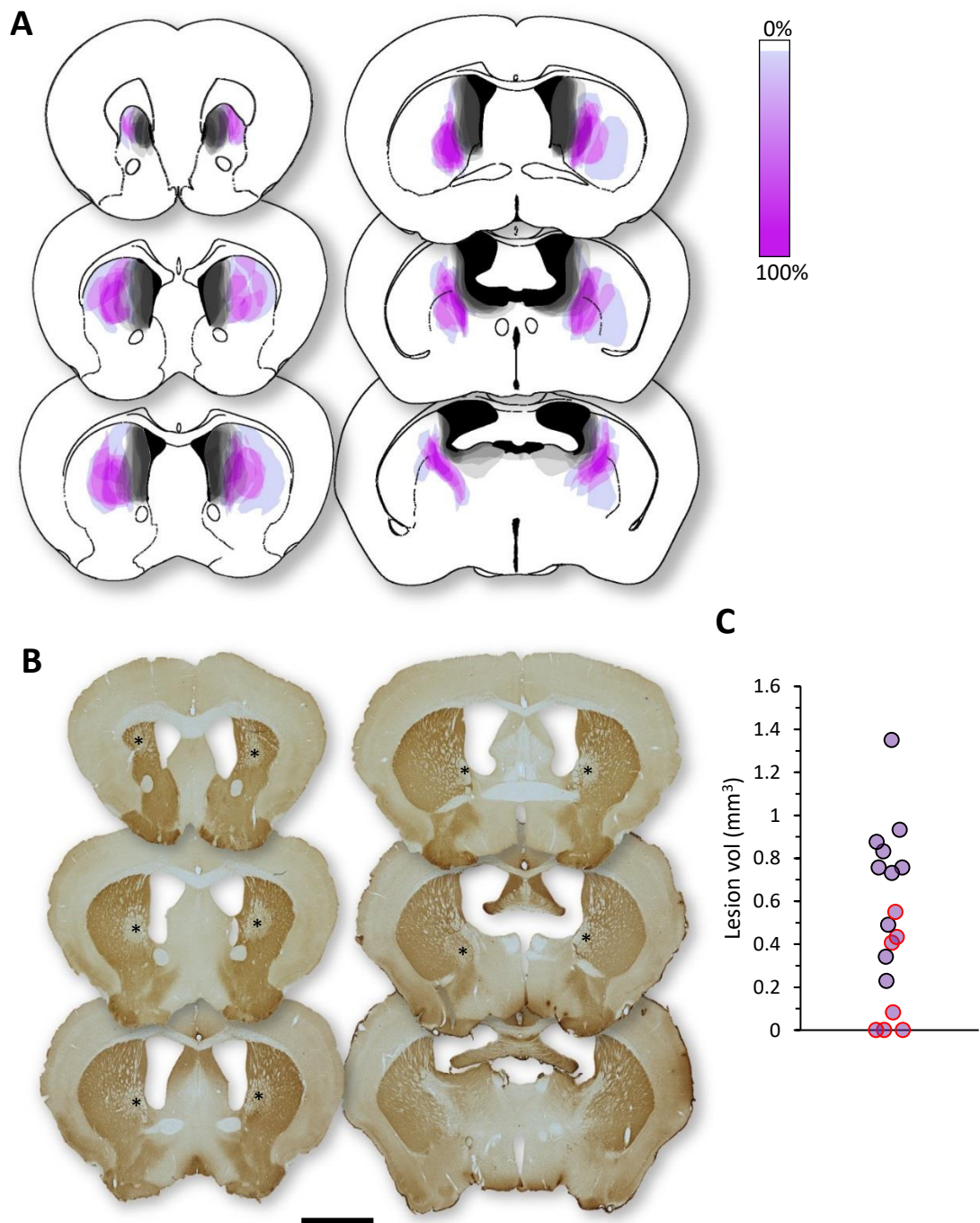


**Figure 5.13** **A** Graphical representation of the size and position of each bilateral QA lesion of mice included in the results. The scale represents the proportion of animals with lesions in the coloured area. **B** Photomicrographs of a typical cross section of a lesioned brain labelled with DARPP-32. Lesions are clearly visible through lack of DAB staining (\*) in the striatum. **C** Graph representing total bilateral lesion volume and group spread, as measured on DARPP-32 labelled brain sections. The red dots represent the animal which were removed from the behavioural analyses due to no visible lesion in one or both hemispheres. Scale bar represents 2mm.

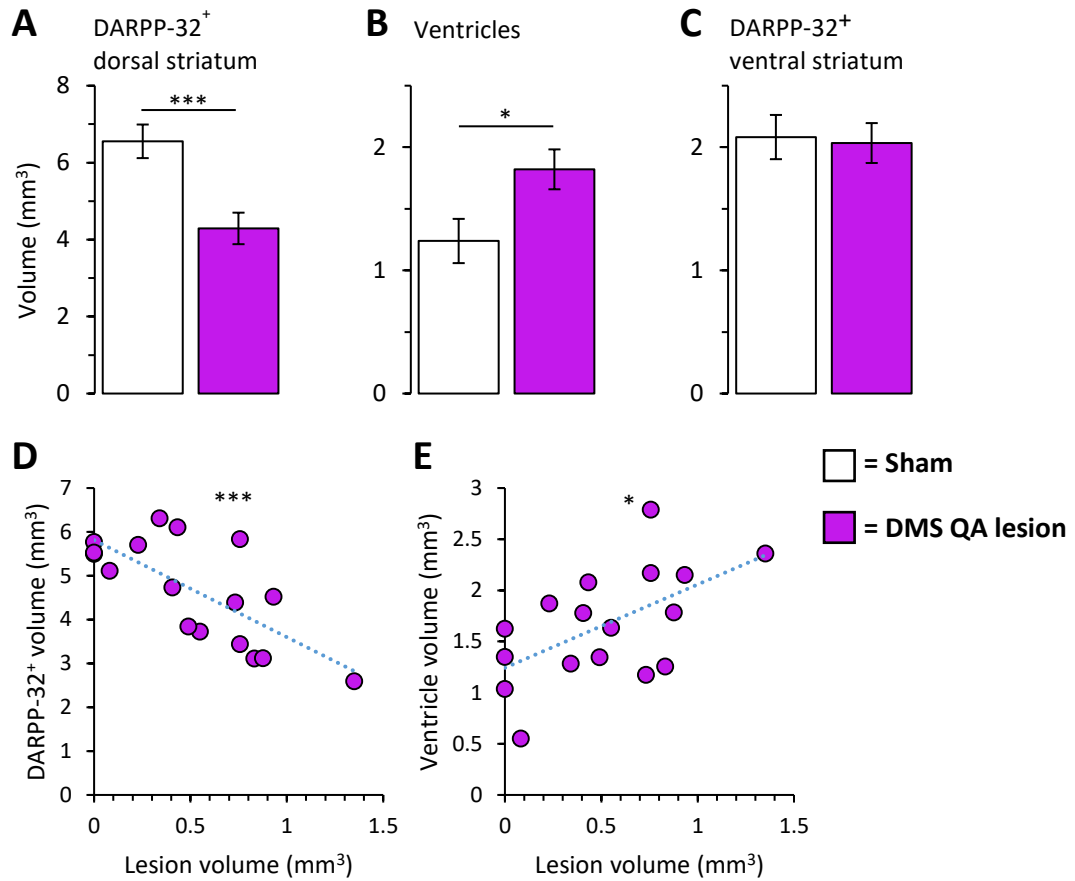


**Figure 5.14** **A** Total volume of dorsal striatum as measured by DARPP-32<sup>+</sup> staining. The DMS QA dorsal striatal volume was reduced compared to the sham animals (\*\*\*)  $p < 0.001$ . **B** Total ventricle volume. The DMS QA ventricle volume was increased compared to the sham group (\*  $p < 0.05$ ). **C** Total volume of ventral striatum as measured by DARPP-32<sup>+</sup> staining. No significant differences between groups were found. **D** Plot showing the correlation between dorsal striatal volume and lesion volume. DARPP-32<sup>+</sup> volume decreased as lesion size increased, \*\*\*  $r = -0.72$ ,  $p < 0.001$ . **E** Plot showing the correlation between ventricle volume and lesion volume. Ventricle volume increased proportionally to lesion volume, \*  $r = 0.57$ ,  $p < 0.05$ .

### Weight

Following surgery there was no difference between the sham and DMS lesioned groups in mean change body weight (Surgery:  $F_{1,20}=1.87$ , ns), **Figure 5.15 A**. Neither was there an effect of surgery on bodyweight during the testing periods for either *ad lib* or water-restricted periods (Surgery:  $t_{20}=0.15$ , ns; and  $t_{20}=0.55$ , ns respectively), **Figure 5.15 B**.

### Non-motor tests

#### Delayed alternation

The DMS lesioned mice were consistently less accurate compared to the shams in the DA task (Surgery:  $F_{1,20}=14.45$ ,  $p<0.001$ ), **Figure 5.16 A**. The number of usable trials performed was comparable at the early time-point, however at the late time-point the lesioned group were completing more trials than the shams (Surgery\*Time:  $F_{1,20}=18.57$ ,  $p<0.05$ ; Surgery (Early):  $t_{29}=1.02$ , ns; Surgery (Late):  $t_{29}=2.69$ ,  $p<0.05$ ), **Figure 5.16 B**.

Accuracy by delay data was analysed separately for the early and late time-points in order to clarify the complicated comparisons, (N.B. No significant Surgery\*Time interaction was shown when analysed together (Surgery\*Time:  $F_{1,20}=3.34$ , ns)). When accuracy was broken down into delay trials it was shown that at the early time-point the sham animals performed to a greater accuracy than the DMS lesioned mice in the shorter delays (0 - 6s), and performance declined at the longer delays whereby there was no difference between groups (Surgery\*Delay:  $F_{1,100}=18.14$ ,  $p<0.001$ ; (0s):  $t_{67}=5.92$ ,  $p<0.001$ ; (2s):  $t_{67}=7.56$ ,  $p<0.001$ ; (4s):  $t_{67}=5.06$ ,  $p<0.001$ ; (6s):  $t_{67}=2.82$ ,  $p<0.05$ ; (8s):  $t_{67}=0.75$ , ns; (10s):  $t_{67}=0.17$ , ns), **Figure 5.16 C**. During the late time-point testing the accuracy of the DMS lesioned mice was lower compared to the shams (Surgery:  $F_{1,20}=4.94$ ,  $p<0.05$ ), however no interaction of surgery and delay was found (Surgery\*Delay:  $F_{1,100}=1.66$ , ns), **Figure 5.16 D**.

Response time (time taken to make a correct response) was increased in the DMS lesioned group compared to the shams at the early time-point, only (Time\*Surgery:  $F_{1,20}=9.31$ ,  $p<0.01$ ; Early (Surgery):  $t_{38}=2.91$ ,  $p<0.05$ ; Late (Surgery):  $t_{38}=0.82$ , ns), **Figure 5.16 E**.

#### Spontaneous alternation

No difference in spontaneous alternation behaviour was found between the DMS lesion and sham groups (Surgery:  $F_{1,20}=0.02$ , ns), **Figure 5.16 F**.

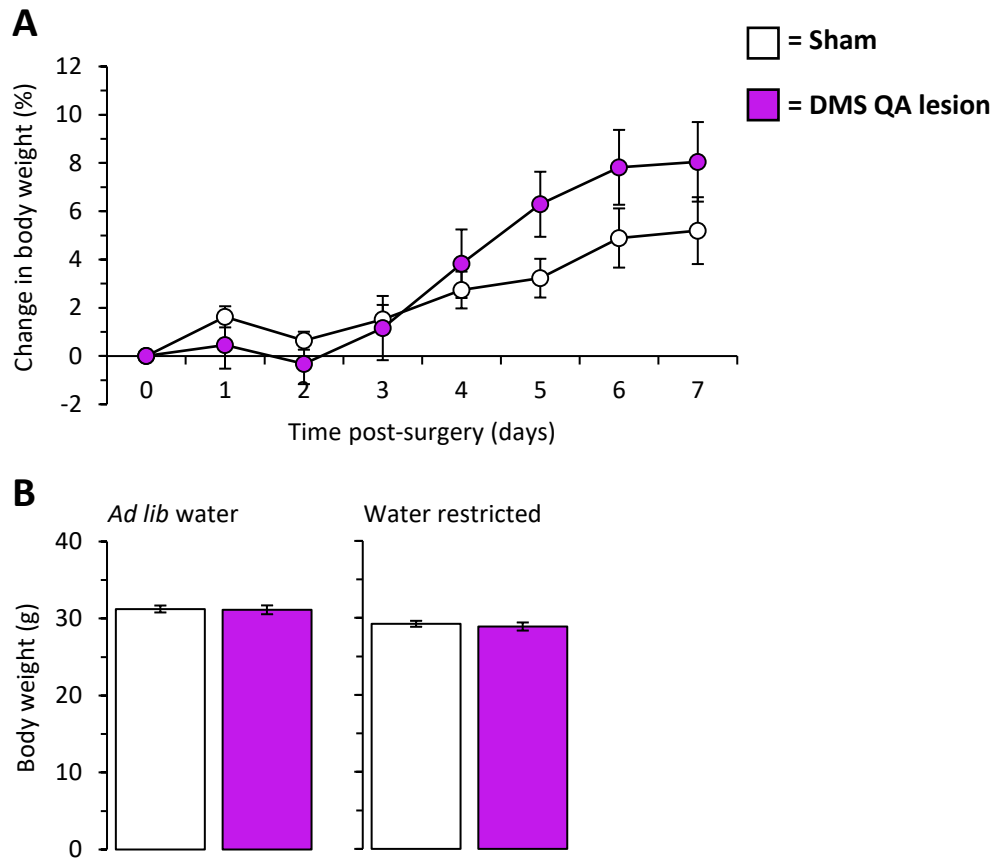


**Figure 5.15** **A** Mean daily body weights of the DMS mice in the week following surgery. There was a no significant difference between the sham and lesion groups. **B** Mean body weights during *ad-lib* feeding and during water restriction periods. There was no difference between groups during free water phases or during food restriction periods.

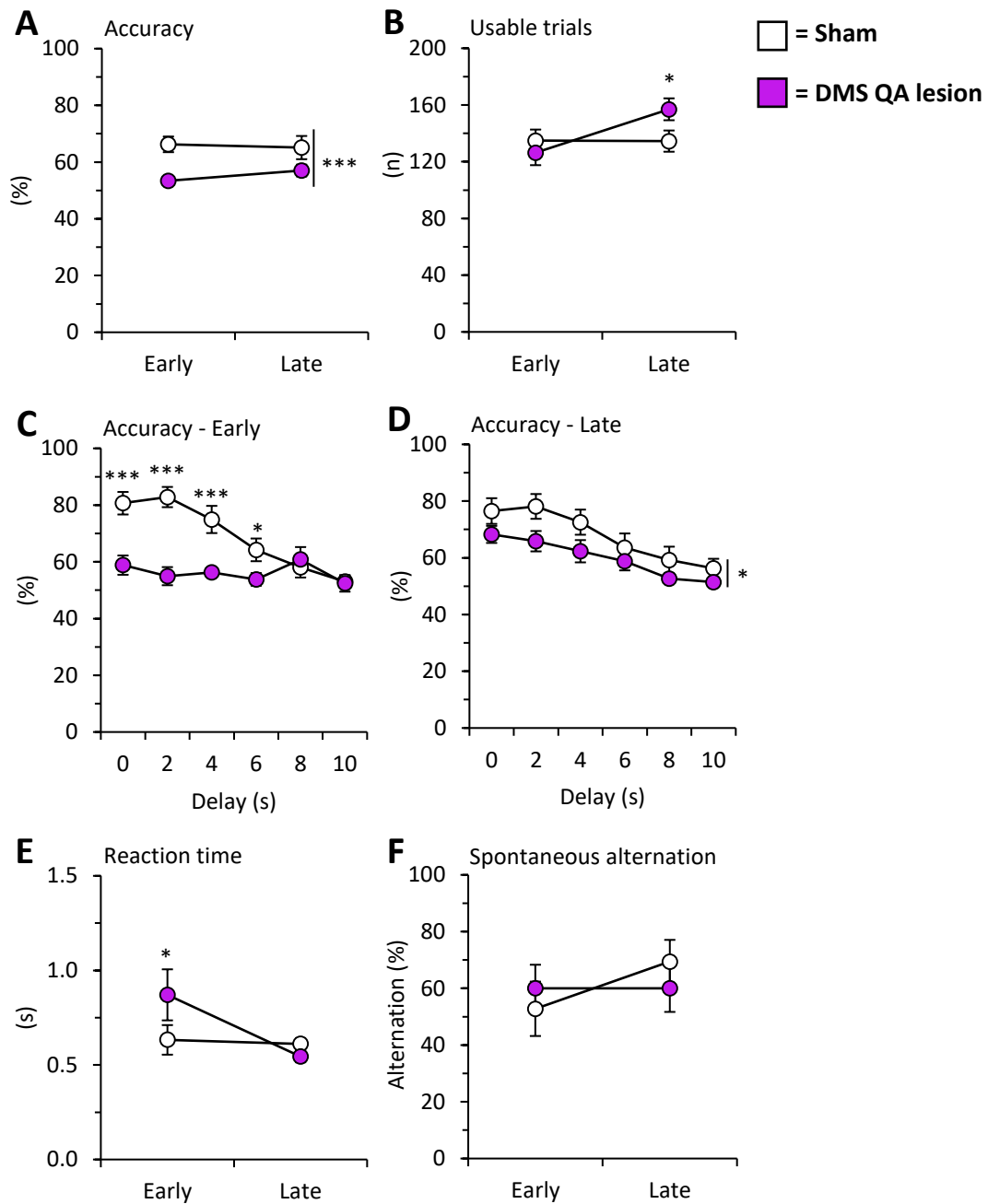


**Figure 5.16** A Total accuracy in the delayed alternation (DA) test. Accuracy calculated as (correct trials / (correct + incorrect)) x 100. The DMS lesioned mice had a lower proportion of correct trials compared to the sham group (\*\**p*<0.001). B Total usable trials in the DA test. There was no difference between the DMS lesion group and the sham group in the number of usable trials at the early time-point, however the lesioned group completed more than the shams at the late time-point (\**p*<0.05). C Accuracy by delay at the early DA time-point. Sham animals performed to a greater accuracy than the DMS lesioned mice in the shorter delays (0 - 6s) (\*\**p*<0.001; \**p*<0.05). D Accuracy by delay at the late DA time-point. Accuracy of the DMS lesioned mice was lower compared to the shams (\**p*<0.05), however no interaction of surgery and delay was found. E Reaction time in the DA task. The DMS had a slower reaction time compared to the shams at the early time-point only (\**p*<0.05). F Proportion of alternating trials in the spontaneous alternation test. There was no effect of surgery in the amount of alternating trials.

### Five-choice serial reaction time task

5CSRTT data was analysed separately for early and late time-points to simplify the complex comparisons. (N.B. No significant Surgery\*Time interactions were shown when analysed together (Accuracy Surgery\*Time:  $F_{1, 19}=3.09$ , ns; RT Surgery\*Time:  $F_{1, 19}=0.27$ , ns; TO Surgery\*Time:  $F_{1, 19}=2.73$ , ns; TTU Surgery\*Time:  $F_{1, 19}=2.26$ , ns)).

Surgery had no effect on attention, as measured by accuracy, in the 5CSRTT at either the early or late time-points (Surgery:  $F_{1, 20}=2.14$ , ns; and  $F_{1, 19}=0.17$ , ns respectively), **Figure 5.17 A**. There was no difference between groups in performance during the distraction probe, during which milkshake was made freely available within the operant chamber (Surgery:  $t_{20}=0.06$ , ns).

The DMS lesioned animals were quicker to make correct responses than the shams at both the early and late time-points (Surgery:  $F_{1, 20}=20.59$ ,  $p<0.001$ ;  $F_{1, 19}=24.53$ ,  $p<0.001$ ), however there was no difference between groups during the distraction probe (Surgery:  $t_{20}=0.12$ , ns), **Figure 5.17 B**.

The number of time-out penalties generated during the early time-point was no different between the DMS lesion group and the shams (Surgery:  $F_{1, 20}=4.33$ , ns), however the DMS lesioned animals made fewer time-out errors than the shams at the late time-point (Surgery:  $F_{1, 19}=24.25$ ,  $p<0.001$ ), **Figure 5.18 A**. No difference was found during the distraction probe (Surgery:  $t_{20}=1.53$ , ns respectively).

DMS lesioned mice generated more usable trials than the sham mice at both the early and late time-points (Surgery:  $F_{1, 20}=6.79$ ,  $p<0.05$  and  $F_{1, 19}=30.44$ ,  $p<0.001$  respectively), but there was no difference between groups in the distraction probe (Surgery:  $t_{20}=0.81$ , ns), **Figure 5.18 B**.

### Reward consumption

There was no effect of surgery on the amount of milkshake consumed in the consumption test (Surgery:  $F_{1, 19}=0.04$ , ns), **Figure 5.19 A**.

### Novel object recognition

Early and late time-point data for the novel object recognition task were analysed separately to simplify the complex comparisons. (N.B. No significant Surgery\*Time interactions was found when analysed together (Surgery\*Time:  $F_{1, 36}=0.14$ , ns)).

At the early time-point, the DMS lesioned mice spent significantly less time than the shams exploring the novel object after the short (15 minute) delay, but there was no difference after the long delay (24 hrs) (Surgery\*Delay:  $F_{1, 18}=6.37$ ,  $p<0.05$ ; Short (Surgery):  $t_{36}=2.44$ ,  $p<0.05$ ; Long (Surgery):  $t_{36}=1.17$ , ns), **Figure 5.19 B**. At the late time-point animals spent less time exploring the novel object after the long delay compared to the short delay (Delay:  $F_{1, 18}=13.80$ ,  $p<0.01$ ), but no difference between groups was found. The mean proportion of time spent exploring the novel object was compared to chance (50%) for each probe. At the early time-point, the shams but not the DMS lesioned mice spent more time exploring the novel object than the familiar one after the short delay (Sham Early Short:  $t_{11}=4.35$ ,  $p<0.001$ ; DMS Early Short:  $t_9=0.77$ , ns). Following the long delay, the shams did not spend significantly longer on the novel object, but the DMS group did (Sham Early Long:  $t_{11}=1.47$ , ns; DMS Early Long:  $t_9=2.72$ ,  $p<0.05$ ). At the late time-point, both the sham and DMS groups spent longer exploring the novel object compared to the familiar after the short delay (Sham Late Short:  $t_{11}=3.42$ ,  $p<0.01$ ; DMS Early Short:  $t_7=4.54$ ,  $p<0.01$ ), however after the long delay, only the sham animals spent significantly more time on the novel object (Sham Late Long:  $t_{11}=2.54$ ,  $p<0.05$ ; DMS Late Long:  $t_7=0.29$ , ns).

### Elevated plus maze

There was no difference between the DMS lesion group and the sham group in the time spent in the open or closed arms of the elevated plus maze (Surgery:  $F_{1, 20}=0.00$ , ns), **Figure 5.19 C**, and neither was there a difference in the number of entries made into the open or closed arms (Surgery:  $F_{1, 20}=0.58$ , ns; and Surgery:  $F_{1, 20}=2.99$ , ns respectively), **Figure 5.19 D**.

### Open field

The DMS lesion group entered the central zone of the open field arena a greater number of times compared to the shams (Surgery:  $F_{1, 20}=6.24$ ,  $p<0.05$ ), however there was no difference in the amount of time spent in the central zone (Surgery:  $F_{1, 20}=0.36$ , ns), **Figure 5.20 A**.

The lesioned mice reared more frequently compared to the sham group (Surgery:  $F_{1, 20}=23.42$ ,  $p<0.001$ ), **Figure 5.20 B**.

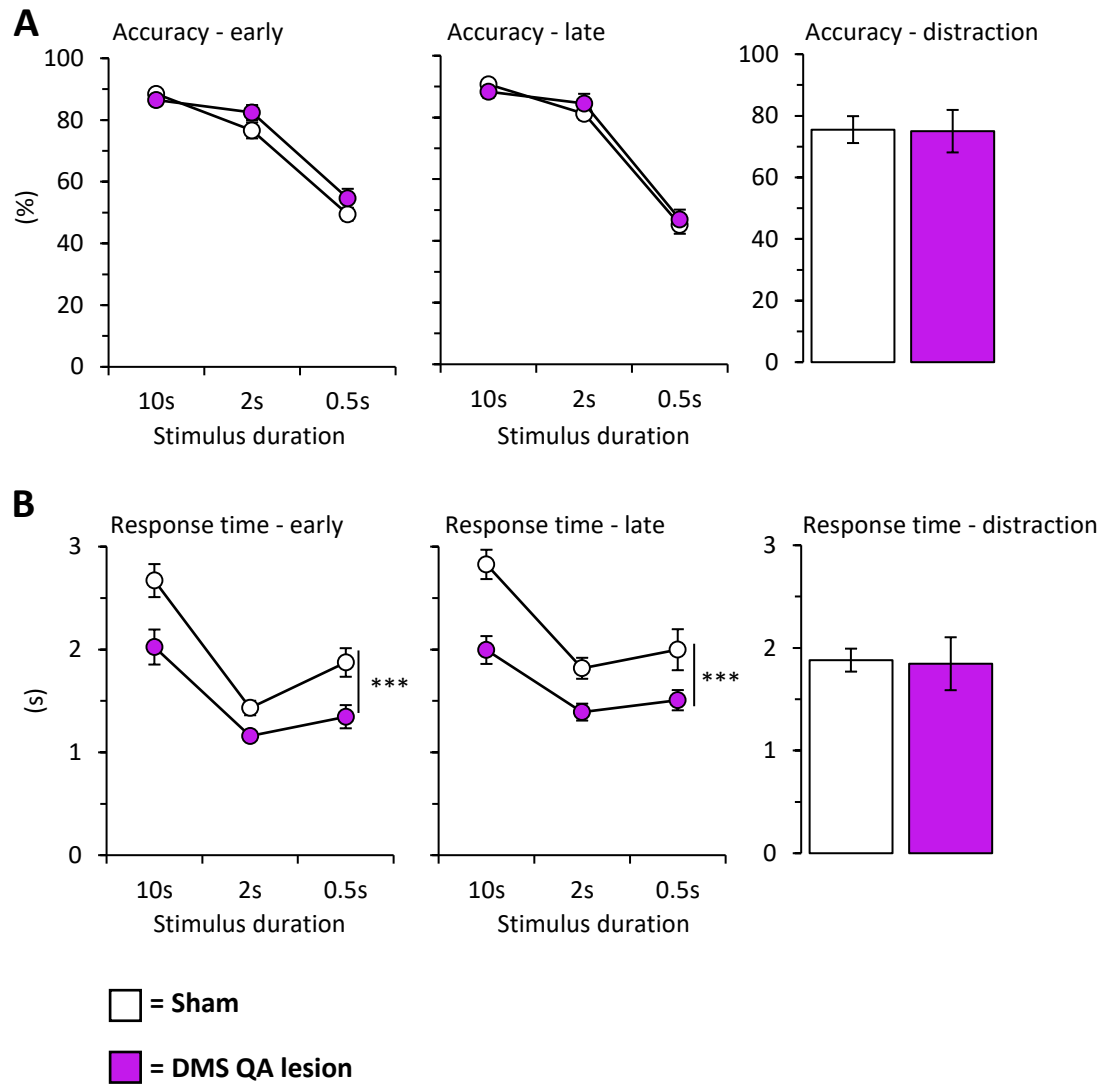


**Figure 5.17** **A** Response accuracy in the 5CSRTT in the early, late and distraction tests. No effect of surgery on accuracy was found. **B** Reaction time of correct responses in the early, late and distraction 5CSRTT. DMS lesioned animals were quicker to respond than the shams at both the early and late time-points, but there was no difference during the distraction probe (\*\*\*) ( $p < 0.001$ ).

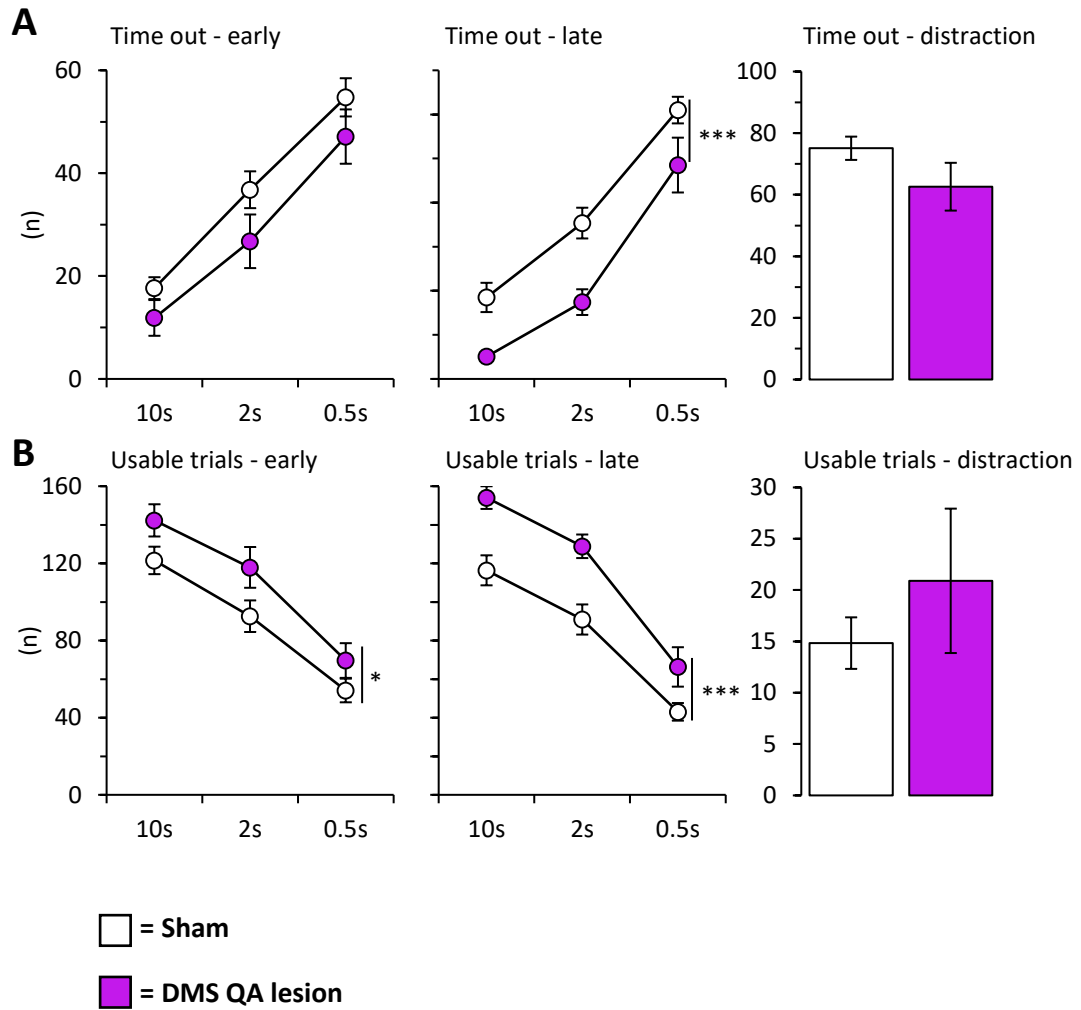


**Figure 5.18** **A** Number of time-out errors in the 5CRTT during the early, late and distraction tests. There was no difference between groups at either the early time-point or distraction probe, however the DMS lesioned animals made fewer time-out errors than the sham at the late time-point (\*\* $p < 0.001$ ). **B** Number of usable trials in the 5CRTT during the early, late and distraction tests. The DMS lesioned mice generated more usable trials than the sham mice at both the early and late time-points (\*  $p < 0.05$ , \*\* $p < 0.001$ ), but there was no difference between groups in the distraction probe.

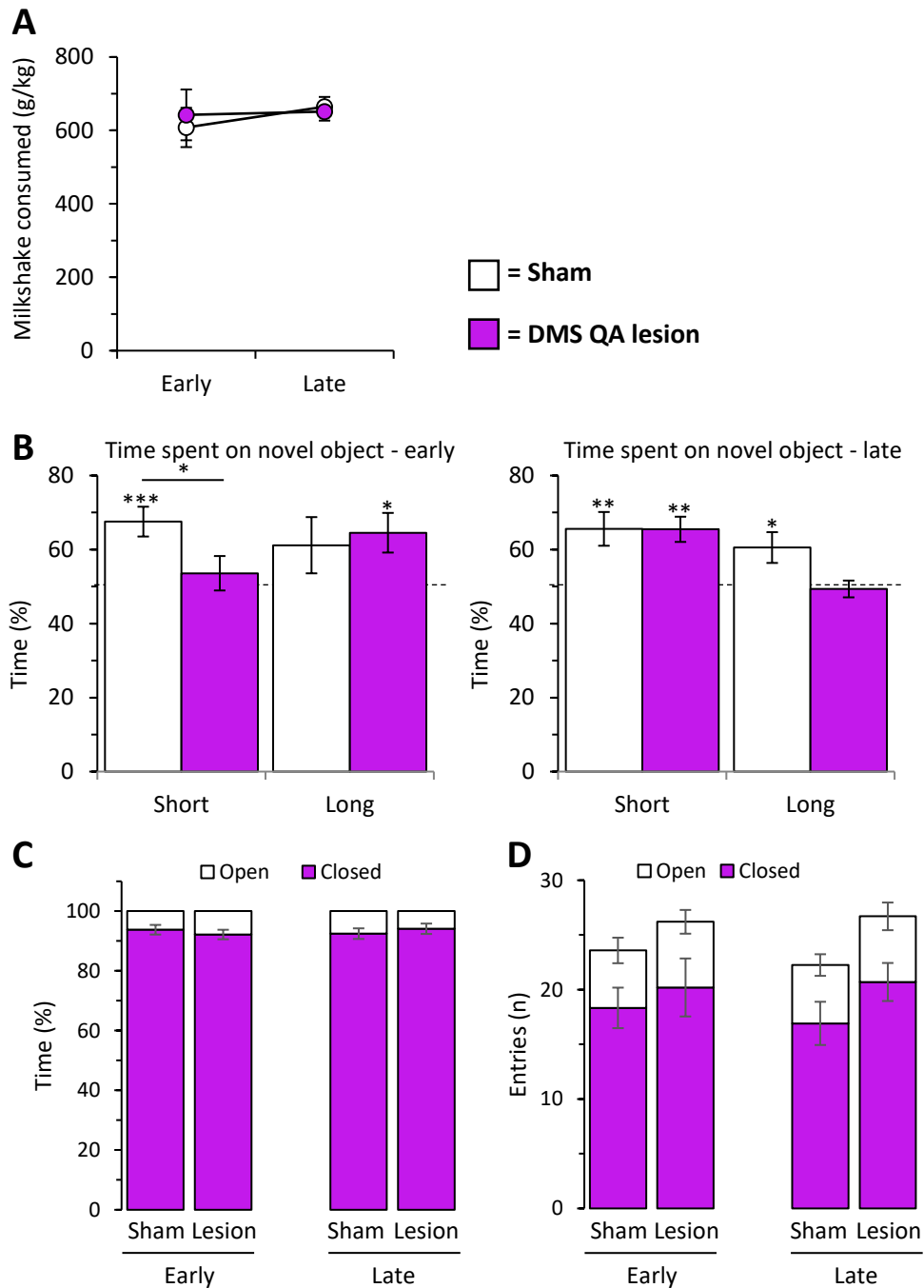


**Figure 5.19** **A** Quantity of milkshake consumed per kg of bodyweight. No difference between groups was found. **B** Time spent exploring novel objects at the early and late time-points during the habituation, short delay (15mins) and long delay (24hr) trials. No effect of time was observed. At the early time-point The DMS lesion group spent less time than the shams exploring the novel object after the short delay (\*  $p < 0.05$ ) but there was no difference after the long delay. At the late time-point animals spent less time exploring the novel object after the long delay compared to the short delay ( $p < 0.01$ ), but no difference between groups was found. When the mean time spent exploring the novel object was compared to chance (50%), the sham animals spent significantly longer in both the early (\*\*\*)  $p < 0.001$  and late short delay probes (\*\*  $p < 0.01$ ) and in the late long delay (\*  $p < 0.01$ ). The DMS lesioned animals spent longer exploring the novel object in only the long probe of the early test (\*  $p < 0.05$ ) and the short probe in the late test (\*\*  $p < 0.01$ ). **C** Proportion of time spent in each segment of the elevated plus maze. There was no difference between groups in the time spent in the open arms. **D** Number of entries into each arm of the elevated plus maze. There was no difference between groups in the number of entries into either the open or closed arms.

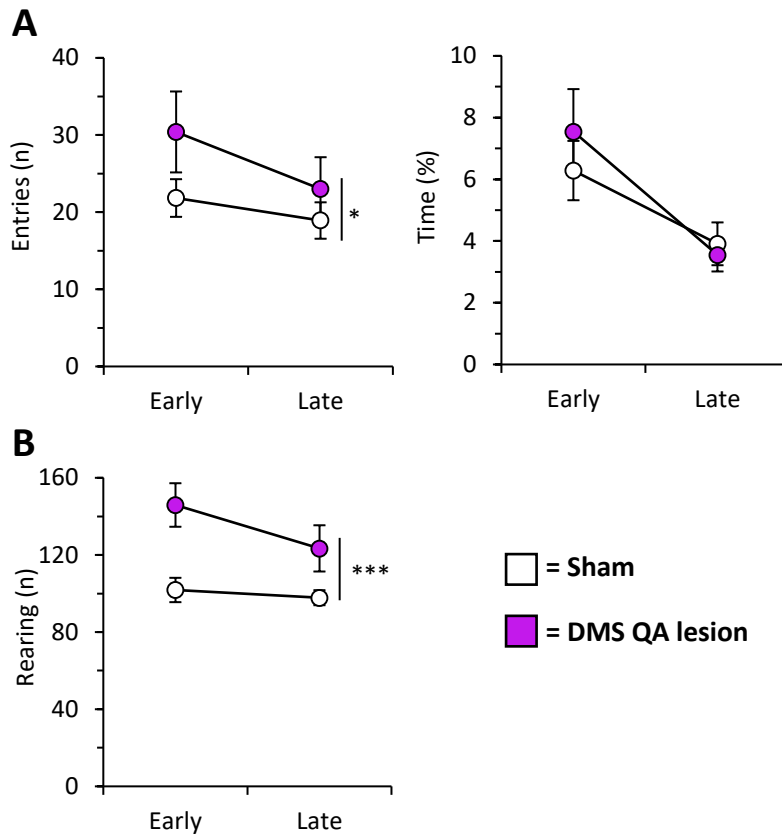


**Figure 5.20** **A** Number of entries made into the central zone of the open field arena and the percentage of time spent within the central zone. The DMS lesion group entered the central zone a greater number of times compared to the shams (\*  $p < 0.05$ ), however there was no difference in the amount of time spent in the central zone. **B** Frequency of rearing behaviour in the open field test. The DMS lesioned animals reared more frequently compared to the shams (\*\* $p < 0.001$ ).

## Motor tests

### Locomotor activity

More beam breaks were made by the DMS animals during the dark period compared to the sham group (Surgery:  $F_{1,20}=22.89$ ,  $p<0.001$ ), **Figure 5.21 A**. Fewer beam breaks were made at the late time-point compared to the early time-point (Time:  $F_{1,20}=24.84$ ,  $p<0.001$ ).

### Open field

The DMS lesion group moved a greater distance and at a higher speed than the sham animals (Surgery:  $F_{1,20}=16.56$ ,  $p<0.001$ ; and Surgery:  $F_{1,20}=16.56$ ,  $p<0.001$  respectively), **Figure 5.21 B & C**. They also spent a higher proportion of time in motion than the shams at the early time-point (Surgery\*Time:  $F_{1,20}=4.77$ ,  $p<0.05$ ; Surgery (Early):  $t_{39}=3.17$ ,  $p<0.01$ ; Surgery (Late):  $t_{39}=0.22$ , ns), and had fewer breaks in movement time (Surgery:  $F_{1,20}=24.42$ ,  $p<0.001$ ), **Figure 5.21 D & E**.

### Gait

No effect of surgery was observed in any gait analysis measures (Stride length Surgery:  $F_{1,20}=2.98$ , ns; Hind base-width Surgery:  $F_{1,20}=4.18$ , ns; Fore base-width Surgery:  $F_{1,20}=0.00$ , ns; Overlap Surgery:  $F_{1,20}=0.02$ , ns), **Figure 5.22 A - C**.

### Balance beam

There was no difference between groups in the time taken to turn on the balance beam (Surgery:  $F_{1,20}=0.18$ , ns), **Figure 5.22 D**, however the DMS lesioned group were faster at crossing the beam than the shams (Surgery:  $F_{1,20}=4.91$ ,  $p<0.05$ ), **Figure 5.22 E**. The time taken to cross was increased at the late time-point compared to the early time-point (Time:  $F_{1,20}=22.26$ ,  $p<0.001$ ). DMS lesioned animals made a greater number of foot-slips than the shams at the early time-point only (Surgery\*Time:  $F_{1,20}=10.53$ ,  $p<0.01$ ; Surgery (Early):  $t_{38}=3.33$ ,  $p<0.05$ ; Surgery (Late):  $t_{38}=0.71$ , ns), **Figure 5.22 F**.

### Rotarod

No difference between groups in the latency to fall from the rotarod was found (Surgery:  $F_{1,20}=1.46$ , ns), **Figure 5.23 A**, however the animals fell sooner at the late time-point compared to the early time-point (Time:  $F_{1,20}=32.06$ ,  $p<0.001$ ).

**Corridor**

There was no effect of surgery on the side bias of animals in the corridor task (Surgery:  $F_{1,19}=1.22$ , ns), **Figure 5.23 B**.

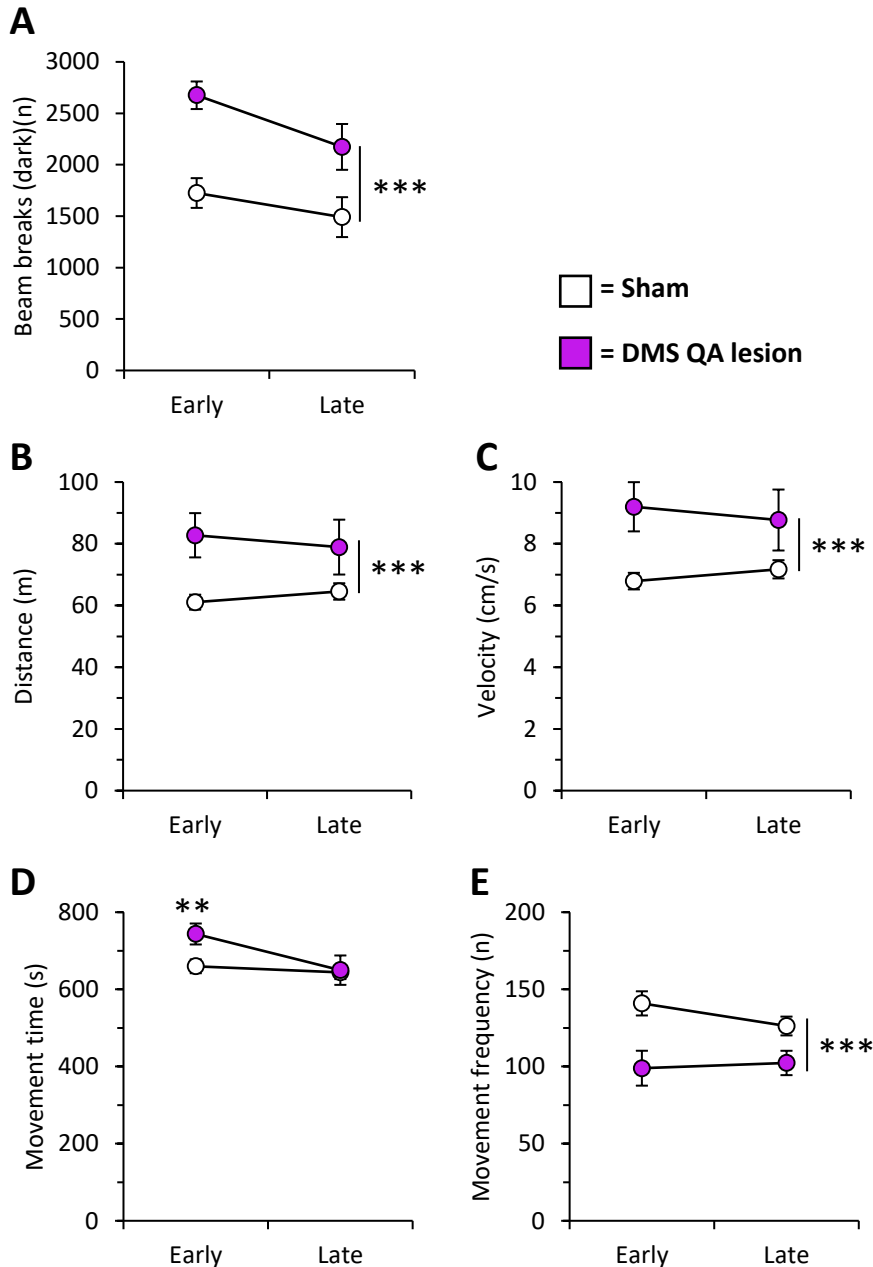


**Figure 5.21** **A** Number of beam breaks during the dark phase of locomotor activity. DMS animals were more active compared to the shams (\*\*\*) Surgery:  $F_{1,20}=22.89$ ,  $p<0.001$ ). Activity levels were decreased at the late time-point compared to the early time-point (Time:  $F_{1,20}=24.84$ ,  $p<0.001$ ). **B** Distance moved in the open field test. The DMS lesioned group moved a greater distance compared to the shams (\*\*\*) Surgery:  $F_{1,20}=16.56$ ,  $p<0.001$ ). **C** Velocity in open field. The DMS group moved at a greater speed than the shams (\*\*\*) Surgery:  $F_{1,20}=16.56$ ,  $p<0.001$ ). **D** Time spent in motion in open field. The DMS animals spent a greater amount of time moving compared to the shams at the early time-point only (Surgery\*Time:  $F_{1,20}=4.77$ ,  $p<0.05$ ; Surgery (Early):  $t_{39}=3.17$ ,  $p<0.01$ ; Surgery (Late):  $t_{39}=0.22$ , ns). **E** Number of bouts of movement during open field tests. The DMS lesioned mice made fewer separate bouts of movement when compared to the shams (\*\*\*) Surgery:  $F_{1,20}=24.42$ ,  $p<0.001$ ).

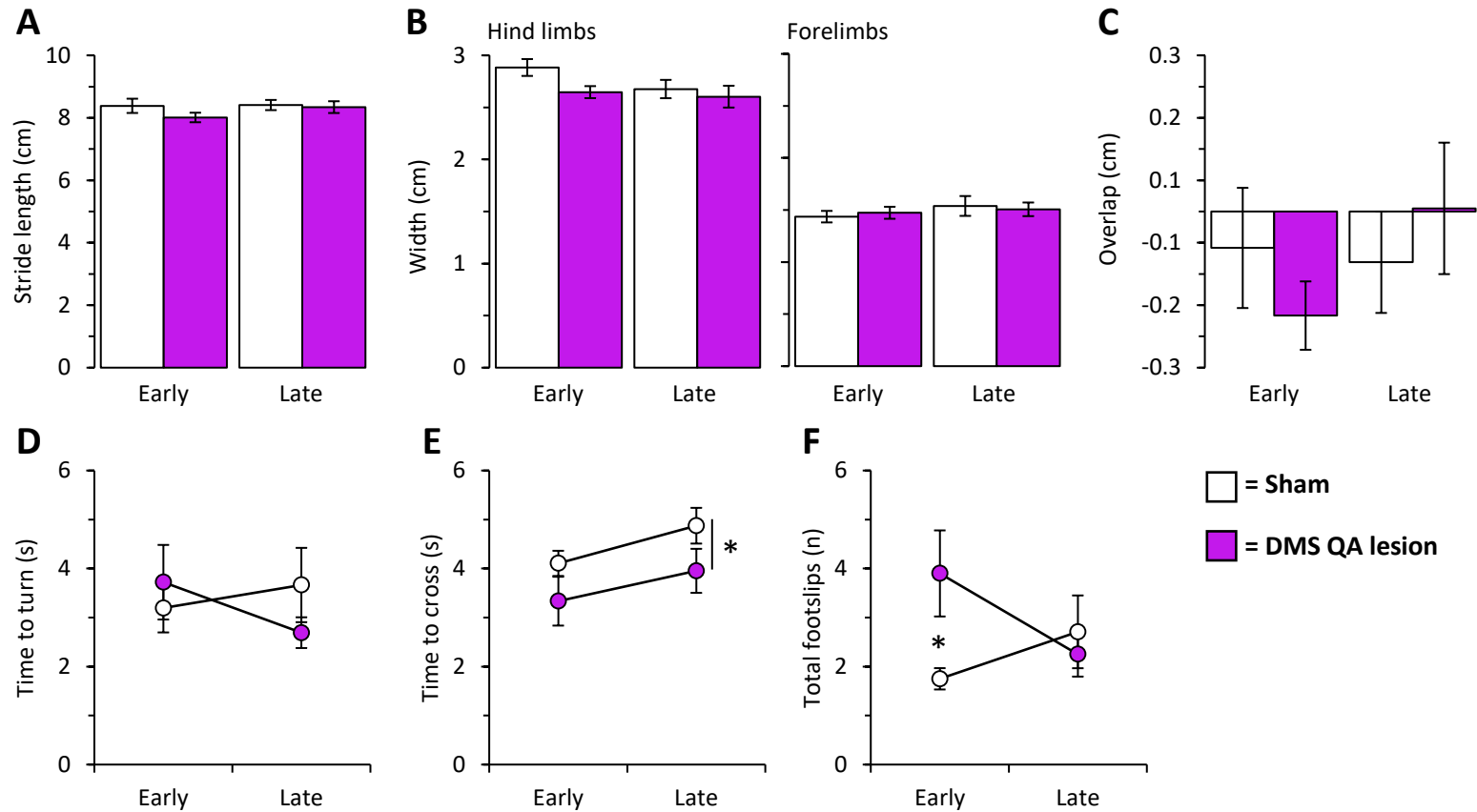


**Figure 5.22** **A** Mean stride length as measured by footprint analysis. No effect of lesion on stride length was found (Surgery:  $F_{1,20}=2.98$ , ns), neither was there a different between the early and late time-points (Time:  $F_{1,20}=1.38$ , ns). **B** Mean base width of the hind and fore paws. No effect of surgery was seen on either hind- or forelimb base-width (Surgery:  $F_{1,20}=4.18$ , ns, and  $F_{1,20}=0.00$ , ns, respectively). **C** Mean overlap of the placement of hind and fore paws. A positive measure represents the placement of the hind paw in front of the fore paw when taking a step. There was no difference in the amount of overlap in the DMS mice compared to sham (Surgery:  $F_{1,20}=0.02$ , ns). **D** Mean time to turn around after placement on the elevated balance beam. No effect of surgery was found in the time taken to turn (Surgery:  $F_{1,20}=0.18$ , ns). **E** Mean time to cross the balance beam. The DMS animals were slower to cross compared to the shams (\* Surgery:  $F_{1,20}=4.91$ ,  $p<0.05$ ). Time to cross increased at the late time-point compared to the early time-point (Time:  $F_{1,20}=22.26$ ,  $p<0.001$ ). **F** Total foot-slips made whilst crossing the balance beam. The DMS mice made more foot-slips than the shams at the early time-point only (Surgery\*Time:  $F_{1,20}=10.53$ ,  $p<0.01$ ; \* Surgery (Early):  $t_{38}=3.33$ ,  $p<0.05$ ; Surgery (Late):  $t_{38}=0.71$ , ns).

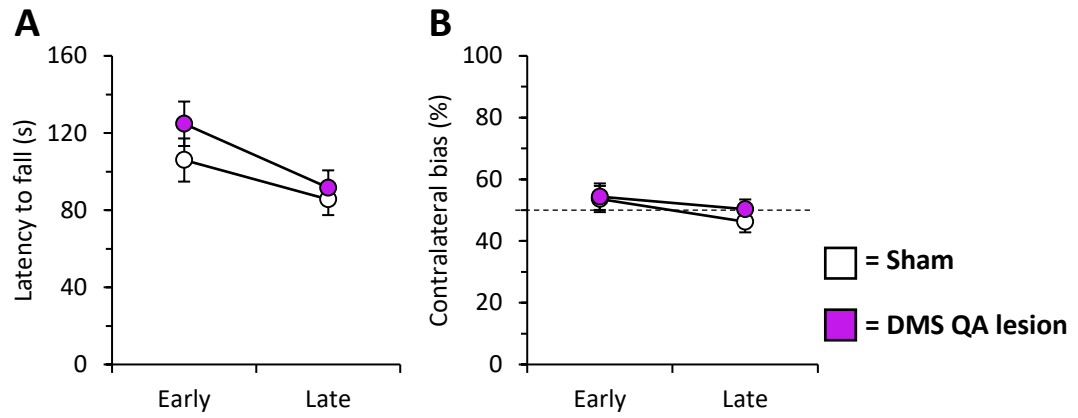


**Figure 5.23** **A** Latency to fall from the accelerating rotarod. There was no difference between groups in the time taken to fall (Surgery:  $F_{1,20}=1.46$ , ns). The animals fell sooner at the late time-point compared to the early time-point (Time:  $F_{1,20}=32.06$ ,  $p<0.001$ ). **B** Side bias in the corridor task. No effect of lesion was found (Surgery:  $F_{1,19}=1.22$ , ns).

## 5.8 Experiment Discussion

This study aimed to establish a behavioural test battery able to detect long-term lesion-induced deficits in a QA mouse model of HD designed to induce cognitive deficits through lesions of the DMS. The purpose of this was to enable their use in future investigations to efficiently test for functional improvements brought about by cell transplantation studies or other therapeutic interventions.

### Lesion quality

Bilateral dorsomedial lesions were confirmed in just 10 of the surviving 17 mice, with the remaining being removed from the study due to no detectable lesion in one or both hemispheres. It is unclear if this was a problem with lesion cannula blocking during surgery or, if in targeting a more medial placement, some toxin was injected into the ventricle in error. Of the lesions that were detected, most were close to the medial edge of the striatum, however in many animals there was sparing of medial tissue, and in all cases at least some sparing of tissue in the most dorsal aspect of the medial striatum.

The variability in lesion accuracy makes an effective bilateral DMS lesion model more difficult to obtain than the DLS, although through refinement of coordinates and perhaps additional injections of toxin at a more dorsal site in the tract could improve the outcomes seen.

The lesions were sufficient to cause a loss of just over 34% of DARPP-32<sup>+</sup> volume and induce behavioural deficits in some of the behavioural test battery. A similar study into DLS and DMS lesioning in rats had similar medial sparing and were able to show a deficit in a simple reaction time task (Hauber and Schmidt, 1994).

As with the DLS lesions, the correlation between lesion volume and the expansion of the ventricles implies that there is tissue loss within the striatum, and therefore the non-DARPP-32<sup>+</sup> volume cannot be taken as an absolute measure of cell loss but is a valid indication of the extent of the lesion.

No disturbance of the ventral striatum was observed; however, it was noted that some lesions extended posteriorly into the globus pallidus externa (GPe) and interna (GPi). Since the cells of the GP are GABAergic, like the striatal MSNs, it can be assumed that some excitotoxic cell loss occurred in this region. As part of the basal ganglia, a disturbance of the inhibitory effect of the GP efferent projections could have an excitatory effect on the

thalamus and hence motor cortex output. Isacson et al. (1986), demonstrated that ibotenic acid lesions to the DMS or GP can cause hyperactive behaviours, therefore any behavioural deficits observed within this chapter cannot necessarily be assumed to be DMS driven since the effects cannot be separated from potential GP disturbances.

### Weight

Bodyweight was unaffected by DMS lesioning and therefore it was assumed to not factor in the results seen.

### The effect of bilateral DMS lesions

The outcome of the tests explored is summarised in **Table 5.4**. Those tests in which a sustained deficit was detected across the two time-points are marked.

Test	Long-term deficits	Measure observed
Delayed alternation	✓	Decrease in accuracy
Spontaneous alternation	✗	No effect
5CSRTT	✗	Decrease in response time only
Milkshake consumption test	✗	No effect
Novel object recognition	✓	Disruption to memory
Elevated plus maze	✗	No effect
Open Field	✓	Increased distance, velocity, movement duration & rearing Increased central zone entries
Nest building	✗	No effect
Locomotor activity	✓	Hyperactivity
Footprint analysis	✗	No effect
Balance beam	✗	Decreased time to cross
Rotarod	✗	No effect
Corridor test	✗	No effect

**Table 5.4** Summary assessment of tests performed. A ✓ indicates test was able to demonstrate stable DLS lesion-induced deficits, a ✗ indicates either no detectable deficits or transient deficit.

## 5.9 Chapter Discussion

The experiments described in this chapter aimed to establish a range of behavioural tests which could detect long-term deficits in QA mouse models of HD. **Experiment 6** utilised a unilateral DLS lesion model intended to probe more motoric impairments, whilst **Experiment 7** used a bilateral DMS lesion model to explore more non-motor behavioural deficits. The two cohorts were lesioned and assessed in a battery of tests at an early (from one-week post-lesion) and late (from sixteen weeks post-lesion) time-point.

### DLS lesions provided more robust lesions compared to DMS

The number of animals excluded from the experiments due to insufficient lesion volume was far greater in the DMS group (n=7) than the DLS (n=1). It might be expected that more would be excluded from the bilateral lesion group simply because each animal must receive two good lesions rather than one. Interestingly, it has previously been shown that DLS lesions of ibotenic acid will diffuse into the tissue more to encompass a greater volume, thereby increasing the chances of obtaining a sufficient lesion. Medial injections, however, tended to remain more confined to the immediate area of injection (Fricker et al., 1996). This also seems to have been the case in this study since those medial lesions that were detectable were mostly small compared to the lateralised lesions. To resolve this problem, it might be necessary to increase the volume of solution injected in the DMS model and include an extra deposit of toxin in a more dorsal site of the injection tract to cover the tissue sparing seen in this region. Throughout the experiments in this thesis the group sizes have been unexpectedly reduced due to poor health of animals following the QA lesioning. Therefore, rather than increasing the amount of toxin *per se*, injecting a greater volume of a less concentrated toxin may be a better solution.

### DLS and DMS lesions elicited different behavioural phenotypes

From the tests which were performed by both DLS and DMS lesioned groups it is clear that the placement of the lesions induced divergent behavioural deficits. Whilst this study did not test if the standard mid-striatal placement of lesions (most commonly used for histology-based transplantation studies) could cause detectable behavioural changes, it did show that the positioning of the lesion is a critical consideration to test certain aspects of behaviour, and therefore therapy-induced recovery. For example, there was a persistent deficit in rotarod performance of the DLS QA group, which was absent in the DMS lesioned group. The

fixed speed or accelerating rotarod test are widely used to test motor coordination, often as the sole test of functional changes, and these results show that the accelerating rotarod is sensitive to the changes induced by dorsolateral striatal lesions. Studies employing lesions more centrally placed within the striatum are also able to demonstrate deficits (Gharaibeh et al., 2016; Lin et al., 2011). Since mid-striatal lesions do not target the DLS specifically, there is sparing of much of the lateral parenchyma, so it could be inferred that rotarod performance is sensitive to small QA induced changes.

The coordination and balance deficits observed in the rotarod test in the DLS lesioned mice were not apparent in the balance beam test. A transient effect on the time to turn at the early time-point only suggests that either the lesions were not of sufficient size to induce a deficit, or the balance beam is not sensitive enough to detect them, or a combination of both. Interestingly there was a decrease in the “time to cross” measure in the DMS lesioned group, possibly linked to their increased speed and hyperactivity (discussed later), whereas this was not seen in the DLS groups despite similar increases in activity and velocity measures in the open field test. A possible explanation for this could be that the DMS lesioned mice, unimpeded by motor impairments, could simply traverse the beam at a greater speed, however, the impaired DLS lesioned animals show a deficit by *not* crossing faster than the sham group, as the DMS group do.

Footprint analysis of gait detected a decrease in the amount of overlap between the hind- and forepaws in the DLS lesioned mice only. Less overlap of paw placement infers less flexibility and more rigid gait posture. In addition, a trend towards reduced stride length in the lesioned animals may have become significant if a larger group size was used. Lesion induced deficits in QA lesioned mice have been shown previously (Ma et al., 2012; Zimmermann et al., 2016), however the lesions in these cases were substantially larger than those discussed here, indicating that a clearer effect might have been seen with greater tissue loss. In addition, the referenced studies utilised automated systems to analyse gait which is likely to be more sensitive to subtle disturbances.

### Both DLS and DMS lesions induce a hyperactive phenotype

Both the locomotor activity and open field demonstrated a significant increase in the locomotor activity levels in both lesioned groups. Since motor impairments in people with HD tend to impede the speed of movement, it was unexpected to find an opposing response in the QA model. However, hyperactivity in lesion rat models of HD has been well reported (Borlongan et al., 1997; Isacson et al., 1986; Sanberg et al., 1986; Shear et al., 1998), and has

also been observed in the early stages of disease progression in the YAC 128 (Slow et al., 2003) and *hdhQ175<sup>+/-</sup>* knock-in mouse models of HD, (Harrison et al., unpublished).

In addition to increased locomotor activity, the open field tests confirmed that the QA lesioned mice were also faster, were active for longer, rested less, and, consequently, moved a greater distance than the sham controls. While superficially these behaviours may seem to be the opposite of the expected deficits, they do represent an imbalance in normal activity control. Since there was no physical disturbance of the ventral striatum, which has been linked to hyperactivity in rats (Costall et al., 1977), it can be assumed that changes in activity are a result of circuitry disturbances originating within the dorsal striatum, particularly in the DLS lesioned animals. This is less clear in the DMS lesioned animals because of the involvement of the GP as previously discussed.

Since these differences are pronounced, consistent and sustained long-term, in addition to being very simple to run, locomotor activity and open field would make useful tests to assess therapy-induced recovery in animal models of HD.

#### Detecting motor deficits in DLS lesioned mice

In addition to the tests described above, the amphetamine and apomorphine rotations were able to demonstrate a significant lesion effect in the motor behaviour of DLS lesioned animals, with the 2mgkg<sup>-1</sup> apomorphine probe demonstrating the greatest effect. Since we would not expect cell therapies to be able to completely restore behaviours to normal levels, it is essential that there is enough of a difference between lesioned animals and the control groups to allow for smaller changes to be identified. For the higher apomorphine dose there is a greater difference in net rotations between the sham and lesioned animals, making it the more effective probe to pull out potential improvements in this behaviour. Importantly, the number of rotations was significantly correlated with lesion volume in the 2mgkg<sup>-1</sup> apomorphine probe, suggesting that improvement in number of rotations could be used to predict the extent of the lesion prior to histological analyses, and potentially measure the effectiveness of grafted MSNs in this model. The lesions in this experiment were shown to span the anterior-posterior striatum, which has been shown to be a factor affecting rotation behaviour. A study utilising ibotenic acid lesions in rats of the anterior or posterior striatum demonstrated that a posterior rather than anterior lesion placement was required for the rats to exhibit apomorphine-induced rotations (Fricker et al., 1996).

For long-term experiments it is worth noting that post-synaptic super-sensitivity to apomorphine in rats can be induced with repeated stimulation of dopamine receptors, depending on how regularly it is administered (Castro et al., 1985; Mattingly and Rowletti, 1989), and this effect has been shown to be exaggerated when administration is paired with environmental cues, such as the rotation equipment, (Mattingly and Gotsick, 1989). Therefore, any behavioural measures utilising repeated exposure to apomorphine should be analysed with this in mind.

A general impairment in skilled paw-reaching was identified in the staircase test, with DLS lesioned animals collecting fewer pellets than those in the sham group. When assessed in conjunction with the sucrose consumption result, this is unlikely to be due to a reduction in palatability or perceived reward value in the lesioned mice since when given free access to the pellets they consumed more than the shams. However, the amount of food restriction could have had a significant impact on the amount of effort mice put in to this task. A clearer result may have been achieved if the mice were restricted to ~85% rather than 90% free feeding weight. With a higher incentive, it is possible the sham animals could have improved their performance to reach more, whereas if the QA lesioned mice were closer to their performance limit, a difference between the groups could be more likely detected. Unilateral lesioned rats tested in the staircase reaching tasks demonstrated a significant bias towards the ipsilateral paw that was not observed in the mice (Fricker et al., 1996), despite similar lesion placement and comparative volume. Applying the idea that increased incentive for the reward could improve the performance in shams to the reach of ipsi- and contralateral sides of the lesioned animals, it's possible that with extra motivation the DLS lesioned mice could have reached more pellets with their ipsilateral paw and thereby revealed an otherwise undetected lateralised bias.

Another potential reason for the lack of lateralised deficits observed includes the physical manoeuvring the animals must do to get in a good reaching position. The task requires the mice to lie flat and reach using one paw and it is assumed that a lateralised impairment would affect only that paw. However, to reach down the animal must use their ipsilateral limb for balance or purchase, and therefore impairments on this paw could affect the reaching capacity of the non-affected paw. This may be unlikely since this does not seem to be an issue with the rats.

The motoric deficits shown in the LCRTT (increased movement time, time-out errors and reduced number of trials) provide a good baseline from which functional improvement could

be measured. However, assessment of motivational changes or information processing deficits would also need to be included in any test battery to determine if any observed effects are purely motoric.

### DLS lesions produced some non-motor effects

Despite DLS lesions being considered as affecting predominantly motor systems, a number of non-motor effects were also detected. Since the medial striatum was unaffected by the lateral lesions it might be theorised that some non-motor synaptic loops could also be associated with the lateral aspect of the striatum. For example, the DLS lesion caused the mice to increase the amount of sucrose they consumed in the consumption test. The DLS has been shown to be involved in the regulation of ingestive behaviours in rats (Lelos et al., 2013), however this was evident only under altered physiological conditions. Other studies have shown motoric but not motivational impairments to consumption in rats with DLS lesions (Eagle et al., 1999). The nucleus accumbens (NAc) is typically associated with perceived reward value (Self and Nestler, 1995), however there was no evidence that the ventral striatum had been disrupted in the histological assessment of the tissue. It is possible that the loss of tissue on the DLS causes compensatory upregulation of the dopamine receptors in the ventral system, and since dopaminergic afferents into this region are associated with the ‘wanting’ incentives (or incentive salience) of reward (Berridge and Robinson, 1998), this could have caused a disruption in the balance of this system, however this would need to be shown through additional experiments.

Visuospatial processing was tested in the BLCRTTs and the DLS lesioned animals showed a deficit in accuracy in responses on the side contralateral to the lesion. In addition, the corridor task demonstrated contralateral neglect of reward pots. This is thought to reflect a disruption in the process of directing a motor response to that side, rather than a deficit in motor ability to move there (Brasted et al., 1997), or visual impairment, as supported in the unilateral version of the task where the mice were able to respond perfectly into the same stimulus hole when presented with only stimuli on the contralateral side. The results shown in the mice reflect lateralised impairments in ibotenic DLS lesioned rats demonstrated previously (Brown and Robbins, 1989), as well as studies in unilaterally dopamine depleted rat and mouse models (Dowd and Dunnett, 2004; Heuer et al., 2013). The BLRTT results also reflect the same differences previously observed between these dopamine lesioned rat and mouse studies, in that the reaction time and number of premature withdrawals was not affected in the mouse lesions, but both were increased in the rat model. Other rat studies

however saw no increase in RT with DLS lesions using alternative RT tests (Brown and Robbins, 1989; Hauber and Schmidt, 1994).

The time spent within the central zone in the open field test, and the number of entries into the open arms of the elevated plus maze were increased in the DLS lesioned animals. It could be hypothesised that the mice are demonstrating inhibition of anxiety related behaviours (Holmes et al., 2003). A normal mouse would tend to spend more time at the edges of the open field or within the closed arms. However, a less anxious mouse may be inclined to exhibit more exploratory rearing behaviour, which was not the case with the DLS mice. Furthermore, the observed results could simply be a consequence of the hyperactive mice moving around in a less controlled way. It is not possible to separate these two potential causes with the data collected without further exploration. Anxiety measures could be further probed through a light-dark exploration test in which avoidance of exploration of brightly lit compartments is probed (Crawley and Goodwin, 1980), or through the novelty-induced hypophagia test in which anxiolytic drugs are used to assess how animals respond to high value food rewards in novel environments (Dulawa and Hen, 2005).

#### Non-motor deficits in DMS lesioned mice

The DMS lesioned mice exhibited a significant deficit in accuracy on the DA task. This was particularly pronounced at the early time-point. Since there was no impairment in spontaneous alternation behaviour, these effects are likely not attributed to generalised deficits in alternation, but most likely due to disruption to executive function, with the animals unable to implement the rule. Impairments to working memory are unlikely to contribute to the results observed since there was no decline in performance in relation to time, and the DMS mice were significantly less accurate in the task even when there was no delay applied.

Some degree of spontaneous recovery or compensation seemed to improve their performance by the late time-point. Spontaneous recovery in the task has been observed in lesioned rats (Dunnett and White, 2006), however the performance of the control groups in this case were able to continue to improve their performance at the same rate as the lesioned animals and thus maintain a significant difference in accuracy score. The DMS lesions did have some medial tissue sparing, leaving some of the cortico-striatal circuitry intact and thus potentially reducing the impact of the deficit. The outcome of this task could be improved with more complete lesions, and potentially by reducing the difficulty of the task by shortening the maximum delay within the trials. In the rat experiments, even though

the delay extends up to 20 seconds, the intact animals can still perform at over 70% accuracy, whereas the sham mice were down to 50% accuracy with a 10 second delay, thus reducing the baseline to which the lesioned animals were compared.

No attentional deficits were shown in the 5CSRRT, in contrast to previous rat studies in which the same cortico-striatal loops were disrupted (Muir et al., 1996), and in mid-striatum lesioned mice (Trueman et al., 2005). In fact, the lesioned mice were able to respond faster than the sham animals. This may be a result of their increased speed and hyperactivity despite the same increase in response time being absent in the DA task. An important distinction is that the DA task requires the mice to remember a previous response and decide where to poke, whereas the 5CSRRT is more straight-forward since they simply have to see a light and poke in it rather than having to make a choice. The relative simplicity of the 5CSRRT may be part of the reason why no deficit was seen, since in a more complex task such as DA, a relatively small disturbance could be enough to disrupt performance. However, it may be that a much greater loss is required in order to elicit a deficit when the processes involved in making a correct response is simplified.

When the contingency was degraded in the 5CSRRT (i.e. the reward was freely available regardless of action outcome) the number of responses were diminished in both the sham and lesioned animals, thus indicating that the lesioned animals were able to inhibit their responses in the boxes (Yin and Knowlton, 2006). However, previous work has implicated the DMS in inhibitory behaviours in the rat (Eagle and Baunez, 2010). It is possible that an alternative probe, such as extinction testing or reward devaluation, could reveal some deficits in this behaviour, or it could be that more complete lesioning is required to elicit these behavioural changes.

The DMS mice demonstrated an early post-lesion deficit on “short-term” memory in the novel object recognition test but “long-term” memory was unaffected. However, when tested at the late time-point the early “short-term” deficit had resolved and an apparent deficit in “long-term” memory had emerged. The DA test did not show any memory deficits, although the delays in the task are significantly shorter than those probes in the novel object task. Previous studies link the DMS with memory processing in rats (Pauli et al., 2012; White and McDonald, 2002), and memory loss is a key feature in people with HD. Short-term memory deficits have been reported in the R6/1 mouse model when under acute stress (Mo et al., 2013). It is possible that the mice could be experiencing a state of stress following lesion surgery which may impact on their behaviour. In addition, short-term disruption

within the DMS caused by the QA could interfere with the process of either storing memory or accessing it. At the late time-point, once the lesion has developed, it is possible that different neural loops are degraded and thereby somehow affecting longer-term memory differentially. It is not possible to draw conclusions from just this one test; however, the data provide an interesting result which could be explored further. If the effect is real, then the novel object recognition task, or other memory tests such as Morris water maze or radial arm mazes could provide a useful tool for probing the efficacy of transplant in attenuating deficits associated with memory.

## 5.10 Conclusions and future work

The experiments described in this chapter aimed to identify a battery of apposite behavioural tests which could detect long-term deficits against which therapeutic interventions, such as cell replacement therapy, could be assessed.

The study found several motor and non-motor behavioural deficits, detection of which was dependant on the lesion placement and volume. Of the tests that were employed, the DLS lesions produced the greater number of demonstrable deficits. This was due partly because of the increased quality of the lesions themselves (i.e. accurate positioning and minimal tissue sparing). Since the DMS lesions were small, only tests capable of detecting subtler lesion-induced disturbances were able to demonstrate changes in behaviour. It is likely that more complete lesioning would confer a greater range of detectable deficits, however these appear to be harder to achieve consistently in the DMS model.

Furthermore, fewer non-motor probes were tested. The number of non-motor tests able to be implemented was restricted by the length of time it takes to train and test mice. Training in the DA task alone took 15 weeks to complete, as a result, fewer cognitive behaviours were probed. Once the mice were trained to respond in the operant boxes it was easy to switch to the 5CSRTT since no further training was required, even so, to complete this test takes an additional three weeks in itself. This is likely to be a major contributing factor to why so few of these tests are carried out in other studies. However, cognitive problems are often cited as having the greatest impact on day to day living by people with HD so characterising these deficits and testing potential therapies should form an essential part of the preclinical process.

To confirm the findings of this experiment, a replication study in different hands would ensure that the models are reproducible, and that the tests are robust against individual interpretation. The DMS model could be improved by increasing the volume of toxin or increasing the number of sites at which the toxin is delivered to reduce the amount of tissue sparing, and through adjusting the posterior coordinates to avoid disruption of the GP to enable a clearer interpretation of the results.

These tests could then be used to assess if changes to the transplantation protocols lead to improved behavioural outcomes, rather than basing improvement solely on the morphological appearance of the grafts, since it is the efficacy of the treatment in improving symptoms which will lead to its use as a therapy in practice.

In conclusion, the proposed lesion parameters and functional tests for future mouse transplantation experiments are:

- Unilateral QA lesion placement
- Dorsolateral coordinates covering both anterior and posterior striatum (AP=+1.2, ML=+2.4, DV=-2.4 and AP=+2.2, ML=+1.8, DV=-2.4).
- 0.2µl 0.9M QA per injection site.
- Apomorphine rotations (2mgkg<sup>-1</sup>).
- Rotarod.
- Sucrose consumption.
- Corridor.
- Bilateral / unilateral choice reaction time tasks.
- Elevated plus maze.

# Chapter 6

## General discussion

Cell replacement therapy offers a unique approach to helping treat people with HD, with the exciting potential of rebuilding lost neural networks and reversing some of the debilitating symptoms of this progressive disease. Preclinical work has been able to show the type of functional effects that a successful treatment could provide, however, the results of the small number of in-patient trials have delivered mixed results for a variety of reasons (study design, incorrect outcome measures etc). Despite this, there have been a number of patients which have exhibited an impressive improvement in quality of life, and for this reason the continued research into understanding the complex mechanisms and interactions of the treatment is essential to progress and refine cell replacement therapies.

Although the success of the technique has been robustly demonstrated in rat models, the mouse models have provided a less successful outcome. This has obstructed the utilisation of the array of genetically altered mouse models which can be more easily manipulated to explicate the mechanisms underlying recovery, and to present the progressive aspects of HD lost in the lesion models.

The objective of the experiments presented in this thesis was to determine factors which may be hindering the success of mouse grafts, and to improve upon the current protocols. The QA model was selected as the basis of the experiments since the best results seen so far have been demonstrated in the QA rat models. The overall aim of the project was to optimise transplantation protocols in the acute QA model so that they may be later applied to the more progressive models.

## 6.1 Key findings

The key findings of each experiment are summarised in the table below;

<b>Experiment 1</b>	<ul style="list-style-type: none"> <li>• The collapse of the striatum following QA lesioning is not sufficient to affect atlas-based co-ordinates for transplantation</li> <li>• The QA lesioned mouse striatum has a greater cell density than that of the rat</li> <li>• Transplantation typically occurs at a time of peak inflammatory activity</li> <li>• The inflammatory response to lesioning is more exaggerated in C57BL6/J mice than in Lister hooded rats</li> </ul>
<b>Experiment 2</b>	<ul style="list-style-type: none"> <li>• Delaying transplantation beyond peak inflammatory response does not improve graft survival or content</li> <li>• Inflammatory response is affected by the age of the host mouse</li> <li>• Transplanting into aged mice has no effect on graft or cell survival</li> </ul>
<b>Experiment 3</b>	<ul style="list-style-type: none"> <li>• Chrm4-EGFP-CD1 tissue does not provoke a greater inflammatory response than other non-EGFP tissue <i>in vivo</i></li> <li>• Matching host and donor strains increases graft survival, but not the size or quality of the surviving grafts</li> <li>• Graft outcome is inconsistent under similar transplantation condition</li> </ul>
<b>Experiment 4</b>	<ul style="list-style-type: none"> <li>• WGE cell suspensions yield better graft outcomes when transplanted at E14 than at E12</li> <li>• Younger tissue survives better when it was not completely dissociated into a single cell suspension</li> <li>• Large differences in the appearance of grafts is evident throughout all groups suggesting other factors may be influencing outcome to a greater extent to those being investigated</li> </ul>
<b>Experiment 5</b>	<ul style="list-style-type: none"> <li>• Animals transplanted earlier within a session had a greater number of surviving cells within grafts</li> <li>• Trypan blue exclusion does not accurately reflect cell viability</li> <li>• Cells remain within the grafting cannula following aliquot expulsion</li> <li>• Creating individual suspensions for each animal did not improve outcome variability</li> </ul>
<b>Experiment 6</b>	<ul style="list-style-type: none"> <li>• The following behavioural tests were able to detect long-term deficits in unilateral DLS lesioned mice; locomotor activity, open field, drug-induced rotations, footprint analysis, rotarod, staircase, sucrose consumption, corridor, BLCRTT, ULCRTT and elevated plus-maze</li> </ul>

## Experiment 7

- The following behavioural tests were able to detect long-term deficits in bilateral DMS lesioned mice; delayed alternation, novel object recognition, open field, locomotor activity
- DLS lesions provided more robust lesions compared to DMS
- DLS and DMS lesions elicited dissimilar behavioural phenotypes

## 6.2 The effect of host

Whilst most of the present experiments investigating the different effects of host on graft outcome did not in themselves yield clear results in terms of graft-improving protocol adaptations, they did highlight potential problems which may have been overlooked previously. Whilst it remains necessary to diagnose the impact of increased microglial activity in the transplanted region and to quantify the activation state of the microglia, the fact that the inflammatory response of mouse hosts is significantly more vigorous than that seen in the rat model was most interesting. The results indicated that further investigations into dampening this effect could be essential in producing a more favourable environment within which transplanted cells could thrive. In fact, the non-steroidal anti-inflammatory drug (NSAID) Metacam, which is used peri-operatively to relieve pain, is a known inhibitor of microglial activation. Therefore, an experiment in which an elongated period of Metacam administration is introduced throughout the time in which grafts are left to mature, might determine if reducing the inflammatory response can aid in graft and/or cell survival. Delaying the transplantation surgery until a period of low post-lesion microglial activity did not resolve this issue, perhaps because the reaction was re-established during the process of transplantation itself. Indeed, it was shown in rats that inserting the transplantation cannula and waiting for at least one hour before injecting cells led to a three-fold increase in dopamine cell survival in the grafts (Sinclair, Fawcett, & Dunnett, 1999). It is proposed that by delaying implantation, exposure of the cells to the hyperacute inflammatory response of the host due to cannula insertion was reduced.

One experiment that did not make it into this thesis was a comparison of grafts transplanted into the intact and lesioned striatum. This would have presented a good opportunity to determine how much of an effect the QA lesion is having on graft outcome, and whether the inflammatory response is indeed impacting of the transplanted cells. Unfortunately, the tissue derived from the experiment was lost due to bacterial infection. Interestingly, neural transplants in rats were shown to be larger in the QA lesioned striatum where increased numbers of microglia, astrocytes and macrophages were present than in intact striatum (W.-M. Duan, Widner, Cameron, & Brundin, 1998). The authors of this

study concluded that inflammation does not lead to rejection. Smaller grafts in the intact striatum could potentially be a result of lack of space in which cells can proliferate. **Experiment 1** has shown that the mouse striatum becomes denser after lesioning (and denser than in the rat on the intact side too), so could the increased cell density of the host parenchyma make it a less appropriate substrate in which to transplant?

Whilst the inflammatory response of the hosts was observed in the current experiments, immune response specifically was not covered within their scope. In fact, the investigation into immune reaction to tissues behind the blood brain barrier could be an entire thesis in itself. Cells within the brain are now known to not be completely protected from the peripheral immune system by the blood brain barrier. For example, microglia can interpret and propagate inflammatory signals that are initiated in the periphery in order to mount an appropriate response to peripheral infection (Norden & Godbout, 2013). Furthermore, cytotoxic T cells, also known as killer T cells, can infiltrate the brain at the site of injury where the blood brain barrier is disrupted, in addition to regions where the barrier may be leaky, such as at the 5<sup>th</sup> lumbar cord (Arima et al., 2013), thereby increasing the risk of graft rejection. These T cells can migrate to and destroy damaged or compromised neuronal cells by expressing cytotoxins that activate cell apoptosis (W.-M. M. Duan, Widner, & Brundin, 1995). Once activated the cytotoxic T cells can increase in number and remain at the site of injury for a prolonged period (Wakim, Woodward-Davis, & Bevan, 2010). Additionally, activated T cells can trigger activation in the microglia, exacerbating the inflammatory process and contributing to chronic transplant rejection processes (Raivich et al., 1999). This process may be exacerbated in cases of transplantation in HD patients since the barrier can become more permeable with aged or unwell individuals (Drouin-Ouellet et al., 2015; Erdő, Denes, & de Lange, 2017). Further examination of the tissues for peripheral immune cells may reveal other differences between the rat and mouse models that lead to the observed poorer outcome in mice.

It has been suggested that the glial component of rat grafts might release immunosuppressive factors and thus enable graft survival in rat models (Devajyothis et al., 1993; Frei et al., 1994). It has not currently been resolved as to whether there is a similar population of cells within mouse grafts releasing protective factors, or if they are absent. Future experiments investigating the transplantation of mouse tissue into rat and vice versa could help to understand this by analysing the presence of these factors within the host and comparing the survival of the grafts. Such secretion could be specific to species, cell type or even donor cell age.

### 6.3 The effect of donor

One way of increasing the proportion of surviving grafts was ensuring host and donor strain matched, however this did not seem to affect the quality of those grafts that survived. Another potential mismatch with the potential to influence rejection is the sex-type of the transplanted tissue. The sex of the embryos that are dissected is not checked and it can be assumed that the cell suspensions used contained a mix of male and female tissue. This could introduce some variance in the way that the host reacts to the cells, particularly if some litters have a skewed sex ratio. This may potentially provide a reason as to why some cells don't survive as well as other. It is possible that sex-matching host and donor tissue may result in improved acceptance of donated tissue. In hindsight, this test could have been incorporated into **Experiment 5** in which individual suspensions were created from single pups. Had these suspensions been sex-typed and transplanted – perhaps into both male and female animals – it could have gone some way to suggesting if tissue sex, or indeed host sex, influence the survival of grafts.

Throughout the present experiments surviving grafts were observed in all experimental groups, however, this is also true for dead or 'unhealthy' looking cells. It is possible that all the grafts were in a continuing state of rejection, albeit at differing rates. The grafts were only taken at twelve weeks post-transplantation, so it remains unclear as to whether graft survival rates would continue to decline beyond that point.

### 6.4 Functional assessment

Without an established battery of functional outcome measures for detecting efficacy of grafts, it was not practicable to test if any protocol changes affected behavioural deficits, despite showing no obvious signs of improved morphological outcome. Whilst targeting lesions to more specific regions of the striatum is technically more difficult than simply producing a lesion within the whole striatum, it seems clear that doing so increases the reliability of induced behavioural deficits, and therefore produces a background against which functional improvements can be assessed. The final experiments of this thesis have identified behavioural deficits in the QA mouse model that could be easily added to any grafting experiment, and if functional improvements can be shown it will enable us to understand more fully the attributes of grafts that lead to the better outcome. Whilst it's true that many of these factors have been identified in rat models, as these experiments have shown, this does not necessarily translate to the mouse.

It is possible that transplanted WGE cells are more inclined to differentiate towards certain types of MSN within the host parenchyma, such as those of the dorsomedial striatum which receive connections from the prefrontal cortex regions, or those of the lateral striatum which receive more connections from the motor-cortex for example. Further investigation into the type of MSNs within grafts and the potential they have for re-instating connections to specific anatomically correct regions could elucidate how some grafts may be more effective than others. Matching DMS lesions with DMS-precursors for example, could provide better functional results than transplanting cells from a contrasting region.

## 6.5 Conclusions

The experiments described in this thesis have shown that deficits in the outcome of striatal transplants in the QA lesion mouse models of HD are contributed to by a combination of host and donor attributes, cell suspension treatment, surgery order and the absence of functional assessments. A disparity in the magnitude and nature of inflammatory responses between the rat and mouse hosts raises important considerations for immunosuppression regimes in mice subject to allografts. Whilst the measures of inflammation used showed no direct correlation on graft size or survival in these experiments, it was postulated that additional factors may be obscuring effects by creating large variations in graft outcome since experimental groups treated under the same transplantation conditions yielded inconsistent results. Metanalysis of all groups, and *in vitro* experiments probing the qualities of cell suspensions over time, revealed that surgery order could be a major source of variation. Therefore, one of the most important steps towards the optimisation of transplant protocols in mice would be to ensure consistent delivery of cells to every individual. Undertaking measures such as screening the health of cells, and aliquoting properly dissociated suspensions prior to surgery, should reduce variability and allow other components of the protocols to be investigated more rigorously.

Furthermore, it was shown that targetting lesions to specific regions of the striatum enables the use of focused behavioural outcome measures which can detect graft-induced functional improvements.

The list of potential factors that could influence the success of transplantation is very long. The experiments presented here aimed to probe a few of those deemed most likely to influence the grafts in order to affect a more successful outcome. The results highlight many potential areas for further investigation which may not have been identified otherwise, and in combination with robust functional testing, it should be possible to progressively apply adaptations to the transplantation methodology to provide a robust system for which many of the ever-advancing genetic models and

techniques can be applied, and progress cell replacement therapies towards becoming a viable treatment option for people with HD.

# Bibliography

Abbott, A., (2004). Laboratory animals: the Renaissance rat. *Nature* 428, 464–6.

Albin, R.L., Young, A.B., Penney, J.B., (1989). The functional anatomy of basal ganglia disorders. *Trends Neurosci.* 12, 366–75.

Alexander, G.E., DeLong, M.R., Strick, P.L., (1986). Parallel organization of functionally segregated circuits linking basal ganglia and cortex. *Annu. Rev. Neurosci.* 9, 357–81.

Alexi, T., (2000). Neuroprotective strategies for basal ganglia degeneration: Parkinson's and Huntington's diseases. *Prog. Neurobiol.* 60, 409–470.

An, M.C., Zhang, N., Scott, G., Montoro, D., Wittkop, T., Mooney, S., Melov, S., Ellerby, L.M., (2012). Genetic Correction of Huntington's Disease Phenotypes in Induced Pluripotent Stem Cells. *Cell Stem Cell* 11, 253–263.

Anderson, S.A., Qiu, M., Bulfone, A., Eisenstat, D.D., Meneses, J., Pedersen, R., Rubenstein, J.L.R., (1997). Mutations of the homeobox genes *Dlx-1* and *Dlx-2* disrupt the striatal subventricular zone and differentiation of late born striatal neurons. *Neuron* 19, 27–37.

Arber, C., Precious, S. V., Cambray, S., Risner-Janiczek, J.R., Kelly, C., Noakes, Z., Fjodorova, M., Heuer, A., Ungless, M.A., Rodríguez, T.A., Rosser, A.E., Dunnett, S.B., Li, M., (2015). Activin A directs striatal projection neuron differentiation of human pluripotent stem cells. *Development* 142, 1375–1386.

Arima, Y., Kamimura, D., Sabharwal, L., Yamada, M., Bando, H., Ogura, H., Atsumi, T., Murakami, M., 2013. Regulation of immune cell infiltration into the CNS by regional neural inputs explained by the gate theory. *Mediators Inflamm.* (2013), 898165.

Arlicot, N., Tronel, C., Bodard, S., Garreau, L., Guilloteau, D., Antier, D., Chalon, S., (2014). Neuroinflammation follow-up in a quinolinic acid rat model of excitotoxicity by translocator protein (18 kDa) mapping with CLINDE. *J. Nucl. Med.* 55, 1796–1796.

Awad, D., Schrader, I., Bartok, M., Mohr, A., Gabel, D., H, U., (2011). Comparative Toxicology of Trypan Blue, Brilliant Blue G, and Their Combination Together with Polyethylene Glycol on Human Pigment Epithelial Cells. *Investig. Ophthalmology Vis. Sci.* 52, 4085.

Aylward, E.H., Anderson, N.B., Bylsma, F.W., Wagster, M. V, Barta, P.E., Sherr, M., Feeney, J., Davis, A., Rosenblatt, A., Pearlson, G.D., Ross, C.A., (1998). Frontal lobe volume in patients with Huntington's disease. *Neurology* 50, 252–8.

Bachoud-Lévi, A.-C., Gaura, V., Brugières, P., Lefaucheur, J.-P., Boissé, M.-F., Maison, P., Baudic, S., Ribeiro, M.-J., Bourdet, C., Remy, P., Cesaro, P., Hantraye, P., Peschanski, M., (2006). Effect of fetal neural transplants in patients with Huntington's disease 6 years after surgery: a long-term follow-up study. *Lancet Neurol.* 5, 303–309.

Bachoud-Lévi, A.-C., Rémy, P., Nguyễn, J.-P., Brugières, P., Lefaucheur, J.-P., Bourdet, C., Baudic, S., Gaura, V., Maison, P., Haddad, B., Boissé, M.-F., Grandmougin, T., Jény, R., Bartolomeo, P., Barba, G.D., Degos, J.-D., Lisovoski, F., Ergis, A.-M., Pailhous, E., Cesaro, P., Hantraye, P., Peschanski, M., (2000). Motor and cognitive improvements in patients with Huntington's disease after neural transplantation. *Lancet* 356, 1975–1979.

Bachoud-Lévi, A., Bourdet, C., Brugières, P., Nguyen, J.P., Grandmougin, T., Haddad, B., Jény, R., Bartolomeo, P., Boissé, M.F., Barba, G.D., Degos, J.D., Ergis, A.M., Lefaucheur, J.P., Lisovoski, F., Pailhous, E., Rémy, P., Palfi, S., Defer, G.L., Cesaro, P., Hantraye, P., Peschanski, M., (2000). Safety and tolerability assessment of intrastriatal neural allografts in five patients with Huntington's disease. *Exp. Neurol.* 161, 194–202.

Baird, A.L., Meldrum, A., Dunnett, S.B., (2001). The staircase test of skilled reaching in mice. *Brain Res. Bull.* 54, 243–250.

Baker-Cairns, B.J., Sloan, D.J., Broadwell, R.D., Puklavec, M., Charlton, H.M., (1996). Contributions of donor and host blood vessels in CNS allografts. *Exp. Neurol.* 142, 36–46.

Baldan Ramsey, L.C., Xu, M., Wood, N., Pittenger, C., (2011). Lesions of the dorsomedial striatum disrupt prepulse inhibition. *Neuroscience* 180, 222–8.

Barker, C.F., Billingham, R.E., (1978). Immunologically Privileged Sites, in: *Advances in Immunology*. Academic Press, pp. 1–54.

Barker, R., (1995). A comparative study of preparation techniques for improving the viability of nigral grafts using vital stains, in vitro cultures, and in vivo grafts. *Cell Transplant.* 4, 173–200.

Barker, R.A., Dunnett, S.B., Faissner, A., Fawcett, J.W., (1996). The time course of loss of dopaminergic neurons and the gliotic reaction surrounding grafts of embryonic mesencephalon to the striatum. *Exp. Neurol.* 141, 79–93.

Barker, R.A., Widner, H., (2004). Immune problems in central nervous system cell therapy. *NeuroRX* 1, 472–481.

Bayer, S.A., (1984). Neurogenesis in the rat neostriatum. *Int. J. Dev. Neurosci.* 2, 163–75.

Beal, M.F., (1994). Neurochemistry and toxin models in Huntington's disease. *Curr. Opin. Neurol.* 7, 542–547.

Beal, M.F., Ferrante, R.J., Swartz, K.J., Kowall, N.W., (1991). Chronic quinolinic acid lesions in rats closely resemble Huntington's disease. *J. Neurosci.* 11, 1649–59.

Beal, M.F., Kowall, N.W., Ellison, D.W., Mazurek, M.F., Swartz, K.J., Martin, J.B., (1986). Replication of the neurochemical characteristics of Huntington's disease by quinolinic acid. *Nature* 321, 168–71.

Bernreuther, C., Dihne, M., Johann, V., Schiefer, J., Cui, Y., Hargus, G., Schmid, J.S., Xu, J., Kosinski, C.M., Schachner, M., (2006). Neural Cell Adhesion Molecule L1-Transfected Embryonic Stem Cells Promote Functional Recovery after Excitotoxic Lesion of the Mouse Striatum. *J. Neurosci.* 26, 11532–11539.

Berridge, K.C., Robinson, T.E., (1998). What is the role of dopamine in reward: hedonic impact, reward learning, or incentive salience? *Brain Res. Rev.* 28, 309–369.

Björklund, A., Dunnett, S.B., Stenevi, U., Lewis, M.E., Iversen, S.D., (1980a). Reinnervation of the denervated striatum by substantia nigra transplants: functional consequences as revealed by pharmacological and sensorimotor testing. *Brain Res.* 199, 307–33.

Björklund, A., Schmidt, R.H., Stenevi, U., (1980b). Functional reinnervation of the neostriatum in the adult rat by use of intraparenchymal grafting of dissociated cell suspensions from the substantia nigra. *Cell Tissue Res.* 212, 39–45.

Björklund, A., Stenevi, U., (1984). Intracerebral neural implants: neuronal replacement and reconstruction of damaged circuitries. *Annu. Rev. Neurosci.* 7, 279–308.

Björkqvist, M., Wild, E.J., Thiele, J., Silvestroni, A., Andre, R., Lahiri, N., Raibon, E., Lee, R. V., Benn, C.L., Soulet, D., Magnusson, A., Woodman, B., Landles, C., Pouladi, M.A., Hayden, M.R., Khalili-Shirazi, A., Lowdell, M.W., Brundin, P., Bates, G.P., Leavitt, B.R., Möller, T., Tabrizi, S.J., (2008). A novel pathogenic pathway of immune activation detectable before clinical onset in Huntington's disease. *J. Exp. Med.* 205.

Boche, D., Perry, V.H., Nicoll, J.A.R., (2013). Review: Activation patterns of microglia and their identification in the human brain. *Neuropathol. Appl. Neurobiol.* 39, 3–18.

Borlongan, C. V., Koutouzis, T.K., Freeman, T.B., Hauser, R.A., Cahill, D.W., Sanberg, P.R., (1997). Hyperactivity and hypoactivity in a rat model of Huntington's disease: the systemic 3-nitropropionic acid model. *Brain Res. Protoc.* 1, 253–257.

Borrell-Pagès, M., Zala, D., Humbert, S., Saudou, F., (2006). Huntington's disease: from huntingtin function and dysfunction to therapeutic strategies. *Cell. Mol. Life Sci.* 63, 2642–60.

Brasted, P.J., Humby, T., Dunnett, S.B., Robbins, T.W., (1997). Unilateral Lesions of the Dorsal Striatum in Rats Disrupt Responding in Egocentric Space. *J. Neurosci.* 17, 8919–8926.

Brasted, P.J., Watts, C., Torres, E.M., Robbins, T.W., Dunnett, S.B., (2000). Behavioral recovery after transplantation into a rat model of Huntington's disease: dependence on anatomical connectivity and extensive postoperative training. *Behav. Neurosci.* 114, 431–6.

Brooks, S., Fielding, S., Döbrössy, M., von Hörsten, S., Dunnett, S., (2009). Subtle but progressive cognitive deficits in the female tgHD hemizygote rat as demonstrated by operant SILT performance. *Brain Res. Bull.* 79, 310–5.

Brooks, S., Higgs, G., Janghra, N., Jones, L., Dunnett, S.B., (2012a). Longitudinal analysis of the behavioural phenotype in YAC128 (C57BL/6J) Huntington's disease transgenic mice. *Brain Res. Bull.* 88, 113–20.

Brooks, S., Higgs, G., Jones, L., Dunnett, S.B., (2012b). Longitudinal analysis of the behavioural phenotype in Hdh(CAG)150 Huntington's disease knock-in mice. *Brain Res. Bull.* 88, 182–8.

Brooks, S.P., Janghra, N., Workman, V.L., Bayram-Weston, Z., Jones, L., Dunnett, S.B., (2012c). Longitudinal analysis of the behavioural phenotype in R6/1 (C57BL/6J) Huntington's disease transgenic mice. *Brain Res. Bull.* 88, 94–103.

Brooks, S.P., Jones, L., Dunnett, S.B., (2012d). Comparative analysis of pathology and behavioural phenotypes in mouse models of Huntington's disease. *Brain Res. Bull.* 88, 81–93.

Brooks, S.P., Trueman, R.C., Dunnett, S.B., (2007). Striatal lesions in the mouse disrupt acquisition and retention, but not implicit learning, in the SILT procedural motor learning task. *Brain Res.* 1185, 179–188.

Brown, G.C., Neher, J.J., (2014). Microglial phagocytosis of live neurons. *Nat. Rev. Neurosci.* 15, 209–16.

Brown, V.J., Robbins, T.W., (1989). Elementary processes of response selection mediated by distinct regions of the striatum. *J. Neurosci.* 9, 3760–5.

Brundin, P., Isacson, O., Björklund, A., (1985). Monitoring of cell viability in suspensions of embryonic CNS tissue and its use as a criterion for intracerebral graft survival. *Brain Res.* 331, 251–9.

Brundin, P., Karlsson, J., Emgård, M., Kaminski Schierle, G.S., Hansson, O., Petersén, Å., Castilho, R.F., (2000). Improving the Survival of Grafted Dopaminergic Neurons: A Review Over Current Approaches. *Cell Transplant.* 9, 179–195.

Bruyn, R.P.M., Stoof, J.C., (1990). The quinolinic acid hypothesis in Huntington's chorea. *J. Neurol. Sci.* 95, 29–38.

Bugos, O., Bhide, M., Zilka, N., (2009). Beyond the rat models of human neurodegenerative disorders. *Cell. Mol. Neurobiol.* 29, 859–69.

Butler, Juurlink, (1987). An atlas for staging mammalian and chick embryos.

Campbell, K., Olsson, M., Björklund, A., (1995). Regional incorporation and site-specific differentiation of striatal precursors transplanted to the embryonic forebrain ventricle. *Neuron* 15, 1259–1273.

Capetian, P., Knoth, R., Maciaczyk, J., Pantazis, G., Ditter, M., Bokla, L., Landwehrmeyer, G.B., Volk, B., Nikkhah, G., (2009). Histological findings on fetal striatal grafts in a Huntington's disease patient early after transplantation. *Neuroscience* 160, 661–675.

Casolini, P., Catalani, A., Zuena, A.R., Angelucci, L., (2002). Inhibition of COX-2 reduces the age-dependent increase of hippocampal inflammatory markers, corticosterone secretion, and behavioral impairments in the rat. *J. Neurosci. Res.* 68, 337–43.

Castro, R., Abreu, P., Calzadilla, C.H., Rodriguez, M., (1985). Psychopharmacology Increased or decreased locomotor response in rats following repeated administration of apomorphine depends on dosage interval. *Psychopharmacology (Berl)*. 85, 333–339.

Caviston, J.P., Holzbaur, E.L.F., (2009). Huntingtin as an essential integrator of intracellular vesicular trafficking. *Trends Cell Biol*. 19, 147–55.

Chen, Z., Phillips, L.K., Gould, E., Campisi, J., Lee, S.W., Ormerod, B.K., Zwierzchoniewska, M., Martinez, O.M., Palmer, T.D., (2011). MHC mismatch inhibits neurogenesis and neuron maturation in stem cell allografts. *PLoS One* 6, e14787.

Cicchetti, F., Saporta, S., Hauser, R.A., Parent, M., Saint-Pierre, M., Sanberg, P.R., Li, X.J., Parker, J.R., Chu, Y., Mufson, E.J., Kordower, J.H., Freeman, T.B., (2009). Neural transplants in patients with Huntington's disease undergo disease-like neuronal degeneration. *Proc. Natl. Acad. Sci.* 106, 12483–12488.

Cicchetti, F., Soulet, D., Freeman, T.T.B., (2011). Neuronal degeneration in striatal transplants and Huntington's disease: potential mechanisms and clinical implications. *Brain* 134, 641–52.

Cisbani, G., Saint Pierre, M., Cicchetti, F., (2014). Single cell suspension methodology favours survival and vascularization of fetal striatal grafts in the YAC128 mouse model of Huntington's disease. *Cell Transplant*. 23, 1267–1278.

Combrinck, M.I., Perry, V.H., Cunningham, C., (2002). Peripheral infection evokes exaggerated sickness behaviour in pre-clinical murine prion disease. *Neuroscience* 112, 7–11.

Coppen, E.M., Roos, R.A.C., (2017). Current Pharmacological Approaches to Reduce Chorea in Huntington's Disease. *Drugs* 77, 29–46.

Corbin, J.G., Rutlin, M., Gaiano, N., Fishell, G., (2003). Combinatorial function of the homeodomain proteins Nkx2.1 and Gsh2 in ventral telencephalic patterning. *Development* 130, 4895–4906.

Costall, B., Naylor, R.J., Cannon, J.G., Lee, T., (1977). Differentiation of the dopamine mechanisms mediating stereotyped behaviour and hyperactivity in the nucleus accumbens and caudate-putamen. *J. Pharm. Pharmacol.* 29, 337–342.

Coyle, J.T., Ferkany, J.W., Zaczek, R., (1983). Kainic acid: insights from a neurotoxin into the pathophysiology of Huntington's disease. *Neurobehav Toxicol Teratol* 5, 617–624.

Crawley, J., Goodwin, F.K., (1980). Preliminary report of a simple animal behavior model for the anxiolytic effects of benzodiazepines. *Pharmacol. Biochem. Behav.* 13, 167–170.

Creighton, S., Almqvist, E., MacGregor, D., Fernandez, B., Hogg, H., Beis, J., Welch, J., Riddell, C., Lokkesmoe, R., Khalifa, M., MacKenzie, J., Sajoo, A., Farrell, S., Robert, F., Shugar, A., Summers, A., Meschino, W., Allingham-Hawkins, D., Chiu, T., Hunter, A., Allanson, J., Hare, H., Schween, J., Collins, L., Sanders, S., Greenberg, C., Cardwell, S., Lemire, E., MacLeod, P., Hayden, M., (2003). Predictive, pre-natal and diagnostic genetic testing for Huntington's disease: the experience in Canada from 1987 to 2000. *Clin. Genet.* 63, 462–475.

Crotti, A., Benner, C., Kerman, B.E., Gosselin, D., Lagier-Tourenne, C., Zuccato, C., Cattaneo, E., Gage, F.H., Cleveland, D.W., Glass, C.K., (2014). Mutant Huntingtin promotes autonomous microglia activation via myeloid lineage-determining factors. *Nat. Neurosci.* 17, 513–521.

Davies, S.W., Roberts, P.J., (1988). Sparing of cholinergic neurons following quinolinic acid lesions of the rat striatum. *Neuroscience* 26, 387–93.

Deacon, T.W., Pakzaban, P., Isacson, O., (1994). The lateral ganglionic eminence is the origin of cells committed to striatal phenotypes: neural transplantation and developmental evidence. *Brain Res.* 668, 211–9.

DeLong, M.R., (1990). Primate models of movement disorders of basal ganglia origin. *Trends Neurosci.* 13, 281–5.

Denaro, M., Oldmixon, B., Patience, C., Andersson, G., Down, J., (2001). EGFP-transduced EL-4 cells from tumors in C57BL/6 mice. *Gene Ther.* 8, 1814–1815.

Devajyothis, C., Kalvakolanus, I., Babcocks, G., Vasavadag, H., Howes, P., Ransohoffli, R., (1993). Inhibition of interferon-gamma-induced major histocompatibility complex class II gene transcription by interferon-beta and type beta 1 transforming growth factor in human astrocytoma cells. Definition of cis-element. *Bio. Chem.* 268(26), 18794-18800.

Devan, B.D., White, N.M., (1999). Parallel Information Processing in the Dorsal Striatum: Relation to Hippocampal Function. *J. Neurosci.* 19, 2789–2798.

Difiglia, M., Rafols, J.A., (1988). Synaptic organization of the globus pallidus. *J. Electron Microsc. Tech.* 10, 247–63.

Dihné, M., Bernreuther, C., Hagel, C., Wesche, K.O., Schachner, M., (2006). Embryonic stem cell-derived neuronally committed precursor cells with reduced teratoma formation after transplantation into the lesioned adult mouse brain. *Stem Cells* 24, 1458–66.

Döbrössy, M.D., Dunnett, S.B., (2008). Environmental Housing and Duration of Exposure Affect Striatal Graft Morphology in a Rodent Model of Huntington's Disease. *Cell Transplant.* 17, 1125–1134.

Döbrössy, M.D., Dunnett, S.B., (2006). Morphological and cellular changes within embryonic striatal grafts associated with enriched environment and involuntary exercise. *Eur. J. Neurosci.* 24, 3223–3233.

Döbrössy, M.D., Dunnett, S.B., (2005). Training specificity, graft development and graft-mediated functional recovery in a rodent model of Huntington's disease. *Neuroscience* 132, 543–52.

Döbrössy, M.D., Dunnett, S.B., (1998). Striatal grafts alleviate deficits in response execution in a lateralised reaction time task. *Brain Res. Bull.* 47, 585–593.

Döbrössy, M.D., Klein, A., Janghra, N., Nikkhah, G., Dunnett, S.B., (2011). Validating the use of M4-BAC-GFP mice as tissue donors in cell replacement therapies in a rodent model of Huntington's disease. *J. Neurosci. Methods* 197, 6–13.

Doig, N.M., Moss, J., Bolam, J.P., (2010). Cortical and thalamic innervation of direct and indirect pathway medium-sized spiny neurons in mouse striatum. *J. Neurosci.* 30, 14610–8.

Dowd, E., Dunnett, S.B., (2004). Deficits in a lateralized associative learning task in dopamine-depleted rats with functional recovery by dopamine-rich transplants. *Eur. J. Neurosci.* 20, 1953–1959.

Dowd, E., Monville, C., Torres, E.M., Dunnett, S.B., (2005). The Corridor Task: A simple test of lateralised response selection sensitive to unilateral dopamine deafferentation and graft-derived dopamine replacement in the striatum. *Brain Res. Bull.* 68, 24–30.

Drouin-Ouellet, J., Sawiak, S.J., Cisbani, G., Lagacé, M., Kuan, W.-L., Saint-Pierre, M., Dury, R.J., Alata, W., St-Amour, I., Mason, S.L., Calon, F., Lacroix, S., Gowland, P.A., Francis, S.T., Barker, R.A., Cicchetti, F., (2015). Cerebrovascular and blood-brain barrier impairments in Huntington's disease: Potential implications for its pathophysiology. *Ann. Neurol.* 78, 160–177.

Duan, W.-M., Brundin, P., Widner, H., (1997). Addition of allogeneic spleen cells causes rejection of intrastriatal embryonic mesencephalic allografts in the rat. *Neuroscience* 77, 599–609.

Duan, W.-M., Widner, H., Cameron, R.M., Brundin, P., (1998). Quinolinic acid-induced inflammation in the striatum does not impair the survival of neural allografts in the rat. *Eur. J. Neurosci.* 10, 2595–2606.

Duan, W.-M.M., Widner, H., Brundin, P., (1995). Temporal pattern of host responses against intrastriatal grafts of syngeneic, allogeneic or xenogeneic embryonic neuronal tissue in rats. *Exp. brain Res.* 104, 227–42.

Duff, K., Paulsen, J.S., Beglinger, L.J., Langbehn, D.R., Stout, J.C., (2007). Psychiatric symptoms in Huntington's disease before diagnosis: the predict-HD study. *Biol. Psychiatry* 62, 1341–6.

Dulawa, S.C., Hen, R., (2005). Recent advances in animal models of chronic antidepressant effects: The novelty-induced hypophagia test. *Neurosci. Biobehav. Rev.* 29, 771–783.

Dunnett, S.B., Björklund, A., (1997). Basic neural transplantation techniques. I. Dissociated cell suspension grafts of embryonic ventral mesencephalon in the adult rat brain. *Brain Res. Brain Res. Protoc.* 1, 91–9.

Dunnett, S.B., Carter, R.J., Watts, C., Torres, E.M., Mahal, A., Mangiarini, L., Bates, G., Morton, A.J., (1998). Striatal transplantation in a transgenic mouse model of Huntington's disease. *Exp. Neurol.* 154, 31–40.

Dunnett, S.B., Nathwani, F., Brasted, P.J., (1999). Medial prefrontal and neostriatal lesions disrupt performance in an operant delayed alternation task in rats. *Behav. Brain Res.* 106, 13–28.

Dunnett, S.B., Rosser, A.E., (2007). Stem cell transplantation for Huntington's disease. *Exp. Neurol.* 203, 279–292.

Dunnett, S.B., White, A., (2006). Striatal grafts alleviate bilateral striatal lesion deficits in operant delayed alternation in the rat. *Exp. Neurol.* 199, 479–489.

Dunnett, S.B., Björklund, A., (1992). *Neural Transplantation: A Practical Approach*. IRL Press.

Eagle, D.M., Baunez, C., (2010). Is there an inhibitory-response-control system in the rat? Evidence from anatomical and pharmacological studies of behavioral inhibition. *Neurosci. Biobehav. Rev.* 34, 50–72.

- Eagle, D.M., Humby, T., Dunnett, S.B., Robbins, T.W., (1999). Effects of Regional Striatal Lesions on Motor, Motivational, and Executive Aspects of Progressive-Ratio Performance in Rats. *Behav. Neurosci.* 113, 718–731.
- Eagle, D.M., Humby, T., Howman, M., Reid-Henry, A., Dunnett, S.B., Robbins, T.W., (1999). Differential effects of ventral and regional dorsal striatal lesions on sucrose drinking and positive and negative contrast in rats. *Psychobiology* 27, 267–276.
- El Akabawy, G., Rattray, I., Johansson, S.M., Gale, R., Bates, G., Mado, M., El-Akabawy, G., (2012). Implantation of undifferentiated and predifferentiated human neural stem cells in the R6/2 transgenic mouse model of Huntington’s disease. *BMC Neurosci.* 13, 97.
- Erdő, F., Denes, L., de Lange, E., 2017. Age-associated physiological and pathological changes at the blood-brain barrier: A review. *J. Cereb. Blood Flow Metab.* 37, 4–24.
- Espey, M.G., Chernyshev, O.N., Reinhard, J.F., Namboodiri, M.A., Colton, C.A., (1997). Activated human microglia produce the excitotoxin quinolinic acid. *Neuroreport* 8, 431–4.
- Evans, A.E., (2013). Characterisation of Foxp1 in striatal development and the adult brain. PhD thesis, Cardiff University, Cardiff.
- Evans, S.J., Douglas, I., Rawlins, M.D., Wexler, N.S., Tabrizi, S.J., Smeeth, L., (2013). Prevalence of adult Huntington’s disease in the UK based on diagnoses recorded in general practice records. *J. Neurol. Neurosurg. Psychiatry* 84, 1156–1160.
- Featherstone, R.E., McDonald, R.J., (2004). Dorsal striatum and stimulus-response learning: Lesions of the dorsolateral, but not dorsomedial, striatum impair acquisition of a simple discrimination task. *Behav. Brain Res.* 150, 15–23.
- Fentress, J.C., Stanfield, B.B., Cowan, W.M., (1981). Observations on the development of the striatum in mice and rats. *Anat. Embryol. (Berl)*. 163, 275–298.
- Finsen, B.R., Sørensen, T., Castellano, B., Pedersen, E.B., Zimmer, J., (1991). Leukocyte infiltration and glial reactions in xenografts of mouse brain tissue undergoing rejection in the adult rat brain. A light and electron microscopical immunocytochemical study. *J. Neuroimmunol.* 32, 159–183.
- Foroud, T., Gray, J., Ivashina, J., Conneally, M., (1999). Differences in duration of Huntington’s disease based on age at onset. *J Neurol Neurosurg Psychiatry* 66, 52–56.

Foster, A., (1983). On the excitotoxic properties of quinolinic acid, 2,3-piperidine dicarboxylic acids and structurally related compounds. *Neuropharmacology* 22, 1331–1342.

Franceschi, C., Capri, M., Monti, D., Giunta, S., Olivieri, F., Sevini, F., Panourgia, M.P., Invidia, L., Celani, L., Scurti, M., Cevenini, E., Castellani, G.C., Salvioli, S., (2007). Inflammaging and anti-inflammaging: A systemic perspective on aging and longevity emerged from studies in humans. *Mech. Ageing Dev.* 128, 92–105.

Freeman, T.B., Cicchetti, F., Hauser, R.A., Deacon, T.W., Li, X.-J., Hersch, S.M., Nauert, G.M., Sanberg, P.R., Kordower, J.H., Saporta, S., Isacson, O., (2000). Transplanted fetal striatum in Huntington's disease: Phenotypic development and lack of pathology. *Proc. Natl. Acad. Sci.* 97, 13877–13882.

Frei, K., Lins, H., Schwerdel, C., Fontana, A., (1994). Antigen Presentation in the Central Nervous System - The Inhibitory Effect of 11-10 on MHC Class II Expression and Production of Cytokines Depends on the Inducing Signals and the Type of Cell Analyzed. *J. Immunol.* 152(6), 2720-2728.

Frick, K.M., Stillner, E.T., Berger-Sweeney, J., Williams, L., (2000). Mice are not little rats: species differences in a one-day water maze task 11, 959–4965.

Fricker-Gates, R., White, A., Gates, M., Dunnett, S.B., (2004). Striatal neurons in striatal grafts are derived from both post-mitotic cells and dividing progenitors. *Eur. J. Neurosci.* 19, 513–520.

Fricker, R.A., Carpenter, M.K., Winkler, C., Greco, C., Gates, M.A., Björklund, A., (1999). Site-specific migration and neuronal differentiation of human neural progenitor cells after transplantation in the adult rat brain. *J. Neurosci.*

Fricker, R. A., Torres, E. M., Dunnett, S. B., (1997). The effects of donor stage on the survival and function of embryonic striatal grafts in the adult rat brain. I. Morphological characteristics. *Neuroscience* 79, 695–710.

Fricker, R., Barker, R., Fawcett, J., Dunnett, S., (1996). A comparative study of preparation techniques for improving the viability of striatal grafts using vital stains, in vitro cultures, and in vivo grafts. *Cell Transplant.* 5, 599–611.

Fricker, R.A., Annett, L.E., Torres, E.M., Dunnett, S.B., (1996). The Placement of a Striatal Ibotenic Acid Lesion Affects Skilled Forelimb Use and the Direction of Drug-Induced Rotation. *Brain Res. Bull.* 41, 409–416.

Gage, F.H., Dunnett, S.B., Brundin, P., Isacson, O., Björklund, A., (1997). Intracerebral grafting of embryonic neural cells into the adult host brain: an overview of the cell suspension method and its application. *Dev. Neurosci.* 6, 137–51.

Gambotto, A., Dworacki, G., Cicinnati, V., Kenniston, T., Steitz, J., Tü Ting, T., Robbins, P., Deleo, A., (2000). Immunogenicity of enhanced green fluorescent protein (EGFP) in BALB/c mice: identification of an H2-K d -restricted CTL epitope. *Gene Ther.* 7, 2036–2040.

Gauthier, L.R., Charrin, B.C., Borrell-Pagès, M., Dompierre, J.P., Rangone, H., Cordelières, F.P., De Mey, J., MacDonald, M.E.M.E., Leßmann, V., Humbert, S., Saudou, F., (2004). Huntingtin Controls Neurotrophic Support and Survival of Neurons by Enhancing BDNF Vesicular Transport along Microtubules. *Cell* 118, 127–138.

Gerfen, C.R., Baimbridge, K.G., Miller, J.J., (1985). The neostriatal mosaic: compartmental distribution of calcium-binding protein and parvalbumin in the basal ganglia of the rat and monkey. *Proc. Natl. Acad. Sci. U. S. A.* 82, 8780–8784.

Gharaibeh, A., Culver, R., Crane, A., Wyse, R., Antcliff, A., Shall, G., Moore, S., Srinageshwar, B., Kolli, N., Story, D., Lossia, O., Frolo, L., Eickholt, A., Dunbar, G., Rossignol, J., (2016). Intra-striatal Transplantation of Mouse Adenovirus-Generated Induced Pluripotent Stem Cells Reduced Behavioral Deficits in the YAC128 Mouse Model of Huntington’s Disease. *Cell Transplant.* 25, 757–758.

Ghosh, C., Marchi, N., Hossain, M., Rasmussen, P., Alexopoulos, A. V, Gonzalez-Martinez, J., Yang, H., Janigro, D., (2012). A pro-convulsive carbamazepine metabolite: Quinolinic acid in drug resistant epileptic human brain. *Neurobiol. Dis.* 46, 692–700.

Gil, J.M., Rego, A.C., (2008). The R6 lines of transgenic mice: A model for screening new therapies for Huntington’s disease. *Brain Res. Rev.* 59, 410–431.

Giulian, D., (1993). Reactive glia as rivals in regulating neuronal survival. *Glia* 7, 102–10.

Godbout, J.P., Chen, J., Abraham, J., Richwine, A.F., Berg, B.M., Kelley, K.W., Johnson, R.W., (2005). Exaggerated neuroinflammation and sickness behavior in aged mice after activation of the peripheral innate immune system. *FASEB J.* 19, 1329–31.

Graveland, G.A., Williams, R.S., DiFiglia, M., (1985). Evidence for degenerative and regenerative changes in neostriatal spiny neurons in Huntington’s disease. *Science* 227, 770–3.

Graybiel, A.M., Liu, F.C., Dunnett, S.B., (1989). Intrastratial grafts derived from fetal striatal primordia. I. Phenotypy and modular organization. *J. Neurosci.* 9, 3250–71.

Guillemin, G.J., Croitoru-Lamoury, J., Dormont, D., Armati, P.J., Brew, B.J., (2003). Quinolinic acid upregulates chemokine production and chemokine receptor expression in astrocytes. *Glia* 41, 371–381.

Guillemin, G.J., Kerr, S.J., Smythe, G.A., Smith, D.G., Kapoor, V., Armati, P.J., Croitoru, J., Brew, B.J., (2001). Kynurenine pathway metabolism in human astrocytes: a paradox for neuronal protection. *J. Neurochem.* 78, 842–853.

Guldin, W.O., Markowitsch, H.J., (1981). No detectable remote lesions following massive intrastratial injections of ibotenic acid. *Brain Res.* 225, 446–451.

Hansson, O., Petersen, A., Leist, M., Nicotera, P., Castilho, R.F., Brundin, P., (1999). Transgenic mice expressing a Huntington's disease mutation are resistant to quinolinic acid-induced striatal excitotoxicity. *Proc. Natl. Acad. Sci. U. S. A.* 96, 8727–8732.

Hargus, G., Cui, Y.F., Schmid, J.S., Xu, J.C., Glatzel, M., Schachner, M., Bernreuther, C., (2008). Tenascin-R promotes neuronal differentiation of embryonic stem cells and recruitment of host-derived neural precursor cells after excitotoxic lesion of the mouse striatum. *Stem Cells* 26, 1973–1984.

Hargus, G., Cui, Y.F., Schmid, J.S., Xu, J.C., Glatzel, M., Schachner, M., Bernreuther, C., (2008). Tenascin-R promotes neuronal differentiation of embryonic stem cells and recruitment of host-derived neural precursor cells after excitotoxic lesion of the mouse striatum. *Stem Cells* 26, 1973–1984.

Harrington, D.L., Smith, M.M., Zhang, Y., Carlozzi, N.E., Paulsen, J.S., (2012). Cognitive domains that predict time to diagnosis in prodromal Huntington disease. *J. Neurol. Neurosurg. Psychiatry* 83, 612–9.

Hauber, W., Schmidt, W.J., (1994). Differential effects of lesions of the dorsomedial and dorsolateral caudate-putamen on reaction time performance in rats. *Behav. Brain Res.* 60, 211–215.

Hauser, R.A., Furtado, S., Cimino, C.R., Delgado, H., Eichler, S., Schwartz, S., Scott, D., Nauert, G.M., Soety, E., Sossi, V., Holt, D.A., Sanberg, P.R., Stoessl, A.J., Freeman, T.B., (2002). Bilateral human fetal striatal transplantation in Huntington's disease. *Neurology* 58, 687–95.

HDCRG, (1993). A novel gene containing a trinucleotide repeat that is expanded and unstable on Huntington's disease chromosomes. The Huntington's Disease Collaborative Research Group. *Cell* 72, 971–83.

Heng, M.Y., Detloff, P.J., Albin, R.L., (2008). Rodent genetic models of Huntington disease. *Neurobiol. Dis.* 32, 1–9.

Herath, S., Le Heron, A., Colloca, S., Patterson, S., Tatoud, R., Weber, J., Dickson, G., (2016). Strain-dependent and distinctive T-cell responses to HIV antigens following immunisation of mice with differing chimpanzee adenovirus vaccine vectors. *Vaccine* 34, 4378–85.

Heuer, A., Vinh, N.-N., Dunnett, S.B., (2013). Behavioural recovery on simple and complex tasks by means of cell replacement therapy in unilateral 6-hydroxydopamine-lesioned mice. *Eur. J. Neurosci.* 37, 1691–1704.

Heyes, M.P., Achim, C.L., Wiley, C.A., Major, E.O., Saito, K., Markey, S.P., (1996). Human microglia convert l-tryptophan into the neurotoxin quinolinic acid. *Biochem. J.* 320 ( Pt 2), 595–7.

Heyes, M.P., Saito, K., Chen, C.Y., Proescholdt, M.G., Nowak, T.S., Li, J., Beagles, K.E., Proescholdt, M.A., Zito, M.A., Kawai, K., Markey, S.P., (2002). Species Heterogeneity Between Gerbils and Rats: Quinolate Production by Microglia and Astrocytes and Accumulations in Response to Ischemic Brain Injury and Systemic Immune Activation. *J. Neurochem.* 69, 1519–1529.

Hickey, W.F., Hsu, B.L., Kimura, H., (1991). T-lymphocyte entry into the central nervous system. *J. Neurosci. Res.* 28, 254–260.

Holmes, A., Kinney, J.W., Wrenn, C.C., Li, Q., Yang, R.J., Ma, L., Vishwanath, J., Saavedra, M.C., Innerfield, C.E., Jacoby, A.S., Shine, J., Iismaa, T.P., Crawley, J.N., (2003). Galanin GAL-R1 Receptor Null Mutant Mice Display Increased Anxiety-Like Behavior Specific to the Elevated Plus-Maze. *Neuropsychopharmacology* 28, 1031–1044.

Hu, J., Ferreira, A., Van Eldik, L.J., (2002). S100 $\beta$  Induces Neuronal Cell Death Through Nitric Oxide Release from Astrocytes. *J. Neurochem.* 69, 2294–2301.

Huang, Y., Henry, C.J., Dantzer, R., Johnson, R.W., Godbout, J.P., (2008). Exaggerated sickness behavior and brain proinflammatory cytokine expression in aged mice in response to intracerebroventricular lipopolysaccharide. *Neurobiol. Aging* 29, 1744–53.

Huntington Study Group, (2015). Safety, tolerability, and efficacy of PBT2 in Huntington's disease: a phase 2, randomised, double-blind, placebo-controlled trial. *Lancet Neurol.* 14, 39–47.

Huntington Study Group, (1996). Unified Huntington's disease rating scale: Reliability and consistency. *Mov. Disord.* 11, 136–142.

Isacson, O., Dawbarn, D., Brundin, P., Gage, F.H., Emson, P.C., Björklund, A., (1987). Neural grafting in a rat model of huntington's disease: Striosomal-like organization of striatal grafts as revealed by acetylcholinesterase histochemistry, immunocytochemistry and receptor autoradiography. *Neuroscience* 22, 481–497.

Isacson, O., Dunnett, S.B., Björklund, A., (1986). Graft-induced behavioral recovery in an animal model of Huntington disease (neuronal transplantation). *Neurobiology* 83, 2728–2732.

Ivkovic, S., Ehrlich, M.E., (1999). Expression of the striatal DARPP-32/ARPP-21 phenotype in GABAergic neurons requires neurotrophins in vivo and in vitro. *J. Neurosci.* 19, 5409–19.

Janeczko, K., (1989). Spatiotemporal patterns of the astroglial proliferation in rat brain injured at the postmitotic stage of postnatal development: a combined immunocytochemical and autoradiographic study. *Brain Res.* 485, 236–43.

Joel, D., Weiner, I., (2000). The connections of the dopaminergic system with the striatum in rats and primates: an analysis with respect to the functional and compartmental organization of the striatum. *Neuroscience* 96, 451–474.

Johann, V., Schiefer, J., Sass, C., Mey, J., Brook, G., Krüttgen, A., Schlangen, C., Bernreuther, C., Schachner, M., Dihné, M., Kosinski, C., (2007). Time of transplantation and cell preparation determine neural stem cell survival in a mouse model of Huntington's disease. *Exp. Brain Res.* 177, 458–470.

Kaba, S.A., Price, A., Zhou, Z., Sundaram, V., Schnake, P., Goldman, I.F., Lal, A.A., Udhayakumar, V., Todd, C.W., (2008). Immune responses of mice with different genetic backgrounds to improved multiepitope, multitarget malaria vaccine candidate antigen FALVAC-1A. *Clin. Vaccine Immunol.* 15, 1674–83.

Kalivas, P.W., Nemeroff, C.B., Prange, A.J., (1984). Neurotensin microinjection into the nucleus accumbens antagonizes dopamine-induced increase in locomotion and rearing. *Neuroscience* 11, 919–930.

Kalonia, H., Kumar, A., (2011). Suppressing inflammatory cascade by cyclo-oxygenase inhibitors attenuates quinolinic acid induced Huntington's disease-like alterations in rats. *Life Sci.* 88, 784–91.

Karperien, A., Ahammer, H., Jelinek, H.F., (2013). Quantitating the subtleties of microglial morphology with fractal analysis. *Front. Cell. Neurosci.* 7, 1–18.

Kelly, C.M., (2005). *Neural Stem Cells for Cell Replacement Therapy in Huntington's Disease*. PhD thesis, Cardiff University, Cardiff.

Kelly, C.M., Precious, S. V, Penketh, R., Amso, N., Dunnett, S.B., Rosser, A.E., (2007). Striatal graft projections are influenced by donor cell type and not the immunogenic background. *Brain* 130, 1317–1329.

Kelly, C.M., Precious, S. V, Scherf, C., Penketh, R., Amso, N.N., Battersby, A., Allen, N.D., Dunnett, S.B., Rosser, A.E., (2009). Neonatal desensitization allows long-term survival of neural xenotransplants without immunosuppression. *Nat. Methods* 6, 271–3.

Kim, J., Min, K.-J., Seol, W., Jou, I., Joe, E., (2010). Astrocytes in injury states rapidly produce anti-inflammatory factors and attenuate microglial inflammatory responses. *J. Neurochem.* 115, 1161–1171.

Klein, A., Lane, E.L., Dunnett, S.B., (2013). Brain Repair in a Unilateral Rat Model of Huntington's Disease: New Insights Into Impairment and Restoration of Forelimb Movement Patterns. *Cell Transplant.* 22, 1735–1751.

Kopyov, O. V, Jacques, S., Lieberman, A., Duma, C.M., Eagle, K.S., (1998). Safety of intrastriatal neurotransplantation for Huntington's disease patients. *Exp. Neurol.* 149, 97–108.

Kraft, A.D., Harry, G.J., (2011). Features of microglia and neuroinflammation relevant to environmental exposure and neurotoxicity. *Int. J. Environ. Res. Public Health* 8, 2980–3018.

Kromer, L.F., Björklund, A., Stenevi, U., (1983). Intracerebral embryonic neural implants in the adult rat brain. I. Growth and mature organization of brainstem, cerebellar, and hippocampal implants. *J. Comp. Neurol.* 218, 433–59.

Kromer, L.F., Björklund, A., Stenevi, U., (1983). Intracerebral embryonic neural implants in the adult rat brain. I. Growth and mature organization of brainstem, cerebellar, and hippocampal implants. *J. Comp. Neurol.* 218, 433–59.

Kumar, P., Kalonia, H., Kumar, A., (2010). Huntington's disease: pathogenesis to animal models. *Pharmacol. Rep.* 62, 1–14.

Kwan, W., Träger, U., Davalos, D., Chou, A., Bouchard, J., Andre, R., Miller, A., Weiss, A., Giorgini, F., Cheah, C., Möller, T., Stella, N., Akassoglou, K., Tabrizi, S.J., Muchowski, P.J., (2012). Mutant huntingtin impairs immune cell migration in Huntington disease. *J. Clin. Invest.* 122, 4737–47.

Lanciego, J.L., Luquin, N., Obeso, J.A., (2012). Functional Neuroanatomy of the Basal Ganglia. *Cold Spring Harb. Perspect. Med.* 2, 10.1101.

Langbehn, D., Brinkman, R., Falush, D., Paulsen, J., Hayden, M., (2004). A new model for prediction of the age of onset and penetrance for Huntington's disease based on CAG length. *Clin. Genet.* 65, 267–277.

Lawrence, J.M., Morris, R.J., Wilson, D.J., Raisman, G., (1990). Mechanisms of allograft rejection in the rat brain. *Neuroscience* 37, 431–462.

Lee, J.-M.H., Ramos, E.M., Lee, J.-M.H., Gillis, T., Mysore, J.S., Hayden, M.R., Warby, S.C., Morrison, P., Nance, M., Ross, C.A., Margolis, R.L., Squitieri, F., Orobello, S., Di Donato, S., Gomez-Tortosa, E., Ayuso, C., Suchowersky, O., Trent, R.J.A., McCusker, E., Novelletto, A., Frontali, M., Jones, R., Ashizawa, T., Frank, S., Saint-Hilaire, M.H., Hersch, S.M., Rosas, H.D., Lucente, D., Harrison, M.B., Zanko, A., Abramson, R.K., Marder, K., Sequeiros, J., Paulsen, J.S., Landwehrmeyer, G.B., Myers, R.H., MacDonald, M.E., Gusella, J.F., (2012). CAG repeat expansion in Huntington disease determines age at onset in a fully dominant fashion. *Neurology* 78, 690–695.

Lelos, M.J., Harrison, D.J., Rosser, A.E., Dunnett, S.B., (2013). The lateral neostriatum is necessary for compensatory ingestive behaviour after intravascular dehydration in female rats. *Appetite* 71, 287–94.

Lelos, M.J., Robertson, V.H., Vinh, N.-N., Harrison, C., Eriksen, P., Torres, E.M., Clinch, S.P., Rosser, A.E., Dunnett, S.B., (2016). Direct Comparison of Rat- and Human-Derived Ganglionic Eminence Tissue Grafts on Motor Function. *Cell Transplant.* 25, 665–675.

Liddel, S.A., Guttenplan, K.A., Clarke, L.E., Bennett, F.C., Bohlen, C.J., Schirmer, L., Bennett, M.L., Münch, A.E., Chung, W.-S., Peterson, T.C., Wilton, D.K., Frouin, A., Napier, B.A., Panicker, N., Kumar, M., Buckwalter, M.S., Rowitch, D.H., Dawson, V.L., Dawson, T.M., Stevens, B., Barres, B.A., (2017). Neurotoxic reactive astrocytes are induced by activated microglia. *Nature* 541, 481–487.

Lin, Y.-T., Chern, Y., Shen, C.-K.J., Wen, H.-L., Chang, Y.-C., Li, H., Cheng, T.-H., Hsieh-Li, H.M., (2011). Human mesenchymal stem cells prolong survival and ameliorate motor deficit through trophic support in Huntington's disease mouse models. *PLoS One* 6, e22924.

Lopez-Paniagua, D., Seger, C.A., (2011). Interactions within and between corticostriatal loops during component processes of category learning. *J. Cogn. Neurosci.* 23, 3068–83.

Loveless, S.E., Hoban, D., Sykes, G., Frame, S.R., Everds, N.E., (2008). Evaluation of the Immune System in Rats and Mice Administered Linear Ammonium Perfluorooctanoate. *Toxicol. Sci.* 105, 86–96.

Luchetti, S., Beck, K.D., Galvan, M.D., Silva, R., Cummings, B.J., Anderson, A.J., (2010). Comparison of immunopathology and locomotor recovery in C57BL/6, BUB/BnJ, and NOD-SCID mice after contusion spinal cord injury. *J. Neurotrauma* 27, 411–21.

Ma, L., Hu, B., Liu, Y., Vermilyea, S.C., Liu, H., Gao, L., Sun, Y., Zhang, X., Zhang, S.-C., (2012). Human Embryonic Stem Cell-Derived GABA Neurons Correct Locomotion Deficits in Quinolinic Acid-Lesioned Mice. *Cell Stem Cell* 10, 455–464.

Ma, L., Morton, A.J., Nicholson, L.F.B., (2003). Microglia density decreases with age in a mouse model of Huntington's disease. *Glia* 43, 274–80.

Magavi, S.S.P., Lois, C., (2008). Transplanted neurons form both normal and ectopic projections in the adult brain. *Dev. Neurobiol.* 68, 1527–1537.

Manfré, G., Doyère, V., Bossi, S., Riess, O., Nguyen, H.P., Massioui, N. El, (2015). Impulsivity trait in the early symptomatic BACHD transgenic rat model of Huntington Disease. *Behav. Brain Res.* 299, 6–10.

Marcora, E., Kennedy, M.B., (2010). The Huntington's disease mutation impairs Huntingtin's role in the transport of NF- $\kappa$ B from the synapse to the nucleus. *Hum. Mol. Genet.* 19, 4373–84.

Martin, D.D.O., Ladha, S., Ehrnhoefer, D.E., Hayden, M.R., (2014). Autophagy in Huntington disease and huntingtin in autophagy. *Trends Neurosci.* 38, 26–35.

Martínez-Serrano, A., Björklund, A., (1996). Protection of the Neostriatum against Excitotoxic Damage by Neurotrophin-Producing, Genetically Modified Neural Stem Cells. *J. Neurosci.* 16, 4604–4616.

Mattingly, B., Gotsick, J., (1989). Conditioning and experiential factors affecting the development of sensitization to apomorphine. *Behav. Neurosci.* 103, 1311–1317.

Mattingly, B.A., Rowletti, J.K., (1989). Effects of Repeated Apomorphine and Haloperidol Treatments on Subsequent Behavioral Sensitivity to Apomorphine. *Pharmacol. Biochem. Behav.* 34, 345–347.

Mayer, E., Brown, V.J., Dunnett, S.B., Robbins, T.W., (1992). Striatal graft-associated recovery of a lesion-induced performance deficit in the rat requires learning to use the transplant. *Eur. J. Neurosci.* 4, 119–26.

Mazzocchi-Jones, D., Döbrössy, M., Dunnett, S.B., (2011). Environmental Enrichment Facilitates Long-Term Potentiation in Embryonic Striatal Grafts. *Neurorehabil. Neural Repair* 25, 548–557.

Mazzocchi-Jones, D., Döbrössy, M., Dunnett, S.B., (2009). Embryonic striatal grafts restore bi-directional synaptic plasticity in a rodent model of Huntington's disease. *Eur. J. Neurosci.* 30, 2134–2142.

McLin, J.P., Thompson, L.M., Steward, O., (2006). Differential susceptibility to striatal neurodegeneration induced by quinolinic acid and kainate in inbred, outbred and hybrid mouse strains. *Eur. J. Neurosci.* 24, 3134–40.

McQuade, J.M.S., Vorhees, C. V., Xu, M., Zhang, J., (2002). DNA fragmentation factor 45 knockout mice exhibit longer memory retention in the novel object recognition task compared to wild-type mice. *Physiol. Behav.* 76, 315–320.

Menalled, L.B., Chesselet, M.-F., (2002). Mouse models of Huntington's disease. *Trends Pharmacol. Sci.* 23, 32–39.

Michou, A.I., Santoro, L., Christ, M., Julliard, V., Pavirani, A., Mehtali, M., (1997). Adenovirus-mediated gene transfer: influence of transgene, mouse strain and type of immune response on persistence of transgene expression. *Gene Ther.* 4, 473.

Mills, C.D., Kincaid, K., Alt, J.M., Heilman, M.J., Hill, A.M., (2000). M-1/M-2 Macrophages and the Th1/Th2 Paradigm. *J. Immunol.* 164, 6166–6173.

Miwa, T., Furukawa, S., Nakajima, K., Furukawa, Y., Kohsaka, S., (1997). Lipopolysaccharide enhances synthesis of brain-derived neurotrophic factor in cultured rat microglia. *J. Neurosci. Res.* 50, 1023–9.

Mo, C., Renoir, T., Pang, T.Y.C., Hannan, A.J., (2013). Short-term memory acquisition in female Huntington's disease mice is vulnerable to acute stress. *Behav. Brain Res.* 253, 318–322.

Moffett, J.R., Espey, M.G., Gaudet, S.J., Namboodiri, M.A., (1993). Antibodies to quinolinic acid reveal localization in select immune cells rather than neurons or astroglia. *Brain Res.* 623, 337–40.

Moffett, J.R., Espey, M.G., Namboodiri, M.A., (1994). Antibodies to quinolinic acid and the determination of its cellular distribution within the rat immune system. *Cell Tissue Res.* 278, 461–9.

Moresco, R., Lavazza, T., Belloli, S., Lecchi, M., Pezzola, A., Todde, S., Matarrese, M., Carpinelli, A., Turolla, E., Zimarino, V., Popoli, P., Malgaroli, A., Fazio, F., (2008). Quinolinic acid induced neurodegeneration in the striatum: a combined in vivo and in vitro analysis of receptor changes and microglia activation. *Eur. J. Nucl. Med. Mol. Imaging* 35, 704–715.

Mosher, K.I., Wyss-Coray, T., (2014). Microglial dysfunction in brain aging and Alzheimer's disease. *Biochem. Pharmacol.* 88, 594–604.

Muir, J.L., Everitt, B.J., Robbins, T.W., (1996). The Cerebral Cortex of the Rat and Visual Attentional Function: Dissociable Effects of Medial Frontal, Cingulate, Anterior Dorsolateral, and Parietal Cortex Lesions on a Five-Choice Serial Reaction Time Task. *Cereb. Cortex* 6, 470–481.

Myers, R.H., MacDonald, M.E., Koroshetz, W.J., Duyao, M.P., Ambrose, C.M., Taylor, S.A.M., Barnes, G., Srinidhi, J., Lin, C.S., Whaley, W.L., Lazzarini, A.M., Schwarz, M., Wolff, G., Bird, E.D., Vonsattel, J.-P.G., Gusella, J.F., (1993). De novo expansion of a (CAG)<sub>n</sub> repeat in sporadic Huntington's disease. *Nat. Genet.* 5, 168–173.

Nakao, N., Frodl, E.M., Duan, W., Widner, H., Brundin, P., (1994). Lazaroids improve the survival of grafted rat embryonic dopamine neurons. *Neurobiology* 91, 12408–12412.

Nakao, N., Grasbon-Frodl, E.M., Widner, H., Brundin, P., (1996). DARPP-32-rich zones in grafts of lateral ganglionic eminence govern the extent of functional recovery in skilled paw reaching in an animal model of Huntington's disease. *Neuroscience* 74, 959–970.

Narang, N., Hunt, M.E., Pundt, L.L., Alburges, M.E., Wamsley, J.K., (1993). Unilateral ibotenic acid lesion of the caudate putamen results in D2 receptor alterations on the contralateral side. *Exp Neurol* 121, 40–47.

Newland, B., Welzel, P.B., Newland, H., Renneberg, C., Kolar, P., Tsurkan, M., Rosser, A., Freudenberg, U., Werner, C., (2015). Tackling Cell Transplantation Anoikis: An Injectable, Shape Memory Cryogel Microcarrier Platform Material for Stem Cell and Neuronal Cell Growth. *Small* 11, 5047–5053.

NIH, (2017). Safety, Tolerability, Pharmacokinetics, and Pharmacodynamics of IONIS-HTTRx in Patients With Early Manifest Huntington's Disease. [www.clinicaltrials.gov/ct2/show/NCT02519036](http://www.clinicaltrials.gov/ct2/show/NCT02519036) [WWW Document].

Njie, E.G., Boelen, E., Stassen, F.R., Steinbusch, H.W.M., Borchelt, D.R., Streit, W.J., (2012). Ex vivo cultures of microglia from young and aged rodent brain reveal age-related changes in microglial function. *Neurobiol. Aging* 33, 195.e1-12.

Norden, D.M., Godbout, J.P., (2013). Review: microglia of the aged brain: primed to be activated and resistant to regulation. *Neuropathol. Appl. Neurobiol.* 39, 19–34.

Novak, M.J.U., Tabrizi, S.J., (2010). Huntington's disease. *BMJ* 340, c3109–c3109.

Olah, M., Biber, K., Vinet, J., Boddeke, H.W.G.M., (2011). Microglia phenotype diversity. *CNS Neurol. Disord. Drug Targets* 10, 108–18.

Olson, L., Seiger, Å., Strömberg, I., (1983). Intraocular Transplantation in Rodents: A Detailed Account of the Procedure and Examples of its Use in Neurobiology with Special Reference to Brain Tissue Grafting. *Adv. Cell. Neurobiol.* 4, 407–442.

Olsson, M., Björklund, A., Campbell, K., (1998). Early specification of striatal projection neurons and interneuronal subtypes in the lateral and medial ganglionic eminence. *Neuroscience* 84, 867–876.

Pauli, W.M., Clark, A.D., Guenther, H.J., O'Reilly, R.C., Rudy, J.W., (2012). Inhibiting PKM $\zeta$  reveals dorsal lateral and dorsal medial striatum store the different memories needed to support adaptive behavior. *Learn. Mem.* 19, 307–14.

Paulsen, J.S., Hoth, K.F., Nehl, C., Stierman, L., (2005). Critical Periods of Suicide Risk in Huntington's Disease. *Am. J. Psychiatry* 162, 725–731.

Paulsen, J.S., Langbehn, D.R., Stout, J.C., Aylward, E., Ross, C.A., Nance, M., Guttman, M., Johnson, S., MacDonald, M., Beglinger, L.J., Duff, K., Kayson, E., Biglan, K., Shoulson, I., Oakes, D., Hayden, M., (2008). Detection of Huntington's disease decades before diagnosis: the Predict-HD study. *J. Neurol. Neurosurg. Psychiatry* 79, 874–80.

Paulsen, J.S., Ready, R.E., Hamilton, J.M., Mega, M.S., Cummings, J.L., (2001). Neuropsychiatric aspects of Huntington's disease. *J. Neurol. Neurosurg. Psychiatry* 71, 310–314.

- Paxinos, G., Franklin, K.B.J., (2004). *The mouse brain in stereotaxic coordinates*, Academic Press.
- Peister, A., Mellad, J.A., Larson, B.L., Hall, B.M., Gibson, L.F., Prockop, D.J., (2004). Adult stem cells from bone marrow (MSCs) isolated from different strains of inbred mice vary in surface epitopes, rates of proliferation, and differentiation potential. *Blood* 103, 1662–1668.
- Perry, V.H., Matyszak, M.K., Fearn, S., (1993). Altered antigen expression of microglia in the aged rodent CNS. *Glia* 7, 60–67.
- Perry, V.H., Teeling, J., (2013). Microglia and macrophages of the central nervous system: the contribution of microglia priming and systemic inflammation to chronic neurodegeneration. *Semin. Immunopathol.* 35, 601–12.
- Phillips, A.G., Carr, G.D., (1987). Cognition and the basal ganglia: a possible substrate for procedural knowledge. *Can. J. Neurol. Sci.* 14, 381–5.
- Portera-Cailliau, C., Hedreen, J., Price, D., Koliatsos, V., (1995). Evidence for apoptotic cell death in Huntington disease and excitotoxic animal models. *J. Neurosci.* 15, 3775–3787.
- Precious, S. V, (2010). Directed Differentiation of mouse embryonic stem cells for transplantation in Huntington's Disease. PhD thesis, Cardiff University, Cardiff.
- Ragozzino, M.E., Jih, J., Tzavos, A., (2002). Involvement of the dorsomedial striatum in behavioral flexibility: role of muscarinic cholinergic receptors. *Brain Res.* 953, 205–214.
- Raivich, G., Bohatschek, M., Kloss, C.U.A., Werner, A., Jones, L.L., Kreutzberg, G.W., (1999). Neuroglial activation repertoire in the injured brain: graded response, molecular mechanisms and cues to physiological function. *Brain Res. Rev.* 30, 77–105.
- Rath, A., Klein, A., Papazoglou, A., Pruszek, J., Garciaa, J., Krause, M., Maciaczyk, J., Dunnett, S.B., Nikkha, G., (2012). Survival and Functional Restoration of Human Fetal Ventral Mesencephalon Following Transplantation in a Rat Model of Parkinson's Disease. *Cell Transplant.* 22, 1281–1293.
- Reading, P.J., Dunnett, S.B., (1995). Embryonic striatal grafts reverse the disinhibitory effects of ibotenic acid lesions of the ventral striatum. *Exp. Brain Res.* 105, 76–86.

Redmond, D.E., Vinuela, A., Kordower, J.H., Isacson, O., (2008). Influence of cell preparation and target location on the behavioral recovery after striatal transplantation of fetal dopaminergic neurons in a primate model of Parkinson's disease. *Neurobiol. Dis.* 29, 103–116.

Reichenbach, D.K., Li, Q., Hoffman, R.A., Williams, A.L., Shlomchik, W.D., Rothstein, D.M., Demetris, A.J., Lakkis, F.G., (2013). Allograft outcomes in outbred mice. *Am. J. Transplant* 13, 580–8.

Reilmann, R., Squitieri, F., Priller, J., Saft, C., Mariotti, C., Suessmuth, S., Nemeth, A., Tabrizi, S., Quarrell, O., Craufurd, D., Rickards, H., Rosser, A., Borje, D., Michaela, T., Angieszka, S., Fischer, D., Macdonald, D., Munoz-Sanjuan, I., Pacifici, R., Frost, C., Farmer, R., Landwehrmeyer, B., Westerberg, G., (2014). Safety and Tolerability of Selisistat for the Treatment of Huntington's Disease: Results from a Randomized, Double-Blind, Placebo-Controlled Phase II Trial (S47.004). *Neurology* 82, S47.004.

Reutzel-Selke, A., Jurisch, A., Denecke, C., Pascher, A., Martins, P.N.A., Keßler, H., Tamura, A., Utku, N., Pratschke, J., Neuhaus, P., Tullius, S.-G., (2007). Donor age intensifies the early immune response after transplantation. *Kidney Int.* 71, 629–636.

Roberton, V.H., (2014). Validation and characterisation of a new method for in vivo assessment of human donor cells. Phd thesis, Cardiff University, Cardiff.

Roberton, V.H., Evans, A.E., Harrison, D.J., Precious, S. V, Dunnett, S.B., Kelly, C.M., Rosser, A.E., (2013). Is the adult mouse striatum a hostile host for neural transplant survival? *Neuroreport* 24, 1010–5.

Roberts, R.C., Ahn, A., Swartz, K.J., Beal, M.F., DiFiglia, M., (1993). Intrastratial Injections of Quinolinic Acid or Kainic Acid: Differential Patterns of Cell Survival and the Effects of Data Analysis on Outcome. *Exp. Neurol.* 124, 274–282.

Rosas, H.D., Liu, A.K., Hersch, S., Glessner, M., Ferrante, R.J., Salat, D.H., van der Kouwe, A., Jenkins, B.G., Dale, A.M., Fischl, B., (2002). Regional and progressive thinning of the cortical ribbon in Huntington's disease. *Neurology* 58, 695–701.

Rosser, A.E., (2002). Unilateral transplantation of human primary fetal tissue in four patients with Huntington's disease: NEST-UK safety report ISRCTN no 36485475. *J. Neurol. Neurosurg. Psychiatry* 73, 678–685.

Rosser, A.E., Kelly, C.M., Dunnett, S.B., (2011). Cell Transplantation for Huntington's Disease: Practical and Clinical Considerations. *Future Neurol.* 6, 45–62.

Saddoris, M.P., Cacciapaglia, F., Wightman, R.M., Carelli, R.M., (2015). Differential Dopamine Release Dynamics in the Nucleus Accumbens Core and Shell Reveal Complementary Signals for Error Prediction and Incentive Motivation. *J. Neurosci.* 35, 11572–82.

Sanberg, P.R., Henault, M.A., Wallace Deckel, A., (1986). Locomotor hyperactivity: Effects of multiple striatal transplants in an animal model of Huntington's disease. *Pharmacol. Biochem. Behav.* 25, 297–300.

Sánchez-Pernaute, R., Ferree, A., Cooper, O., Yu, M., Brownell, A.-L., Isacson, O., (2004). Selective COX-2 inhibition prevents progressive dopamine neuron degeneration in a rat model of Parkinson's disease. *J. Neuroinflammation* 1, 6.

Sapp, E., Kegel, K.B., Aronin, N., Hashikawa, T., Uchiyama, Y., Tohyama, K., Bhide, P.G., Vonsattel, J.P., Difiglia, M., (2001). Early and Progressive Accumulation of Reactive Microglia in the Huntington Disease Brain. *J. Neuropathol. Exp. Neurol.* 60, 161–172.

Schackel, S., Pauly, M.-C., Piroth, T., Nikkhah, G., Döbrössy, M.D., (2013). Donor age dependent graft development and recovery in a rat model of Huntington's disease: histological and behavioral analysis. *Behav. Brain Res.* 256, 56–63.

Schmidt, R.H., Björklund, A., Stenevi, U., (1981). Intracerebral grafting of dissociated CNS tissue suspensions: a new approach for neuronal transplantation to deep brain sites. *Brain Res.* 218, 347–356.

Schwarcz, R., Hökfelt, T., Fuxe, K., Jonsson, G., Goldstein, M., Terenius, L., (1979). Ibotenic acid-induced neuronal degeneration: a morphological and neurochemical study. *Exp. Brain Res.* 37, 199–216.

Seiger, A., Olson, L., (1977). Quantitation of fiber growth in transplanted central monoamine neurons. *Cell Tissue Res.* 179, 285–316.

Self, D.W., Nestler, E.J., (1995). Molecular Mechanisms of Drug Reinforcement and Addiction. *Annu. Rev. Neurosci.* 18, 463–495.

Shear, D.A., Dong, J., Gundy, C.D., Haik-creguer, Kr.L., Dunbar, G.L., Shear, A., Haik-Creguer, K.L., (1998). Comparison Of Intrastratial, Injections Of Quinolinic Acid And 3-Nitropropionic Acid For Use In Animal Models Of Huntington's Disease. *Prog. Nemo-Psychopharmacol. & Biol. Psychiat* 22, 1217–1240.

Shelbourne, P.F., Killeen, N., Hevner, R.F., Johnston, H.M., Tecott, L., Lewandoski, M., Ennis, M., Ramirez, L., Li, Z., Iannicola, C., Littman, D.R., Myers, R.M., (1999). A Huntington's Disease CAG Expansion at the Murine Hdh Locus Is Unstable and Associated with Behavioural Abnormalities in Mice. *Hum. Mol. Genet.* 8, 763–774.

Shemesh, N., Sadan, O., Melamed, E., Offen, D., Cohen, Y., (2009). Longitudinal MRI and MRSI characterization of the quinolinic acid rat model for excitotoxicity: peculiar apparent diffusion coefficients and recovery of N-acetyl aspartate levels. *NMR Biomed.* 23, 196–206.

Shiigi, S., Mishell, B., (1996). *Selected Methods in Cellular Immunology*, W H Freeman & Co. Oxford, UK. Elsevier.

Shin, E., Palmer, M.J., Li, M., Fricker, R.A., Shin, Eunju; Palmer, Mary J; Li, Meng; Fricker, R.A., (2012). GABAergic Neurons from Mouse Embryonic Stem Cells Possess Functional Properties of Striatal Neurons In Vitro, and Develop into Striatal Neurons In Vivo in a Mouse Model of Huntington's Disease. *Stem Cell Rev.* 8, 513–31.

Shiwach, R.S., Patel, V., (1993). Aggressive behaviour in Huntington's disease: a cross-sectional study in a nursing home population. *Behav. Neurol.* 6, 43–7.

Sinclair, S., Fawcell, J., Dunnett, SB., (1999). Delayed implantation of nigral grafts improves survival of dopamine neurones and rate of functional recovery. *NeuroReport.* 10(6), 1263-1267.

Skelton, D., Satake, N., Kohn, D., (2001). The enhanced green fluorescent protein (eGFP) is minimally immunogenic in C57BL/6 mice. *Gene Ther.* 8, 1813–1814.

Slow, E.J., van Raamsdonk, J., Rogers, D., Coleman, S.H., Graham, R.K., Deng, Y., Oh, R., Bissada, N., Hossain, S.M., Yang, Y.-Z., Li, X.-J., Simpson, E.M., Gutekunst, C.-A., Leavitt, B.R., Hayden, M.R., (2003). Selective striatal neuronal loss in a YAC128 mouse model of Huntington disease. *Hum. Mol. Genet.* 12, 1555–67.

Smart, I.H.M., Sturrock, R.R., (1979). *The Neostriatum*. Elsevier.

Smialowicz, R., (1994). Effects of 2,3,7,8-Tetrachlorodibenzo-p-dioxin (TCDD) on Humoral Immunity and Lymphocyte Subpopulations: Differences Between Mice and Rats. *Toxicol. Appl. Pharmacol.* 124, 248–256.

Smythe, G.A., Braga, O., Brew, B.J., Grant, R.S., Guillemin, G.J., Kerr, S.J., Walker, D.W., (2002). Concurrent Quantification of Quinolinic, Picolinic, and Nicotinic Acids Using Electron-Capture Negative-Ion Gas Chromatography–Mass Spectrometry. *Anal. Biochem.* 301, 21–26.

Sriram, K., Miller, D.B., O'Callaghan, J.P., (2006). Minocycline attenuates microglial activation but fails to mitigate striatal dopaminergic neurotoxicity: role of tumor necrosis factor- $\alpha$ . *J. Neurochem.* 96, 706–718.

Stefanova, N., Hainzer, M., Stemberger, S., Couillard-Després, S., Aigner, L., Poewe, W., Wenning, G.K., (2009). Striatal transplantation for multiple system atrophy--are grafts affected by alpha-synucleinopathy? *Exp. Neurol.* 219, 368–71.

Steffan, J.S., (2010). Does Huntingtin play a role in selective macroautophagy? *Cell Cycle* 9, 3401–13.

Steiner, H., Gerfen, C.R., (1998). Role of dynorphin and enkephalin in the regulation of striatal output pathways and behavior. *Exp. Brain Res.* 123, 60–76.

Stenevi, U., Björklund, A., Svendgaard, N.A., (1976). Transplantation of central and peripheral monoamine neurons to the adult rat brain: techniques and conditions for survival. *Brain Res.* 114, 1–20.

Streit, W.J., Mrak, R.E., Griffin, W.S.T., (2004). Microglia and neuroinflammation: a pathological perspective. *J. Neuroinflammation* 1, 14.

Stripecke, R., Del, M., Villacres, C., Skelton, D., Satake, N., Halene, S., Kohn, D., (1999). Immune response to green fluorescent protein: implications for gene therapy. *Gene Ther.* 6, 1305–1312.

Suri, R.E., Albani, C., Glattfelder, A.H., (1997). A dynamic model of motor basal ganglia functions. *Biol. Cybern.* 76, 451–8.

Tai, Y.F., Pavese, N., Gerhard, A., Tabrizi, S.J., Barker, R.A., Brooks, D.J., Piccini, P., (2007a). Microglial activation in presymptomatic Huntington's disease gene carriers. *Brain* 130, 1759–66.

Tai, Y.F., Pavese, N., Gerhard, A., Tabrizi, S.J., Barker, R.A., Brooks, D.J., Piccini, P., (2007b). Imaging microglial activation in Huntington's disease. *Brain Res. Bull.* 72, 148–51.

Tang, T.-S., Slow, E., Lupu, V., Stavrovskaya, I.G., Sugimori, M., Llinas, R., Kristal, B.S., Hayden, M.R., Bezprozvanny, I., (2005). Disturbed Ca<sup>2+</sup> signaling and apoptosis of medium spiny neurons in Huntington's disease. *Proc. Natl. Acad. Sci.* 102, 2602–2607.

Tasaki, M., Saito, K., Nakagawa, Y., Ikeda, M., Imai, N., Narita, I., Takahashi, K., (2014). Effect of donor–recipient age difference on long-term graft survival in living kidney transplantation. *Int. Urol. Nephrol.* 46, 1441–1446.

The Jackson Laboratory, (2017). [Jax.org/strain/000664](http://jax.org/strain/000664) [WWW Document].

The U.S.-Venezuela Collaborative, T.U.S. –Venezuel. C.R., Wexler, N.S., Lorimer, J., Porter, J., Gomez, F., Moskowitz, C., Shackell, E., Marder, K., Penchaszadeh, G., Roberts, S.A., Gayan, J., Brocklebank, D., Cherny, S.S., Cardon, L.R., Gray, J., Dlouhy, S.R., Wiktorski, S., Hodes, M.E., Conneally, P.M., Penney, J.B., Gusella, J., Cha, J.-H., Irizarry, M., Rosas, D., Hersch, S., Hollingsworth, Z., MacDonald, M., Young, A.B., Andresen, J.M., Housman, D.E., de Young, M.M., Bonilla, E., Stillings, T., Negrette, A., Snodgrass, S.R., Martinez-Jaurieta, M.D., Ramos-Arroyo, M.A., Bickham, J., Ramos, J.S., Marshall, F., Shoulson, I., Rey, G.J., Feigin, A., Arnheim, N., Acevedo-Cruz, A., Acosta, L., Alvir, J., Fischbeck, K., Thompson, L.M., Young, A.B., Dure, L., O'Brien, C.J., Paulsen, J., Brickman, A., Krch, D., Peery, S., Hogarth, P., Higgins, D.S., Landwehrmeyer, B., (2004). Venezuelan kindreds reveal that genetic and environmental factors modulate Huntington's disease age of onset. *Proc. Natl. Acad. Sci.* 101, 3498–3503.

Thomas, F.T., Contreras, J.L., Bilbao, G., Ricordi, C., Curiel, D., Thomas, J.M., (1999). Anoikis, extracellular matrix, and apoptosis factors in isolated cell transplantation. *Surgery* 126, 299–304.

Torres, E.M., Trigano, M., Dunnett, T.B., (2015). Translation of Cell Therapies to the Clinic: Characteristics of Cell Suspensions in Large-Diameter Injection Cannulae. *Cell Transplant.* 24, 737–749.

Torres, E.M., Monville, C., Gates, M., Bagga, V., Dunnett, S.B., (2007). Improved survival of young donor age dopamine grafts in a rat model of Parkinson's disease. *Neuroscience*, 146(4), 1606-1617.

Trueman, R.C., Brooks, S.P., Dunnett, S.B., (2005). Implicit learning in a serial choice visual discrimination task in the operant 9-hole box by intact and striatal lesioned mice. *Behav. Brain Res.* 159, 313–322.

Turmaine, M., Raza, A., Mahal, A., Mangiarini, L., Bates, G.P., Davies, S.W., (2000). Nonapoptotic neurodegeneration in a transgenic mouse model of Huntington's disease. *Proc. Natl. Acad. Sci. U. S. A.* 97, 8093–7.

Twelvetrees, A.E., Yuen, E.Y., Arancibia-Carcamo, I.L., MacAskill, A.F., Rostaing, P., Lumb, M.J., Humbert, S., Triller, A., Saudou, F., Yan, Z., Kittler, J.T., (2010). Delivery of GABAARs to Synapses Is Mediated by HAP1-KIF5 and Disrupted by Mutant Huntingtin. *Neuron* 65, 53–65.

van der Kooy, D., Fishell, G., (1987). Neuronal birthdate underlies the development of striatal compartments. *Brain Res.* 401, 155–161.

Vijitruth, R., Liu, M., Choi, D.-Y., Nguyen, X. V, Hunter, R.L., Bing, G., (2006). Cyclooxygenase-2 mediates microglial activation and secondary dopaminergic cell death in the mouse MPTP model of Parkinson's disease. *J. Neuroinflammation* 3, 6.

Voorn, P., Vanderschuren, L.J.M., Groenewegen, H.J., Robbins, T.W., Pennartz, C.M., (2004). Putting a spin on the dorsal–ventral divide of the striatum. *Trends Neurosci.* 27, 468–474.

Wakim, L.M., Woodward-Davis, A., Bevan, M.J., (2010). Memory T cells persisting within the brain after local infection show functional adaptations to their tissue of residence. *Proc. Natl. Acad. Sci. U. S. A.* 107, 17872–9.

Walker, F.O., (2007). Huntington's disease. *Lancet* 369, 218–228.

Wang, T.-Y., Bruggeman, K.F., Kauhausen, J.A., Rodriguez, A.L., Nisbet, D.R., Parish, C.L., (2016). Functionalized composite scaffolds improve the engraftment of transplanted dopaminergic progenitors in a mouse model of Parkinson's disease. *Biomaterials* 74, 89–98.

Wang, Z., Kai, L., Day, M., Ronesi, J., Yin, H.H., Ding, J., Tkatch, T., Lovinger, D.M., Surmeier, D.J., (2006). Dopaminergic control of corticostriatal long-term synaptic depression in medium spiny neurons is mediated by cholinergic interneurons. *Neuron* 50, 443–52.

Watts, Brasted, P.J., Dunnett, S.B., (2000a). Embryonic donor age and dissection influences striatal graft development and functional integration in a rodent model of Huntington's disease. *Exp. Neurol.* 163, 85–97.

Watts, Brasted, P.J., Dunnett, S.B., (2000b). The Morphology, Intergration, and Functional Efficacy of Striatal Grafts Differ Between Cell Suspensions and Tissue Pieces. *Cell Transplant.* 9, 395–407.

Watts, C., Dunnett, S.B., Rosser, A.E., (1997). Effect of embryonic donor age and dissection on the DARPP-32 content of cell suspensions used for intrastriatal transplantation. *Exp. Neurol.* 148, 271–80.

Wei, J., Wu, F., Sun, X., Zeng, X., Liang, J., Zheng, H., Yu, X., Zhang, K., Wu, Z., (2013). Differences in microglia activation between rats-derived cell and mice-derived cell after stimulating by soluble antigen of IV larva from *Angiostrongylus cantonensis* in vitro. *Parasitol. Res.* 112, 207–214.

White, A., Dunnett, S.B., (2006). Fronto-striatal disconnection disrupts operant delayed alternation performance in the rat. *Neuroreport* 17, 435–41.

White, N.M., McDonald, R.J., (2002). Multiple Parallel Memory Systems in the Brain of the Rat. *Neurobiol. Learn. Mem.* 77, 125–184.

Wictorin, K., Ouimet, C.C., Bjorklund, A., (1989). Intrinsic Organization and Connectivity of Intrastratial Striatal Transplants in Rats as Revealed by DARPP-32 Immunohistochemistry: Specificity of Connections with the Lesioned Host Brain. *Eur. J. Neurosci.* 1, 690–701.

Yin, H.H., Knowlton, B.J., (2006). The role of the basal ganglia in habit formation. *Nat Rev Neurosci* 7, 464–476.

Yin, H.H., Knowlton, B.J., Balleine, B.W., (2004). Lesions of dorsolateral striatum preserve outcome expectancy but disrupt habit formation in instrumental learning. *Eur. J. Neurosci.* 19, 181–189.

Yun, K., Garel, S., Fischman, S., Rubenstein, J.L.R., (2003). Patterning of the lateral ganglionic eminence by the *Gsh1* and *Gsh2* homeobox genes regulates striatal and olfactory bulb histogenesis and the growth of axons through the basal ganglia. *J. Comp. Neurol.* 461, 151–165.

Zdzienicka, E., Rakowicz, M., Mierzewska, H., Hoffman-Zacharska, D., Jakubowska, T., Poniatowska, R., Sułek, A., Waliniowska, E., Zalewska, U., Kulczycki, J., Zaremba, J., (2002). [Clinical and genetic study of juvenile form of Huntington's disease]. *Neurol. Neurochir. Pol.* 36, 245–58.

Zimmermann, T., Remmers, F., Lutz, B., Leschik, J., (2016). ESC-Derived BDNF-Overexpressing Neural Progenitors Differentially Promote Recovery in Huntington's Disease Models by Enhanced Striatal Differentiation. *Stem cell reports* 7, 693–706.

# Appendices

## Appendix 1

### Solution recipes

#### Antifreeze solution (4°C)

Di-sodium hydrogen orthophosphate anhydrous 5.45g  
 Sodium dihydrogen phosphate 1.57g  
 dH<sub>2</sub>O 400ml  
 Ethylene glycol 300ml  
 Glycerol 300ml

#### Cresyl violet solution

Cresyl violet acetate 7g  
 Sodium acetate (anhydrous) 5g  
 dH<sub>2</sub>O 600ml  
 pH 3.5 w/ glacial acetic acid  
 dH<sub>2</sub>O make up to 1L  
 Stir o/n and filter

#### DAB (3,3'-Diaminobenzidine) stock solution (-20°C)

DAB 1g  
 TNS 100ml  
 Freeze in 2ml aliquots

#### DAB working solution

2ml DAB stock solution  
 40ml fresh TNS  
 12µl hydrogen peroxide

#### PBS (Phosphate-buffer) 0.1M solution (4°C)

Di-sodium hydrogen phosphate (dihydrate) 18g  
 Sodium chloride 9g  
 dH<sub>2</sub>O 1L  
 pH 7.3 w/ orthophosphoric acid

#### PBST (0.3% Triton X-100 in PBS)

PBS 100ml  
 Triton X-100 100µl

#### PFA (Paraformaldehyde) 4% (4°C)

PFA 40g  
 PBS 1L  
 Heat <65°C for 3hrs to dissolve  
 Cool o/n  
 pH 7.3 w/ NaOH / orthophosphoric acid

#### Pre-wash see PBS

#### Sucrose solution 25% (4°C)

Sucrose 250g  
 PBS (make up to 1L)  
 pH 7.3 w/ orthophosphoric acid

<b>TBS (Tris Buffered saline) 4X stock solution (4°C)</b> Tris base 96g Sodium chloride 76g dH <sub>2</sub> O 2L pH 7.4 w/ HCl	<b>TBS 1X working solution</b> TBS stock solution 500ml dH <sub>2</sub> O 1.5L pH 7.4 w/ HCl
<b>TNS (Tris non-saline) (4°C)</b> Trizma base 6g dH <sub>2</sub> O 1L pH 7.4 w/ HCl	
<b>TXBBS (0.2% Triton X-100 in TBS) (4°C)</b> TBS 250ml Triton X-100 500µl pH 7.4 w/ HCl	
<b>QA (quinolinic acid) 0.12M stock solution (-20°C)</b> QA 125g PBS 750µl 10M sodium hydroxide 800µl Sonicate 15mins PBS 3200µl 10M sodium hydroxide 50µl PBS 2200µl	<b>QA 0.09M working solution (RT)</b> QA stock solution 50µl PBS 16.7µl
<b>Quench</b> Methanol 10ml Hydrogen peroxide 30% 10ml dH <sub>2</sub> O 80ml	

## Appendix 2

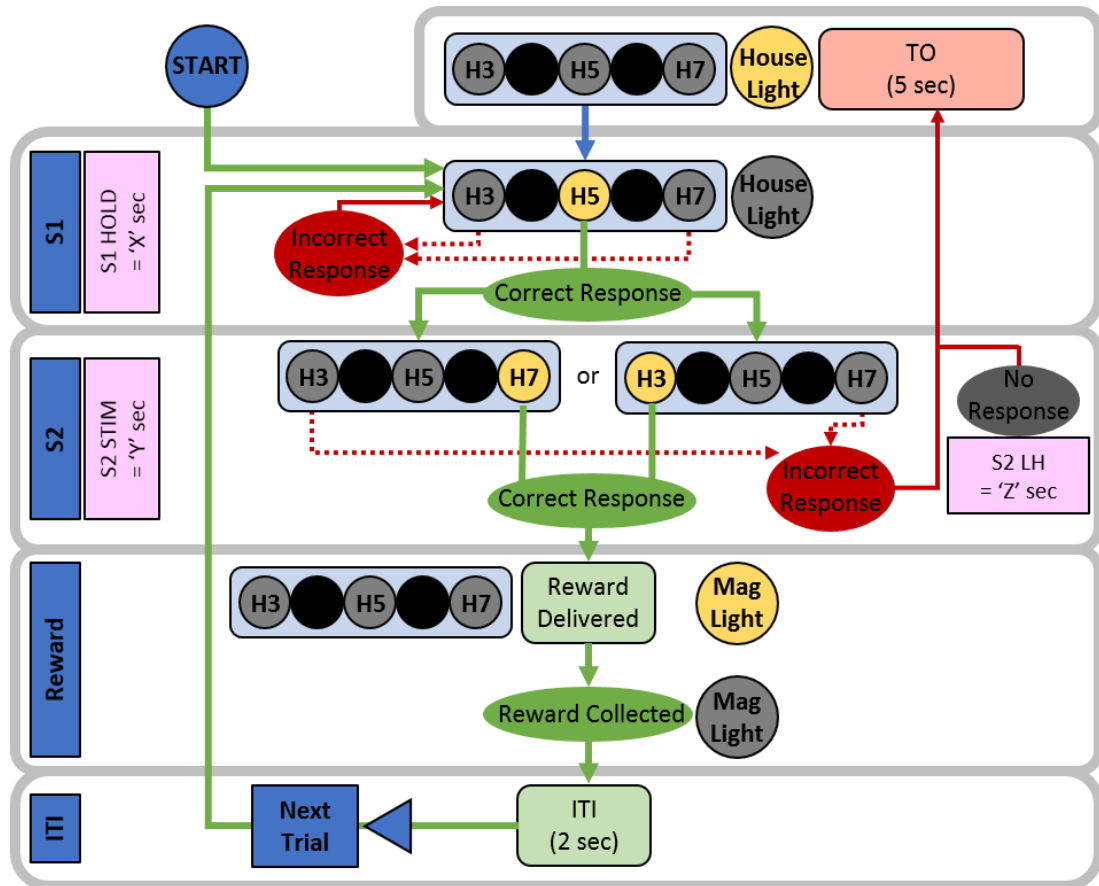
### Antibodies

Primary antibody	Type	Supplier	Product Code	Concentration	Blocking serum	Secondary antibody (all at 1:200)
<b>β-tubulin</b> (neurons)	Mouse	Sigma, UK	T8578	1:500	Goat	Alexa594
<b>CTIP2</b> (early MSNs)	Rat	Abcam, UK	ab18465	1:500	Goat	Alexa594
<b>DARPP-32</b> (mature MSNs)	Mouse	Cornell University, USA	-	1:10000	Horse	Horse anti-mouse
<b>FoxP1</b> (early MSNs)	Mouse	Abcam, UK	ab32010	1:500	Goat	Alexa488
<b>GFAP</b> (astrocytes)	Rabbit	Abcam, UK	ab7260	1:500	Goat	Alexa488
<b>GFP</b> (Chrm4-EGFP-CD1 cells)	Rabbit	Invitrogen, UK	A-11122	1:1000	Goat	Goat anti-rabbit
<b>Hoechst</b> (Nuclei)	-	Fisher Scientific, UK	62249	1:10000	-	-
<b>Iba1</b> (microglia & macrophages)	Rabbit	Wako, Germany	019-19741	1:8000	Goat	Goat anti-rabbit
<b>NeuN</b> (neuronal nuclei)	Mouse	Abcam, UK	ab104224	1:1000	Goat	Goat anti-mouse
<b>Parvalbumin</b> (subset of interneurons)	Mouse	Sigma, UK	P3088	1:4000	Horse	Horse anti-mouse

## Appendix 3

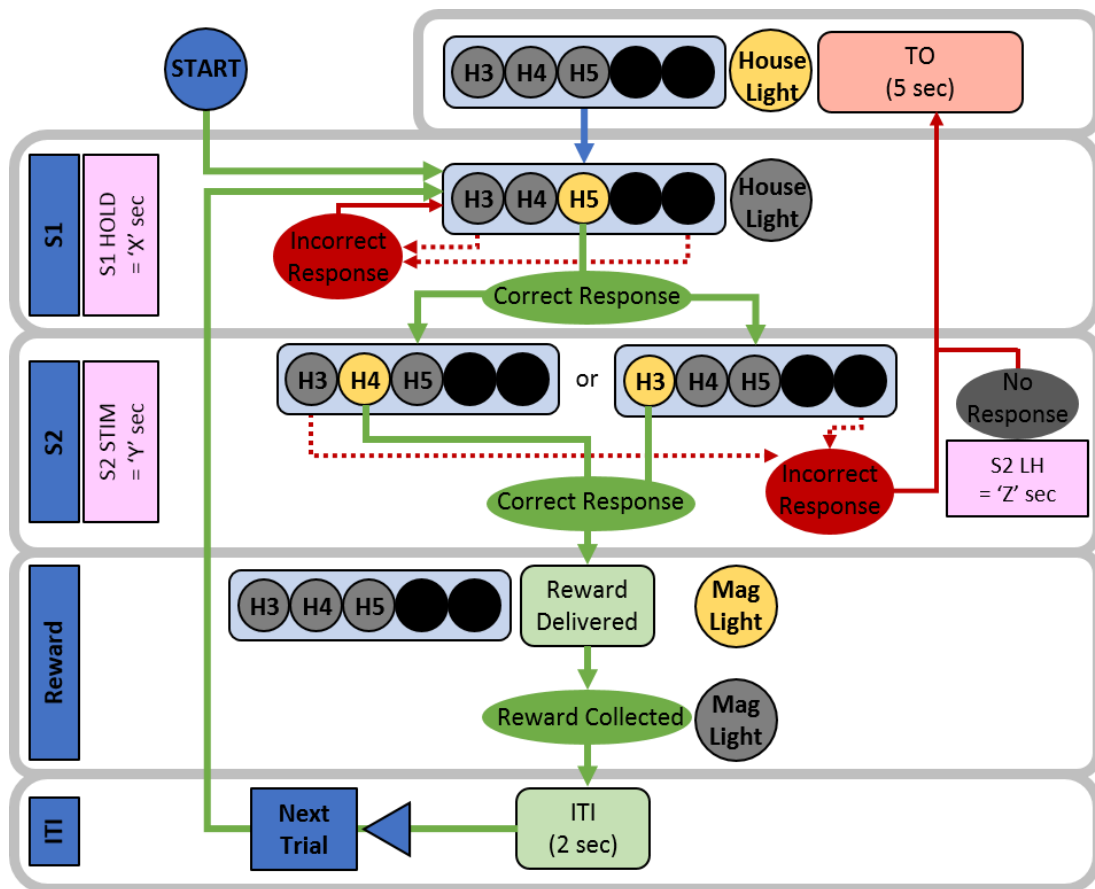
## Operant test programs

## Bilateral lateralised choice reaction time task



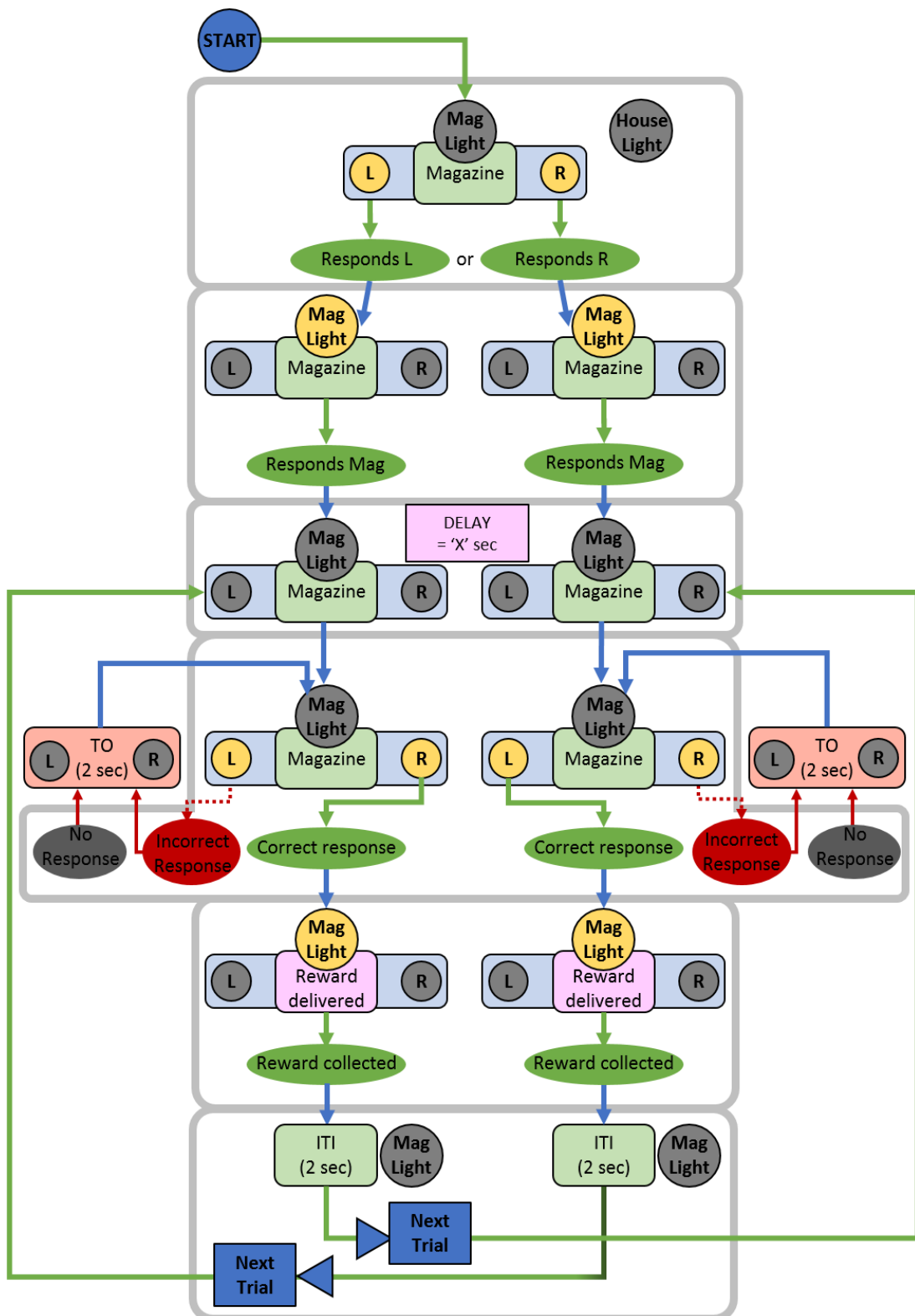
**Appendix 3 Figure 1** Schematic to represent the bilateral lateralised choice reaction time task. H3 = hole 3, H5 = hole 5, H7 = hole 7, Mag Light = magazine light, S1 = stimulus 1, S2 = stimulus 2, TO = time out, ITI = inter-trial interval, S1 Hold = the duration for which a mouse must hold their nose in S1 hole before S2 will begin, S2 STIM = the duration for which S2 will be illuminated and S2 LH = limited hold or how long the mouse has to respond to S2 once it has been illuminated. NB S1 Hold duration is selected pseudo-randomly from a pool of four values to make it unpredictable and encourage attention, see **Appendix 3 Table 1**.

## Unilateral lateralised choice reaction time task



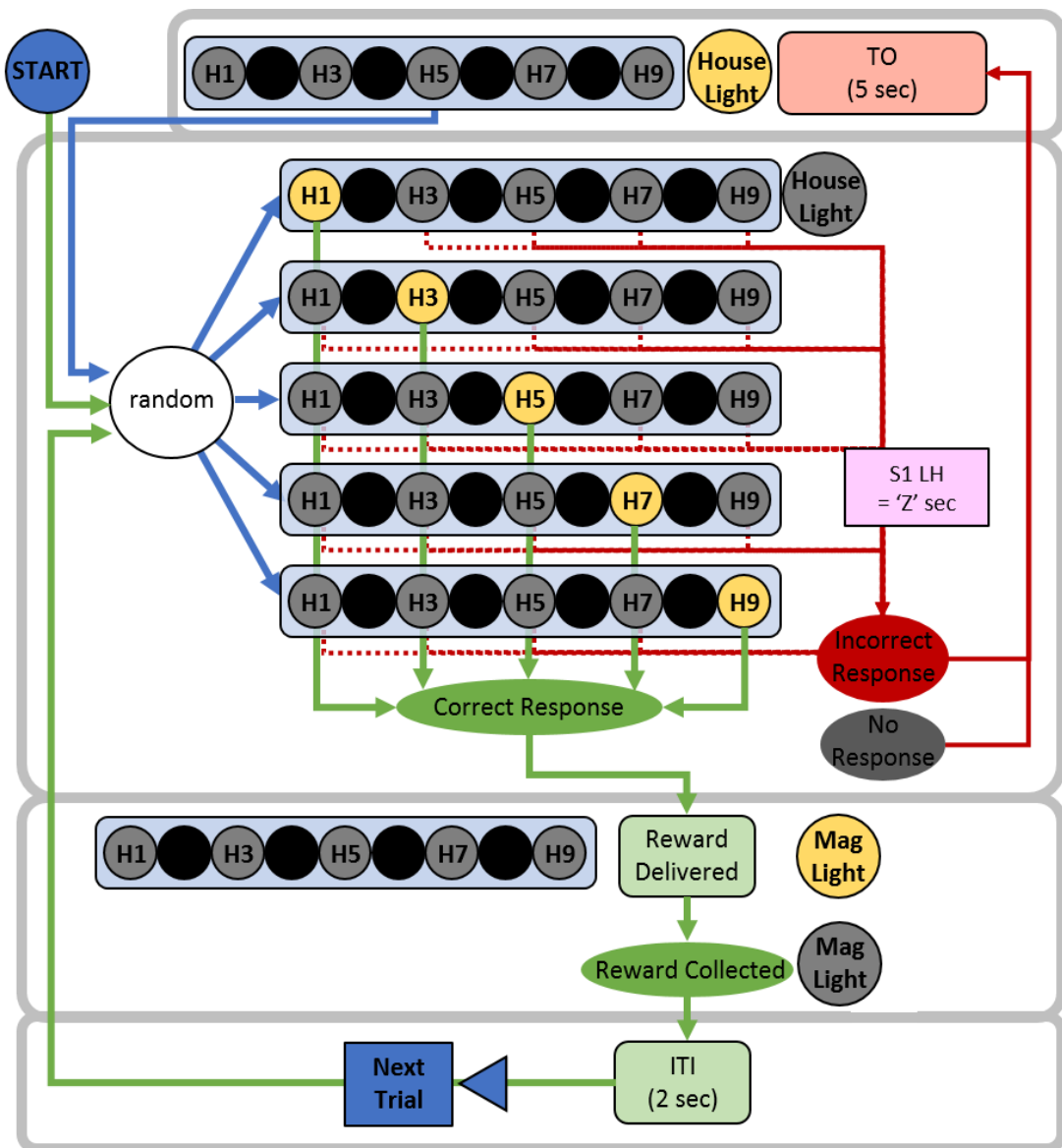
**Appendix 3 Figure 2** Schematic to represent the unilateral lateralised choice reaction time task. H3 = hole 3 (far), H4 = hole 4 (near), H5 = hole 5, Mag Light = magazine light, S1 = stimulus 1, S2 = stimulus 2, TO = time out, ITI = inter-trial interval, S1 Hold = the duration for which a mouse must hold their nose in S1 hole before S2 will begin, S2 STIM = the duration for which S2 will be illuminated and S2 LH = limited hold or how long the mouse has to respond to S2 once it has been illuminated. NB S1 Hold duration is selected pseudo-randomly from a pool of four values to make it unpredictable and encourage attention, as listed in **Appendix Table 1**.

Delayed alternation



**Appendix 3 Figure 3** Schematic to represent the delayed alternation task. L = left hole, R = right hole, Mag Light = magazine light, TO = time out and ITI = inter-trial interval. NB Delay time 'x' is selected pseudo-randomly from the values listed in Appendix Table 2.

**Five-choice serial reaction time task**



**Appendix 3 Figure 4** Schematic to represent the five-choice reaction time task. H1 = hole 1, H3 = hole 3, H5 = hole 5, H7 = hole 7, H9 = hole 9, Mag Light = magazine light, TO = time out and ITI = inter-trial interval. NB S1 location is selected pseudo-randomly to ensure all locations are represented equally but unpredictably.

Training stage	S1 HOLD length X (ms)				S2 STIM length Y (ms)	S2 Limited Hold Z (s)
	1	2	3	4		
1	5	5	5	5	10000	10
2	5	5	5	5	5000	10
3	5	5	5	5	2000	10
4	5	5	5	5	1000	10
5	25	25	25	25	1000	10
6	50	50	50	50	1000	5
7	25	25	50	50	500	5
8	75	75	75	75	500	5
9	100	100	100	100	500	5
10	125	125	125	125	300	5
11	150	150	150	150	300	5
12	200	200	200	200	300	5
<b>Pre-lesion testing</b>	<b>100</b>	<b>150</b>	<b>175</b>	<b>200</b>	<b>300</b>	<b>5</b>
<b>Post-lesion testing</b>	<b>25</b>	<b>50</b>	<b>75</b>	<b>100</b>	<b>300</b>	<b>5</b>

**Appendix 3 Table 1** List of program parameters used for training and testing in the bilateral lateralised choice reaction time task. S1 Hold = the duration for which a mouse must hold their nose in first stimulus (S1) hole before the second stimulus (S2) will begin, S2 STIM = the duration for which S2 will be illuminated and S2 limited hold = how long the mouse has to respond to S2 once it has been illuminated. NB S1 Hold duration is selected pseudo-randomly from a pool of four values to make it unpredictable and encourage attention. Because responses are expected to be reduced following lesioning, the post-lesion testing has an S1 hold value set with shorter durations than the pre-lesion testing.

Training stage	Delay length X (s)						STIM length (s)
	1	2	3	4	5	6	
1	0	0	0	0	0	0	10
2	0	0	0.5	1	1.5	2	10
3	0	1	2	3	4	5	10
4	0	2	3	4	5	6	10
5	0	2	4	6	8	10	10
<b>Testing</b>	<b>0</b>	<b>2</b>	<b>4</b>	<b>6</b>	<b>8</b>	<b>10</b>	<b>10</b>

**Appendix 3 Table 2** List of program parameters used for training and testing in the delayed alternation task. Delay length = duration assigned to the delay period between a correct response in a trial and the subsequent stimulus presentation, STIM length = the duration for which the stimuli are presented before a time out penalty is activated.

## Appendix 4

The Effect of Tissue Preparation and Donor Age on Striatal Graft Morphology  
in the Mouse

Published November 2017 in Cell Transplantation Vol. 27(2) 230-244

# The Effect of Tissue Preparation and Donor Age on Striatal Graft Morphology in the Mouse

Cell Transplantation  
2018, Vol. 27(2) 230–244  
© The Author(s) 2018  
DOI: 10.1177/0963689717744788  
journals.sagepub.com/home/ctj  


David J. Harrison<sup>1</sup>, Victoria H. Robertson<sup>1</sup>, Ngoc-Nga Vinh<sup>1</sup>,  
Simon P. Brooks<sup>1</sup>, Stephen B. Dunnett<sup>1</sup>, and Anne E. Rosser<sup>1</sup>

## Abstract

Huntington's disease (HD) is a progressive neurodegenerative disease in which striatal medium spiny neurons (MSNs) are lost. Neuronal replacement therapies aim to replace MSNs through striatal transplantation of donor MSN progenitors, which successfully improve HD-like deficits in rat HD models and have provided functional improvement in patients. Transplants in mouse models of HD are more variable and have lower cell survival than equivalent rat grafts, yet mice constitute the majority of transgenic HD models. Improving the quality and consistency of mouse transplants would open up access to this wider range of rodent models and facilitate research to increase understanding of graft mechanisms, which is essential to progress transplantation as a therapy for HD. Here we determined how donor age, cell preparation, and donor/host strain choice influenced the quality of primary embryonic grafts in quinolinic acid lesion mouse models of HD. Both a within-strain (W-S) and a between-strain (B-S) donor/host paradigm were used to compare transplants of donor tissues derived from mice at embryonic day E12 and E14 prepared either as dissociated suspensions or as minimally manipulated tissue pieces (TP). Good graft survival was observed, although graft volume and cellular composition were highly variable. The effect of cell preparation on grafts differed significantly depending on donor age, with E14 cell suspensions yielding larger grafts compared to TP. Conversely, TP were more effective when derived from E12 donor tissue. A W-S model produced larger grafts with greater MSN content, and while high levels of activated microglia were observed across all groups, a greater number was found in B-S transplants. In summary, we show that the effect of tissue preparation on graft morphology is contingent on the age of donor tissue used. The presence of microglial activation in all groups highlights the host immune response as an important consideration in mouse transplantation.

## Keywords

cell transplantation, Huntington's disease, primary embryonic tissue, striatal grafts, mouse models, medium spiny neurons

## Introduction

Huntington's disease (HD) is an inherited neurodegenerative disease caused by an expanded polyglutamate cytosine-adenine-guanine (CAG) repeat in the Huntingtin gene on chromosome 4<sup>1</sup>. The resultant mutant Huntingtin protein leads to progressive neuronal dysfunction and loss, with medium spiny neurons (MSNs) primarily affected in the early stages of the disease<sup>2</sup>. HD is a debilitating disease causing a broad range of physical and mental deficits, and currently there is no disease-modifying treatment.

The relatively targeted nature of the primary neuronal loss in HD makes it an ideal candidate for cell replacement therapy. Primary neuronal progenitors derived from the whole ganglionic eminence (WGE; from which the striatum develops) and transplanted directly into the quinolinic acid

(QA)-lesioned striatum develop into MSNs, integrate into the parenchyma, and form functional connections with host neural circuitry in rats<sup>3,4</sup>. A number of clinical trials confirm that transplantation of fetal WGE in HD is safe, and there is preliminary evidence that it can improve some disease

<sup>1</sup> Brain Repair Group, School of Biosciences, Cardiff University, Cardiff, United Kingdom

Submitted: August 19, 2017. Revised: October 13, 2017. Accepted: November 1, 2017.

### Corresponding Author:

David J. Harrison, Brain Repair Group, School of Biosciences, Cardiff University, Museum Avenue, Cardiff CF10 3AX, United Kingdom.  
Email: harrisondj2@cf.ac.uk



symptoms in people with HD.<sup>5–8</sup> However, more work is required. First, tests must be conducted to determine whether fetal transplantation can reliably improve function in people with HD, and second it should be determined whether the efficacy and consistency of this approach can be improved, before its development as a potential treatment. Moreover, optimizing the protocols for achieving successful embryonic WGE grafts will solve many issues that are also relevant to pluripotent stem cell-derived grafts, which are currently being developed as a more sustainable source of donor cells.

Protocols have been optimized and are well established for rat-to-rat striatal transplants, with extensive preclinical literature showing consistent large and functional grafts from embryonic day (E)14 to E16 WGEs<sup>9,10</sup>. Rat protocols have been refined over many years, with donor age and tissue preparation identified as critical factors affecting graft survival, morphology, and function of rat-to-rat striatal transplants<sup>11–13</sup>; however, these factors have not been systematically investigated in mice. It is evident throughout the literature,<sup>14–18</sup> and from experience within this lab, that the direct translation of these protocols to mice results in considerable graft variability. Graft survival is lower and surviving grafts are smaller and contain less striatal-like tissue compared to rat striatal grafts. This suggests that either there are unrecognized differences between rat and mouse host models and the way in which they interact with transplanted tissue or species differences in the way the transplanted tissue develops following transplantation, or both.

Typically, immunosuppressive treatment is not required when transplanting rat cells into the rat brain, even using outbred stocks, with good graft integration and functional recovery<sup>19,20</sup>. It has therefore been assumed that transplants in mice would also not require immunosuppression in the supposed “immune-privileged” brain. However, as the immunological response to transplanted tissue is likely to be critical for graft survival, we have considered the host response to transplantation (including the disparity in immunological background between donor and host and the preparation of transplanted cells) as a potential factor in survival of neural mouse grafts.

Establishing a reliable protocol in the mouse is essential to use the array of well-characterized genetic HD mouse models for cell transplantation, as well as a wide range of transgenics that could be used to contribute to a better understanding of graft survival integration and functional mechanisms. The present study examined whether modifications to current standard transplant protocols could produce more reliable and effective striatal grafts in mouse models of HD, both within and between strains. The effects of donor tissue age and cell preparation were assessed by characterizing the cell content of striatal grafts of mouse primary embryonic tissue and analyzing the activated microglial response. The QA lesion model of HD was used, as it is the most widely used and well-validated model to date for preclinical studies and provides a reliable starting point for later translation to genetic models of HD.

## Materials and Methods

This experiment was subject to project, personal, and facilities licenses and local ethical review in accordance with the United Kingdom Animals (Scientific Procedures) Act 1986 as amended.

### Subjects

Young adult male C57BL6/J ( $N = 32$ ) and CD1 ( $N = 32$ ) mice (20 to 30 g, Harlan, Bicester, UK) were housed in pairs under standard conditions in a 12:12-light/dark cycle. Temperature and humidity were maintained at  $21 \pm 2$  °C and  $60\% \pm 1\%$ , respectively. Food and water were available *ad libitum*.

### QA Lesion Surgery

Mice received unilateral QA (P6320-4; Sigma-Aldrich, Gillingham, UK) lesions to the right striatum, with 2 mice of each strain retained as intact controls. Fresh 0.09 M QA solution was prepared each day in 0.1 M phosphate buffer (10010-056; Thermo Fisher, Loughborough, UK). All animals were anesthetized in an induction chamber using 4% isoflurane gas in oxygen, the head shaved, and a subcutaneous (sc) injection of meloxicam 2.5 mg/kg (Metacam, Boehringer Ingelheim, Germany) given as pain relief prior to surgery. Mice were transferred to a stereotaxic frame and maintained on 1.5% to 2% isoflurane in a mixture of oxygen and nitrous oxide (2:1). The skull was exposed and a small hole drilled at the following stereotaxic coordinates: anterior-posterior (AP) +0.8 mm and medial-lateral (ML) –2.0 mm from bregma. A 30-gauge stainless steel cannula attached to a 10  $\mu$ L microvolume syringe (2035; SGE Analytical Sciences, Thermo Fisher) driven by a mechanical pump was used to inject 0.75  $\mu$ L of 0.09 M QA at dorso-ventral (DV) –3.0 mm below dura. The QA was infused over 6 min and the cannula left in position for an additional 3 min to prevent back flow of solution. The cannula was removed and the incision closed using 5-0 Vicryl dissolvable sutures (W9915; Ethicon, Livingston, UK). 0.5ml of 0.9% glucose saline (FKE1323; Baxter, Newbury, UK) was administered sc during surgery to reduce dehydration and a 7.5 mg/kg intramuscular injection of diazepam (Hameln Pharmaceuticals Ltd, Gloucester, UK) was given post-anesthesia prevent seizures. Mice were placed into a warm recovery chamber for 2 to 3 h until completely awake and returned to their home cages for 10 d. The general health of mice was monitored daily and mice were fed a wet mash of standard food in their cages for at least 3-d post surgery. In the week following lesion surgery, 7 C57BL6/J mice became unwell, necessitating hand-feeding of wet mash via a syringe daily until weight was regained. In addition, 4 pairs of C57BL6/J mice were separated due to fighting. Animals that did not fully recover from illness or fighting were removed from the study ( $n = 8$ ).

**Table 1.** Summary of Survival Rates and Untransformed Data for Surviving Grafts.

Host Strains	Groups	Number of Surviving Grafts	Graft Volume ( $\times 10^6 \mu\text{m}^3$ )	Number of NeuN <sup>+</sup> Cells ( $\times 10^3$ )	P-zone Volume ( $\times 10^6 \mu\text{m}^3$ )	Number of DARPP-32 <sup>+</sup> Cells ( $\times 10^3$ )	Percentage of DARPP-32 <sup>+</sup> Patches (%)
C57BL6/J	E12 CS	4 of 5 (80%)	110.3 $\pm$ 52.4	11.1 $\pm$ 5.1	61.2 $\pm$ 42.4	1.4 $\pm$ 0.7	51.0
C57BL6/J	E12 TP	5 of 5 (100%)	301.6 $\pm$ 88.5	28.4 $\pm$ 8.0	180.6 $\pm$ 67.7	2.5 $\pm$ 0.8	55.5
C57BL6/J	E14 CS	4 of 4 (100%)	188.9 $\pm$ 32.7	12.9 $\pm$ 4.1	127.6 $\pm$ 5.7	2.4 $\pm$ 0.4	74.4
C57BL6/J	E14 TP	2 of 6 (33%)	97.0 $\pm$ 16.3	6.8 $\pm$ 0.5	44.7 $\pm$ 3.7	0.8 $\pm$ 0.5	48.1
CD1	E12 CS	5 of 6 (83%)	226.0 $\pm$ 52.9	11.1 $\pm$ 2.4	91.1 $\pm$ 31.1	2.1 $\pm$ 0.5	34.0
CD1	E12 TP	6 of 7 (86%)	335.6 $\pm$ 46.5	16.4 $\pm$ 2.8	237.5 $\pm$ 66.4	4.2 $\pm$ 0.7	68.4
CD1	E14 CS	6 of 7 (86%)	194.0 $\pm$ 21.6	9.6 $\pm$ 1.4	84.3 $\pm$ 16.9	2.3 $\pm$ 0.4	44.3
CD1	E14 TP	3 of 7 (43%)	146.9 $\pm$ 36.8	6.6 $\pm$ 1.6	119.0 $\pm$ 25.6	2.5 $\pm$ 0.3	89.9

Note: Untransformed data presented  $\pm$  standard error of the mean. High graft survival rates were seen in most groups with the exception of those derived from E14 TP. Large differences in graft volume and cell numbers were observed within group. CS = single-cell preparation; TP = tissue piece.

### Donor Tissue

Two transplant paradigms were used incorporating common strain combinations studied within the lab: a within-strain (W-S) model with CD1 tissue transplanted into CD1 hosts and a between-strain (B-S) model with Chrm4-EGFP-CD1 tissue transplanted into C57BL/6J hosts. The CD1 mouse is used as a standard transplantation model for assessing graft survival and composition, chosen primarily for their large litter sizes. The C57BL/6J/Chrm4-EGFP-CD1 model is used to investigate the functional efficacy of transplants, as C57BL/6J mice are particularly adept at performing behavioral tasks and are the background strain for many of the genetically modified HD mouse models. The bacterial artificial chromosome (BAC) Chrm4-EGFP-CD1 mice express green fluorescent protein (GFP) attached to M4 receptors in a subset of MSNs<sup>19</sup>, allowing easy identification of donor-derived MSNs.

Time-mated CD1 and Chrm4-EGFP-CD1 mice from an in-house colony (originally purchased from Harlan, and MMRRRC, Farmington, CT, USA, respectively) were sacrificed by cervical dislocation at E12 or E14, and the embryos dissected into Dulbecco's modified Eagle's medium: nutrient mixture F-12 (DMEM/F12; 12634-028; Thermo Fisher). Using a dissecting microscope in a laminar flow hood, the brains were removed and, following a longitudinal cut in the medial cortex, the whole (medial and lateral) striatal primordium was identified on the floor of the lateral ventricle and removed via a horizontal cut as described<sup>21</sup>. Four transplant preparations were made for each donor strain: (1) E12 cell suspension (CS), (2) E12 tissue pieces (TP), (3) E14 CS, and (4) E14 TP. Transplantation surgery was spread across multiple days with fresh suspensions made each morning for each group.

### Transplantation Surgery

Approximately 10-d postlesion mice were randomly assigned to experimental groups with 20 C57BL6/J and 27 CD1 mice receiving primary tissue transplants ( $n = 4$  to 7

per group, see Table 1). In addition, a group of mice from each strain were retained as lesion-only controls (C57BL6/J,  $n = 2$ ; CD1,  $n = 3$ ). Surgery was conducted using the same anesthetic regime described for lesions; however, no diazepam was administered post-transplantation. Cell preparations were injected at the lesion coordinates via the same burr hole,  $-3.2$  and  $-2.8$  mm below dura.

### Single-cell Preparations

CS preparations consisted of pooled E12 WGEs (Chrm4-EGFP-CD1,  $n = 26$ ; CD1  $n = 24$ ) or E14 WGEs (Chrm4-EGFP-CD1,  $n = 22$ ; CD1,  $n = 26$ ) for each strain. Tissue was incubated at 37 °C for 10 min in 0.1% bovine trypsin (25300-054; Thermo Fisher) + 0.05% deoxyribonuclease (DNase) (D4527; Sigma-Aldrich) in DMEM/F12 solution, before adding 0.01% bovine trypsin inhibitor (T6522-250MG; Sigma-Aldrich) for an additional 5 min, and washing with direct addition of DMEM/F12 followed by centrifugation for 3 min at 1,000 rpm. Cells were resuspended in DMEM/F12 and triturated using a Gilson pipette with a 200  $\mu\text{L}$  tip to mechanically dissociate into a single CS. Cell number and viability were determined with trypan blue (T8154 20ML; 0.4% trypan blue solution, Sigma-Aldrich, UK) exclusion using a hemocytometer, confirming all suspensions had >90% viability. Cells were concentrated at 250,000 cells/ $\mu\text{L}$  for transplantation in DMEM/F12. 1  $\mu\text{L}$  of suspension was injected at each depth using a 10  $\mu\text{L}$  microvolume syringe (2035; SGE Analytical Sciences, Thermo Fisher), depositing approximately 500,000 cells in total into the lesioned striatum over 2 min (1  $\mu\text{L}/\text{min}$ ), with the syringe left in situ for an additional 3 min to allow diffusion and reduce backflow. All suspensions were kept in the dark at room temperature.

### Tissue Piece Preparations

For TP preparations, no cell counts could be conducted directly from nondissociated tissue, therefore WGE units equating to approximately 500,000 cells (the number of cells

**Table 2.** Summary of Transplanted Cell Numbers and Associated Proportion of WGE Used in Each Group.

Donor Strains	Embryonic Age	Preparation	Cells per WGE	Proportion WGE Transplanted	Number Cells Transplanted
Chrm4-EGFP-CD1	E12	CS	180,769	2.77	500,000
Chrm4-EGFP-CD1	E12	TP	180,769	2.00	361,538
Chrm4-EGFP-CD1	E14	CS	577,273	0.87	500,000
Chrm4-EGFP-CD1	E14	TP	577,273	1.00	577,273
CD1	E12	CS	357,143	1.40	500,000
CD1	E12	TP	357,143	2.00	714,286
CD1	E14	CS	1,041,667	0.48	500,000
CD1	E14	TP	1,041,667	1.00	1,041,667

Note: The number of cells per WGE was estimated based on the mean cell counts of the CS preparations. The number of WGEs used in the TP preparations was adjusted based on the mean number of cells in the WGE for each particular donor strain and age with the aim of transplanting a similar number of cells in each group. Since it was only possible to use whole WGE units in the nondissociated TP preparations, the number of cells transplanted could not be exactly matched but was kept as close to 500,000 as possible. Subsequently, the proportion of WGE transplanted was used to transform the data to account for the differences in proliferative potential of the cells transplanted. CS = single-cell preparation; TP = tissue piece; WGE = whole ganglionic eminence.

transplanted in the CS groups) were transplanted. Cell counts calculated from the CS dissections showed this to equal approximately a pair of WGEs for E12 tissue and a single WGE for E14 (see Table 2). Separate preparations were made for each individual surgery, with WGEs treated with bovine trypsin, DNase, and trypsin inhibitor as described above. However, after gentle washing, tissue was transferred directly into ~4  $\mu$ L DMEM/F12 for transplantation, with no trituration, therefore minimizing mechanical manipulation to maintain integrity of the TPs. TP preparations were injected as above, at a rate of 1  $\mu$ L/min over 4 min (2 min at each depth). Mice were monitored daily until full recovery.

### Perfusion and Immunohistochemistry

At 12 wk after transplantation surgery, mice were perfused and the brains were processed for histological analysis of the grafts. Animals received a terminal intraperitoneal injection of sodium pentobarbital (Euthatal, Merial Animal Research, Woking, UK) and were transcardially perfused using phosphate buffered saline (PBS, pH 7.3) followed by 150 mL of 4% paraformaldehyde solution (PFA, pH 7.3; 10131580; Fisher Scientific, Loughborough, Lutterworth, UK) over 4 min. Brains were removed, postfixed in 4% PFA for 4 h, and transferred to 25% sucrose solution in PBS for at least 48 h. Brains were cut at 40  $\mu$ m on a freezing microtome, and sections stored in antifreeze—5.45 g disodium-hydrogen-orthophosphate (28029.26; VWR, UK), 1.57 g sodium-dihydrogen-orthophosphate (28013.264; VWR), 300 mL ethylene glycol (102466-2.5L; Sigma-Aldrich), and 300 mL glycerol (G7893-2L; Sigma-Aldrich) in 400 mL dH<sub>2</sub>O—at -20 °C until immunohistochemical analysis. The 1:12 series were incubated at room temperature as free-floating sections with primary antibodies for neuronal nuclei (NeuN) (MAB377; 1:2,000; Millipore, Watford, UK), ionized calcium-binding adapter molecule 1 (Iba1) (019 19741; 1:8,000; Wako, Chuo-ku, Japan), parvalbumin (P3088; 1:4,000; Sigma-Aldrich) or anti-GFP (AB11122; 1:1,000; Invitrogen, Loughborough, UK), and streptavidin–biotin reaction (PK-6100; Dako,

Glostrup, Denmark), then stained using 3,3'-diaminobenzidine (DAB, D5637-1G; Sigma-Aldrich). Parvalbumin series were double-stained with dopamine- and cAMP-regulated phosphoprotein antibody (DARPP-32) (1:30,000; the kind gift of Professor H. C. Hemmings, Cornell University<sup>22</sup>) and Vector SG kit (SK-4700; Dako). Sections were mounted onto gelatinized slides and left to air-dry overnight before being dehydrated and cover-slipped with distyrene plasticizer and xylene (DPX) mounting medium (12658646; Fisher Scientific).

### In Vitro Primary Cultures

Time-mated CD1 dams were sacrificed at E12 or E14 ( $n = 3$  per group), and WGEs were dissected as described previously<sup>21</sup>. Tissue from each litter was pooled to prepare 3 separate suspensions for each embryonic age, as described above. Cells were resuspended in neuronal differentiation media—DMEM/F12 + 1% FCS (10270-106; Thermo Fisher, Waltham, MA, USA) + 2 $\times$  B27 (17504-044; Thermo Fisher, Waltham, MA, USA) and plated on poly-L-lysine treated coverslips at 100,000 cells per well. CS of 30  $\mu$ L was left for approximately 1 h before flooding with 500  $\mu$ L of differentiation media and incubated at 37 °C in humidified 5% CO<sub>2</sub> and 95% atmospheric air. A complete media change was performed after 3 d in culture using the same media described above. After 24 h and 7 d *in vitro*, 12 wells of each suspension were fixed with 4% PFA and stored at 4 °C until immunocytochemical staining.

### Immunocytochemistry

Cells were quenched in 100% ethanol for 2 min, washed 3 times in PBS, and then blocked with PBS + 0.3% Triton X-100 (PBST; X100-500ML; Sigma-Aldrich) + 1% BSA (A3059; Sigma-Aldrich) + 1% serum at RT for 1 h. Cells were then incubated at 4 °C overnight with the following pairs of primary antibodies in PBS + PBST + 1% BSA + 1% horse serum (16050-122; Thermo Fisher, USA): neuronal marker  $\beta$ III-tubulin (T2200; 1:500; Sigma-Aldrich) and astrocyte marker glial fibrillary acidic protein antibody

(GFAP AB32010; 1:500; Abcam, Cambridge, UK) or early MSN marker forkhead box P1 (FoxP1 AB16645; 1:500; Abcam) and COUP-TF-interacting protein 2 (CTIP2) AB18465; 1:500; Abcam, UK). Cells were washed with PBST before incubating for 2 h in the dark at RT with the following fluorescent secondary antibodies in PBS (1:200): Alexa594 (A11037; Thermo Fisher, UK) for  $\beta$ III-tubulin and CTIP2 and Alexa488 (A11034; Thermo Fisher, UK) for GFAP and FoxP1. After washing with PBS, a Hoechst (23000-1000; 1:10,000; Fisher Scientific) counterstain was applied for 5 min. Cells were washed again in PBS and coverslips mounted onto microscope slides with aqueous mountant (PBS: glycerol; G7893-2L; Sigma-Aldrich, 1:1) and stored in the dark at 4 °C. Five regions per coverslip were counted, and the mean count from each suspension recorded.

### Analysis of Grafts and Statistics

The location of grafts in the C57BL6/J hosts was identified through immunohistochemical labeling of the transplanted Chrm4-EGFP-CD1 tissue using an anti-GFP antibody (A11122; Invitrogen, Loughborough, UK), and corresponded to clearly identifiable regions of NeuN<sup>+</sup> staining within the lesioned striatum (Fig. 1A). CD1 hosts were transplanted with CD1 tissue, and therefore could not be identified through GFP staining, consequently NeuN<sup>+</sup> staining was used to identify the graft location in these animals. The presence of fully differentiated adult neurons (NeuN<sup>+</sup> cells) within the grafted area was used to determine graft survival in all groups (Fig. 1B), with grafts with no positive NeuN staining excluded from graft analyses. These animals were however retained in the analysis of microglial immune response. It is important to note that while successful grafts are defined here as those containing NeuN<sup>+</sup> cells, survival of other cell types, such as immature neurons and glial cells, cannot be excluded. Volumes were calculated by measuring cross-sectional areas of NeuN<sup>+</sup> (total graft volume) and DARPP-32<sup>+</sup> graft regions (P-zones) across 1:12 series and using the formula: volume = ( $\Sigma A \times M$ )/ $f$ , where  $A$  = area of graft ( $\mu\text{m}^2$ ),  $M$  = section thickness ( $\mu\text{m}$ ), and  $f$  = section frequency (Fig. 1B and C).

For larger grafts, total cell numbers were calculated by unbiased stereology. For smaller grafts, stereological analysis would generate a large sampling error, therefore these were counted manually using Image J v1.45 software (National Institutes of Health (NIH), Bethesda, MD, USA) following imaging of grafted sections. Mean cell diameter was obtained for NeuN<sup>+</sup>, DARPP-32<sup>+</sup>, and parvalbumin<sup>+</sup> cells by measuring the minimum and maximum diameters of 10 cells per graft using Image J.

Iba1-labeled series were used to grade the host microglial response in the grafted area using an established semi quantitative rating scale<sup>23</sup>. Each section was graded 0 to 4 according to the following categories: (0) no specific activated microglia in the graft area, (1) low number of activated

microglia distributed as scattered single cells or clustered in a few small patches in or around the graft, (2) several activated microglia distributed as single cells or clustered in multiple prominent patches, (3) dense immunostaining of the graft area and a large number of activated microglia in and around the graft, and (4) very dense immunostaining of the whole graft area and a very large number of activated microglia in and around the graft. Activated microglia were easily identified by their morphological appearance<sup>24</sup> (Fig. 1D). The highest grade given to any section for each animal was the grade assigned to that animal.

As TP were not dissociated, transplants were prepared by WGE units rather than by cell number as in the CS preparations. Embryos used for CS and TP were collected from the same litters, so although cell number could not be determined, an estimate of the number of cells per WGE at each age was calculated using total counts from the CS and dividing by the total number of WGEs dissociated (see Table 2). Since E12 WGE contained approximately half the number of cells of E14 WGE, a pair of E12 WGEs were transplanted for each E14 WGE to maintain a consistent total cell number, as close to 500,000 as possible. However, transplanting different proportions of WGE raises the issue that the E12 TP grafts of 2 WGEs may have twice the proliferative potential of the single WGE E14 TP. As it is not possible to control for both cell number and quantity of WGE transplanted, graft outcome measures were subsequently transformed to account for the proportion of WGE transplanted as described below:

Cell counts and volume data were corrected for the proportion of WGE transplanted using the following transformations:  $Tn = n/\text{proportion of WGE transplanted}$  and  $Tvol = \text{vol}/\text{proportion of WGE transplanted}$ , where proportion of WGE transplanted = number of cells transplanted/mean number of cells in WGE,  $Tn$  = corrected cell count,  $n$  = actual cell count,  $Tvol$  = corrected volume, and  $\text{vol}$  = actual volume.

Transformed data from successful grafts in all groups were analyzed together using 3-way analyses of variance (ANOVAs) in Genstat for Windows v16.1 software. If a significant main effect of strain was found, then B-S and W-S groups were subsequently analyzed in separate 2-way ANOVAs. Consequently, NeuN<sup>+</sup> graft volume, DARPP 32<sup>+</sup> graft volume, DARPP-32<sup>+</sup> cell count, proportion of parvalbumin<sup>+</sup> cells, and activated microglia scores were analyzed in separate ANOVAs for the B-S and W-S groups. For immune response data, transplanted mice with no detectable surviving grafts, as well as lesion only controls, were also included in the analyses.

## Results

Mouse donor cells from E14 and E12 WGE were prepared either as standard dissociated single-CS or as nontriturated partially digested TPs. These cell preparations were transplanted into the striatum of 2 commonly used laboratory

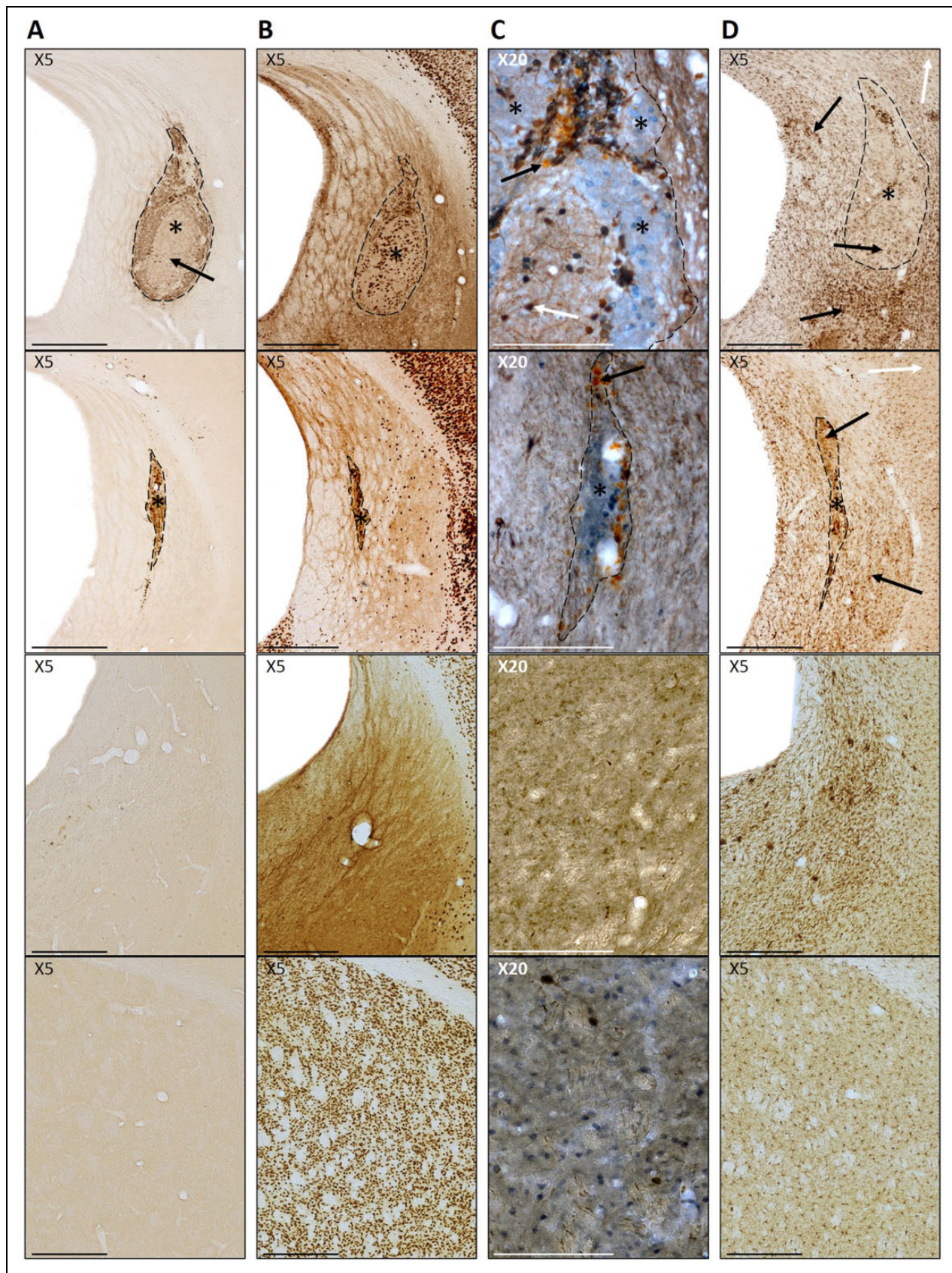


**Fig. 1.** Photomicrographs of typical large and smaller grafts (first and second row, respectively), lesion only and control (third and final row, respectively). (A) GFP<sup>+</sup> staining identifying Chrm4-EGFP-CD1-grafted tissue (indicated by \*) within the host parenchyma. Paler areas of

mouse donor/host strain paradigms; a B-S and a W-S model. Grafts were analyzed using immunohistochemistry 12 wk later and graft size, neuronal content, DARPP-32<sup>+</sup> MSN, and parvalbumin<sup>+</sup> interneuron number compared, as well as the microglial reaction to the graft by the host. CS of each donor age was also analyzed after 24 h and 7 d *in vitro* to assess whether the age at which tissue is harvested affects the development of cells independently from the host environment.

### Graft Survival

The presence of DAB-labeled GFP<sup>+</sup> Chrm4-EGFP-CD1 donor cells corresponded with areas of NeuN<sup>+</sup> and DARPP-32<sup>+</sup> staining in the C57BL6/J hosts, confirming the donor origin of the cells (Fig. 1A and B). Transplanted cells could be clearly identified within the lesioned host striatum by staining for NeuN<sup>+</sup> mature neurons in all hosts, including those transplanted with non-GFP donor cells (Fig. 1B). The proportion of surviving grafts for each group and raw untransformed data for surviving grafts are shown in Table 1. There was no effect of donor/host on NeuN<sup>+</sup> graft survival ( $t_6 = 0.208$ , *ns*), and a high proportion of NeuN<sup>+</sup> grafts was identified in all groups (80% to 100%) except for E14 TP, of which only 5 of 13 (43%) transplanted mice had NeuN<sup>+</sup> cells in the grafted region after 12 wk. Graft volumes varied both within and between groups, ranging from just  $12 \times 10^6 \mu\text{m}^3$  up to  $588 \times 10^6 \mu\text{m}^3$ .

### Graft Volume and Cellular Composition

Figure 2A shows the volumes of NeuN<sup>+</sup> tissue in the surviving grafts for each group and a comparison of mean graft volume of B-S (Chrm4-EGFP-CD1 tissue into C57BL6/J hosts; B-S) and within strain (CD1 tissue into CD1 hosts; W-S) groups. Grafts from the W-S group were significantly larger than those observed in the B-S group ( $F_{1, 27} = 19.08$ ,  $P < 0.001$ ). Preparations of E14 CS yielded significantly larger grafts than E14 TP in the B-S model, while the younger E12 tissue produced larger grafts when prepared as TP than as CS (age  $\times$  preparation:  $F_{1, 11} = 14.52$ ,  $P < 0.01$ ). In the W-S model, E14 CS also yielded significantly larger grafts than E14 TP; however, there was no significant difference between grafts derived from different preparations of E12 tissue (age  $\times$  preparation:  $F_{1, 16} = 17.14$ ,  $P < 0.001$ ).

Distinct regions of DARPP 32<sup>+</sup> staining were observed within all surviving grafts (Fig. 1C). The volume of DARPP-32<sup>+</sup> patches (P-zones) within each graft is shown in Fig. 2B. W-S transplants yielded significantly larger total P-zone volumes than B-S (strain:  $F_{1, 27} = 6.50$ ,  $P < 0.05$ ). B-S

transplants contained larger P-zone volumes when transplanted as CS than TP at E14, while the reverse was true for E12 tissue (age  $\times$  preparation:  $F_{1, 11} = 18.27$ ,  $P < 0.001$ ). A similar trend was observed in the W-S groups; however, a statistically significant interaction was not found. As Fig. 2C shows, there were no differences in the proportion of DARPP-32<sup>+</sup> P-zone volume (out of total NeuN<sup>+</sup> graft volume) in B-S and W-S groups. B-S transplants showed a trend toward higher proportion of P-zones in E14 CS compared to E14 TP, although this was not statistically significant. No difference in the B-S E12 preparations was observed. W-S E12 groups again showed a tendency for higher proportions of P-zone tissue from E12 transplants as TP rather than CS. However, at E14, TP produced the larger DARPP-32<sup>+</sup> proportion compared to CS—the only measure in which E14 TP outperformed E14 CS (strain  $\times$  preparation:  $F_{1, 27} = 10.73$ ,  $P < 0.01$ ).

There was no difference between B-S and W-S transplants in the total number of mature NeuN<sup>+</sup> neurons within the grafts (Fig. 2D). Cell counts reflected the data patterns observed in graft volume, with E14 CS yielding more cells than E14 TP, and E12 TP yielding more cells than E12 CS (age  $\times$  preparation:  $F_{1, 27} = 23.43$ ,  $P < 0.001$ ). The W-S grafts contained more DARPP-32<sup>+</sup> cells than B-S (strain:  $F_{1, 27} = 21.43$ ,  $P < 0.001$ ; Fig. 2E). Grafts of E14 tissue contained more DARPP-32<sup>+</sup> cells than those of E12 origin in both W-S and B-S groups (age:  $F_{1, 16} = 13.6$ ,  $P < 0.01$  and  $F_{1, 11} = 6.71$ ,  $P < 0.05$ , respectively). E14 tissue yielded higher DARPP-32<sup>+</sup> content when transplanted as CS than TP, while there was trend for E12 to produce more as TP in both W-S and B-S groups (age  $\times$  preparation:  $F_{1, 16} = 8.94$ ,  $P < 0.01$  and  $F_{1, 11} = 17.25$ ,  $P < 0.01$ , respectively).

The W-S models yielded the greatest proportion of DARPP-32<sup>+</sup> cells within the grafts compared to the B-S group (strain:  $F_{1, 27} = 4.46$ ,  $P < 0.05$ ; Fig. 2F). Grafts derived from E14 tissue contained a higher proportion of DARPP-32<sup>+</sup> cells than those from E12 in the W-S model (age:  $F_{1, 16} = 9.88$ ,  $P < 0.01$ ). In addition, TP preparations in the W-S model yielded a greater proportion than the CS (preparation:  $F_{1, 16} = 12.97$ ,  $P < 0.01$ ).

Significantly more parvalbumin<sup>+</sup> cells were found in W-S transplants compared to B-S (strain:  $F_{1, 27} = 20.67$ ,  $P < 0.001$ ; Fig. 3A). In addition, E14 generated more parvalbumin<sup>+</sup> cells than E12 tissue in both W-S and B-S groups (age:  $F_{1, 16} = 19.39$ ,  $P < 0.001$  and  $F_{1, 11} = 14.14$ ,  $P < 0.01$ , respectively), and CS yielded more than TP preparations (preparation:  $F_{1, 16} = 4.49$ ,  $P < 0.05$  and  $F_{1, 11} = 8.05$ ,  $P < 0.05$ , respectively) although this effect was mostly due to very high numbers in the E14 CS groups compared to all other combinations. E14 CS grafts contained significantly

**Fig. 1.** (Continued) non-medium spiny neurons cell types are seen within the graft (indicated by arrow). Scale bar represents 500  $\mu\text{m}$ . (B) NeuN<sup>+</sup> staining of mature neurons. Areas of grafted cells can be clearly identified within the lesioned striatum (\*). Scale bar represents 500  $\mu\text{m}$ . (C) DARPP-32<sup>+</sup> staining (blue) shows distinct P-zones within the grafts (\*). Parvalbumin<sup>+</sup> interneurons (brown stain; white arrow) are present throughout the grafts. Black arrows highlight the nonspecific orange-colored staining of spherical dead cells. Scale bar represents 100  $\mu\text{m}$ . (D) Iba1<sup>+</sup> staining of microglia. Resting-state ramified cells (white arrow) can be seen on the peripheral cortex areas. Clusters of darker, amoeboid activated cells (black arrow) can be seen within the grafts (\*) and the surrounding striatum. Scale bar represents 500  $\mu\text{m}$ .

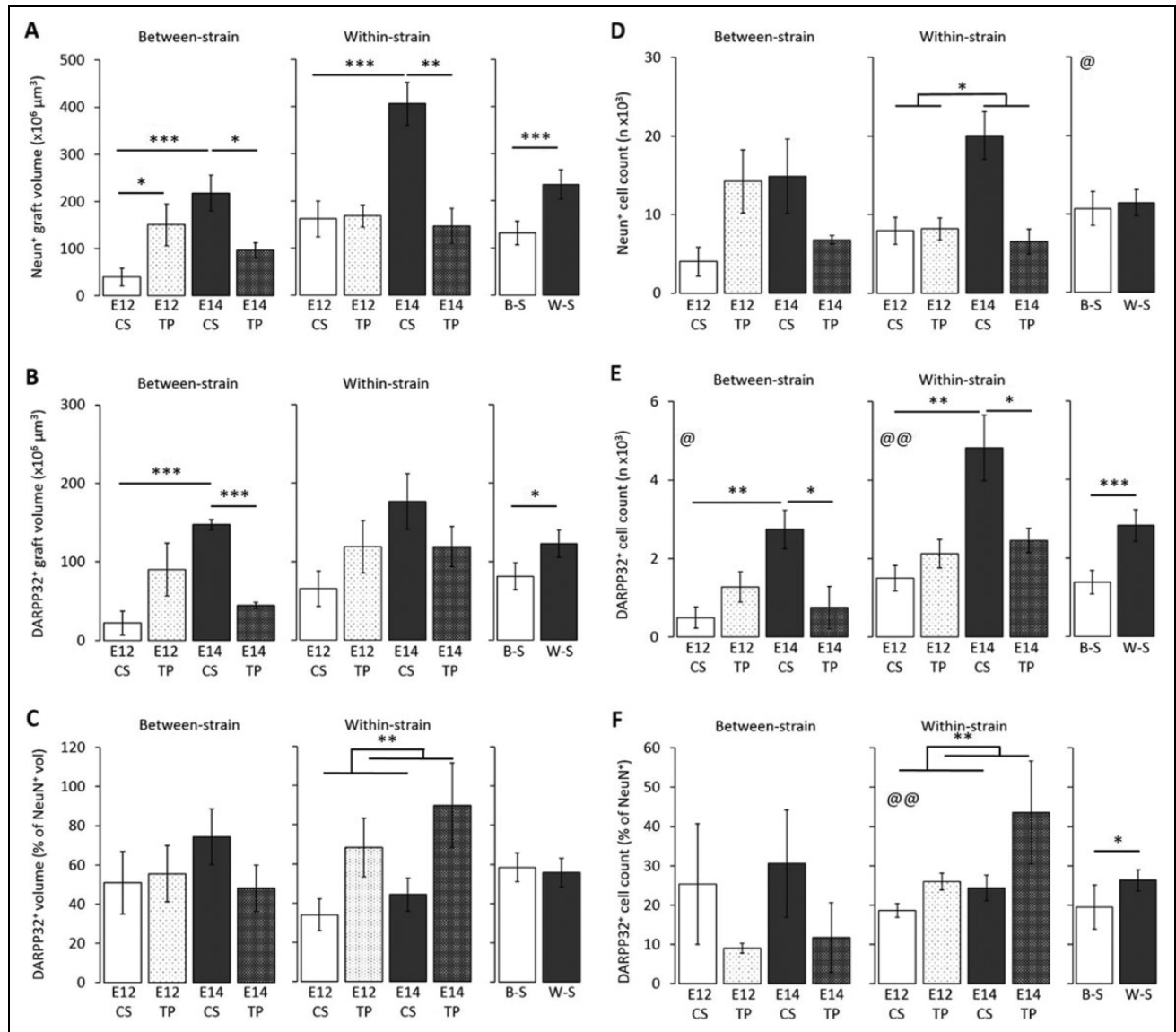


**Fig. 2.** (A) NeuN<sup>+</sup> graft volumes. Within-strain (W-S) transplants were larger than the between-strain (B-S) transplants ( $***P < 0.001$ ). E14 tissue yielded a larger volume than E12 tissue when transplanted as single-cell preparation (CS) in both strain models ( $***P < 0.001$ ). E14 tissue produced larger grafts when transplanted as CS than tissue piece (TP) style preparation in B-S ( $*P < 0.05$ ) and W-S ( $**P < 0.01$ ) models. E12 tissue yielded a larger volume when transplanted as TP than CS in the B-S model only ( $*P < 0.05$ ). (B) DARPP32<sup>+</sup> graft volumes. W-S transplants contained a larger volume of DARPP32<sup>+</sup> tissue than the B-S ( $*P < 0.05$ ). The B-S CS transplants yielded a larger DARPP32<sup>+</sup> volume using E14 tissue than E12 ( $***P < 0.001$ ), and E14 tissue yielded a larger volume when transplanted as CS than TP ( $***P < 0.001$ ). (C) Proportion of DARPP32<sup>+</sup> graft tissue (proportion = [DARPP32<sup>+</sup> volume/NeuN<sup>+</sup> volume] × 100). There was no difference in the proportion of DARPP32<sup>+</sup> tissue in the different models; however, CS transplants yielded a higher proportion of DARPP32<sup>+</sup> tissue in the B-S groups than in the W-S groups ( $P < 0.05$ ). TP yielded a higher proportion of DARPP32<sup>+</sup> tissue than CS in the W-S groups ( $**P < 0.01$ ). (D) NeuN<sup>+</sup> graft cell counts. No effect of model on neuronal cell counts was detected. E14 tissue yielded a greater number of neurons than E12 ( $@P < 0.05$ ). CS transplants contained more NeuN<sup>+</sup> cells than the TP in the W-S transplants ( $P < 0.05$ ); however, TP grafts comprised of more NeuN<sup>+</sup> cells than CS at age E12 ( $P < 0.05$ ). (E) DARPP32<sup>+</sup> cell counts. More DARPP32<sup>+</sup> cells were present in the W-S grafts than the B-S ( $***P < 0.001$ ). E14 tissue produced a greater number of DARPP32<sup>+</sup> cells compared to E12 in the B-S ( $@P < 0.05$ ) and W-S model ( $@@P < 0.01$ ). CS transplants yielded more DARPP32<sup>+</sup> cells using E14 tissue than E12 in both the BS ( $**P < 0.01$ ) and W-S ( $**P < 0.01$ ) models. E14 tissue yielded a higher DARPP32<sup>+</sup> cell count when transplanted as CS than TP in the B-S ( $*P < 0.05$ ) and W-S ( $*P < 0.05$ ). (F) DARPP32<sup>+</sup> cell counts as a proportion of total NeuN<sup>+</sup> cells. W-S grafts yielded a greater proportion of DARPP32<sup>+</sup> cells within the graft than the B-S ( $*P < 0.05$ ). In the W-S groups, E14 tissue produced a greater proportion of DARPP32<sup>+</sup> cells compared to E12 ( $@@P < 0.01$ ) and TP preparations produced a greater proportion than CS ( $*P < 0.01$ ).

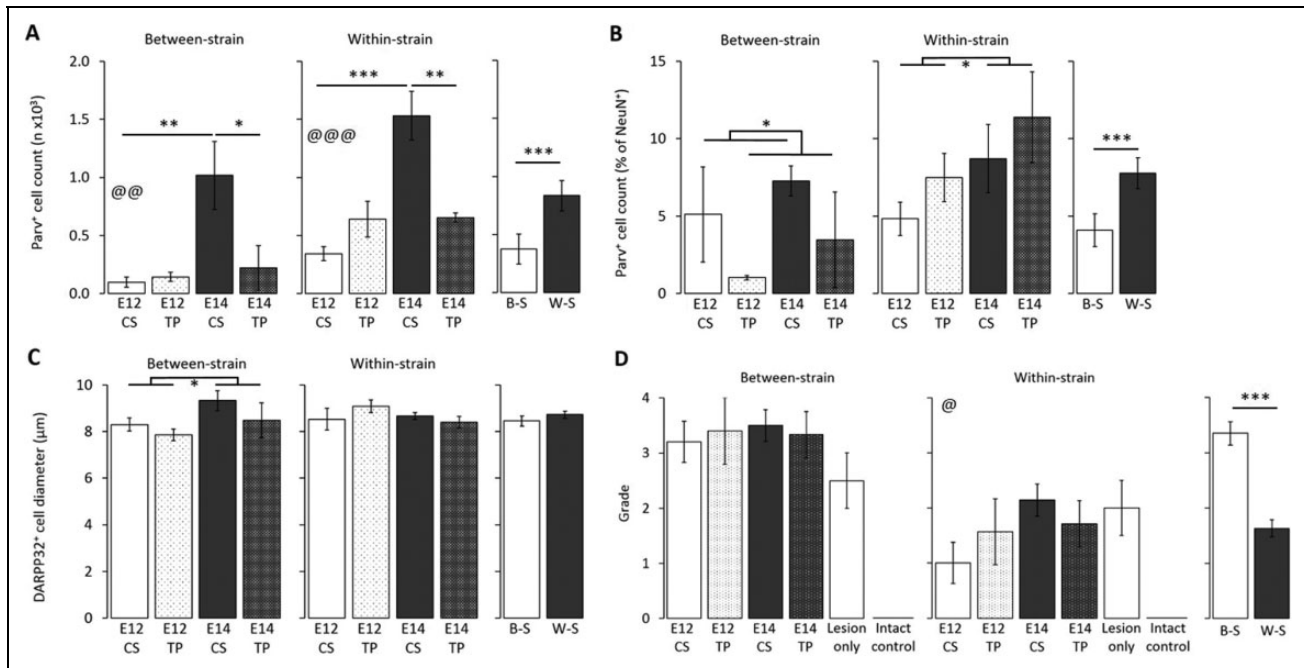


**Fig. 3.** (A) Parvalbumin<sup>+</sup> cell counts. A greater number of parvalbumin<sup>+</sup> interneurons were present in the within-strain (W-S) model than the between-strain (B-S) model (\*\**P* < 0.001). E14 tissue yielded a greater number of parvalbumin<sup>+</sup> interneurons than E12 in both the B-S (@@*P* < 0.01) and W-S (@@@*P* < 0.001) models. E14 tissue yielded a higher parvalbumin<sup>+</sup> cell count when transplanted as single-cell preparation (CS) than tissue piece style preparation (TP) in the B-S (\**P* < 0.05) and W-S (\*\**P* < 0.01) models. All data presented in Fig. 1 are adjusted for proportion of whole ganglionic eminence transplanted. (B) Parvalbumin<sup>+</sup> cell counts as a proportion of total NeuN<sup>+</sup> cells. W-S grafts yielded a greater proportion of parvalbumin<sup>+</sup> cells within the graft than the B-S (\*\**P* < 0.001). E14 tissue produced a greater number of parvalbumin<sup>+</sup> cells compared to E12 in the W-S (\**P* < 0.05). CS preparations produced a greater number of parvalbumin<sup>+</sup> cells compared to TP in the B-S (\**P* < 0.05). (C) DARPP-32<sup>+</sup> cell diameter. There was no difference in DARPP-32<sup>+</sup> cell diameter between the B-S and W-S groups. Cells derived from E14 tissue were larger than those taken from E12 tissue in the B-S groups (\**P* < 0.05). (D) Grading score for activated microglia (0 to 4) in the grafted striatum in the B-S groups, W-S groups, and the mean grading score for activated microglia in all grafted groups. Higher levels of activated microglia were found in B-S transplants than W-S (\*\**P* < 0.001). W-S transplants of E14 tissue produced an increased microglial response than E12 (@*P* < 0.05). No effect of age on microglial response was found in the B-S groups.

more parvalbumin<sup>+</sup> cells than E14 TP in both W-S and B-S groups (age × preparation:  $F_{1, 16} = 18.40$ ,  $P < 0.001$  and  $F_{1, 11} = 10.13$ ,  $P < 0.01$ , respectively), and there was a trend for E12 TP to yield more than E12 CS, but this did not reach significance.

The proportion of parvalbumin<sup>+</sup> cells (as a percentage of NeuN<sup>+</sup> cells) was greatest in the W-S model (strain:  $F_{1, 27} = 12.97$ ,  $P < 0.001$ ; Fig. 3B). CS preparations yielded a higher proportion compared to TP in the B-S groups (Preparation:  $F_{1, 11} = 7.13$ ,  $P < 0.05$ ), and E14 tissue yielded a higher proportion than the E12 in the W-S groups (age:  $F_{1, 16} = 5.76$ ,  $P < 0.05$ ).

There was no difference in the diameter of the DARPP-32<sup>+</sup> cells between the B-S and W-S groups; however, those derived from E14 tissue in the B-S groups were significantly larger compared to those from E12 tissue (age:  $F_{1, 13} = 12.98$ ,  $P < 0.01$ ).

### Microglial Response

Iba1 labeling revealed dense areas of microglial activation, not only within the grafted area but also extending beyond

the transplant boundaries to the host striatum in all mice except for intact control animals (Fig. 1D). Numerous dead cells and cellular debris were observed within most grafts and needle tracts, visible in sections stained with DAB as spherical clusters of paler staining (arrows in Fig. 1C).

Figure 3D shows the graded microglial response for each group. Activation of microglia was significantly higher in B-S than in W-S groups ( $F_{1, 39} = 99.09$ ,  $P < 0.001$ ). Grafts derived from E14 tissue in the W-S model induced a greater microglial activation than those of E12 tissue ( $F_{1, 23} = 5.54$ ,  $P < 0.05$ ); however, this effect was not seen in the B-S groups. No difference was detected between TP and CS preparations.

### Differentiation In Vitro

To investigate the development and maturation of cells from E12 and E14 donor embryos independent of the host environment, CS from CD1 embryos was prepared as described for transplantation and cultured for 24 h and 7 d *in vitro*. As TP preparations were not dissociated, it was not possible to culture these comparably. Cell counts from primary cultures are shown in Fig. 4. There was no difference in the

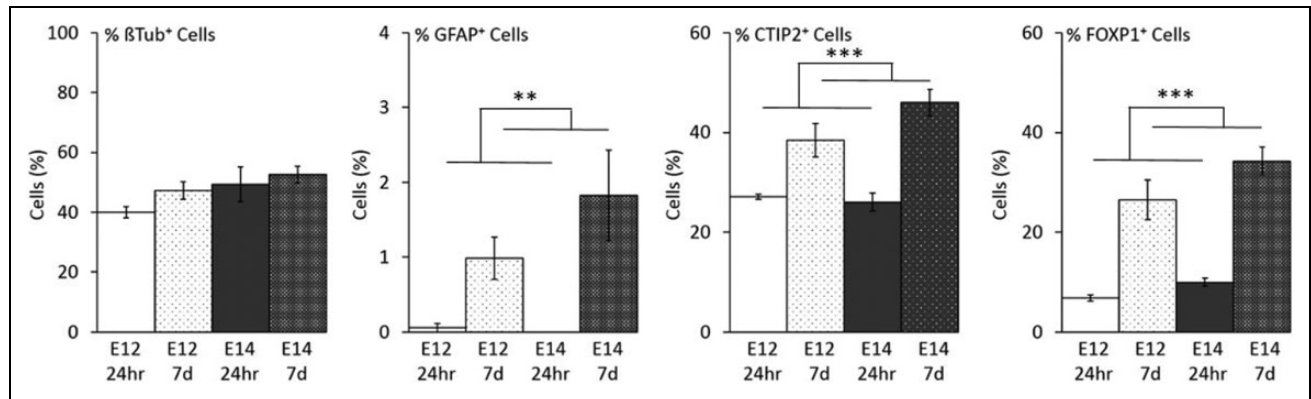


**Fig. 4.** Cell counts from plate downs of 100,000 cells from E12 and E14 single-cell suspensions after 24 h and 7 DIV. No differences were observed in the number of neurons across groups ( $\beta$ Tub<sup>+</sup> staining). Compared to 1 DIV, the cultures at 7 DIV contained a significantly higher percentage of astrocytes (\*\*GFAP<sup>+</sup>,  $P < 0.01$ ) and medium spiny neurons precursors (\*\*CTIP2<sup>+</sup>,  $P < 0.001$ ; \*\*FOXP1<sup>+</sup>,  $P < 0.001$ ).

proportion of  $\beta$ -tubulin<sup>+</sup> cells across any age or time point; however, there was a trend toward a greater number of  $\beta$ -tubulin<sup>+</sup> cells at 7-d post plate-down compared to 24 h, as well as for E14 compared to E12. Very few GFAP<sup>+</sup> cells were found in any group; however, there were significantly more after 7 d in both E12 and E14 donor age groups ( $F_{1, 8} = 16.99$ ,  $P < 0.01$ ). There was a significant increase in the proportion of CTIP2<sup>+</sup> cells at 7 days *in vitro* (DIV) compared to 24 h ( $F_{1, 8} = 44.52$ ,  $P < 0.001$ ) but there was no effect of embryonic age. FoxP1<sup>+</sup> MSN precursor cells also accounted for a higher proportion of the population at 7 DIV compared to 24 h ( $F_{1, 8} = 78.21$ ,  $P < 0.001$ ) with no effect of embryonic age.

## Discussion

The effect of donor age, cell preparation (single CS or dissociated TP), and variability in donor/host strain on primary embryonic striatal graft development and the host microglial response was investigated. Preparation as a CS is the method most routinely used, with trituration following enzymatic digestion to form a quasi-single CS. The TP style preparation used in this study, although not an identical treatment to other chopped tissue piece preparations,<sup>25–27</sup> provides a less severe treatment than standard CS protocol<sup>28,29</sup>. Cells underwent the same enzymatic digestion to aid in the transplantation process, but did not undergo manual trituration, thus leaving the tissue relatively intact, thus theoretically reducing cell stress. To provide information on how model selection could affect the host response to transplants and subsequent graft survival/development, 2 different donor/host strain combinations were used: a B-S model transplanting Chrm4-EGFP-CD1 tissue into C57BL/6/J hosts and a W-S model with CD1 tissue transplanted into CD1 mice.

A high percentage of graft survival was found across all groups, except for E14 TP in both strains, which was the least effective transplant protocol in terms of graft survival (see Table 1). These data show that transplanted cells can survive under a variety of protocol conditions, yet survival

rates were still not as high as usually seen in rat studies, and considerable variation in graft volume and content was seen within experimental groups. Graft cells were analyzed for the expression of the mature neuron marker NeuN, MSN marker DARPP-32, and the interneuron marker parvalbumin. Some NeuN<sup>+</sup> cells did not appear to express either DARPP-32 or parvalbumin and could be MSN cells not yet producing DARPP-32, nonstriatal neural cells, or nonparvalbumin interneurons.

## Donor Age

In general, E14 tissue produced grafts containing a higher number of mature neurons, DARPP32<sup>+</sup> MSN cells, and parvalbumin<sup>+</sup> interneurons compared to preparations transplanted using E12 tissue after considering the number of progenitor cells transplanted. Neural graft volume was larger for E14 preparations than E12 in the W-S groups, and this trend was also seen in the B-S groups, although not reaching significance—possibly due to small group sizes.

CS preparations produced more NeuN<sup>+</sup> cells, larger graft volumes, and more DARPP32<sup>+</sup> and interneuron content when harvested at E14 than at E12. Additionally, B-S transplants of E14 CS produced a higher proportion of P-zone tissue than E12 CS. In contrast, there was no effect of age on TP in any of the above measures, although a consistent trend was apparent showing the opposite effect, with TP yielding better grafts at E12 than at E14. Striatal transplants of E14 preparations in rats have been shown to produce larger grafts and DARPP-32<sup>+</sup> P-zones within the graft compared to older tissue as well as the greatest functional recovery.<sup>10,30,31</sup> Given that the developmental stage at E14 in rats is equivalent to age E12.5 in mice, by comparing the Carnegie stages of development<sup>32</sup>, it would be expected that E12 TP in mice should reflect the results seen in E14 TP rat studies. It is possible that the digestion process and trituration of the mouse CS have more of a detrimental effect on the cells at this younger age than at E14 and are less tolerant to the treatment than rat cells. This could lead to a reduced capability of mouse E12 CS cells

to survive and develop posttransplantation. In addition, it is possible that the Carnegie stages are not perfectly translated from rat to mouse and E12 could be more representative of a younger stage than the estimated E14 rat stage. This could have important implications for fetal age selection in primary human tissue transplants.

No effect of donor age was found in the *in vitro* measures investigated, including numbers of mature neurons ( $\beta$ -tubulin), early MSNs (FoxP1, CTIP2), and astrocytes (GFAP). E12 and E14 cells were equally viable at the time of transplantation/cell plating. However, *in vitro* conditions are not reflective of the *in vivo* environment, and differences seen *in vivo* may suggest that it is the interaction of cells with the host environment affecting the apparent differences in development. It has been shown that neuronal cells under stress are more likely to be destroyed by the host<sup>33</sup>, therefore if younger cells are more susceptible to stress, they may be more susceptible to the host immune response. The high levels of activated microglia seen within the grafted regions, and even in the lesion only controls, confirm that the immune response could play a critical role in the long-term survival of cells<sup>14</sup>.

Parvalbumin<sup>+</sup> interneurons were more abundant in grafts derived from E14 CS than those from any other, an indication that these grafts may contain a greater proportion of this interneuron population than the other groups, thereby presenting a cell population more characteristic of the normal striatum<sup>34</sup>. To obtain the neural diversity in grafts closest to that seen in the adult striatum, it is necessary to transplant both the lateral ganglionic eminence (LGE) and the medial ganglionic eminence (MGE)<sup>13,35</sup>. In mice, the LGE, the source of striatal progenitors<sup>36</sup>, is visible by E12, while the MGE, where interneurons are born, is visible as early as E11<sup>35,37</sup>, indicating that E12 might be the earliest time point for obtaining all the necessary cell types in mice. It is known that interneuron populations contribute to normal striatal function and development<sup>35</sup>, and these may be playing a supportive role in the development of the MSNs within the graft<sup>38</sup>. The MGE is much larger at E14 than at E12, and as this is the origin of interneuron progenitors<sup>39,40</sup>, would most likely contribute a greater proportion of interneurons to the transplanted population. In turn, this may have resulted in the improved development of E14 grafts<sup>13,35</sup>.

It is interesting to note that the mean cell body diameter of DARPP32<sup>+</sup> grafted cells from Chrm4-EGFP-CD1 tissue was significantly larger in the E14 age groups than in the E12, although this was not seen in the CD1 grafts. Given that at the time of perfusion all grafted cells were 12 wk old, under normal physiological conditions, it would be expected that they would have reached the same level of maturity and hence size. This may be an indication that the E14 cells are less inhibited by the local environment after transplantation into the host than the E12 cells, although contrasting evidence suggests that older cells, once past their proliferative stage, may be able to compensate less well<sup>12</sup>. Alternatively, E12 tissue could be undergoing proliferation for a longer

time posttransplantation, thus giving rise to cells until much later. These, at the time of sacrifice, could be less mature than those born closer to the time of transplantation. Changes in cell size may also be because of shrinkage or swelling due to physiological processes. For example, increases in cell size have been linked to necrosis<sup>41</sup>, while cells in the early process of apoptosis are reduced in size<sup>42</sup>. In this case, it is possible that more E14-derived cells could be necrotic or that more E12-derived cells are undergoing apoptosis; however, this could not be determined within the current study. No difference in the cell size of parvalbumin<sup>+</sup> interneurons was seen (data not presented).

### Cell Preparation

There are potential benefits of delivering the transplant as tissue pieces rather than triturated CSs. Limiting the manipulation of the tissue can reduce disruption and death of neuronal populations within the preparation, and the retention of the extracellular matrix may protect cells during transplantation and in the initial postgraft period. However, it has been suggested that the transplantation of whole tissue pieces may induce a stronger immune response due to the presence of the intact donor vasculature and antigen presenting cells (APCs)<sup>26,43</sup>. Although the use of nonimmunogenic bioengineered scaffolds could avoid this issue<sup>44,45</sup>, protocols generally require dissociation of cells prior to seeding into a scaffold, therefore still posing a risk to neuronal populations. Preparing tissue as partly digested tissue pieces without trituration<sup>28,29</sup> may prevent disruption to MSN precursors prior to transplantation and thus improve graft survival.

The results show a significant difference in the effect of preparation type on graft morphology depending on the age of the tissue used. E14 tissue prepared as CS produced grafts that are phenotypically superior to those transplanted as TP in almost all parameters including graft survival. Dissociated cell preparations are thought to provoke less of a host immune response when transplanted because the immunogenic donor vasculature is at least partially destroyed prior to implantation<sup>43,46</sup>. In addition, trypsinized single-cell preparations provide an advantage over solid pieces of tissue by potentially allowing transplanted cells access to the host capillary network more easily. The necessity of establishing contact in order to nourish the grafted tissue was demonstrated early on in studies implanting in vessel-rich and vessel-poor microenvironments<sup>47</sup>. Rat-to-rat grafts from CS transplants produce a greater proportion of striatal-like tissue, with more DARPP-32 expressing cell populations than those from TP, as well as providing greater innervation of the host parenchyma<sup>29</sup>. Cells transplanted as TP within a surrounding matrix may be restricted in terms of migration and integration into the host brain. The present study suggests that the benefits of transplanting dissociated CSs may outweigh those of a supportive matrix provided by TP transplants and that the trituration process is not too harsh to affect survival of the transplant at E14.

Conversely, E12 tissue produced larger grafts with greater striatal-like content when prepared as TP over CS. Previous studies in rats have shown that, for transplants of TP, older donor tissue is tolerated less and that younger tissue has a better chance of survival<sup>11,12,47</sup> corresponding to what we find in mouse TP transplants. It is unclear why the dissociation processes involved in CS preparation would reverse this trend, although, as discussed above, it seems that mouse WGE tissue is better able to withstand dissociation when processed at E14 than at E12 as evidenced through E14 CS transplants yielding improved long-term graft survival and larger grafts. Studies have suggested that different subpopulations of rat neurons are more sensitive to trypsinization than others<sup>12</sup>. Mouse cells may also be more sensitive, particularly at different developmental stages, warranting a systematic study of the effect of trypsinization on mouse precursors.

E12 TP survived transplantation with an improved capacity to produce successful grafts, although it is unclear why the same results are not reflected with E14 TP. Potentially, the less mature cells within the E12 TP are more proliferative and migratory at this early stage of development, therefore not restricted by the surrounding matrix. The particularly low survival rate in E14 TP preparations may indicate that TP at this age are not as amenable to integration as those at E12, potentially due to an increased potential of their vasculature and APCs to induce an immune response in the host<sup>43</sup>. In addition, following expulsion from the graft cannula, cells within the E14 TP might be more densely packed within the host striatum than single cells which could impede diffusion and timely integration with the capillary<sup>18,46</sup>.

### Strain Effects

The models selected for the purposes of this study were the 2 most commonly used paradigms within the lab, with the aim of determining how the choice of these particular models could affect the graft outcome.

We showed that the use of the different W-S and B-S models did not affect the number of surviving grafts. However, the transplants in the W-S model yielded the largest grafts in terms of neuronal volume compared to the B-S paradigm and had a higher number and proportion of DARPP32<sup>+</sup> cells. The CD1 grafts also contained more interneuron cells. A previous study using the same Chrm4-EGFP-CD1 donor tissue observed much larger grafts and survival<sup>19</sup>, although notably this CD1-derived tissue was transplanted into CD1 hosts rather than the C57BL/6.

The results suggest that the choice of strain and matching of donor and host animals for transplantation studies could be critical in achieving robust results. Iba1 staining revealed a significant amount of microglial activation within the grafted areas of all mice except the intact controls, including those in the lesion only group and those with no detectable surviving grafts. A significantly higher grading of activated

microglia was found in the B-S than in the W-S groups. Allotransplants elicit a greater immune response than isogenic tissue, and while neither of the models investigated here are inbred strains, it is clear that the response is increased when immunological disparity is greater<sup>43</sup>. This, in turn, can be linked to reduced transplant survival. Since the CD1 hosts received tissue derived from the same strain, it is likely that this was tolerated more than the tissue in the mismatched B-S groups. In addition, some studies have shown that the GFP marker associated with the Chrm4-EGFP-CD1 donor tissue could in itself be immunogenic<sup>48</sup>, although it is unclear if this is the case in striatal transplants in the C57BL/6 model<sup>49</sup>. It is also plausible that the C57BL/6 strain is inherently more prone to an exaggerated inflammatory response compared to the CD1 mice. It has been demonstrated that C57BL/6 mice have a strong bias to M1 inflammatory reaction, whereas other strains, such as Balb/c, tend toward a more supportive M2 response<sup>50</sup>. The separation of the effects of immunogenicity of the different donor tissues used and the reactivity of the hosts is beyond the scope of this study; however, it does warrant further investigation.

E14 tissue transplanted into the W-S models induced a greater microglial reaction than the E12 tissue. It is possible that tissue pieces transplanted from later embryonic ages contain more vasculature and hence could invoke a greater immune response, although this is yet to be tested. The fact that this pattern was not detected in the B-S model could be a result of a ceiling effect since the microglial response was consistently high in all B-S groups.

The higher levels of activated microglia in the C57BL/6/J hosts could explain the lower surviving cell number and graft volume<sup>51,52</sup>. It was noted that the area of activation exceeded the area of transplantation, suggesting secondary activation or recruitment of microglia to the site of transplantation. Interestingly, the glial response appeared reduced in individuals with rejected grafts, presumably because the transplanted cells had already been subjugated and the immune response had entered a post reactive phase. The ongoing proliferation of activated glial cells in and around the grafts is suggestive of ongoing reactivity with the surviving implanted cells. This could be an indication that the grafts surviving to 12 wk may be hampered long-term by the immune response of the hosts. Therefore, the study of immunosuppressive regimes in mouse to mouse transplantation could be a key to resolving the less than optimum quality of the grafts seen, as immunosuppression is generally only considered to be required for xenotransplant models.

### Conclusions

The results highlight a capacity of mouse transplants to survive under a variety of conditions and a need for protocols to be optimized to improve consistency and reliability. Donor age and tissue preparation technique are important factors that affect the morphology of primary fetal grafts. The data

from this study suggest that more successful grafts are derived from single-cell preparations of E14 tissue or from less dissociated tissue pieces at E12.

We found large variation in grafts across all the experimental groups, which implies the influence of other factors that may be more fundamental than the methodological modifications investigated in this study. Any impact of changes in cell preparation or donor age may be reduced by other more influential factors in the mouse to mouse model, highlighted by the differences between the strains investigated here. High levels of activated microglia in the grafted zones, particularly in the B-S transplants, and the presence of dead cells in all groups suggest that further investigation into immune response of mouse hosts to specific tissues is warranted.

### Authors' Note

The DARPP-32 antibody used in this study was kindly provided as a gift by Professor H. C. Hemmings, Cornell University, USA. Technical support was provided by Jane Heath, Anna Burt, Tom Steward, and Harry Potter.

### Ethical Approval

Ethical Approval is not applicable.

### Statement of Human and Animal Rights

This experiment was subject to project, personal, and facilities licenses and local ethical review in accordance with the United Kingdom Animals (Scientific Procedures) Act 1986 as amended.

### Statement of Informed Consent

There are no human subjects in this article and informed consent is not applicable.

### Declaration of Conflicting Interests

The author(s) declared no potential conflicts of interest with respect to the research, authorship, and/or publication of this article.

### Funding

The author(s) disclosed receipt of the following financial support for the research, authorship, and/or publication of this article: This work was funded by the Medical Research Council and the Wellcome Trust (VHR supported by a Wellcome Trust PhD studentship), with additional support from the CHDI Foundation and Repair-HD and Neurostemcell Repair projects of the EU FP7 programme.

### References

- Huntington's Disease Collaborative Research Group (HDCRG). A novel gene containing a trinucleotide repeat that is expanded and unstable on Huntington's disease chromosomes. The Huntington's Disease Collaborative Research Group. *Cell*. 1993;72(6):971–983.
- Graveland GA, Williams RS, DiFiglia M. Evidence for degenerative and regenerative changes in neostriatal spiny neurons in Huntington's disease. *Science*. 1985;227(4688):770–773.
- Dunnett SB, Nathwani F, Björklund A. The integration and function of striatal grafts. *Prog Brain Res*. 2000 Chapter 16; 127:345–380.
- Victorin K. Anatomy and connectivity of intrastriatal striatal transplants. *Prog Neurobiol*. 1992;38(6):611–639.
- Hauser RA, Furtado S, Cimino CR, Delgado H, Eichler S, Schwartz S, Scott D, Nauert GM, Soety E, Sossi V, et al. Bilateral human fetal striatal transplantation in Huntington's disease. *Neurology*. 2002;58(5):687–695.
- Rosser AE. Unilateral transplantation of human primary fetal tissue in four patients with Huntington's disease: NEST-UK safety report ISRCTN no 36485475. *J Neurol Neurosurg Psychiatry*. 2002;73(6):678–685.
- Bachoud-Lévi A, Bourdet C, Brugières P, Nguyen JP, Grandmougin T, Haddad B, Jény R, Bartolomeo P, Boissé MF, Barba GD, et al. Safety and tolerability assessment of intrastriatal neural allografts in five patients with Huntington's disease. *Exp Neurol*. 2000;161(1):194–202.
- Reuter I, Tai YF, Pavese N, Chaudhuri KR, Mason S, Polkey CE, Clough C, Brooks DJ, Barker RA, Piccini P. Long-term clinical and positron emission tomography outcome of fetal striatal transplantation in Huntington's disease. *J Neurol Neurosurg Psychiatry*. 2008;79(8):948–951.
- Schmidt RH, Björklund A, Stenevi U. Intracerebral grafting of dissociated CNS tissue suspensions: a new approach for neuronal transplantation to deep brain sites. *Brain Res*. 1981; 218(1–2):347–356.
- Fricker RA, Torres EM, Dunnett SB. The effects of donor stage on the survival and function of embryonic striatal grafts in the adult rat brain. I. Morphological characteristics. *Neuroscience*. 1997;79(3):695–710.
- Kromer LF, Björklund A, Stenevi U. Intracerebral embryonic neural implants in the adult rat brain. I. Growth and mature organization of brainstem, cerebellar, and hippocampal implants. *J Comp Neurol*. 1983;218(4):433–459.
- Björklund A, Stenevi U. Intracerebral neural implants: neuronal replacement and reconstruction of damaged circuitries. *Annu Rev Neurosci*. 1984;7:279–308.
- Watts Brasted PJ, Dunnett SB. Embryonic donor age and dissection influences striatal graft development and functional integration in a rodent model of Huntington's disease. *Exp Neurol*. 2000;163(1):85–97.
- Robertson VH, Evans AE, Harrison DJ, Precious S V, Dunnett SB, Kelly CM, Rosser AE. Is the adult mouse striatum a hostile host for neural transplant survival? *Neuroreport*. 2013;24(18): 1010–1015.
- El Akabawy G, Rattray I, Johansson SM, Gale R, Bates G, Modo M, El-Akabawy G. Implantation of undifferentiated and predifferentiated human neural stem cells in the R6/2 transgenic mouse model of Huntington's disease. *BMC Neurosci*. 2012;13(1):97.
- Johann V, Schiefer J, Sass C, Mey J, Brook G, Krüttgen A, Schlangen C, Bernreuther C, Schachner M, Dihné M, et al. Time of transplantation and cell preparation determine neural stem cell survival in a mouse model of Huntington's disease. *Exp Brain Res*. 2007;177(4):458–470.

17. Kelly CM, Precious SV, Penketh R, Amso N, Dunnett SB, Rosser AE. Striatal graft projections are influenced by donor cell type and not the immunogenic background. *Brain*. 2007; 130(5):1317–1329.
18. Cisbani G, Saint Pierre M, Cicchetti F. Single-cell suspension methodology favors survival and vascularization of fetal striatal grafts in the YAC128 mouse model of Huntington's disease. *Cell Transplant*. 2014;23(10):1267–1278.
19. Döbrössy MD, Klein A, Janghra N, Nikkhah G, Dunnett SB. Validating the use of M4-BAC-GFP mice as tissue donors in cell replacement therapies in a rodent model of Huntington's disease. *J Neurosci Methods*. 2011;197(1):6–13.
20. Lelos MJ, Robertson VH, Vinh N-N, Harrison C, Eriksen P, Torres EM, Clinch SP, Rosser AE, Dunnett SB. Direct comparison of rat- and human-derived ganglionic eminence tissue grafts on motor function. *Cell Transplant*. 2016;25(4):665–675.
21. Dunnett SB, Björklund A. Dissecting embryonic neural tissues for transplantation. In: Dunnett SB, Boulton AA, Baker GB, editors. *Neural transplantation methods*. Totowa (NJ): Humana Press; 2000. p. 3–25.
22. Hemmings HC, Greengard P. DARPP-32, a dopamine- and adenosine 3':5'-monophosphate-regulated phosphoprotein: regional, tissue, and phylogenetic distribution. *J Neurosci*. 1986;6(5):1469–1481.
23. Duan W-MM, Widner H, Brundin P. Temporal pattern of host responses against intrastriatal grafts of syngeneic, allogeneic or xenogeneic embryonic neuronal tissue in rats. *Exp Brain Res*. 1995;104(2):227–242.
24. Boche D, Perry VH, Nicoll JAR. Review: activation patterns of microglia and their identification in the human brain. *Neuropathol Appl Neurobiol*. 2013;39(1):3–18.
25. Bachoud-Lévi A-C, Rémy P, Nguyễn J-P, Brugières P, Lefaucheur J-P, Bourdet C, Baudic S, Gaura V, Maison P, Haddad B, et al. Motor and cognitive improvements in patients with Huntington's disease after neural transplantation. *Lancet*. 2000; 356(9246):1975–1979.
26. Redmond DE, Vinuela A, Kordower JH, Isacson O. Influence of cell preparation and target location on the behavioral recovery after striatal transplantation of fetal dopaminergic neurons in a primate model of Parkinson's disease. *Neurobiol Dis*. 2008;29(1):103–116.
27. Freeman TB, Sanberg PR, Nauert GM, Boss BD, Spector D, Olanow CW, Kordower JH. The influence of donor age on the survival of solid and suspension intraparenchymal human embryonic nigral grafts. *Cell Transplant*. 1995;4(1):141–154.
28. Rath A, Klein A, Papazoglou A, Pruszek J, Garcia J, Krause M, Maciaczyk J, Dunnett SB, Nikkhah G. Survival and functional restoration of human fetal ventral mesencephalon following transplantation in a rat model of Parkinson's disease. *Cell Transplant*. 2013;22(7):1281–1293.
29. Watts Brasted PJ, Dunnett SB. The morphology, integration, and functional efficacy of striatal grafts differ between cell suspensions and tissue pieces. *Cell Transplant*. 2000;9(3):395–407.
30. Watts C, Dunnett SB, Rosser AE. Effect of embryonic donor age and dissection on the DARPP-32 content of cell suspensions used for intrastriatal transplantation. *Exp Neurol*. 1997; 148(1):271–280.
31. Schackel S, Pauly M-C, Piroth T, Nikkhah G, Döbrössy MD. Donor age dependent graft development and recovery in a rat model of Huntington's disease: histological and behavioral analysis. *Behav Brain Res*. 2013;256:56–63.
32. Butler H, Juurlink BHJ. *An atlas for staging mammalian and chick embryos*. Boca Raton (FL): CRC Press; 1987.
33. Brown GC, Neher JJ. Microglial phagocytosis of live neurons. *Nat Rev Neurosci*. 2014;15(4):209–216.
34. Fentress JC, Stanfield BB, Cowan WM. Observations on the development of the striatum in mice and rats. *Anat Embryol (Berl)*. 1981;163(3):275–298.
35. Olsson M, Björklund A, Campbell K. Early specification of striatal projection neurons and interneuronal subtypes in the lateral and medial ganglionic eminence. *Neuroscience*. 1998; 84(3):867–876.
36. Deacon TW, Pakzaban P, Isacson O. The lateral ganglionic eminence is the origin of cells committed to striatal phenotypes: neural transplantation and developmental evidence. *Brain Res*. 1994;668(1–2):211–219.
37. Smart IHM, Sturrock RR. *The neostriatum*. Amsterdam, Netherlands: Elsevier; 1979:127–146.
38. Gerfen CR, Baimbridge KG, Miller JJ. The neostriatal mosaic: compartmental distribution of calcium-binding protein and parvalbumin in the basal ganglia of the rat and monkey. *Proc Natl Acad Sci U S A*. 1985;82(24):8780–8784.
39. Anderson SA, Qiu M, Bulfone A, Eisenstat DD, Meneses J, Pedersen R, Rubenstein JLR. Mutations of the homeobox genes *Dlx-1* and *Dlx-2* disrupt the striatal subventricular zone and differentiation of late born striatal neurons. *Neuron*. 1997; 19(1):27–37.
40. Campbell K, Olsson M, Björklund A. Regional incorporation and site-specific differentiation of striatal precursors transplanted to the embryonic forebrain ventricle. *Neuron*. 1995; 15(6):1259–1273.
41. Healy E, Dempsey M, Lally C, Ryan MP. Apoptosis and necrosis: Mechanisms of cell death induced by cyclosporine A in a renal proximal tubular cell line. *Kidney Int*. 1998;54(6):1955–1966.
42. Elmore S. Apoptosis: a review of programmed cell death. *Toxicol Pathol*. 2007;35(4):495–516.
43. Chen Z, Phillips LK, Gould E, Campisi J, Lee SW, Ormerod BK, Zwierchoniewska M, Martinez OM, Palmer TD. MHC mismatch inhibits neurogenesis and neuron maturation in stem cell allografts. *PLoS One*. 2011;6(3):e14787.
44. Wang T-Y, Bruggeman KF, Kauhausen JA, Rodriguez AL, Nisbet DR, Parish CL. Functionalized composite scaffolds improve the engraftment of transplanted dopaminergic progenitors in a mouse model of Parkinson's disease. *Biomaterials*. 2016;74:89–98.
45. Newland B, Welzel PB, Newland H, Renneberg C, Kolar P, Tsurkan M, Rosser A, Freudenberg U, Werner C. Tackling cell

- transplantation anoikis: an injectable, shape memory cryogel microcarrier platform material for stem cell and neuronal cell growth. *Small*. 2015;11(38):5047–5053.
46. Baker-Cairns BJ, Sloan DJ, Broadwell RD, Puklavec M, Charlton HM. Contributions of donor and host blood vessels in CNS allografts. *Exp Neurol*. 1996;142(1):36–46.
  47. Stenevi U, Björklund A, Svendgaard NA. Transplantation of central and peripheral monoamine neurons to the adult rat brain: techniques and conditions for survival. *Brain Res*. 1976;114(1):1–20.
  48. Stripecke R, Del M, Villacres C, Skelton D, Satake N, Halene S, Kohn D. Immune response to green fluorescent protein: implications for gene therapy. *Gene Ther*. 1999;6(7):1305–1312.
  49. Skelton D, Satake N, Kohn D. The enhanced green fluorescent protein (eGFP) is minimally immunogenic in C57BL/6 mice. *Gene Ther*. 2001;8(23):1813–1814.
  50. Mills CD, Kincaid K, Alt JM, Heilman MJ, Hill AM. M-1/M-2 macrophages and the Th1/Th2 paradigm. *J Immunol*. 2000;164(12):6166–6173.
  51. Perry VH, Teeling J. Microglia and macrophages of the central nervous system: the contribution of microglia priming and systemic inflammation to chronic neurodegeneration. *Semin Immunopathol*. 2013;35(5):601–612.
  52. Raivich G, Bohatschek M, Kloss CUA, Werner A, Jones LL, Kreutzberg GW. Neuroglial activation repertoire in the injured brain: graded response, molecular mechanisms and cues to physiological function. *Brain Res Brain Res Rev*. 1999;30(1):77–105.